Industrial Applications of Thermal Spray Technology

19

Abbreviations

ACP	Amorphous calcium phosphate
ALTM	Air Lock Transition Module
APS	Air plasma spraying
APS	Atmospheric plasma spraying
AS	As-sprayed
BAG	Bioactive glass
BM	Base material
BOF	Basic oxygen furnace
BRT	Burner Rig Test
CAPS	Controlled atmosphere plasma spraying
CFRP	Carbon fiber-reinforced plastic
CMAS	Acronym for CaO, MgO, Al_2O_3, SiO_2
CNT	Carbon nanotubes
CS	Cold Spray
C-SSCS	Composite of Stainless Steel-Carbon Steel
CTE	Coefficient of thermal expansion
CVD	Chemical Vapor Deposition
CW	Corrosion-Wear
dBA	Decibel Authorized
DC	Direct current
D-gun	Detonation-gun
DRC	Diamond-reinforced composite
DWTS	Direct write thermal spray
EAF	Electric arc furnace
EB-PVD	Electron Beam-Physical Vapor Deposition
EC	Erosion-Corrosion
EHC	Electrolytic hard chrome
EIS	Electrochemical impedance spectroscopy
EMI	Electromagnetic interference
EW	Erosive-Wear
FAC	Fe-based alloy coatings
FBC	Fluidized-bed combustor
fcc	Face-centered cubic
FDA	Food and Drug Administration
FG	Functionally graded
FGC	Functionally graded coating
FW	Fatigue wear
GDC	Acronym for, $Ce_{0.8}$ $Gd_{0.2}$ $O_{1.9}$
GS	Gas shroud
HA	Hydroxyapatite Ca_{10} $(PO_4)_6$ $(OH)_2$
HAT	HA top coating
HB	Hardness Brinell
HC	Hard chrome
HCC	Hard chromium coating
HEPS	High-energy plasma spray
HIP	Hot isostatically pressed
HPAL	High-pressure acid-leach
HPPS	High-power plasma spray
HTBC	HA/TiO_2 (50 vol.% each) Bond Coat
HTH	HA/(HA/TiO_2) Bond Coat
HVAF	High-velocity air fuel
HVFS	High-velocity flame spraying
HVLF	High-velocity liquid fuel
HVOF	High-velocity oxy fuel
HVPS	High-velocity plasma spray
HVSFS	High-velocity suspension flame spraying
ICP	Inductively Coupled Plasma
IACS	International Annealed Copper Standard
IPS	Induction plasma spraying
JTST	*Journal of Thermal Spray Technology*
LaMA	Acronym for $LaMgAl_{11}O_{19}$
LBT	Land-based turbines
LPPS	Low-pressure plasma spraying
LPPS-TF	Low Pressure Plasma Spray-Tin Film
LSCF	Acronym for, $La_{0.6}$ $Sr_{0.4}$ $Co_{0.2}$ $Fe_{0.8}$ $O_{32-\delta}$
LTA	Acronym for, $LaTi_2Al_9O_{19}$
LTE	Local thermodynamic equilibrium
MLCC	Multilayer ceramic capacitors
MMC	Metal matrix composite
MSWI	Municipal solid waste incinerator
NTSRS	Net thermal spraying residual stress
ODS	Oxide-dispersion strengthened
OEM	Original equipment manufacturer

M. I. Boulos et al. (ed.), *Thermal Spray Fundamentals*, https://doi.org/10.1007/978-3-030-70672-2_19

PA-12	Polyamide-12
PAH	Progressive abradability hardness
PE-CVD	Plasma Enhanced-CVD
PEEK	Poly-ether-ether-ketone
PEI	Polyetherimide
PGDS	Pulsed gas dynamic spraying
PM	Post-melted
PMC	Polymer matrix composite
PS	Plasma spraying
PSD	Particle size distribution
PS-PVD	Plasma Spray-PVD
PTA	Plasma-transferred arc
PTS	Polymer thermal spray
PVD	Physical vapor deposition
QC	Quality control
RCF	Rolling contact fatigue
RF	Radio frequency
RF-IPS	RF-Induction Plasma Spraying
RH	Relative air humidity
SBF	Simulated body fluid
SER	Specific energy requirement
SFW	Surface fatigue wear
SPS	Spark Plasma Sintering

19.1 Introduction

At its early stages of development, thermal spray (TS) technology was mostly used for surface protection against corrosion and erosion, as well as for the rebuilding, retrofitting, and wear repair [Davis JR (Ed) (2004)]. Up to the early 1980s, the basic phenomena involved in most of thermal spray processes were poorly understood, with the process parameters based more on the operator experience and skills rather than on a solid scientific understanding of the phenomena involved. This often resulted in unsatisfactory process reproducibility and reliability. The wider acceptance of the technology for industrial-scale production started in the late 1980s and early 1990s, with applications limited to high added-value components in the aerospace and nuclear industry. These were mostly driven by the fact that no viable alternate solutions were available, and design engineers and scientists were used to work with rather complex processes.

Since the turn of the century, the range of industrial-scale applications of the thermal spray industry expanded considerably penetrating into new industrial sectors such as biomedical, electric and electronics industry, and high-end automobile industry. These were mostly considered for tribological and wear-resistant applications including lubricity and low-friction surfaces, resistance to corrosion and/or oxidation, thermal protection, electrical and optical components, electromagnetic shielding, electrical insulation, abradable seals, biomedical applications, as well as ornamental applications. The surge was manifested by a major increase in the volume of the scientific literature published in this field as illustrated in Fig. 19.1, which shows the cumulative number of technical manuscripts submitted to the *Journal of Thermal Spray Technology* (JTST), one of the leading scientific journals in this field, during the period 2004–2010. Particularly relevant to note is the very rapid increase of TS

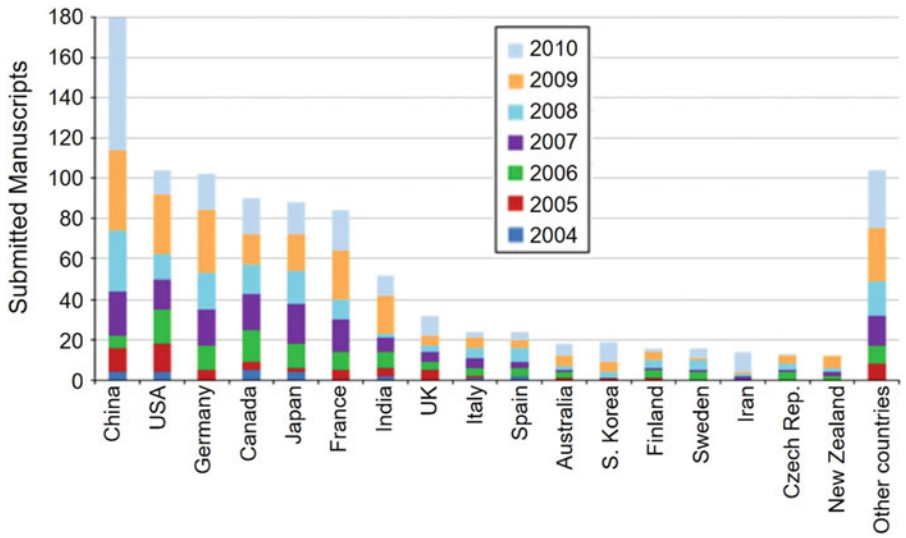

Fig. 19.1 Cumulative number of technical papers submitted to the *Journal of Thermal Spray Technology* over the period 2004–2010. [Dorfman and Sharma (2013a, b)]

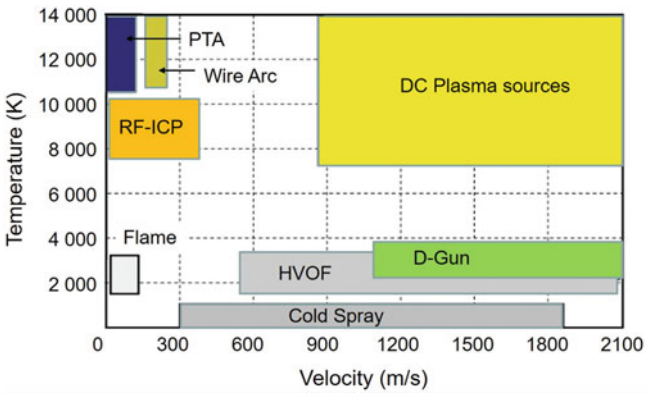

Fig. 19.2 Gas temperatures versus velocity mapping associated with different thermal spray processes

research activities over this period in China and the sustained research and development (R&D) activities in the USA, Germany, Canada, Japan, and France.

The choice of a specific coating and/or thermal spray process technology, for a given service condition, depends, however, on the expectation of the user and the cost that could be tolerated for the application. This affected, in turn, the selection of the material to be applied for the coating and the spray process used, which, as shown in Fig. 19.2, can offer widely different spraying conditions in terms of spray medium velocity and temperature range. The design of functional coatings, however, is often complicated by the fact that components are not always devoted to a single requirement such as wear or corrosion, electrical insulation, or thermal insulation. In most cases, coatings had to satisfy multiple combined needs such as, for example, wear and corrosion resistance.

It is important to point out that, contrary to general perception, because of the specific features of each of these TS technologies, they are mostly complementary, rather than competitive. Any overlap between them in terms of application is not very broad with the majority of TS technologies differing in terms of coating functional properties, and economic factors. To choose between them, it is important to know the advantages and limitation of each of these processes and to make the proper decision of the best process for each application.

In this chapter, a comparative analysis of thermal spray processes is given highlighting their principal characteristics and limitations. This is followed by a classification of the different areas of application of TS technologies for surface modification depending on functional needs and service conditions. Review of the principal TS coating applications by industrial sector and by country is presented next, followed by a simplified economic analysis of the different thermal spray processes. A summary of coating applications by industry and listing of the range of materials that can be used for different applications are provided respectively in Appendices A and B at the end of this chapter.

19.2 Comparative Analysis of Thermal Spray Processes

In this section, a comparative analysis is presented of different thermal spray processes described in detail in Part II, Thermal Spray Technologies, of this book. These are grouped in terms of energy source used in the process, the form of precursor used with each of these processes, and key features of the technology that orients its field of industrial applications.

19.2.1 Cold Spraying

As discussed in Chap. 6, cold spray (CS) is a kinetic process utilizing high-pressure compressed gas (2–4 MPa), such as nitrogen or helium or their mixture, at near room temperature, or preheated up to 700–800 °C, to produce high-velocity supersonic gas jets that act as spray medium to entrain and accelerate the spray material in the form of fin powder to velocities up to 300–1500 m/s. On impact of the particles on the surface of the substrate, they plastically deform creating the coating. The process requires impact particle velocities higher than a so-called *critical velocity*, which depends on the nature of the particle material, its particle size distribution (PSD), and particle morphology.

Cold spray is limited to the spraying of ductile metals, ferrous and nonferrous, metal alloys, composites, and cermets on virtually any substrate. The main advantage of the technology is its ability to avoid the in-flight oxidation of the powder and achieving high coating densities and minimal heating of the substrate during the deposition process, which allows it to be used for the coating of heat-sensitive substrates. With this spray process, the oxide content of the coating reflects essentially that of the sprayed powder (for example, <100 ppm for copper). The mechanical and electrical properties of as-sprayed (AS) coatings are remarkably close to those of bulk materials, especially with very good tensile properties. The ductility of cold-sprayed coatings can, however, be rather low due to the important work hardening inherent to the process.

Other than its principal limitation with respect to the material to be sprayed, the process is rather noisy reaching up to 110 decibels authorized (dBA), thus requiring special protective equipment for the operator. Its need for high gas flow rates can be prohibitively costly especially when using helium, even when mixed with nitrogen. Recycling helium requires that the spray process be carried out in a controlled atmosphere chamber, adapted to the size of the parts to be coated. The chamber should be equipped with an airlock transition module (ALTM) allowing for the introduction and removal of the parts from the chamber without contaminating its gaseous content. Gas recycling also

requires important investments in gas recycling pumping system, filters, and high-pressure gas storage tanks. In this case, the noise level associated with the process is reduced to that of the surrounding equipment. Deposition rates are typically in the range of 2–10 kg/h, with deposition efficiencies of 40–90% depending on sprayed materials.

The first and very successful application of CS was for copper metallization. Other industrial-scale applications include its use for metal restoration and sealing, engine blocks, castings, molds and dies, refrigeration equipment, heat exchangers, aluminum piston heads, manifolds, disk brakes, heat sinks for microelectronics (Al and Cu), solid lubricant matrix with base metals, electronically conductive coatings (Cu or Al on ceramic or polymeric components), electromagnetic shielding, as well as localized corrosion protection (Zn or Al coatings).

19.2.2 Combustion-Based Thermal Spraying

As presented in Chap. 7, combustion-based thermal spray technologies are the first to be developed in the early twentieth century and remains one of the most widely used spray-coating processes because of their favorable economics. The principal limitation of the technology is in the nature of the material to be sprayed since the maximum flame temperature is generally below 3500 K. Moreover, because the oxidizing atmosphere predominate in the flame, flame-spray coatings of metals usually contain a few wt.% of oxide (1–4 or 5 wt.% depending on metal reactivity, torch design, and oxygen-to-fuel ratio). Over the years, their wider acceptance of combustion-based thermal spraying driven by scientific and technical improvements as well as growing market demand has led to the development of the following three distinct technologies.

19.2.2.1 Flame Spraying

Flame spraying (FS) is at the origin of all combustion-based thermal spray technologies, making use of mostly oxyacetylene torches achieving premixed combustion temperatures up to about 3000 K. Flame velocities are generally below 100 m/s. Sprayed materials are introduced generally axially into the spray gun either in the form of powder—"powder flame spraying"—or as wire, rod, or cord—"wire flame spraying".

In "powder flame spraying," the sprayed materials are mostly metals or polymers, which are rather easy to melt and spray. Particles are axially injected into the flame. Coatings present a high porosity (>10 vol.%) and a low adhesion (<30 MPa). Powder feed rates are typically between 2 and 10 kg/h, depending on sprayed material and torch used. The deposition efficiency is around 50%. In-flight oxidation of the powder occurs during processing (oxide content up to 6–12 wt.%). They are mostly used for wear-resistance applications under low load. Substrate and coating must be cooled during spraying. Flame spraying is generally rather noisy (90–125 dBA).

Flamed-sprayed, self-fluxing alloys contain Si and B (for example, CrBFeSiCNi) that are used as deoxidizers. When the coating is heat-treated at about 1030 °C, they diffuse toward the coating surface trapping the oxygen. It results in coatings with almost no porosity, an excellent adhesion by diffusion at the substrate–coating interface. It is also very easy to deposit materials of brazing type, and composite coatings are possible. Such coatings are generally limited to substrates that can tolerate the fusing temperature (steel and not aluminum, for example) and possibly any induced distortion. They are mostly used against abrasion (friction, erosion) and corrosion (cold or hot).

Flame spraying can also be used with wires, rods, or cords. In this case, a compressed air jet atomizes the melted tip of the wire (metallic and ductile) or cored wires (containing ceramics or nonductile materials), rod, or cord (for ceramics). Due to the compressed gas atomization, the noise level is not negligible. Compared to powders, the variety of materials that can be sprayed as wires, rods, or cords are larger. Wires of self-fluxing alloys can also be sprayed. Oxides are of course generated during the process, but less than with powders (about 4–8 wt.%), and the deposition efficiency is better (around 70%). Compared to powders the material flow rate varies from 5 to 25 kg/h. With wires the coating adhesion is slightly better than that obtained with powders. The porosity is similar to that obtained with powders except for ceramic materials that are more porous but present an excellent wear resistance. Generally, the metal or alloy coatings are used against wear—especially abrasion or adhesion under low load, for example, in rotating heavy equipment, piston rings, and synchronizing rings—and atmospheric corrosion: bridges, large steel structures, galvanized tubing, or ships. The wire flame-spray noise level is between 118 and 122 dBA, while with rods it is about 125 dBA.

19.2.2.2 High-Velocity Flame Spraying

High-velocity flame spraying (HVFS), or as commonly referred to as "high-velocity oxy fuel" (HVOF) or "high-velocity air fuel" (HVAF), are also combustion-driven processes with internal combustion at pressure below 1 MPa for those with gaseous fuel and slightly higher for those with liquid fuels. They produce very-high-velocity spray medium streams, thanks to a convergent–divergent nozzle design following the combustion chamber. They work mostly with powder spray materials injected axially, or radially, into the flame with some spray gun designs, with a few processes developed to spray wires. Power levels for HVOF guns working with gaseous fuels are in the range of 100–120 kW, with a noise level of 125–135 dBA. For those working

with liquid fuels, the power can reach 300 kW with a noise level of 133 dBA or more. The actual trend is to increase particle velocities and reduce their temperatures in order to limit their oxidation, the high kinetic energy of particles compensating for the lower temperature. This was first realized with HVAF guns working with air and where the noise level was 133 dBA or more. In the high-power guns, especially designed for that, the addition of inert gas such as nitrogen in the combustion chamber, at flow rates up to 2000 standard liter per minute (slm), is used to reduce gas temperature and increase its velocity.

Globally this process, working mainly with metals, alloys, and cermets (one of their most successful application), has deposition efficiencies of about 70% at powder feed rates up to 7.2 kg/h for gaseous-fuel guns, and up to 12 kg/h for liquid-fuel guns with deposition efficiencies roughly of 60–80%. Resulting coating porosities are a few vol.%, with a good adhesion (>50–60 MPa) and low oxygen content (between 0.5 and a few wt.%). Due to shot-peening effect, compressive stresses can be achieved in rather thick coatings (up to 6.4 mm). Of course, the process is noisy, dusty, and requires special safety precautions for the handling of large flow rates of explosive gases. HVOF and HVAF spraying are mostly used for wear and corrosion protection. Resistance to wear of the coating, sliding/adhesive wear, fretting, erosion, or cavitation is generally excellent depending on the material and process parameters used. The corrosion resistance is also very good with the high density of coatings and, according to the sprayed material, they are used for hot corrosion, oxidation, and against acidic or alkaline atmospheres and liquids. Substrate and coating must be cooled during spraying.

19.2.2.3 Detonation-Gun Spraying

Detonation-gun (D-gun) spraying, commonly referred to as "D-gun spraying" or "pulsed detonation spraying," was developed in the 1950s. The technology is closer to cold spray or HVOF/HVAF than conventional thermal spray coating since it relies heavily on the acceleration of particles to be sprayed to high velocities, projecting them toward the substrate in essentially a soften solid-state where they deform on impact forming the coating. In contrast to other combustion processes, where the flame is a subsonic wave sustained by a chemical reaction, detonation wave is a shock wave sustained by the energy of chemical reactions in a compressed explosive gas mixture. The ideal detonation wave travels in gases at speeds between 1500 and 3000 m/s, depending on the type and composition of the fuel-oxidizer mixture. The pressure just behind the detonation wave can be as high as 20–30 times the ambient pressure.

This process is pulsed at a frequency between 6 and 100 Hz. Particle velocities are due to the energy of a detonation (explosion). The resulting deposit is extremely hard, dense, and tightly bonded to the substrate. The process is the noisiest of all the thermal spray processes (more than 145 dBA). Coating porosity is low (below 1 vol.%) and its oxygen content is between 0.1 and 0.5 wt.%. The deposition efficiency is around 90%, but powder flow rates are limited to the 1–2 kg/h range. Sprayed materials in powder form range from metals, alloys, and cermets. Some oxides can also be sprayed by this technique as long as their average particle size is below 20 μm. The main applications are abrasion and adhesion (friction) under low load as well as corrosion. Substrate and coating must be cooled during spraying.

19.2.3 Plasma Spraying

As described in Chaps. 7, 8, and 9, plasma spraying (PS) is based on the concept of generation of a high-temperature, high-velocity spray jet through the striking of an electric arc between two electrodes, or inductive coupling of the electric energy into a discharge that is heated through resistive energy dissipation by the current flowing through the gas at sufficiently high temperatures to have appreciable degrees of ionization and high electrical conductivities. Two distinct features of the technology in general are:

- Electric energy is the sole source of energy in the process.
- Extensive flexibility on the chemistry of the spray medium allowing the process to be carried out in an inert, reducing, or oxidizing atmosphere.

For most plasma-forming gases, the required temperatures at atmospheric pressure are above 8000 K. By definition, in a thermal arc the thermodynamic state of the plasma generally approaches local thermodynamic equilibrium (LTE), which includes kinetic and chemical equilibrium, except for the arc fringes or that close to a cooled wall.

Direct current (DC) plasma spray technology has been the principal driver in this field, leading to the development of a wide range of technologies such as:

- Atmospheric plasma spraying (APS)
- Controlled atmosphere plasma spraying (CAPS)
- Vacuum plasma spraying (VPS)
- Ultra-low-pressure plasma spraying (ULPPS)

Radio frequency induction plasma spraying (RF-IPS), on the other hand, has been developed in parallel mostly for high-end, high-purity applications such as preform cladding with high-purity silica in the fiber optic industry and high-purity crystal growing.

With temperatures over 8000 K, any material, whether metallic or ceramic, can be melted. The technology is essentially based on the in-flight heating and melting of the sprayed material injected into the plasma stream, either

radially as in most DC plasma torches or axially as in RF-IPS or a few multi-electrode DC plasma sources. Feed material used is mostly in powder form with a mean particle diameter in the micron size range. Alternately, solution and suspension plasma spraying have been gaining wider acceptance for specific applications such as the spraying of nanostructured coatings.

19.2.3.1 Atmospheric Plasma Spraying

Atmospheric plasma spraying or air plasma spraying (APS) is carried out mostly with DC plasma torches in an open-air atmosphere using Ar, Ar/H_2, Ar/He, or Ar/N_2 as plasma gas operating at power levels ranging from 30 to 90 kW with, in most cases, radial powder injection. For plasma spray torches with one-stick type cathode, and power levels in the range 40–50 kW, the powder flow rate is between 3 and 6 kg/h, the deposition efficiency around 50%, and the torch noise level between 110 and 125 dBA. With high-power torches (150–250 kW), powder flow rates as high as 15–20 kg/h can be reached. With tri-cathode torches such as the Oerlikon-Metco Triplex Torch or the Northwest Mettech Axial III comprising of three plasma jets converging in the torch nozzle, particles are axially injected into the emerging plasma jet.

Typical spraying distance is in the range of 100–120 mm, the heat flux to the substrate is among the highest ($\approx$2 MW/m^2), and the substrate as well as the coating must be cooled. To avoid oxidation, spraying must be performed under controlled atmosphere or soft vacuum conditions. APS coating porosities are between 2 and 8 vol.%, the oxygen content of metal or alloy coatings is between 1 and 5 wt.%, and their adhesion is good (>40–50 MPa). They are mainly used to spray oxides. However, they present good resistance to abrasive, adhesive, fretting, or sliding wear. They also produce thermally conductive or resistant surfaces.

19.2.3.2 Controlled Atmosphere Plasma Spraying

Controlled atmosphere plasma spraying (CAPS) is used when oxidation is a problem. Metals with high-melting temperature and non-oxide ceramics can be sprayed only in inert atmosphere (e.g., chamber filled with argon), at atmospheric pressure or slightly over. The technique is mostly used to melt materials with high melting temperature, such as TaC ($T_m \approx 4150$ K). The controlled atmosphere chamber must be water-cooled if its volume is below 10 m^3, and industrial-scale production of such coatings requires using an airlock transition module (ALTM) to introduce and remove parts from the chamber without allowing for air penetrating into the main chamber. The noise level is that of the surrounding pumps, fans, and power supply. The equipment is more complex than APS requiring the use of robots with adequate thermal protection depending on the ambient temperature in the chamber. With all the equipment required, including that of argon gas recycling, the investment and operating cost is considerably higher than that of APS.

19.2.3.3 Vacuum Plasma Spraying

Vacuum plasma spraying (VPS) is similar to CAPS with the exception that the operation is carried out under sub-atmospheric pressures, in the range of tens of kPa ($5 > p_a > 70$ kPa). VPS is carried out in large vacuum chamber with volumes of a few m^3 up to 10–20 m^3, typically 1.5–2.5 m in diameter by 3–4 m long, which houses the substrate, often on a carousel holding more than one part to be coated, a DC plasma torch, and a robotic torch manipulator adequately protected for operation in a hot dusty atmosphere. The chamber is normally water-cooled with a large access door for ease of servicing, placing the parts to be coated on the carousel substrate holder and retrieving them at the end of the coating cycle. Torch operation is similar to that of APS torches, that is, with similar arc currents, plasma gas selections and flow rates, power levels, and powder flow rates. The torch-to-substrate distance is longer than normally used in APS, typically in the range of 250 and 500 mm. According to the plasma jet expansion, the mean ambient temperature in the chamber is over 200 °C. The noise level is similar to CAPS being essentially that of ambient fans, vacuum pumps, and power supply. The equipment is more complex and consequently is the most expensive of all spray processes, with the exception of ultra-low-pressure plasma spraying (ULPPS). One of the advantages of the process, besides the significant reduction in oxidation, is the possibility to remove the oxide layer from the substrate prior to the spraying operation using the plasma torch in a reversed-polarity-transferred arc mode. The part can also be preheated to a sufficiently high temperature to achieve diffusion bonding between the sprayed metal or alloy and substrate. This step can be carried out using the same transferred arc approach used in surface cleaning from oxides, in straight polarity with the part being then the anode of the transferred arc. VPS is by far one of the most expensive thermal spray installations that is mostly used for coating of high added-value parts, such as turbine blades.

19.2.3.4 Ultra-Low-Pressure Plasma Spraying

Ultra-low-pressure plasma spraying (ULPPS), also identified as very-low-pressure plasma spraying (VLPPS) or plasma spray physical vapor deposition (PS-PVD) and referred to by Oerlikon-Metco as low-pressure plasma spraying–thin film (LPPS®-TF), is a relatively new technology that bridges the gap between conventional VPS and physical vapor deposition (PVD) processes, in which the coating is formed through the deposition of the coating material from the

vapor phase at lower temperatures at relatively low deposition rates compared to VPS. ULPPS was developed in direct competition to (EB-PVD), for the production of ceramic TBC coatings with equivalent quality as (EB-PVD) technology, at considerably higher deposition rates and lower cost. The two technologies, ULPPS and (EB-PVD), differ essentially in the way the precursor is transformed into the vapor phase with ULPPS based on the in-flight heating and evaporation of the precursor in powder form using the plasma jet, while (EB-PVD) makes use of an electron beam for the precursor evaporation from a solid target or powder. This difference has a significant impact on their respective operating pressure and the deposition rates associated with each of the two technologies, with the ULPPS process operating at pressures <200 Pa with deposition rates in the range of μm/s, in contrast to the electron beam technology that required considerably lower operating pressures (<5 Pa), has lower deposition rates in the 0.1–100 μm/min range, and significantly higher investment cost.

19.2.3.5 Induction Plasma Spraying

Radio frequency induction plasma spraying (RF-IPS) is usually carried out under controlled atmosphere at atmospheric pressure, or soft vacuum conditions, down to 10 kPa. The process is essentially similar to DC-VPS with the exception that the torch is fixed with respect to the chamber walls, while the substrate has to be translated in a linear or rotating movement across the stream of molten droplets emerging from the torch at the required spraying distance. With torches i.d. in the range of 30–100 mm, against below 10 mm for DC ones, the velocity of the plasma jet is considerably lower (<100 m/s) than that of a corresponding DC plasma torch at a comparable power rating and chamber pressures. It allows spraying bigger particles (up to 200–250 μm) than those sprayed with DC torches. Typical plasma power ratings for radio frequency vacuum induction plasma spraying (RF-VIPS) installations are in the 50–200 kW range, with corresponding powder feed rates of 2–10 kg/h, depending on the sprayed material. Because of the radio frequency (RF) of the supplied power to the induction coil of the torch (mostly in the 1–5 MHz range), special precautions need to be implemented for the electromagnetic interference (EMI) shielding of the plasma torch from the rest of the process and control equipment. RF-IPS is mostly used for the spraying of metals and ceramics on small parts with a high added value and coating densities close to 98% of the theoretical value. Vacuum induction plasma spraying (VIPS) is used on an industrial production scale for the deposition of high-purity silica on fiber optics and refractory metals on X-ray targets. The technology is also extensively used for powder spheroidization and the synthesis of nanostructured or nanosized powders for a wide range of applications beyond the thermal spray industry.

19.2.4 Wire Arc Spraying

Wire arc spraying (WAS) is the oldest of thermal spray processes, which can be traced back to 1915 with the issuing of its first patents in the USA. It was only in the 1960s that the real potential of the technology was recognized, and its applications greatly expanded. WAS is essentially a plasma spray coating process based on the concept of melting the material to be sprayed in wire or cord form using an electric arc struck between the tips of two wires, or a wire and a non-consumable electrode, and atomizing the formed molten metal by a high-velocity gas stream, which projects the droplets toward the substrate. As with conventional thermal spraying, the molten droplets form splats that rapidly solidify on impact with the substrate surface building up the coating in successive layers. The process can be maintained in a continuous mode by electrically connecting the two wires to a DC power supply, and continuously feeding the wires in a closely controlled speed to compensate for the melting of their respective tips such as to maintain a constant gap between them, and consequently a constant arc voltage. A high-velocity gas flow injected between the two wires removes constantly formed molten material from the wire tips, breaks down the larger droplets into smaller ones in a secondary atomization process, and propels them toward the substrate. The maximum arc current can vary from 200 to 1500 A. With this process, the spray rates are between 5 and 30 kg/h, with deposition efficiency of about 80%, higher than most other spray processes. Consequently, it is one of the most economical processes, as long as the materials to be sprayed can be obtained in the form of wires or cored wires. The noise level is similar to that of wire flame process, which is in the range of 118–122 dBA. The oxide content depends strongly on the sprayed materials but is rather high, over 25 wt.% for Al, for example. Using nitrogen instead of air as atomizing gas can reduce the oxidation level in the deposit though, depending on the required gas flow rates (around 1.0 m^3/min or more), the process can become rather expensive. Porosity is usually over 10 vol.% and the coating adhesion is medium, in the 40 MPa range. As the atomizing gas is at room temperature, the process has the added advantage of minimal heating of the substrate during the spraying operation, while the divergence of the spray pattern is a disadvantage. Like other spray processes, it is noisy and dusty. Coatings can be used for abrasion and adhesion (friction) under low load, though their main use is for atmospheric or marine corrosion protection and a broad range of electrical applications.

19.2.5 Plasma-Transferred Arc Deposition

Plasma-transferred arc (PTA) deposition is a combination of welding and thermal spraying process that requires

electrically conductive substrates acting mostly as the anode. The feedstock is wires or powder form with particle sizes in 50–150 μm range. Metals, alloys, and cermets are sprayed using PTA techniques. The different guns are characterized by the maximum current varying from 200 to 600 A. The coating is different from those obtained from other thermal spray coating processes because the arc melts to some degree the substrate material, and the molten powder of the coating material is mixed with the molten substrate material. The consequence is that a good metallurgical bond or fusion bond is achieved, and that the porosity is very low; however, the heat penetration region, and in particular the region where the coating material is mixed with the substrate material, can change the properties of both the substrate and the coating. This mixing region is expressed in terms of the "dilution." Torches used are divided into three different categories according to the deposition rate and the power used: micro PTA with deposition rates of 0.1–2 kg/h, used for small components, or components with complex shapes; regular PTA for deposition rates of 2–10 kg/h; and high-power PTA for deposition rates between 10 and 20 kg/h. Coatings are thicker than those of other spray processes; they can be 10 mm thick or more and fused with a metallurgical bond to the substrate. The substrate must be kept as horizontal as possible during spraying. No porosity is observed, and the deposition efficiency is over 90%. The resistance to wear is excellent as well as that to high-temperature corrosion. These coatings are used to achieve high-quality rebuilding of worn surfaces, to coat large and heavy parts without cracks or deformation, and to produce smooth and highly wear-resistant surfaces. PTA coatings are mostly used against wear in different mining, pulp and paper, oil and gas, and power industries.

19.3 Thermally Sprayed Coating Applications

In this section, a review is presented of the principal applications of thermal spray coating technology. The objective is to provide typical examples of present and potential industrial applications of each of these technologies rather than presenting an exhaustive review of each of these topics. The reader must keep in mind, however, that the TS coatings can have mechanical, thermal, and service properties that are distinctly different from those of bulk ones. These depend on the real contacts between layered splats, porosities, crack types and distributions, oxide inclusions, and possible partial modification of the chemistry of the sprayed particles during the deposition process. Coating morphologies and microstructure are also linked to the spray process used, the properties of the sprayed particles, the spray parameters, the substrate used, the coating thickness, and the possible posttreatments of coatings.

19.3.1 Wear-Resistant Coatings

"Wear is the problem" and it occurs in almost all industries where thermally sprayed coatings are used. In all cases, it is a progressive loss of material at the active surface due to the relative movement of another part or particles on this surface. The life time of the coating depends on its resistance to wear and its thickness, which can reach up to 10 mm with PTA coatings. Examples of coatings are presented for the different types of wear described in the following according to American Welding Society (1985), Cartier (2003), Zhum Gahr (1987), Chattopadhyay (2001), Pawlowski (1995), Champagne (2007), and Sobolev et al. (2004).

19.3.1.1 Abrasive Wears

Abrasive wear (AW) corresponds to weight loss with grooves, pits, and scores at the surface due to cutting or deformation, which results from:

- *Two-body abrasion*, where asperities or defects of one of the surface plough or abrade the counter-face.
- *Three-body abrasion*, where hard particles move freely between both surfaces, or are imbedded in one of them.

The phenomena are promoted when temperature, humidity, and aggressiveness of the environment (corrosion) increase. The three-body abrasion depends also on the shape, grain size, and hardness of the abrasive particles and the relative speed of the two bodies.

As a general rule, abrasion increases significantly as soon as the hardness of one metal or alloy becomes equal to that of the abrasive particles. If the abrasive particle belongs to the surrounding medium, the contact must be protected from it and wear debris must be removed or trapped. The roughness of the harder surface must also be reduced to the minimum. It must be emphasized that abrasion wear represents more than 50% of wear. In most cases, wear-resistant coatings are hard with a good resistance to heat and chemical attack. In the following, examples are given of materials commonly used for abrasive wear resistance coatings [American Welding Society (1985)].

Self-Fluxing Alloys

Self-fluxing alloys have generally excellent corrosion resistance. Due to their hardness, not being particularly high, they cannot compete with cermets for sliding wear resistance unless they are either *heat-treated* or sprayed with *hard particles*.

The effect of heat treatment on the wear resistance of self-fluxing alloys was investigated by Bolelli and Lusvarghi (2006) for HVOF-sprayed Co-28%, Mo-17%, and Cr-3% Si coatings. Comparing the as-sprayed coatings with those heat-treated at 200, 400, and 600 °C for 1 h, significant degree of

splat boundary oxidation was observed in the as-sprayed coating, because of exothermic oxidative reaction occurring at $T > 810$ °C. The as-sprayed coating had low hardness and toughness, resulting in poor tribological performance. Post-treatment at 600 °C caused the appearance of submicrometric crystalline regions improving hardness and elastic modulus and the sliding wear performance at room temperature was improved. Sakata et al. (2007) flame sprayed Co-based (Co–Cr–W–B–Si) self-fluxing alloy coating on steel substrate followed by a diffusion treatment at 1370–1450 K for 10–100 min under Ar atmosphere. Two types of fine compounds were precipitated in Co-based matrix: a chromium boride dissolving cobalt, and a tungsten boride containing cobalt and chromium. The size of each precipitate became larger with increasing treatment temperature and time. A coating with the proper size borides showed a superior wear resistance with substantially improved abrasion resistance.

The effect of mixing hard metal particles with the self-fluxing alloy during the spraying process on the wear resistance property of the coating was tested by Kulu and Hailing (1998) who flame sprayed NiCrSiB self-fluxing alloy-base composite powders, containing 15–50 wt.% WC–Co hard metal powders. They compared the coating obtained with D-gun-sprayed WC–Co particles. The wear resistance to abrasive particles at *small impact angles* increased with the increase in the hardness of the matrix phase, and the increase in hard phase content in the composite. However, at *straight impact angles* the wear resistance remained relatively low. Further study by Kulu and Pihl (2002) showed for the spraying of self-fluxing alloys, containing tungsten carbide-based hard metal particles (NiCrSiB-[WC-Co]), using the HVOF JP 5000 that a good resistance to oblique and normal impact can be obtained provided the coatings have the following properties: minimum porosity (less than 3 vol.%), hardness higher than that of the abrasive, and a metal matrix structure containing particles of WC–Co granules, or WC–Co particles.

Cermet Coatings

Coating quality is strongly linked to the spray process and parameters, especially with WC particles. If corrosion problems are also to be considered, Cr is important in the metal matrix. For example, Schwetzke and Kreye (1999) have sprayed different WC–Co and WC–Co–Cr powders with various HVOF spray systems such as Jet Kote, Top Gun, Diamond Jet (DJ) Standard, DJ-2600, DJ-2700, JP-5000, and Top Gun-K. Powders exhibited various degrees of phase transformation during the spray process depending on type of powder, spray system, and spray parameters. Phase transformations increased when the injection of the powder occurred in a region where the flame temperature was highest, for example, into the combustion chamber of the Top Gun system. Decarburization of agglomerated and sintered WC–Co 83–17 powder ranged from 25 to 70% for the various spray systems and fuels. When the carbon loss remained below 60%, the properties of the coatings such as hardness and wear resistance were not significantly influenced. The decarburization seemed to be compensated by the hardening with the formation of a solid solution of cobalt (tungsten, carbon) and hard W_2C and h-phases. While the wear resistance of WC–Co–Cr coatings were comparable to those of WC–Co, the corrosion resistance of WC–Co–Cr was considerably higher.

Kasparova et al. (2011) have evaluated the abrasive wear resistance and adhesive strength of HVOF-sprayed WC–Co and the Cr_3C_2–NiCr coatings. They found that high-stress abrasive conditions change the coating behavior very significantly, particularly that of the Cr_3C_2–NiCr coating. The high plastic deformation and pulling out of entire splats or splat blocks, especially during abrading by the alumina sand, were detected under the high-stress abrasive conditions for both coatings, but much more with Cr_3C_2–NiCr. As pointed out by Houdkova et al. (2010), the spraying angle is one of the deposition parameters that influences the quality of thermally sprayed coatings. They HVOF (TAFA JP-5000) sprayed WC–Co and Cr_3C_2–NiCr coatings with different spray angles. Their results showed that the wear resistance of the coating was not affected up to 30° angle diversion from the normal spray direction for WC–Co, and 15° angle diversion for Cr_3C_2–NiCr coatings. Tillmann et al. (2010) used statistical design of experiments to identify the most relevant factors influencing the HVOF spraying of fine $75Cr_3C_2$–25(Ni20Cr) powders and to find an optimum setting of these factors to produce coatings with improved morphological and mechanical properties. Fine structured coatings obtained showed an extremely dense and finely dispersed structure (porosity < 2 vol.%), a high surface quality (Ra < 2 μm), and a high adhesive strength. These coatings showed a high potential to be used as wear-resistant coatings for large tools without any posttreatment or surface finish.

Considerable emphasis has been placed recently on HVOF thermal spraying of nanostructured WC/Co to achieve high hardness combined with excellent wear resistance. However, it appeared difficult to achieve dense coatings and avoid decarburization. Skandan et al. (2000) have HVOF sprayed homogeneously mixed powders. These consisted of WC/12 Co agglomerates in the range 15–40 μm with a carbide grain size of 2–5 μm (70 vol.% of the mixture) and WC/5 Co, forming particles in the range 0.1–0.5 μm with each particle composed of many WC nanometer-sized crystals (~30 nm in diameter). The coating was dense and had no decarburized phases. The abrasion wear resistance was at least 50% better than that of a pure coarse-grained WC/Co coating. In their review, Lima and Marple (2007) presented superior abrasion and sliding wear

performance of nanostructured ceramic coatings (Al_2O_3, Al_2O_3–13 wt.% TiO_2, Al_2O_3–3 wt.% TiO_2, TiO_2, and YSZ) when compared to those of conventional coatings. By employing HVOF and nanosized ceramics, the abrasion wear levels could be reduced by up to 90% in comparison with the wear performance of optimized APS conventional ceramic coatings. It was generally observed that the nanostructured coatings were not harder than the conventional ones; however, they tended to be much tougher. Kim and Walker (2007) have developed nanostructured titania coating specifically for ball valves destined for high-pressure acid-leach (HPAL) service. These coatings were compared to conventional ones. The nanostructured titania coating provided significantly superior resistance against abrasive and erosive wear—the better wear performance attributed to improved toughness.

Gawne et al. (2001) have plasma sprayed ball-milled mixture of glass and alumina powders to produce alumina–glass composite coatings. The alumina raised the mean hardness from 300 Vickers hardness (HV) for pure glass coatings to 900 HV for a 60 wt.% alumina–glass composite coating. The scratch resistance increased by a factor of 3 and the wear resistance by a factor of 5, and maximum value obtained with 40–50 vol.% alumina. This alumina content corresponded to the changeover from a glass matrix to an alumina matrix. Cipri et al. (2007) produced thick aluminosilicate coatings by plasma spray technique. Coatings, efficiently coupling to metallic substrates even after plastic deformation, exhibited very interesting performance in terms of mechanical properties and fracture toughness (elastic modulus of 43 GPa and K_{1c} of about 2 MPa $m^{1/2}$ for 850 μm thick coatings) and compliance. Excellent refractory behavior allows a wide use of such coatings, as wear-resistant thermal barrier coatings (TBCs) in metallurgical and glass plants and in high-temperature heat exchangers. To illustrate the interest of such coatings, Kang et al. (2012) used detonation-gun to spray three different WC–Co–Cr, Cr_3C_2–NiCr, and Stellite-21 coatings on high-tensile steel rotavator blades. The wear rates of Cr_3C_2–NiCr and Stellite-21 coated blades showed significant superiority over the uncoated blade, but not as much as that obtained by WC–Co–Cr coated blades.

19.3.1.2 Erosive Wear

Erosive wear (EW) occurs when hard particles carried by a fluid hit the surface. The impact angle plays an important role on the wear rate depending on the nature of the surface material; ductile, hard metal, ceramic [Zhum Gahr KH (1987), Chattopadhyay R (2001)]. To reduce the wear, one must choose a coating material harder than the abrasive particles, with toughness high enough, especially for impact angles between 30 and 45°, which must be avoided if possible. It is also important to avoid turbulences in service conditions because they increase erosion and reduce coating roughness to a minimum.

Erosion wear is much more complex than abrasive wear in which the wear resistance is predominantly influenced by the hardness of the coatings. The erosion wear resistance depends on the response of coatings to the impact of erosive particles at high velocity. It is usually considered that erosion wear of cermet coatings is predominately influenced by their microstructures including the splat size, carbide particle size, carbide content, and its distribution within a splat, as well as cohesion between the splats [Kim HJ, et al. (1994), Wang BQ, Luer K (1994)].

Kim et al. (1994) showed that inter-splat cohesive strength of coatings, measured by a simple bonding test, was the most significant factor relating to the wear rate of plasma-sprayed WC-12 wt.% Co coatings. As previously emphasized, the microstructure strongly depended on starting powder, spray system, and spray conditions. Other parameters, such as the influence of time, solid loading, impingement angle, temperature, particle velocity, as well as the erosion–corrosion (E-C) mechanism, must also be considered [Kenichi S, et al. (2005)]. When comparing the influence of dry and slurry erosion on HVOF coatings, it was shown that erosion rates in dry particle impact were about three orders of magnitude higher than those in slurry systems. This difference probably reflects the real erodent target impact velocities, which are mitigated in the slurry test by the water medium [Hawthorne HM, et al. (1999)]. A few examples are presented below.

Ji et al. (2007) HVOF sprayed Cr_3C_2–NiCr coatings and erosion tests were performed at different jet angles of abrasive particles. The erosion occurred dominantly by spalling of splats from the lamellar interfaces, spalling resulting from the propagation of cracks parallel to the interfaces between the lamellae exposed at the surface and underlying coating. The carbide particle size and content in the coating influenced significantly the erosion performance of Cr_3C_2–NiCr coatings. Yang et al. (2008) compared the high-temperature erosion behavior of HVOF-sprayed Cr_3C_2–NiCr coating with that of mild steel for circulating fluidized-bed boiler tubes. The erosion rate of the HVOF-sprayed Cr_3C_2–NiCr coating was not influenced by the temperature in the range of 300–800 °C, while for mild steel at 800 °C the erosion rate was four times that at 300 °C at an erosion angle of 30°.

Osawa et al. (2005) have shown for WC–Co HVOF-sprayed coatings that the substrate also played a role in coating erosion resistance. For the studied variety of steel substrates, the near-surface hardness of the substrate resulting from the work hardening caused by peening during the grit blasting and HVOF spraying played a dominant role. It improved the ability of the substrate to support the coating and thus the integrated coating–substrate performance during impact loading. Kulu et al. (2005) sprayed, by D-gun, HVOF

JP-5000 spraying, and spray fusion processes, tungsten carbide-based hard metal, nickel-based self-fluxing alloy, and composites NiCrSiB. For all of them the erosion was strongly affected by particle impact angle. The erosion rate was five to six times higher at elevated temperature for all materials tested, while in that case, the influence of impact angle had no great effect.

Ramesha et al. (2011) plasma sprayed Inconel-718 (thicknesses of 200 μm and 250 μm) on mild steel. Increased coating thickness decreased the porosity and increased the hardness significantly. Inconel-718 coatings exhibited improved slurry (containing 3.5 vol.% NaCl) erosive wear resistance when compared to uncoated mild steel. The wear resistance also increased with coating thickness. Higuera Hidalgo et al. (2001a, b) compared the behavior of plasma- and flame-sprayed modified nickel–chromium alloy (with small aluminum and titanium additions) subjected to the action of simulated post-combustion gases from a coal-fired boiler combustor. With flame, the adherence was much lower even with a bond coat. High-temperature oxidation rate of nickel–chromium coatings in post-combustion gases from coal-fired boilers (atmospheres with 3–3.5 vol.% of free oxygen) was low. The embedment of fly ash particles on the surface of coatings was especially important at higher temperatures (800 °C). The erosion behavior of nickel-chromium flame and plasma-sprayed coatings at medium temperatures (500 °C) was characterized by low erosion rates and a ductile erosion mechanism. At 800 °C the wear was essentially corrosive.

Krishnamurthy et al. (2012) studied the erosion resistance of plasma-sprayed alumina and calcia-stabilized zirconia coatings on Al-6061 substrate. It was found that erosion of coating systems occurred through spalling of lamella exposed on coating surface resulting from cracking along the lamellar interface. Erosion wear was more at 45° angle of impact. Pores seemed to act as stress concentrators and decreased the load-bearing surface.

The promising behavior of unconventional nanoscale composite coatings must be underlined. Branagan et al. (2005)] have wire arc sprayed (WAS) amorphous SHS-7170. Coatings were found to develop an amorphous matrix structure containing starburst-shaped boride and carbide crystallites with sizes ranging from 60 to 140 nm. The performance of the SHS-7170 coatings in boiler environments was measured via elevated temperature erosion experiments conducted at 300, 450, and 600 °C using bed ash from a circulating fluidized-bed combustor (FBC) boiler, and the results were compared with those for existing boiler coatings. The elevated temperature erosion resistance of the SHS-7170 wire arc coatings was found to be superior, based on thickness loss, compared with the existing wire arc coatings that have been tested. SHS-7170 coatings have resisted to erosion almost independently of contact angle.

19.3.1.3 Friction and Adhesive Wear

Friction and adhesive wear occur when particles are transferred from one interacting surface to the other. When different materials are in contact, particles are mainly transferred from the softer or weaker material onto the harder one. This type of wear is promoted by the increase in the load and/or the temperature, under dry friction or poor lubrication. It depends on the structure, composition, hardness, and melting temperature of the material.

To reduce it, dry friction must be avoided and, if not possible, coatings containing solid lubricants or retaining lubricants must be used. The compatibility of materials is also important since the friction coefficient, f, defined by Eq. 19.1, depends on the couple of materials rubbing against each other.

$$f = \frac{T}{N} \tag{19.1}$$

Where,

T tangential force
N normal force

The friction coefficient is also linked to the load, P (or more precisely the pressure, p), and the relative velocity, v, between both parts (in principle the product, $p \cdot v$, must be below 1 MPa m/s) [Cartier M (2003)]. The roughness of surfaces in contact must also be as low as possible and from a rough surface (Ra of a few μm) to a smooth one (Ra < 0.1 μm), f, can be reduced by 60%.

Dry friction usually results in high local heating and, even with a very low relative velocity, the friction coefficient, f, increases with temperature. Low friction coefficients can be achieved with solid lubricants ($f = 0.001$–0.05), but the relative velocity must be low. Using materials with a high thermal conductivity (both coating and substrate) reduces the heating due to friction. As wear increases with the energy of adhesion, it is also important to avoid micro welding, that is, to use materials with a low solubility and a narrow range of solid solution (e.g., Fe/Al, Fe/Cu). The work of adhesion decreases with the following couples: metal–metal, metal–ceramic, ceramic–ceramic, metal–polymer, ceramic–polymer, and polymer–polymer. A few examples are presented in the following.

High stress, due to too high average pressure or very high local pressure that exceed the elastic limit, might be favorable when it strengthens the material by work hardening, but it might result in surface embrittlement of surface layers reducing their fatigue strength. It is promoted by an increase in the friction coefficient or temperature. Here again the worst occurs when cracks propagate.

Ceramic Materials

Pantelis et al. (2000) plasma sprayed a 450 μm thick Al_2O_3 coating deposited on cast iron substrate. Wear tests were carried out with normal force varying from 50 to 160 N, sliding speed of 1.40 m/s, and average relative humidity of 60%, using as a counter-body a quenched D-2 tool steel (D-type tool steels contain between 10% and 18% chromium; D-2 steel is very wear resistant but not as tough as lower alloyed steels). The coating wear rate presented three stages.

- During the first one, the wear rate was decreasing rapidly, and the wear of the coating proceeded via adhesion mechanism.
- During the second stage, wear rate remained almost constant and the wear of the coating was taking place via a combined "polishing/abrasion/fatigue" wear mechanism.
- During the third and last stage, wear rate increased rapidly due to the "easy" removal of the remaining completely cracked ceramic coating.

Sanchez et al. (2008) plasma sprayed Al_2O_3–13 wt.%TiO_2 coatings on stainless steel substrates from conventional and agglomerated nanostructured powders. The wear resistance of conventional coatings was shown to be lower than that of nanostructured coatings. As already emphasized in Chap. 16, Nanocrystalline and Nanostructured Coatings, Darut et al. (2008) found that the friction coefficient of Al_2O_3 suspension plasma sprayed (SPS) coatings decreased by a factor of 2 and wear rates were 30 times lower for SPS layers compared to coatings obtained with micrometer-sized particles.

Bolelli et al. (2009a, b) HVOF sprayed alumina suspensions and compared them to coatings obtained with conventional powders sprayed with APS and HVOF. With the suspension, porosity is much lower, and pores are smaller than in conventional coatings. Moreover, few inter- or intralamellar cracks exist, resulting in reduced pore interconnectivity (evaluated by electrochemical impedance spectroscopy [EIS]). Such strong interlamellar cohesion favors much better dry sliding wear resistance at room temperature and at 400 °C.

Ahn and Kwon (1999) studied the tribological behavior of plasma-sprayed chromium oxide coatings against cast iron both in dry, at 450 °C, and lubricated wear tests at room temperature and 200 °C. Under dry sliding conditions, dispersed smooth surface films were formed by plastic deformation of compacted debris particles that adhered to the surface and these films strongly influenced the friction coefficient and wear rate of the coating. Considerable quantity of CrO_3 was detected at room temperature, whereas CrO_2 (more favorable than CrO_3 in reducing friction) was detected at 450 °C. Under lubricated sliding conditions, tribo-chemical reaction films of different species of carbon–oxygen bond units were formed depending on the test temperature and they appeared to be effective in reducing friction and preventing wear. Pratap Singh et al. (2011) studied the tribological behaviors of plasma-sprayed conventional and nanostructured (agglomerated nanoparticles) Cr_2O_3–3% TiO_2 ceramic coatings. Samples coated with nanostructured powder exhibited better properties such as higher hardness and less porosity as compared to conventional powder-coated samples. Dry sliding wear resistance of nanostructured powder under 60 N load was better than the wear resistance offered by conventional powder under 50 and 60 N load for similar testing conditions. In general, nanostructured powder exhibits a better wear resistance than conventional powder.

Tao et al. (2010) deposited Al_2O_3 and Cr_2O_3 coatings on stainless steel by atmospheric plasma spraying and tested their dry sliding tribological properties against copper alloy using a block-on-ring configuration at room temperature. The wear resistance of Al_2O_3 coating was superior to that of the Cr_2O_3 coating under these conditions. This was mainly attributed to the better thermal conductivity of Al_2O_3 coating (about 2.8 W/m K for alumina against 2.4 for chromia at 400 °C), which was considered to effectively facilitate the dissipation of tribological heat and alleviate the reduction of hardness due to the accumulated tribological heat. Bolelli et al. (2006a, b, c) plasma sprayed ceramic coatings (Al_2O_3, Al_2O_3–13 wt.% TiO_2, Cr_2O_3) and tested them through pin-on-disk and dry sand–steel wheel tests. The toughest coating (Al_2O_3) displayed the highest wear resistance, which in fact overcame HVOF-sprayed cermets and Cr electroplating, when a low number of wheel revolutions was considered. Against the alumina ball, Al_2O_3 and Al_2O_3–TiO_2 coatings showed high wear rates and friction coefficients (due to chemical affinity), while Cr_2O_3 had better wear resistance, lower friction coefficient, and inflicted less wear on the counterpart. Cr_2O_3 wear scar consisted in plastically deformed splats and debris forming a quite adherent protective tribo-film. In pin-on-disk tests, no coating underwent wear loss against the 100Cr6 ball that possessed lower hardness. Ramachandran et al. (2012) studied the friction and wear behaviors of yttria-stabilized zirconia (YSZ) coatings, lanthanum zirconate (LZ) coatings, and Inconel-738 Base Material (BM) sliding under unlubricated conditions, against a sintered tungsten carbide surface in a pin-on-disk configuration. They found that the wear resistance of the ceramic coatings got deteriorated with the increase in the percentage volume of porosity.

Cermets

Dallaire (2001) studied a cored wire, referred to as Alpha 1800, developed to produce tailored arc-sprayed coatings that were tough enough to resist particle impacts at 90° and sufficiently hard to deflect eroding particles at low-impact angles. Results showed that coatings produced with the new cored wire are at least five times more erosion resistant and

ten times more abrasion resistant than coatings produced by arc spraying commercial cored wires.

Yang et al. (2006a, b) sprayed by an HVOF system three-agglomerated WC-12 wt.% Co powders with different carbide grain size distributions. Dry sliding friction and wear behavior of the WC-12 wt.% Co coatings were investigated using sintered alumina (Al_2O_3) as the mating material at 200 °C, 300 °C, and 400 °C. The specific wear rate of the coatings increased when increasing the carbide grain size at a given testing temperature. It decreased when increasing the temperature for a given carbide grain size. The specific wear rate was reduced by more than one order of magnitude when the test temperature was increased from room temperature to 400 °C. The tribo-film formed at higher temperature was denser and more adhesive to the underlying surface, thus providing more surface protection against wear. The results showed that the formation of dense and well-adhered tribo-films played an important role in the low sliding wear rate of the coatings at elevated temperatures.

Yandouzi et al. (2012) sprayed by pulsed gas dynamic spraying (PGDS) process both cryo-milled particles made of an Al matrix reinforced with B_4C powders (Al-5356 + 20% B_4C) and conventional composite. The presence of homogeneously distributed fine B_4C reinforcement particles embedded within the nanostructured Al-5356 matrix significantly improved the dry sliding wear resistance of the coating. Li et al. (2008) cold sprayed dense Al5356/TiN composites with TiN particles uniformly dispersed in the matrix (50 wt.% TiN). The coating porosity was less than 1 vol.%. The deposited composite coating presented an excellent performance compared to that of the composite sprayed without using the ball-milled powder.

Qiao et al. (2001) studied the resistance to abrasive and unlubricated sliding wear of 40 WC/Co coatings applied by HVOF, high-energy plasma spray (HEPS), and high-velocity plasma spray (HVPS), using commercial and nanostructured experimental powders. Phase analysis by X-ray diffraction (XRD) revealed various amounts of decarburization in the coatings, some of which contained WC, W_2C, W, and h-phase. The wear resistance was lowered by decarburization, which produced a hard but brittle phase.

Jacobs et al. (1999) investigated the microstructural properties of WC–Co–Cr and WC–Co coatings deposited by HVOF and HVAF processes. The HVAF-sprayed coatings showed better sliding wear resistance compared to the HVOF coatings. The prime wear mechanism in the WC–Co HVAF coatings was adhesive wear; the lubricious cobalt matrix resulted in very low wear rates and low debris generation. The WC–Co–Cr HVOF coating wear was linked to "pullouts" that became trapped in the contact zone and acted as a third-body abrasive. The HVAF/WC–Co–Cr coatings exhibited better resistance.

Bolelli et al. (2012a, b) studied the tribological performance of two Colferoloy Fe–Cr–Ni–Si–B–C coatings HVOF sprayed and they compared them to other coatings. Under sliding wear conditions, these coatings were a good alternative to Ni-based alloy coatings, but they could not replace Cr_3C_2–NiCr cermets (best sliding wear). These coatings were unsuitable for dry particle abrasion conditions. At 400 °C, all coatings were softened, and their sliding wear behavior was dominated by more severe abrasive grooving and all differences were reduced.

Alam et al. (2001) studied the tribological characteristics of low-pressure plasma spraying (LPPS) aluminum bronze coatings against steel ball. Under optimum operating conditions, the test samples exhibited a dense microstructure with high hardness, low coefficient of friction, and high wear resistance.

Ouyang et al. (2001) studied the tribological properties of VPS ZrO_2–CaF_2–Ag_2O composite coating (ZFA). At 300–700 °C, the ZFA coating exhibited lower friction and wear than at room temperature, 200 °C, or 800 °C. Ag_2O and CaF_2 acted as solid lubricants effectively at 300–400 °C and 600–700 °C, respectively. But with the increase in temperature up to 800 °C, the severe adhesive sliding caused more material transfer and tearing out of coating, and finally led to a high friction and wear.

Metals

Ahn et al. (2005) studied the wear resistance, on a low-carbon steel substrate, of plasma-sprayed molybdenum blend coatings consisting of powders of bronze and aluminum–silicon alloy powders mixed with molybdenum. The wear test results revealed that the wear rate of all coatings increased with rising wear load and that the blended coatings had better wear resistance than the pure molybdenum coatings, although its hardness was lower. The molybdenum coating blended with bronze and aluminum–silicon alloy powders exhibited excellent wear resistance because hard phases such as $CuAl_2$ and Cu_9Al_4 formed inside the coating.

Bolelli et al. (2012a, b) studied the tribological performance of two Fe–Cr–Ni–Si–B–C (Colferoloy) alloy coatings manufactured by HVOF thermal spraying, through rubber-wheel dry particle abrasion test and ball-on-disk sliding wear tests. Colferoloy coatings were validated as alternatives to Ni-based alloys and electroplated chromium under sliding wear conditions but appeared unsuitable for particle abrasion resistance. The different sliding wear behaviors of HVOF-sprayed coatings were explained by coupling micro- and nano-hardness to scratch testing, which reflected cracking resistance and plastic deformability.

Rodriguez et al. (2003) compared NiCrBSi alloys sprayed by either plasma or flame but then fused for the latter. Four sets of specimens were tested varying the composition (with

the presence or not of WC in the powders). Coatings were tested in a reciprocating pin on plate wear machine able to select loads ranging from 50 to 200 N and temperatures up to 500 °C. NiCrBSi alloys, deposited by thermal spray techniques, maintained their wear-resistant performances up to bulk temperatures of 500 °C. The alloys deposited by flame spraying with fusion had better wear resistance than those deposited by plasma spraying. The presence of tungsten carbide in the powders was not a beneficial factor on the wear performance of thermally sprayed NiCrBSi coatings. PTA is used to increase wear resistance mainly in steel industry.

Polymers

At low temperatures polymers can be used against friction. Niebuhr and Scholl (2005) sprayed with high-energy plasma polymer–steel coatings for high-contact pressure rolling/sliding systems. Polymers were applied as a thin film (75–100 μm) over a thicker (250–750 μm) steel coating. Twin roller rolling/sliding tests were performed at 5 and 35% creep and contact loads of 1700 N on a 5 mm contact face. A lower coefficient of friction (0.10–0.15) with increased durability compared with that of AISI-1080 steel thermally sprayed coating (coefficient of friction of 0.46) was observed under these rolling–sliding contact conditions.

Li et al. (2002) deposited, using the flame spray process, poly-ether-ether-ketone (PEEK) coatings with three kinds of crystallinities. Investigations were performed under dry sliding conditions against a 100C6 counter-body. The average friction coefficients appeared to decrease while increasing the sliding velocity but were insensitive to the applied load in the range of investigation. The higher was the crystallinity of the coating, the lower was its average friction coefficient. The wear mechanisms of the different coatings were explained in terms of plastic deformation, plough marks, and fatigue tearing.

Li et al. (2007) flame sprayed polyamide1010 (PA-1010) and its composite with nanometer-sized silica (PA-1010/n-SiO_2). The dry friction and wear behaviors of both coatings were investigated under dry sliding conditions. The results showed that the addition of nanometer-sized silica increased the crystallinity of the coatings and reduced friction and wear compared to pure PA-1010. The nano-composite coatings, containing 1.5 wt.% nanosized silica, displayed better properties.

19.3.1.4 Cavitation Wear

Cavitation wear characterized by the formation of pits and pores occurs when the velocity difference between the liquid and solid surfaces is important. They result from sudden variations of pressure in the fluid leading to the creation of shock waves due to implosion combined with fatigue phenomenon. Cavitation wear can be significantly reduced or eliminated by simply redesigning the solid surface profiles and reducing low-pressure areas. Surface polishing is also very important since a low Ra can reduce the wear by a factor of 5. Alternately, the use of high-toughness alloys with a good resistance to micro-crack formation is essential.

Wire arc spraying (WAS) has been extensively used against cavitation with results depending on surface hardness and internal coherency of the coating. According to Kim and Lee (2010), among ten different coating materials tested, stainless steel with the highest hardness showed the best performance against the cavitation erosion. With Al-based coatings, the addition of silicon to the alloy (12 wt.% Si) improved both the hardness and bond strength, resulting in significant improvement in cavitation erosion resistance by almost 40 times. Unfortunately, the addition of Si to Al-based coatings caused surface pitting similar to those of Zn-based coatings. In both the Cu- and Fe-based coatings, interfacial oxidation occurred in between the coating and steel substrate.

Hahn and Fischer (2010) tested the cavitation resistance of WAS- and HVOF-sprayed $FeC_{0.8}$ coating, and $FeCr_{19}C_{0.1}B_{1.6}$ coating deposited by plasma-transferred arc (PTA) fed with wire. They showed that for all coatings the weight loss immediately starts with the beginning of the test. The major acting wear mechanism within cavitation was surface fatigue with splat delamination and crack propagation along splat interfaces, the worst being when coating had a very low ductility. Kumar et al. (2005) reported that out of 21 different TS coatings, HVOF-sprayed coatings generally exhibited lower cavitation wear rates than plasma-sprayed coatings. The lowest cavitation rate was for TS Stellite-6 coating, which had a cavitation erosion rate of 11.7 mg/h. The results, however, were still considerably higher than that obtained with weld deposited 308 stainless steel, which was 3.2 mg/h. In contrast, slurry erosion wear testing showed that the volume loss for Stellite-6 coatings was 5.33 mm^3/h, which was considerably lower than the volume loss of 11.17 mm^3/h reported for 304 stainless steel.

Factor and Roman (2002) have subjected a selection of WC–Co and Cr_3C_2–25% NiCr coatings produced by PS and HVOF deposition techniques to various wear tests designed to simulate abrasion, cavitation, sliding, and particle erosion type wear mechanisms. Cr_3C_2–25 wt.% NiCr outperforms the WC–Co samples, and it appeared that the WC–12 wt.% Co sample performed better than the WC–17 wt.% Co samples. For all samples the wear loss mechanism was clearly that of the delamination of flakes of material. With WC–Co samples, corrosion mechanisms played an important role, possibly through enhanced corrosion resulting from the cavitation mechanisms causing pit corrosion or similar behavior. Wu et al. (2012a, b) studied a WC–Co–Cr coating deposited by HVOF onto a $CrNi_{18}Ti_9$ stainless steel substrate to increase its cavitation erosion resistance. The microstructural analysis of the coating after the cavitation

erosion tests indicated that most of the corruptions took place at the interface between the unmolten or half-melted particles and the Co–Cr matrix, the edge of the pores in the coating, and the boundary of the twin and the grain in the stainless steel $CrNi_{18}Ti_9$.

Santa et al. (2009) studied the slurry and cavitation erosion resistance of six thermal spray coatings and compared them to that of an uncoated martensitic stainless steel. The results showed that the slurry erosion resistance of the steel could be improved by up to 16 times through the application of the thermally sprayed coatings. On the other hand, none of the coated specimens showed better cavitation resistance than the uncoated steel in the experiments.

Lima et al. (2004) deposited the following four different coatings onto an AISI- 1020 steel substrate:

- WC–12%Co
- As-sprayed (AS) 50%WC–12%Co + 50%NiCr
- Post-melted (PM) 50%WC–12%Co + 50%NiCr
- A duplex system comprising WC–12%Co top layer and NiCrAl interlayer

The worst performance in cavitation erosion tests was observed for the WC–12%Co coating, which showed the highest mass loss throughout the test. Conversely, the PM 50%WC–12%Co + 50%NiCr coating exhibited the best cavitation resistance and a correlation between coating toughness and cavitation resistance could be established.

Ding et al. (2011) reported that for conventional, submicron, and multimodal WC–12Co cermet HVOF-deposited coatings, the multimodal WC–12Co coating exhibited the best cavitation erosion resistance among the three coatings tested. The erosion rate was approximately 40% that of the conventional coating, and the cavitation erosion resistance of multimodal WC–12Co coating was enhanced by >150% in comparison with the conventional coating. Dense nanostructure, high microhardness, and strong cohesive strength of WC–12Co coating contributed to the increase in the cavitation erosion performance of multimodal WC–12Co coating.

19.3.1.5 Fatigue Wear

Fatigue wear (FW) is a form of material wear that can result from either surface fatigue, thermal fatigue, or thermal chock fatigue. In the following, highlights of these different fatigue-wear mechanisms are discussed identifying their main features, probable causes, and the role thermal spray coating can play to control them.

Surface Fatigue Wear

Surface fatigue wear (SFW) results in the development of surface defects such as pits and pores that can extend to depths of several tenths of millimeters due to cyclic loading contacts, with stresses induced by rolling, shocks, or sliding in a lubricated regime. They depend on material properties such as structure, cohesion, elastic limit, toughness, and residual stresses. If tangential stress is predominant, fatigue will start in the "skin" while if shear stress is more important, fatigue will occur essentially in the subsurface. The worst SFW occurs when cracks propagate. The best materials to limit SFW are hard ones with a high toughness with smooth surfaces with no irregularities where cracks are initiated.

Stewart and Ahmed (2002) made, in 2002, an extensive review of the thermally sprayed coatings used in rolling contact fatigue (RCF). The following coatings were applied to steel substrate using different thermal spray technologies:

- WC–12%Co, WC–17%Co, and WC–10%Co–4%Cr were sprayed using APS or HVOF
- NiBSiCrFeC, Al_2O_3–TiO_2, Cr_2O_3–SiO_2–TiO_2, and Mo were sprayed by APS
- WC–Co and WC–Cr–Ni were sprayed by HVOF
- WC–12%Co, WC–15%Co, and Al_2O_3 were sprayed by D-gun

The HVOF-deposited coatings presented superior RCF performance, probably because of their dense microstructure and high cohesive strength combined with a minimum number of detrimental brittle phases. Cermet coatings displayed superior RCF performance followed by ceramic and metallic coating, respectively. Thermal and mechanical mismatch between the coating and the substrate influenced the RCF performance of the coating through the control of the degree of compressive residual stress. Coatings thicker than 200 μm displayed superior RCF performance over thinner ones.

Ahmed and Hadfield (2002) studied cermet (WC–Co) and ceramic (Al_2O_3) coatings deposited by D-gun, HVOF, and high-velocity plasma-spraying techniques, in a range of coating thicknesses (20–250 μm) on various steel substrates to deliver an overview of the various competing failure modes in rolling/sliding contact. Four modes of fatigue failure, competing during fatigue failure and that can be combined, were identified: abrasion, delamination, bulk deformation, and spalling. The authors concluded that *abrasion* can be controlled by appropriate selection of contacting pair and lubrication conditions while *delamination* and *catastrophic* failure mode can be avoided by appropriate selection of coating thickness and fracture toughness. Controlling the hardness of substrate and also increasing the coating thickness can avoid bulk failure. Coating failures were attributed to micro- and macro-cracking of either the coating material or the coating–substrate interface, which also resulted in the attenuation of compressive residual stress.

Savarimuthu et al. (2001) studied the possible replacement of chromium electroplating with WC–Co-sprayed coatings for commercial aircraft applications. Decarburization, volume percent and distribution of hard particles, and porosity

might more strongly influence wear behavior than residual stresses. Zhang et al. (2008) addressed the fatigue behavior and failure mechanisms of plasma-sprayed CrC–NiCr cermet coatings in rolling contact. As emphasized previously, failure modes of coatings could be classified into four main categories, that is, surface abrasion, spalling, and delamination within the coating, and at the coating/substrate interface. The interfacial delamination was the main failure mode of the coatings at high contact stress. The failure mechanisms of coatings were associated with the microstructures and the bonding strengths of coatings, the depths of the orthogonal shear stress, and the maximum shear stress.

Berger et al. (2011) studied the dependence on substrate hardness of the rolling contact fatigue of HVOF-sprayed WC–17%Co coatings used for gears and other components with high load-bearing capacity. The durability of HVOF-sprayed WC–17 wt.% Co coatings under rolling contact fatigue loading was significantly improved through the use of substrates of different hardnesses. The highest endurable Hertz pressure for a probability of survival of 50% at 5×10^7 cycles was obtained with quenched and tempered substrates of intermediate hardness of 400 Hardness Brinell (HB). Crack formation and subsequent delamination appeared to be the main causes of failure.

Bolelli et al. (2012a, b) studied the tribological performance of two coatings of Fe–Cr–Ni–Si–B–C (Colferoloy) alloy HVOF sprayed. They compared results to those obtained on Ni–Cr–Fe–Si–B–C and Cr_3C_2–NiCr layers (also HVOF sprayed), hard chromium electroplating, and bulk tool steel. Colferoloy coatings were validated as alternatives to Ni-based alloys and electroplated chromium under sliding wear conditions but appeared unsuitable for particle abrasion resistance. The different sliding wear behaviors of HVOF-sprayed coatings could be explained by coupling micro- and nano-hardness to scratch testing, which reflected cracking resistance and plastic deformability.

Ganesh Sundara Raman et al. (2007) D-gun sprayed Cu–Ni–In coatings on two substrate materials: Ti–6Al–4V and Al-alloy AA-6063. The Cu–Ni–In coating was found to be beneficial on the Ti-6-4 alloy, while deleterious on the Al-alloy substrate under both plain fatigue and fretting fatigue loading. The results were explained in terms of differences in the values of surface hardness, surface roughness, surface residual stress, and friction stress.

Akebono et al. (2008) investigated the factors that most strongly influenced fatigue properties of steel flame sprayed with Ni-based self-fluxing alloy and prepared three types of thermally sprayed specimens, which differed in heating time in the fusing process. The sprayed specimens fused for longer time exhibited lower fatigue strength, because of the segregation of the chromium compound in the coated microstructures. Performing the fusion for a shorter time was effective for producing sprayed materials of enhanced fatigue-resistant properties.

Thermal Fatigue Wear

Thermal fatigue occurs in components subjected to high temperature gradients resulting from friction or operating environment (for example, external surface subjected to hot gases). It results in high stresses, surface fatigue, and mechanical transfer (transfer of the softer body to the harder one). When thermal fatigue tests are performed in air, very often oxidation problems take an important part in coating performance. For thermal fatigue testing, the heat flux to the sample is applied using a flame, followed by air cooling, with or without convection. As it could be expected, most studies were devoted to thermal barrier coatings (TBCs). The following two examples are not related, however, to TBCs.

Aoh and Chen (2001) investigated high-temperature (700 °C) wear characteristics of Stellite-6 alloy containing Cr_3C_2 after thermal fatigue and oxidation treatment at 700 °C. The coating was deposited by plasma-transferred arc (PTA) process. Thermal fatigue cracks initiated from the surface of Stellite-6 with Cr_3C_2 and propagated into the coating along carbide boundaries. No thermal fatigue crack was observed on sprayed Stellite-6 layer. The Cr_3C_2 content in the alloy enhanced the formation of the oxide layer. Surface oxidation was beneficial to the improvement of wear resistance and the coating exhibited the lowest wear loss if an oxidation treatment at 700 °C/100 h was achieved prior to the wear testing.

According to D'Ans et al. (2011), the major wear mode of steel in the aluminum foundry industry is thermal fatigue, especially affecting die-casting dies. Steel is also intensively corroded by molten aluminum and, sometimes, sliding wear occurs when extracting the molded parts from the die. D'Ans et al. (2011) conducted thermal fatigue tests with samples of hot work tool steel, either simply borided, or protected by a multilayer of YSZ, followed by a nickel superalloy and then a borided layer. The multilayer coating resistance to thermal fatigue (heating between 500 and 800 °C) turned out to be lower than for a single-treatment solution (boriding) and for plain steel.

Eriksson et al. (2011) subjected air plasma-sprayed TBC to isothermal and cyclic heat treatments (thermal cycling fatigue: TCF). Specimen subjected to TCF and isothermal oxidation gave very similar interface between thermally grown oxide (TGO) thickness and TGO composition. The heat treatment influences the adhesion of TBCs: isothermal oxidation up to 290 h has been shown to have a beneficial effect on adhesion compared to the as-sprayed condition, while cyclic heat treatment has been shown to decrease adhesion. Kwon et al. (2006) studied a TBC with topcoat deposited by APS and bond coat by HVOF. Thermal fatigue did not affect the stress–strain curves, except for thermal

fatigue for 500 h. However, the thermally grown oxide (TGO) layer thickness was dependent on the exposure time under thermal fatigue, showing a nominal thickness of approximately 4 μm after thermal fatigue for 500 h, independent of the number of thermal fatigue cycles. As the exposure time was increased in the thermal fatigue experiments, the damage to the topcoat was inhibited with less crack coalescence. The higher stiffness in the bond coat induced cracking or delamination at the interface between the bond coat and the substrate, whereas thermal fatigue increased the mechanical properties, especially the elastic modulus, of the bond coat and enhanced the damage tolerance of the TBC system.

Thermal Shock Fatigue Wear

Thermal shock occurs when the thermal gradient causes different parts of an object to expand by different amounts, generating stress or strain. At some point, this stress can exceed the strength of the material, causing a crack to form. If nothing stops this crack from propagating through the material, it will cause the object's structure to fail. The thermal shock resistance is tested by alternate high-temperature exposure and cooling cycles until failure. The heating is achieved by a furnace (moderate thermal gradients), followed by cooling using cold water (high thermal gradients). Alternately, the heating is made with a flame on one side of the sample, while the opposite side of the sample is air-cooled (high thermal gradients). The cooling step can also be achieved through replacing the flame by an air jet (moderate thermal gradients). The heating step can also be achieved with a fluidized bed or a laser.

Luo et al. (2011) deposited by high-velocity wire arc spraying using cored wires FeMnCrAl/Cr_3C_2 and FeMnCrAl/Cr_3C_2–Ni9Al coatings onto low-carbon steel substrates. The specimens were placed inside a furnace at 800 °C, held for 15 min, and then quenched into a water bath (25 °C). The first type of coating consisted of layered splat of mainly Fe solid solution phases mixed with oxide phases, unmelted particles, and pores. The second type of coating exhibited higher bonding strength; Ni and Fe formed the diffusion layer that improved the thermal shock resistance. The cracks in the coatings were mainly initiated and propagated along the oxide phases during the thermal shock test. The uniformly shaped pores in the coatings helped prevent crack initiation and propagation.

Pan et al. (2012) studied the effect of SiC particles on thermal shock resistance of Al_2O_3–20 wt.% 8YSZ coatings air plasma sprayed. The thermal shock resistance of Al_2O_3/8YSZ coatings was increased greatly from 5 to 83 cycles with addition of SiC particles at 1000 °C. Some silicate fibers were formed on the coating surface and through thickness after thermal shock. The $Al_2O_3{\cdot}xSiO_2$ silicate fibers increased greatly the thermal shock resistance of ceramic coatings.

Gu et al. (2011) plasma sprayed NiCoCrAlY/8YPSZ coating on aluminum alloy (5A06). The failure after thermal shock tests (furnace heating at 400 °C for 0.5 h, then quenched with cold water, and dried by warm air) was mainly due to the stress caused by thermal expansion mismatch between the bond coat and the substrate as well as the galvanic corrosion of the aluminum alloy. Ni–P, Ni–W–P, and Ni–Cu–P as interlayers were electrolessly deposited on the substrate in order to mitigate the thermal stress. Diffusion layers mainly composed of AlNi, Al_3Ni_2, and Al_3Ni were observed between the interlayers and the substrate after thermal shock test. The oxidation of the substrate was effectively inhibited. Ni–P interlayer was superior to the other two interlayers and enhanced the thermal shock life from 38 to more than 200 cycles.

Kokini et al. (2002) studied plasma-sprayed yttria-stabilized zirconia (YSZ)–NiCoCrAlY bond coat alloy compositionally graded TBC onto Inconel steel subjected to a thermal shock loading. The thermal loading was applied using a continuous CO_2 laser. The results showed that for a given thermal resistance, as the compositional gradation was increased, the maximum surface temperature at which horizontal cracks initiated in the TBC increased.

Liang and Ding (2005) deposited by APS nanostructured and conventional zirconia coatings and studied, by the water quenching method, the thermal shock resistances of as-sprayed coatings. The results showed that the nanostructured as-sprayed coating possessed better thermal shock resistance than the conventional one. The difference in microstructure and microstructural changes occurring during thermal shock cycling explained those results. Gilbert et al. (2008) investigated the reduction in time-dependent deformation through the addition of mullite to YSZ-based TBCs. Fracture mechanics analyses were performed for three coating architectures: monolithic YSZ, monolithic mullite, and a mullite–YSZ composite. The effect of coating architecture and surface crack morphology on interface fracture was investigated. They found that mullite and YSZ combined to influence the thermal shock behavior of the composite coatings. Composite coatings experienced a reduced driving force for interface fracture compared to monolithic YSZ coatings while having a higher thermal resistance compared to monolithic mullite coatings.

19.3.1.6 Other Forms of Wear

Wear by Very High Stresses

Wear by very high stresses is mostly characterized by dry sliding with a pin-on-disk test and depends on the high load applied and sliding distance, the wear response being dominated by subsurface cracking and removal of materials when sliding. Martials used include APS-formed ceramic coating, and HVOF, or D-gun with cermets. Bolleli et al.

(2006a, b, c) have investigated through pin-on-disk and dry sand–steel wheel tests the wear resistance of APS ceramic coatings (Al_2O_3, Al_2O_3–13%TiO_2, Cr_2O_3). These have their best performance in dry particle abrasion conditions, because they never undergo abrasive grooving but only splat detachment. In the pin-on-disk test, the ability to form a smooth and compact surface film by local plastic deformation was the key property determining coating performance. Al_2O_3 and Al_2O_3–13%TiO_2 did not form an adequately compact tribo-film and therefore showed unfavorable properties in terms of sample wear rate, pin wear rate, and friction coefficient. Cr_2O_3, on the other hand, had the ability to form a compact tribo-film by splat plastic deformation giving rise to performances comparable to HVOF-sprayed ceramics. However, its rather low deposition efficiency (below 45%) and its propensity to possibly form Cr_6^+ by in-flight thermal alteration represented serious shortcomings that must be considered. Bolleli et al. (2006a, b, c) also found that Al_2O_3 coatings, manufactured by the high-velocity suspension flame spraying (HVSFS) technique using a nanosized powder suspension, resulted in few interlamellar or interlamellar cracks, inducing reduced pore interconnectivity. Such strong interlamellar cohesion favored much better dry sliding wear resistance at room temperature and at 400 °C.

Ahmaniemi et al. (2002a, b) showed that the aluminum phosphate sealing treatment changed stress states of the alumina and chromia coatings toward compression. Tensile stress state of the Al_2O_3 coating decreased during the sealing treatment and was even compressive when measured with hole-drilling method. Dry abrasion resistance increased correlatively. Stress state of sealed Cr_2O_3 coating was more sensitive to sealing treatment temperature. Higher sealing treatment temperature led to higher compressive stress state and better abrasion wear resistance.

Chen and Hutchings (1998) plasma sprayed coatings of tungsten carbide with 9, 12, and 17 wt.% Co by both air (APS) and low-pressure (VPS) methods. VPS coatings had a lower porosity, better inter-pass bonding, and higher WC contents; these correlated with greater abrasion resistance. All coatings showed poor resistances to high-stress abrasive wear, which was associated with widespread fracture of the carbide constituents of coatings under these conditions. Under low-stress abrasion, however, all coatings showed a substantially greater wear resistance than the steel control. The presence of hard carbides was beneficial, and the VPS coatings all showed a greater wear resistance than the APS ones.

Venkateswarlu et al. (2009) sprayed diamond-reinforced composite (DRC) coatings deposited with both oxyacetylene flame and HVOF techniques. The feedstock material used for the coating consisted of tungsten carbide (WC; average particle size: ~2 μm), bronze (average particle size: ~30 μm), and diamond (average particle size: ~25 μm) powders. In addition to the high hardness of HVOF-sprayed coating, the uniform distribution of diamond particles in the matrix was considered important in view of reduced matrix deformation. HVOF-sprayed specimen, owing to its lower porosity and higher bond strength between reinforced particulates and the matrix, led to substantial reduction in the deformation of matrix, which in turn facilitated higher wear resistance. To improve the resistance of HVOF-sprayed cermets, different means were used. For example, Stoica et al. (2005) have HVOF (JP-5000) sprayed functionally graded (FG) WC–NiCrBSi coatings and heat-treated them at 1200 °C in argon environment. It was possible to achieve higher wear resistance, both in terms of coating wear and the total wear of the test couples. This was attributed to the improvements in the coating microstructure during the heat treatment, which resulted in an improvement in coating's mechanical properties through the formation of hard phases, elimination of brittle W_2C and W, and the establishment of metallurgical bonding within the coating microstructure and at the coating–substrate interface.

Valarezo et al. (2010) tested the effective damage tolerance of a functionally graded coating (FGC) deposited by HVOF. The thick FGC (≈1.2 mm) consisted of six layers with a stepwise change in composition from 100 vol.% ductile AISI-316 stainless steel (bottom layer) to 100 vol.% hard WC–12Co (top layer) deposited onto an AISI-316 stainless steel substrate. The FGC structure showed the ability to reduce cracking with increased compliance in the top layer during static and dynamic normal contact loading, while retaining excellent sliding wear resistance (ball-on-disk tests). One of the main problems seemed to be the poor characteristics of HVOF-sprayed stainless steel. It suffered from extensive oxidation and phase alteration during spraying, which compromised its mechanical strength and probably impaired its adhesion to the substrate.

Bolelli et al. (2012a, b) manufactured HVOF-sprayed functionally graded coating, consisting of two NiAl/WC–Co composite layers with increasing cermet content and a pure WC–Co topmost layer. Results showed that the WC–Co/NiAl FGC could provide good wear and corrosion protection to the substrate under very severe conditions, when very thick layers were demanded. This architecture also solved many of the problems highlighted by the previously considered WC–Co/stainless steel FGC.

Stoica et al. (2004) compared the sliding wear performance of as-sprayed and hot isostatically pressed (HIP) thermal spray cermet (WC–12Co) coatings. Results indicate that HIP technique can be successfully applied to posttreat thermal spray cermet coatings for improved sliding wear performance, not only in terms of coating wear but also in terms of the total volume loss for test couples. The process induced

phase transformations: elimination of secondary phase W_2C and metallic tungsten W, and alteration of amorphous binder phase through recrystallization of Co leading to precipitation of the η carbides. It also developed the metallurgical bonding at the interface between the constituent lamellae of the coating, thereby increasing the coating's Young's modulus after posttreatment with HIP technique.

Wear by Fretting and Fretting-Corrosion

Fretting occurs when the two interacting mating surfaces are subjected to an oscillatory motion of small amplitude. It can be more important when corrosion or oxidation occurs, producing for example oxides with ferrous materials (fretting corrosion). In the latter case, the extent and kinetics of phenomena are linked to the balance between the formation of products and their removal through wear. Besides the material properties, the design of the machine must eliminate the micro-movement, trap or remove debris, and limit the contact with the environment. Jin et al. (2006) have underlined that surface coating may protect the contact area from the fretting damage; however, specific contact condition would govern the effectiveness of the coating. They proposed to classify coatings into two major types: hard and soft. Hard coatings are used in the contact conditions where fretting wear is present or dominant, while soft coatings are used to reduce the fretting fatigue-induced failure since they could act as a self-lubricant and reduce the coefficient of friction resulting in improvement in fretting fatigue life. Of course, fretting resistance depends on coating and substrate on the one hand and contact conditions (lubricant, pressure, and amplitude of the movement) on the other. For example, Kim and Korsunsky (2011) studied a pad and a substrate made of Ti-6Al-4V alloy on which was plasma sprayed a metallic interlayer of Cu59–Ni36–In5. A dry film lubricant layer was then applied on the metallic interlayer and on the pad in the form of epoxy matrix loaded with MoS_2 particles. The coated specimen was clamped between two pads that were pressed against the specimen surface with a contact pressure of ∼125 MPa, conditions simulating the geometric and loading conditions experienced in aerospace components. Each fretting test was performed at a frequency of 2.5 Hz. The durability of the coating was increased when increasing its thickness. Jin et al. (2006) studied Cu–Al coating on Ti-6Al-4V substrate under fretting fatigue condition. At the low applied-stress amplitudes, the coating survived up to one million cycles. At the high applied-stress amplitudes, either the coating was separated from the substrate due to insufficient interfacial strength or the specimen fractured at locations away from the contact area.

Mary et al. (2011) performed fretting wear tests up to 500 °C. A representative punch (Ti17)/plane (CuNiIn plasma coating) interface was investigated under air conditions. Wear was studied by varying pressure, sliding amplitude, and temperature. A threshold pressure $p_{th} \approx 85$ MPa was identified for the transition from a low- to a high-wear regime. Temperatures in the range of 20–450 °C did not modify the respective wear processes and consequently did not affect the related wear rates.

Hager Jr et al. (2008) conducted, for titanium compressor bladed disk assemblies, an in-depth wear analysis on the gross slip fretting wear of Ti-6Al-4V-mated surfaces as well as Ti6Al4V worn against plasma-sprayed CuNiIn, Al–bronze, Mo, and Ni. Tests were performed at room temperature and 450 °C. To eliminate the stress concentrations, the test geometry was an ellipsoid on a flat plate. They determined that all coatings caused significant damage to the mating Ti6Al4V surfaces and that the wear mechanisms were all similar to those of the uncoated baseline case. In gross slip fretting, these soft thermal spray coatings did not effectively protect the mating Ti6Al4V surfaces without solid lubrication.

Koiprasert et al. (2004) HVOF sprayed four types of coating (≈300–400 μm), namely, WC–17% Co ($T < 500$ °C), Cr_3C_2–25%NiCr ($T < 800$ °C), AlSi graphite, and CoMoCrSi ($T < 800$ °C) on stainless steel substrates. They used an in-house flat-on-flat fretting wear tester at 500 °C. At that temperature, WC–Co did not perform well, and Cr_3C_2–25%NiCr outperformed WC-Co; but the formation of Cr_2O_3 by oxidation caused rapid wear, and AlSi graphite coating did not provide additional wear resistance to the stainless steel. Only the CoMoCrSi coating, with its low porosity, moderate-to-high hardness, and good high-temperature corrosion resistance, exhibited the best wear property.

Hager Jr et al. (2009) plasma sprayed nickel graphite composite coatings with 5–20% graphite and studied mitigated fretting wear within Ti-6Al-4V contacts at room temperature and 450 °C. The embedded graphite particles reduced the friction of the nickel thermally sprayed coatings during both low- and high-temperature fretting wear experiments. The wear reduction on the mated Ti-6Al-4V surfaces was due to the formation of uniform transfer film graphite based at room temperature and NiO based at 450 °C.

Carrasquero et al. (2008) investigated the fretting wear performance of a Ni–Cr-based alloy, containing B and C, HVOF sprayed onto a SAE-1045 steel substrate. Tests were conducted on both the uncoated and coated substrate, under unlubricated dry conditions, at different applied normal loads, cycles, and amplitudes. They showed that at constant wear amplitude, the wear volume increased with the applied normal load and that at under constant load conditions, the wear volume decreased as the wear test amplitude also decreased, becoming insignificant when it was less than ∼100 μm.

Tian et al. (2008) studied the fretting wear behavior, against a steel ball, of conventional and nanostructured

Al_2O_3–13 wt.% TiO_2 plasma spray. The improved fretting wear resistance of nanostructured coatings was attributed to the nanometer-sized grains, reduced lamellar structures, and amorphous phases. Fretting wear often occurs in hip joints that must be replaced after about 10 years of use.

Sathish et al. (2011) reported on the sliding wear performance of the nanostructured Al_2O_3–$13TiO_2$, ZrO_2, and the bilayered (ZrO_2/Al_2O_3–$13TiO_2$) coated biomedical Ti–13Nb–13Zr alloy in simulated body fluid (SBF) condition. The bilayered coating exhibited 200- and 500-fold increase in the wear resistances when compared with that of the nanostructured Al_2O_3–$13TiO_2$ and ZrO_2 coatings. This substantial improvement was attributed to the lower porosity and higher adhesion strength of the bilayered coating.

19.3.1.7 Replacement of Hard Chromium

Electrolytic hard chromium plating is extensively used against wear and sometimes corrosion. However, the chromium plating baths contain chromic acid, in which the chromium is in hexavalent state, which is known to be carcinogenic. Considering the harmful effects of the technology on the environment and public health, combined with some intrinsic technical limitations, research efforts were devoted since the beginning of the 1990s to its replacement by sprayed coatings, especially HVOF-sprayed cermets. In the following a few examples are given.

Savarimuthu et al. (2001) studied sliding wear characteristics of HVOF-sprayed WC coatings and electroplated chrome tested against Al–Ni–Bz blocks, Cu–Be blocks, and against themselves. The fatigue resistance of WC coatings increased in the presence of compressive residual stresses.

Sahraoui et al. (2004) investigated and compared microstructural properties, wear resistance, and potentials of HVOF-sprayed Tribaloy©-400 (T-400), Cr_3C_2–25 wt.% NiCr, and WC–12 wt.% Co coatings for a possible replacement of hard chromium plating in gas turbine shaft repair. HVOF carbide-based coatings exhibited higher hardnesses and superior performances in wear resistance than hard chromium coatings. In the case of shaft repair, hard chromium plating process proved to be time consuming and to involve high costs.

Ishikawa et al. (2005) used a commercial HVOF and a gas shroud (GS) attachment HVOF to prepare WC/CrC/Ni cermet coatings under various combustion conditions. The density of coatings improved as the velocity of sprayed particles increased. With the gas-shrouded HVOF, high density was achieved with a lower degree of WC degradation. Such coatings could be alternative candidates of hard chrome (HC) plating.

Guilemany et al. (2005) compared wear and corrosion properties of Cr_3C_2–NiCr (CC-TS) HVOF sprayed and hard chromium coatings (HCCs) obtained on a steel substrate. Three orders of magnitude lower volume loss was found for CC-TS (HVOF) after friction tests compared with HC. The best corrosion resistance was also obtained for the CC-TS by HVOF.

Picas et al. (2006) compared the mechanical and tribological properties of HVOF CrC75–(NiCr20)25 coatings sprayed from three different agglomerated feedstock powders with various powder size distributions and compared results with conventional hard chromium plating. The CrC–NiCr coating, obtained with the lowest feedstock powder size, presented the best wear resistance under all studied conditions and demonstrated superior performance to hard chrome with regard to mechanical and tribological properties.

Bolelli et al. (2006a, b, c) studied mechanical properties and tribological behavior (abrasion and unlubricated sliding wear resistance) of various kinds of electrolytic hard chrome (EHC) coatings and of metallic and cermet HVOF-sprayed coatings (WC–17Co, WC–10Co–4Cr, Co–28Mo–17Cr–3Si). HVOF-sprayed cermet coatings were harder but less tough than EHC ones. Therefore, they underwent a comparable or even higher mass loss when subjected to three-body abrasion conditions. However, their two-body sliding resistance definitely overcame that of EHC coatings, because they form a tough and uniform surface film protecting them from further damage.

Deng et al. (2007) used high-velocity oxygen/air fuel (HVO/AF) to spray WC-17Co and WC-10Co4Cr on 300M ultrahigh-strength steel. WC-17Co coating exhibited higher fracture toughness than that of WC-10Co4Cr coating. WC-17Co coating demonstrated better impingement resistance than WC-10Co4Cr, and the impingement resistance of chrome electroplating fell between that of WC-17Co and WC-10Co4Cr coatings.

Abdi and Lebaili (2008) flame sprayed NiCrBSiCFe coatings for a possible replacement of hard chromium plating in mechanical parts' repair. Coatings presented a high hardness after cyclic heat treatment, an excellent resistance to wear and friction, a good corrosion resistance, and an excellent adhesion to steel. Tests have been also positive for the replacement of hard chromium in landing gear by HVOF-sprayed WC–CoCr coatings [Krishnan N, et al. (2008), Matthäus G, et al. (2009)].

Heydarzadeh and Ghadami (2010) plasma deposited WC–12 wt.% Co using APS onto steel substrates. Heat treatment of the coatings in an inert atmosphere above 900 °C promoted the formation of Z-carbides from the amorphous phase. Microhardness of coatings for different heat-treating conditions was relatively higher than that of the conventional hard chromium electro deposit.

Lu et al. (2011) compared the microstructure and corrosion behavior of hard chromium coating (HCC) and plasma-sprayed Fe-based alloy coating (FAC) on low-carbon steel, using the salt-spray test and electrochemical corrosion test.

After 60 days of salt-spray test, the weight loss of the FAC was only about 10% of HCC. After sealing treatment, the defects of pores and micro-cracks existing in FAC disappeared. The sealing treatment further decreased the weight loss of FAC to be about 4% of HCC.

Staia et al. (2012) investigated the tribological behavior of a VPS sprayed Cr_2C_3–25 wt.% NiCr chromium carbide coating both in the as-deposited and heat-treated conditions. The samples were subsequently annealed for 2 h at 600 °C, 800 °C, and 900 °C in Ar. The wear values indicated a satisfactory behavior from the tribological point of view. However, the heat treatment had no important consequences on the tribological performance of these coatings. The only problem is that VPS coating is about four times more expensive than HVOF.

19.3.2 Corrosion- and Oxidation-Resistant Coatings

Corrosion and oxidation correspond to a chemical or electrochemical reaction with the surrounding atmosphere. As a general rule, except for sacrificial coatings, those used against corrosion must be as dense as possible and, in most cases, a posttreatment such as fusion of self-fluxing alloys, heat-treatment, sealing, austempering, or laser glazing is necessary for optimal performance.

19.3.2.1 Room Temperature Corrosion

Corrosions at room temperature can roughly be categorized into atmospheric or marine corrosion, and chemical or parachemical corrosion.

Atmospheric and Marine Corrosion

Large steel structures such as bridges, pipelines, oil tanks, towers, radio and television masts, overhead walkways, and large manufacturing facilities in the metallurgical, chemical, energy, and other industries must be protected from corrosion. It is the same, but with more difficulties, with structures exposed to moist atmospheres and seawater such as ships, offshore platforms, and seaports [Evdokimenko Yu I, et al. (2001)]. Sørensen et al. (2009) have presented a review of anticorrosive coatings for containers, offshore constructions, wind turbines, storage tanks, bridges, rail cars, and petrochemical plants and "marine corrosion" corresponding to coatings for ballast tanks, cargo holds and cargo tanks, decks, and engine rooms on ships.

Flame and wire arc spraying meet such requirements. However, coatings obtained by these methods are relatively porous (up to 20%). Sacrificial coatings (for example, Zn or Al on steel) are mainly used. Such coatings must have a cathodic behavior relatively to the ions of the metal to be protected, steels in almost all cases. The cathodic protection can be porous without any corrosion of the underneath metal. Zinc performs better than aluminum in alkaline conditions, while aluminum is better in acidic conditions. Zinc–aluminum (Zn–15 wt.% Al) seems to combine advantages of both materials. Against marine biofouling, undesirable accumulation of marine organisms on artificial surfaces that are immersed in the sea, Murakami and Shimada (2009) have studied flame-sprayed aluminum–copper alloy powders, aluminum–copper blend powders, aluminum–zinc blend powders, and a zinc powder. Coatings were immersed in the sea and their corrosion and marine fouling behaviors were examined. The aluminum–copper coatings had poor anticorrosion and antifouling properties. The aluminum–zinc coating with high zinc content and the zinc coating possessed the anticorrosion and antifouling properties.

Of course, other treatments are possible such as plastic deformation. For example, the initial porosities of 4–14% (depending on spray conditions) of aluminum coatings, wire arc sprayed, were reduced to 0.16–0.83% after being shot-peened with SiC glass beads of 0.21–0.3 mm [Pacheo da Silva C et al (1991)]. Sealers can also present antifouling properties. Chun-long et al. (2009) have arc sprayed aluminum on steel panels and then sealed coatings with nanocomposite epoxies especially developed for sealing them. In order to test their performance, some panels were tested in the East China Sea. Test panels were mounted respectively for 3 years, in the marine atmosphere zone, seawater splash zone, tidal zone, and full-immersion zone. Tests included marine atmospheric outdoor exposure test, seawater corrosion test, and coating adhesion test. It was found that the appearance of coating panels was as fine as original but with a little sea species adhering to panels on tidal zone and full-immersion zone. Basically, no change in the morphology and bond strength, and no visible coating crack, blister, rust, and break-off was observed. Schmidt et al. (2006) investigated the corrosion protection performance of 17 different Zn and Al sacrificial coating system configurations during marine atmospheric exposure (20-month exposure time) at Kure Beach, NC, USA. The coating systems incorporated several conversion coating layers, primers, and organic topcoats. The sacrificial Zn coatings provided sacrificial protection at the defects. Of the two thermal spray Zn coatings, flame spray coatings were more protective than arc spray.

Han et al. (2009) wire arc sprayed aluminum wire on special treatment steel (STS) 304 base metal. The electrochemical experiment was performed in natural seawater. The coating with the higher thickness represented good corrosion resistance in seawater. Esfahani et al. (2012) deposited aluminum coating on mild steel by arc spraying. The corrosion behavior was evaluated by electrochemical impedance spectroscopy (EIS) and polarization tests in 3.5 vol.% NaCl solution. The as-coated samples were also subjected to a

1500-h salt-spray assay. EIS measurements showed that the corrosion performance of the coating was improved during a long-time immersion and exposure to saline mist. This could be due to plugging of pores by corrosion products, which hinder further penetration of the electrolyte through the coating. The twin wire arc sprayed aluminum coatings could reliably protect steel structures against corrosion in chloride-containing aqueous solutions.

Gorlach (2009) has developed wire (Zn–Al) spraying by HVAF process. Coatings showed considerably higher bond strength than those obtained by the conventional methods, an advantage in areas where the adhesion strength was critically important. The highly dense coating structure also eliminated the need for a top paint coat, usually applied on metal-sprayed coatings to extend service life. Concrete bridge structural deterioration in coastal marine environments or in areas where deicing salts are used for snow and ice removal is a problem.

To limit atmospheric or marine corrosion, if anodic protection is used (for example, nickel is anodic to steel and the cathodic area of steel exposed controls the rate), the coating should be as dense as possible (if necessary sealed). Cramer et al. (1999), as well as Holcomb et al. (1997), have proposed a cobalt-catalyzed, non-consumable, thermally sprayed titanium anode as an alternative to thermally sprayed zinc anodes for impressed current cathodic protection (ICCP). Ti was wire arc sprayed [Cramer SD, et al. (1999)], the atomization being performed with nitrogen to limit as much as possible the formation of γ-TiO_2. The titanium anode had a porous heterogeneous structure composed of α-titanium containing interstitial oxygen and nitrogen, and a face-centered cubic (fcc) phase thought to be Ti(O,N). The final titanium anode thickness was 50–150 μm. Electrochemical aging was studied using catalyzed titanium anodes thermally sprayed on concrete slabs containing a steel mesh cathode. Cobalt catalyst, applied to the anode as an aqueous cobalt nitrate–amine complex, penetrated the anode and accumulated at the anode–concrete interface and in cracks within the concrete adjacent to the interface. Anodic polarization during and after application converted the cobalt to the active catalyst, Co_3O_4. With aging, cobalt catalyst dissolved in the increasingly acid environment of the interface and dispersed into the Ca-deficient, silica-rich reaction zone to reprecipitate and form a more diffused site for the anode reactions. Stable operation of catalyzed anodes was maintained for a period equivalent to 23 years' service at Oregon Department of Transportation (DOT) bridge ICCP conditions with no evidence that operation would degrade with further aging. Early results from the field experiment at the Depoe Bay Bridge suggested anodes may age more slowly at low current densities with lesser impact from acidification.

To improve the marine corrosion resistance of stainless steel coatings fabricated by high-velocity oxy fuel (HVOF) spraying with a gas shroud attachment, Kawakita et al. (2005) increased the molybdenum (Mo) content of stainless steel with a chemical composition of Fe balance-18 wt.% Cr-22 wt.% Ni-2–8 wt.% Mo. The corrosion rate in sulfuric acid was improved when increasing the molybdenum content. The pitting corrosion resistance in artificial seawater was shifted toward the noble direction with increases in the molybdenum content. The number of rust spots formed by crevice corrosion in artificial seawater decreased after the addition of molybdenum to the coatings.

Chemical or Parachemical Corrosion

Non-sacrificial coatings will never protect the substrate if connected porosities and oxide networks exist, which is the case of most thermally sprayed coatings. The substrate protection requires using a protective bond coat or producing dense coatings or sealing them, which is generally possible if the service temperature is below few hundreds of Celsius degrees. Austenitic stainless steels, aluminum bronze, nickel-base alloys, MCrAlY, cermets with WC, Cr_2C_3, and matrices containing chromium or nickel, or both, are used against corrosion, often associated with wear. A few examples will be presented below.

Moskowitz (1993) pointed out that the use of vacuum chambers or posttreatments can eliminate most defects, but these methods are costly and impractical on a large scale. Thus, he proposed using modified HVOF process using unique inert gas shrouding to achieve highly dense, low-oxide coatings of metallic alloys. Coatings of corrosion-resistant alloys for severe corrosion applications in petroleum industry, such as type 316L stainless steel and Hastelloy C-276, were shown to act as true corrosion barriers. The oxide content also played a role. For example, 316L stainless steel coatings formed by HVAF and HVOF were applied on carbon steel panels and their resistance to salt spray was tested as sprayed or sealed [Zeng Z, et al. (2008)]. When coatings were sealed, corrosion was less on the HVAF coatings than that on the sealed HVOF coating, and almost no corrosion was observed on the sealed coating sprayed with powder of the largest particles (highest porosity) after even 500 h of salt-spray testing. While the amount of through pores dominated the corrosion resistance of as-sprayed coatings, the degree of oxidation of the coatings (much less with HVAF) determined the corrosion resistance when sealing was applied.

For applications with a severe wear in oil and gas industry, cermets are used, with however some problems for offshore installations. According to Meng (2010), the choice between the wide varieties of tungsten carbides with different alloying binders is not simple. The corrosion resistance must be improved by the proper choice of binder. For example,

Souza and Neville (2007) have shown that WC–CrNi exhibited passive behavior, as stainless steel, and would be compatible for use as a coating/substrate system when exposed to seawater, which was not the case for WC–CrC–CoCr. As previously mentioned, the coating porosity and its oxide content must be as low as possible, which implied using HVOF guns resulting in higher impact velocities (low coating porosity) and lower particle temperatures (less oxidation). This was illustrated by the work of Ishikawa et al. (2005) who used a commercial HVOF with a gas shroud attachment (GS-HVOF) to prepare WC–CrC–Ni coatings. The density of coatings improved as the velocity of sprayed particles increased. Results of corrosion test indicated that through porosity was eliminated at velocities above 770 m/s with a lower degree of WC degradation. Wear resistance and hardness of coatings prepared by GS-HVOF were superior to those prepared by the conventional HVOF. Fedrizzi et al. (2007) showed that Cr_3C_2–NiCr coatings, in sodium chloride solution under sliding wear, presented good barrier properties, and substrate corrosion was never observed. Moreover, when chromium was added to the metal matrix of WC–Co-based systems, tribo-corrosion behavior was enhanced, and lower tribo-corrosion rates were measured. Plasma-sprayed Cr_2O_3–8 wt.% TiO_2 coating was used on hydraulic cylinder piston rods and rolls, but the substrate was rapidly corroded by the diffusion of the corrosive solution through pores: the bond coating was destroyed by the aggressive solution and ceramic coating flakes dropped off. Zhang et al. (2011) have sealed coatings with epoxy and silicone resins. The sealing treatment improved the corrosion resistance of coatings significantly by blocking the open pores and cracks of the coating. Sealed by silicone resin, the coating gained remarkable anticorrosion properties, as after 1200-h salt-spray test, there was still no rust on the silicone resin-sealed coating.

For chemical corrosion, the coating material must be adapted to the corrosive medium. Coatings are often used to reduce costs, especially when solutions have been found in the use of sophisticated materials that are oxidation- and corrosion-resistant at high and low temperatures with high strength such as nickel-base superalloy Inconel 625. However, coatings of these materials on cheaper metals would be cheaper than bulk super alloy. Tuominen et al. (2000) have shown that Inconel 625 HVOF sprayed presented mechanical and corrosion properties typically inferior to wrought materials due to the chemical and structural inhomogeneity of the thermally sprayed coating material. Laser remelting, with high-power continuous wave Nd:YAG laser equipped with large beam optics, resulted in homogenization of the sprayed structure. This strongly improved the performance of the laser-remelted coatings in adhesion, wet corrosion, and high-temperature oxidation testing.

A rudder is one of the essential ship components for navigation and safety and services in the complex conditions of cavitation erosion and marine corrosion [Tuominen J, et al. (2000)]. Kim and Lee (2011) have investigated ten different coatings arc sprayed with Al-, Zn-, Cu-, and Fe-based wire feedstock for a rudder application. In terms of marine corrosion resistance, aluminum coating was the best, while stainless steel coating presented the highest resistance against cavitation erosion. Si addition improved both the hardness and bond strength of Al-based coatings, resulting in drastic increment of cavitation erosion resistance by about 40 times when adding 12 wt.% Si. With Cu- and Fe-based coatings, interfacial oxidation occurred in between the coating and steel substrate, leading to interfacial cracks and coating delamination. The same authors, also for rudders, wire arc sprayed Al–Zn and then sealed them with F–Si sealer, spread with the brush at room temperature for several times. The corrosion rate of the sealed specimen after coating was lower and the hardness higher and they presented good cavitation resistance characteristics.

Dent et al. (1999) studied the corrosion characteristics in 0.5 M H_2SO_4 of two Ni–Cr–Mo–B alloy powders HVOF sprayed. Both coatings exhibited comparable resistance to corrosion. Microstructural examination of samples revealed the prevalence of degradation at splat boundaries, especially where significant oxidation of the deposit occurred. Ishikawa et al. (2001) wire arc sprayed a duplex coating composed of aluminum on 80Ni–20Cr alloy undercoat. The duplex coating presented an excellent performance in a hot, near-neutral aqueous environment. The role of the undercoat layer of the sprayed 80Ni–20Cr alloy was to decrease the surface area of the steel substrate to be protected and reduce the sacrificing load for the aluminum and also to increase the adhesion of the aluminum topcoat by its roughness.

Magnesium alloys present low density and excellent physical and mechanical properties. They are particularly suitable for their use in automotive and aerospace applications, where replacement of steel and aluminum components by magnesium components would contribute to energy savings and reduced environmental impact. However, their drawback is their relatively high corrosion susceptibility and low wear resistance. That is why many studies of thermal spray coatings have been performed to improve their corrosion resistance. Pardo et al. (2009) wire arc sprayed aluminum/silicon carbide composite coatings on AZ31, AZ80, and AZ91D magnesium–aluminum alloys. Presence of SiC particles provides higher hardness and wear resistance but not necessarily a better corrosion resistance. Corrosion was investigated in 3.5 wt.% NaCl solution at 22 °C. Al/SiC composite coatings in the as-sprayed state revealed high level of porosity with poor bonding at the Al/SiC and coating/substrate interfaces, facilitating the degradation of the magnesium substrates by galvanic corrosion. Cold-pressing

posttreatment produced more compact coatings with improved corrosion performance. Arrabal et al. (2010) evaluated also the corrosion behavior of wire arc sprayed Al/SiC coatings on AZ31, AZ80, and AZ91D Mg–Al–Zn alloys in neutral salt fog (ASTM B 117) and high relative humidity (98% relative air humidity [RH], 50 °C) environments. Pardo et al. (2009) found that the application of a cold-pressing posttreatment improved the corrosion performance of the coatings. In high-humidity atmosphere, corrosion signs were only visible at the Al/SiC interfaces in the outermost surface of the coatings and in salt fog environment the galvanic corrosion of the substrates was delayed.

Pokhmurska et al. (2008) deposited on magnesium substrates (AM20, AZ31, AZ91) by wire arc spraying Zn, ZnAl4, and ZnAl15 solid wires and cored wires in aluminum core with powder filling containing different hard particles, such as boron, silicon, and tungsten carbide or titanium oxide. Remelting of thermal spray coatings was carried out by means of continuous irradiation of $C\square_2$ laser in nitrogen or argon atmosphere, electron beam in vacuum, and focused tungsten halogen lamp line heater in atmosphere. Electrochemical behavior of modified surface layers was mostly improved due to alloying, homogenization of element distribution, and strong decrease in as-sprayed coating porosity.

19.3.2.2 High-Temperature Corrosion

Hot corrosion degradation of metals and alloys is a serious problem for many high-temperature aggressive environment applications, such as thermal barrier coatings (TBCs), boilers, fluidized-bed combustors, and industrial waste incinerators. At high temperatures, corrosion reactions can take place through oxidation, carburization, nitriding, sulfidation, molten-salt corrosion, and halogen erosion. They are generally addressed using appropriate gas-tight thermally sprayed coatings adapted to the predominant corrosion mechanism as briefly listed below.

- *Against oxidation*, nickel and/or cobalt-based alloyed coatings are used.
- *Against carburization*, nickel and chromium-containing alloys are often used.
- *Against nitriding*, austenitic stainless steel and nickel-base alloys present a good resistance.
- *Against sulfidation*, certain Hastelloy and CoCrAlY are used.
- *Against molten glass*, among the most corrosive media, high-chromium-containing alloys (NiCrMo: Hastelloy or Nistelle, CoCrSiMo: Tribaloy and MCrAlYs) are used.
- *Against molten salt corrosion* resulting from sodium sulfates (such as Na_2SO_4), sodium chlorides (such as NaCl), and vanadium oxides (such as V_2O_5), no protection exists.

In the following, examples are reviewed of corrosion-resistant coating for some of the listed high-temperature corrosion situations and mechanisms commonly met in an industrial environment.

As summarized by Mohan et al. (2010) and Jones (1997) for TBCs, when cost-effective alternative fuels containing appreciable levels of elemental impurities such as V, Na, S, P, and Ca are used, corrosive compounds such as vanadates and sulfates might arise as combustion by-products. In addition, TBCs are also increasingly susceptible to degradation by air-ingested oxide deposits such as CaO, MgO, Al_2O_3, and SiO_2 (CMAS) [Hitchman LN, Knapp J (2010)], especially in aircraft engines that operate in a dust-laden environment.

Mohan et al. (2010) studied the degradation of thermal barrier coatings (TBCs) by fuel impurities and CMAS (CaO, MgO, Al_2O_3, SiO_2) at temperatures up to 1400 °C. The study was carried out on yttria-stabilized zirconia (YSZ) and CoNiCrAlY coatings (300 μm) on free-standing grit-blasted graphite substrates. The degradation by V_2O_5 and a laboratory-synthesized CMAS was due to the destabilizing effect of molten deposits on the YSZ leading to the formation of YVO_4, and reacting with the thermally grown oxide (TGO) forming various reaction product and phase transformations. CMAS melt readily dissolved the YSZ and then reprecipitated ZrO_2 with a composition based on local melt chemistry that deviates in the content of the Y_2O_3 stabilizer. Extensive dissolution of the TGO α-Al_2O_3 from freestanding APS CoNiCrAlY coatings by CMAS melt was observed. Enriching CMAS composition with Al promoted the crystallization of anorthite platelets and $MgAl_2O_4$ spinel and mitigated CMAS ingression [Hitchman LN, Knapp J (2010)]. Li et al. (2010a, b) investigated, in laboratory scale, the effect of CMAS. They found that the porous nature of the thermally sprayed TBCs made them vulnerable to CMAS attack even before discernible chemical reaction started. A denser coating had the potential to resist the CMAS attack for a longer time than a more porous coating.

Habibi et al. (2012) compared the hot corrosion performance of YSZ, $Gd_2Zr_2O_7$, and YSZ + $Gd_2Zr_2O_7$ composite coatings in the presence of molten mixture of Na_2SO_4 + V_2O_5 at 1050 °C. For YPSZ, results were similar to those of Mohan et al. (2010). For the second composite coating, by the formation of $GdVO_4$, the amount of YVO_4 formed was significantly reduced. Molten salt also reacted with $Gd_2Zr_2O_7$ to form $GdVO_4$ but under 1050 °C, these coatings were more stable, both thermally and chemically, than YPSZ and exhibited a better hot corrosion resistance. $LaTi_2Al_9O_{19}$ (LTA) exhibited [Xie X, et al. (2012)] promising potential as a new kind of TBC material, with its excellent high-temperature capability and low thermal conductivity. Xie et al. (2012) demonstrated its good chemical stability in molten salt of Na_2SO_4 and NaCl at 1000 °C. However, the

molten salt infiltrated to the bond coat, dissolving the TGO and resulting in hot corrosion of the bond coat.

Mei et al. (2012) studied the corrosion kinetics and mechanisms of NiCoCrAlTaY cold-sprayed coating and uncoated Mar-M247 superalloy in molten Na_2SO_4 salt vapor. Mass gain and microstructures after 200 h indicated that the NiCoCrAlTaY coating provided good oxidation and corrosion resistance in this vapor at 900 °C. Sidhu et al. (2006a. b) HVOF sprayed NiCrBSi, Cr_3C_2–NiCr, Ni–20Cr, and Stellite-6 coatings on a nickel-base superalloy and tested them at 900 °C in the molten salt (Na_2SO_4–60%V_2O_5) environment under cyclic oxidation conditions. Among them, Ni–20Cr-coated superalloy imparted maximum hot corrosion resistance, whereas Stellite-6 coated superalloy indicated minimum resistance. The hot corrosion resistance of all the coatings was attributed to the formation of oxides and spinels of nickel, chromium, or cobalt.

Chatha et al. (2012a, b) deposited by HVOF process 80Ni–20Cr and 75Cr_3C_2–25(Ni–20Cr) coatings on T91 boiler tube steel. Hot corrosion was studied on bare and HVOF-coated steel specimens after exposure to a molten salt (Na_2SO_4–60%V_2O_5) environment at 750 °C under cyclic conditions. The 80Ni–20Cr coating was found to be more protective than the cermet coating. Tani and Harada (2007) examined the corrosion resistance of Ni–50Cr alloy coating, plasma sprayed onto the fireside of steam-generating tubes in a heavy oil-fired boiler. This coating, applied on steam-generating tubes at Tocalo Co. Ltd., had remained for more than 20 years (about 140,000 h) demonstrating the corrosion-resistant effect. Bala et al. (2010) studied the corrosion resistance of Ni–50Cr coatings cold sprayed on two boiler steels SA-213-T22 and SA 516 (Grade 70). The aggressive environment consisted of Na_2SO_4–60%V_2O_5 under cyclic conditions at 900 °C. The Ni–50Cr coated steels showed lesser weight gains than the bare metals and the oxide scales remained intact till the end of the experiment. According to Matsubara et al. (2007), nickel-based self-fluxing alloy coating extended the service life of furnace wall tubes at waste incineration plants due to its excellent corrosion resistance and heat resistance. Fusing of such coatings by induction heating offered improved efficiency and reliability of products. A successful experimental application of 11 units in a waste incinerator revealed virtually no corrosion on the exposed surfaces and showed an improved water heating efficiency over that of the original tubes.

Chatha et al. (2012a, b) investigated the corrosion resistance of HVOF-sprayed Cr_3C_2–NiCr coating on ASME-SA213-T91 boiler steel without and with posttreatment of the coating by sealing and heat treatment. Corrosion tests consisted of exposure to a molten salt (Na_2SO_4–60% V_2O_5) environment at 900 °C under cyclic conditions. Posttreated coating resulted to be more effective than as-deposited coating in enhancing the corrosion resistance of T91 steel. Tao et al. (2009) HVAF sprayed conventional and nanostructured NiCrC coatings. Hot corrosion was conducted in the Na_2SO_4–30%K_2SO_4 environment, in the temperature range of 550–750 °C for periods up to 160 h. Both types of dense coatings possessed high corrosion resistance, especially the nanostructured NiCrC coating. The enhanced grain boundary diffusion in the nanostructured coating not only promoted the formation of a denser Cr_2O_3 scale with a higher rate but also helped to mitigate the Cr depletion at the metal/scale interface. Ceramic coatings are also used against corrosion.

Jansen et al. (2002) compared the performance of dicalcium silicate-based coatings plasma sprayed to that of YPSZ coatings. Coatings were exposed to a V_2O_5–15 wt.% Na_2SO_4 slag at 700 and 900 °C. At 700 °C, gaseous sulfidation was stimulated by an addition of 0.5 vol.% sulfur dioxide in air. The dicalcium silicate withstood combined attack without debonding, while the YPSZ coating deteriorated and spalled. Hirata et al. (2003) investigated the influence of impurities of Al_2O_3 on the hot corrosion resistance against V_2O_5–Na_2SO_4 molten salt. Thickness of damage zone in Al_2O_3 ceramics, whose purity was high, depended linearly on the holding time. On the other hand, thickness of damage zone in Al_2O_3 whose purity was relatively low depended on square root of holding time. In the impurities, SiO_2 especially affected the corrosion rate influencing the diffusion rate of corrosive elements through grain boundaries and thus the corrosion rate.

Two examples of mold protection are presented. For the protection of aluminum for injection mold tools, Gibbons and Hansell (2008) HVOF or plasma sprayed 100 ± 20 μm thick coatings of WC–10Co–4Cr, Cr_2C_3–20(Ni20Cr), 316 Stainless Steel, or Al_2O_3–40TiO_2. Substrates were made of three grades of aluminum: 2014 (90.4–95.0Al 3.9–5.0Cu 0.5–1.2Si 0.4–1.2Mn), 5083 (92.4–95.6Al 4.0–4.9Mg 0.4–1.0Mn), and 6082 (94.7–98.8Al 0.7–1.3Si 0.4–1.0Mn 0.06–1.2Mg). HVOF, except for the alumina–titania coating only plasma sprayed, was the most suitable of the two types of thermal spray systems evaluated, since APS was unable to provide high bond strengths. Furthermore, the processing by HVOF was not found to be detrimental to the fatigue life of the aluminum substrate. Mizuno and Kitamura (2007) HVOF sprayed on AISI-316L substrate MoB/CoCr, a novel cermet material with high durability in molten alloys for aluminum die-casting parts and for hot continuous dipping rolls in Zn and Al–Zn plating lines. This coating presented a much higher durability without dissolution in the molten Al–45 wt.% Zn alloy. Using undercoat was effective to reduce the influence of large difference in thermal expansion between the MoB/CoCr topcoat and stainless-steel substrate.

Combinations of topcoat and undercoat thickness were optimized to obtain intrinsic performance.

19.3.2.3 Oxidation

A variety of oxides can form on the surface and the further oxidation depends on the oxide layer forming a stable and continuous film. Of course, the oxidation depends on the oxygen affinity of the elements forming the alloy. In most cases Cr and Al additions to the coating's matrix are used to form the oxidation barrier. Their quantity must be important enough to provide the renewal of the oxide layer that must be tough, well adhered, and self-healing. Up to 430 °C, chromium–molybdenum steel presents a good resistance to oxidation. Up to 980 °C, the high-chromium-containing (16–28 wt.%) alloys—NiCr, Inconel (Ni–Cr alloys), stellites (Co–Cr alloys), and stainless steel—present a good resistance. Over that temperature superalloys with aluminum (up to 5 wt.%) are used, because aluminum forms an alumina film, which is more adherent than Cr_2O_3, thin enough to be ductile, and nonvolatile at temperatures $\geq$ 1000 °C.

Many studies were devoted to the bond coat and the thermally grown oxide (TGO) layer formation. The problem is that MCrAlY coatings contain only limited aluminum content because high values can lead to brittleness and potential crack. For example, Koolloos and Houben (2000) have shown that pre-oxidation of the bond coat had a beneficial effect on lifetime when the oxidation was the main cause of failure. The pre-oxidation time and temperature were chosen such that a dense alumina layer was formed, and the forming of spinel-type structures avoided. Fossati et al. (2012) sprayed by VPS CoNiCrAlY coatings onto CMSX-4 single-crystal nickel superalloy disk substrates. As-sprayed samples were annealed at high temperatures in low vacuum. Three kinds of finishing processes were carried out producing three types of samples:

- As-sprayed
- Mechanically smoothed by grinding
- PVD coated by using aluminum targets in an oxygen atmosphere

Samples were tested under isothermal conditions, in air, at 1000 °C, and up to 5000 h. Several differences were observed: grinding operations decreased the oxidation resistance, whereas the PVD process can increase the performances over longer time with respect to the as-sprayed samples.

Jiang et al. (2010) designed gradient coating that could provide a balance between high Al content and high stress-bearing ability. The gradient coating showed better performance of re-healing alumina β scale due to its possession of more β phase as Al reservoir. The improved high-temperature performance of the gradient coating was due to the enrichment of Al in the outer layer.

Yuan et al. (2008) sprayed the MCrAlY bond coat by HVOF and D-gun processes. The isothermal oxidation rate at 1100 °C of the TBC system with the HVOF bond coat was two times lower than that of the TBC system with the detonation-sprayed bond coat. The rough surface of the detonation-sprayed bond coat created a large specific surface area and unfavorable oxides on the bond coat.

Pint et al. (2000) investigated by furnace cycling several different oxidation-resistant substrates with dry, flowing oxygen at temperatures from 1000 to 1200 °C. They determined the cyclic lifetimes of YSZ topcoat plasma sprayed or EBPVD deposited. For NiAl + Zr (0.05–0.08 wt.% Zr) substrate, the testing revealed that a more adherent alumina scale may extend the lifetime of commercial EBPVD and PS coatings. Oxide-dispersion strengthened (ODS) FeCrAl substrates with YSZ topcoat seemed promising for the metallic skin of the next-generation space shuttle.

Limarga et al. (2005) produced Al_2O_3/ZrO_2 functionally graded (FG) thermal barrier coating system incorporating an oxygen barrier layer between bond coat and topcoat. Alumina has been highlighted as a potential material as oxygen barrier to improve the oxidation resistance of the bond coat since it has very low oxygen diffusivity. The results showed that FG systems exhibited superior mechanical properties and oxidation resistance at the expense of a slightly lower thermal insulating effect. Thin interlayer was preferred in order to minimize the detrimental effect of phase transformation of γ-Al_2O_3 to α-Al_2O_3 that resulted in tensile residual stresses at the interface.

High-temperature oxidation and corrosion phenomena in boilers are the source of many problems. Both the HVAF-sprayed conventional and nanostructured NiCrC coatings possess good properties against the oxidation and hot corrosion attacks [Chatha SS, et al. (2012a, b)]. Compared with its conventional counterpart, nanostructured NiCrC coating exhibited better performance, which was believed to result from the faster formation of Cr_2O_3 scale with a denser structure. Even after thermal exposure at 650 °C for over 100 h, the nanostructured coating still kept its mean grain size less than 100 nm and seemed to be stable. Consequently, a large number of grain boundaries in the nanostructured coating served as "short circuit" channels for Cr diffusion [Chatha SS, et al. (2012a, b)].

Sidhu et al. (2007) HVOF sprayed WC-NiCrFeSiB coating on Ni-based superalloy (Superni 75) and Fe-based superalloy (Superfer 800H). The coated as well as uncoated specimens were exposed to air and molten salt (Na_2SO_4–25% NaCl) environment at 800 °C under cyclic conditions. The oxides of active elements of the coatings, formed in the surface scale as well as at the boundaries of nickel and tungsten rich splats, contributed to the oxidation and hot

corrosion resistance. These oxides acted as barriers for the diffusion/penetration of the corrosive species through the coatings.

Ramesh et al. (2011) HVOF sprayed Ni-based hard facing NiCrFeSiB alloy powder on three kinds of boiler tube steels. Thermo-cyclic oxidation studies were performed in static air at 900 °C. NiCrFeSiB-coated steels showed slow oxidation kinetics and considerably lower weight gains than uncoated steels. The superior performance was attributed to continuous and protective thin oxide scale of amorphous SiO_2 and Cr_2O_3 formed on the surface of the oxidized coatings.

Kaur et al. (2011) deposited with D-gun Cr_3C_2–NiCr coating on T22 boiler steel. High-temperature oxidation in air and oxidation–erosion in actual boiler environment at 700 °C under cyclic conditions were carried out. While the uncoated boiler steel suffered from a catastrophic degradation in the form of intense spalling of the scale, the Cr_3C_2–NiCr coating showed good adherence to the boiler steel during the exposures with no tendency for spallation of its oxide scale.

Singh et al. (2006) deposited by a shrouded plasma spray process Stellite-6 on two Ni-base superalloys, Superni-601 and Superni-718, and one Fe-base superalloy, Superfer 800H. Oxidation studies were conducted on the coated superalloys in air at 900 °C under cyclic conditions for 50 cycles. The rate of oxidation was observed to be high in the early cycles of the study for the coated superalloys, which may be attributed to the interconnected network of pores and splat boundaries present in the coating structure. The Stellite-6 coating after exposure to air oxidation showed the presence of mainly oxides in its surface scale. The phases revealed where oxides of Cr and Co and spinels containing CoCr mixed oxides were present, oxides reported to be protective in nature against the high-temperature oxidation. Bala et al. (2011) deposited by cold spray Ni–20Cr and Ni–50Cr coatings on two boiler steels. The coatings, in general, were found to follow the parabolic rate of oxidation and were successful in maintaining surface contact with their respective substrate steels.

19.3.2.4 Corrosive Wear

Corrosive wear occurs when the effects of corrosion and wear (C-W) are combined, resulting in a more rapid degradation of the material's surface. A surface that is corroded or oxidized may be mechanically weakened and more likely to wear at an increased rate. Furthermore, corrosion products including oxide particles that are dislodged from the material's surface can subsequently act as abrasive particles. Stress corrosion failure results from the combined effects of stress and corrosion. At high temperatures, reactions with oxygen, carbon, nitrogen, sulfur, or flux result in the formation of oxidized, carburized, nitrided, sulfidized, or slag layer on the surface. Temperature and time are the key factors controlling the rate and severity of high-temperature corrosive attack [Chattopadhyay R (2001)].

The effect of fluids containing solid particles is complex and depends on the surface temperature. At low temperature, the main phenomenon is erosion; with increasing temperature both erosion and oxide scale formation are similar. The loss of oxide prevails with further increase in temperature (chipping of the brittle scale). It is thus necessary to use a compatible matrix with hard reinforcing phases such as carbides and oxides. It is also necessary to limit residual stresses within coating for example by using graded layers.

The problem of erosion–corrosion of materials at elevated temperatures is that the extent of wastage in such environments is dependent on a wide variety of parameters, which include properties of the impacting particles (angularity, for example), impact angle, target material, and nature of the corrosive environment, as well as the composition of the oxide scale formed during the erosion–oxidation process.

Low Temperature

Hill et al. (2012) investigated HVOF-sprayed coatings of Fe–Cr–C and Fe–Cr–V–C on high-chromium high-carbon tool steels in the as-processed state and after a quenching and tempering treatment. Coatings were also achieved by super solidus liquid phase sintering (SLPS). In comparison, sintered steels were analyzed in the quenched and tempered conditions only. The performed heat treatment was able to improve the properties of both steels leading to an increase in hardness due to martensite formation (SLPS and HVOF) and also carbide precipitation (HVOF) and an assumed increase in wear. The lower corrosion resistance of the high-vanadium tool steel X420CrVMo18-16 in comparison to X190CrVMo20-4 was due to a lower concentration of dissolved chromium in the metal matrix. The HVOF coatings showed a decrease in corrosion resistance in relation to the sintered material because of smaller precipitates and formation of chromium oxides. Kembaiyan and Keshavan (1995) deposited, on drill bits in mining, and oil and gas drilling, 82W–15Co–3C by Super-D-gun, 80Ni–10Cr–4Fe–4Si–1.8B–0.4C by spray fused and laser cladded, Fe–Cr–Ni by wire feed and fuse welded, WC-based by plasma, and 36Ni–44W–6Cr–6Co–1.8Si–1.9Fe–1.35B by flame and laser cladded, and all were heat-treated afterward. The D-gun coating offered beneficial compressive residual stresses on the inserts and cone shell, thereby being the best coating protecting three cone drill bits from corrosion and fluid erosion. Uozato et al. (2003) plasma sprayed Fe–C powders, with or without nickel added (up to 14 wt.%), on a cast AA383 aluminum alloy plate. Corrosion and wear tests in engine oil with or without sulfuric acid water solutions added were performed as well. The corrosion performance was dependent upon the nickel content.

Souza and Neville (2007) studied the influence of microstructure on the overall material loss in erosion–corrosion environments for WC–Co–Cr coatings applied by HVOF

and D-gun processes. The work was devoted to the enhancement of erosion due to corrosion effects. HVOF coatings had a slightly lower corrosion resistance than the D-gun coatings but higher overall erosion–corrosion resistance. The formation of different tungsten species, η phases, and a higher Cr amount reduced the toughness of WC–Co–Cr coatings and the corrosion rates under erosion–corrosion. Stainless steel components coated with Inconel-625 are very common in the oil/gas industry. That is why Al-Fadhli et al. (2006) HVOF sprayed Inconel-625 on three different metallic surfaces:

- Plain stainless steel (SS)
- Spot-welded stainless steel (SW-SS)
- Composite surface of stainless steel and carbon steel welded together (C-SS-CS)

The erosion experiment was carried out using a jet impingement rig through which natural seawater (pH = 8.3) or sand slurry was circulated. The coating exhibited excellent erosion–corrosion resistance, as it was not highly affected by the type of substrate material. The coating was found to be highly sensitive to the presence of sand particles in the impinging fluid. As the period of coating exposure to the flow of slurry fluid increased, weight loss increased significantly, the increment being dependent on the type of substrate material.

Polymer coatings have received increased attention as protection against corrosion and wear for several environmental conditions mainly in the automotive, petrochemical, oil, and gas industries. Lima et al. 2012) flame sprayed (Terodyn-System-2000 gun of Eutectic) polyetherimide (PEI), poly-ether-ether-ketone (PEEK), and polyamide-12 (PA-12) polymers onto carbon steel substrates. The obtained coatings had formed a dense and smooth deposit with good adhesion and no significant defects. The abrasive wear test showed a better performance for PA-12 samples, almost twice better than PEEK and 20% better than PEI. PA-12 and PEEK coatings showed no corrosive attack in a very aggressive H_2SO_4 40 vol.% solution after 2000 h of testing. Under the experimental conditions used in their work [Lima CRC, et al. (2012)], PEEK and PA-12 coatings had a better corrosion performance, but PA-12 had much better abrasive wear performance.

As the presence of sand and mineral particles flowing in a corrosive fluid produced a high degradation rate of the hydrotransport equipment, Flores et al. (2009) studied the erosion–corrosion behavior of two tungsten carbide cermet coatings obtained by PTA process. Two variations of the CNiCrFeBSi matrix, called soft and hard, with different concentration of Cr, C, and B were evaluated with and without reinforcing hard phase. Important microstructural differences were identified between the two metal matrix composites (MMCs). Elongated precipitates rich in W and Cr were identified near the WC grains and in the matrix phase of the WC-hard overlay. Needle-like precipitates with a lower concentration of W were identified in the WC-soft overlay. For both MMCs the γ-Ni phase and silicides were present in the matrix phase. The MMC with the harder matrix showed the lower mass loss and the erosive degradation was predominant in the overall erosion–corrosion process at the lower temperature. A different behavior was observed when the temperature of the testing solution was increased, and a low sand concentration was used. PTA coatings are excellent, when wear and corrosion are present at low temperature.

High Temperature

Sidhu and Prakash (2006) evaluated the erosion–corrosion (E-C) behavior of as-sprayed plasma and laser remelted Stellite-6 coatings on boiler tube steels (three different ones) in the actual coal-fired boiler environment at 755 °C. Coating has been found to be effective in increasing the E-C resistance of boiler steels in the coal-fired boiler environment. Among the as-coated steels the highest E-C resistance has been observed for T11 steel, probably due to the presence of a continuous chromium-rich band lying at bond coat–substrate interface. A less porous structure obtained after laser remelting was found to be effective for increasing E-C resistance to the given environment for this coated T11 steel.

Wang (1996) HVOF sprayed Cr_3C_2–NiCr coating and tested them in conditions simulating erosive conditions in tubular heat exchangers of fluidized-bed combustor boilers. These coatings showed excellent E-C behavior as compared with 1018 steel and A213 T22 steel. Coating high E-C resistance was attributed to its high compactness, fine grain size structure, and the homogeneous distribution of the skeletal network of hard carbides within a ductile, corrosive-resistant metal binder. Uusitalo et al. (2002) sprayed various coatings by HVOF, wire arc, and plasma and simulated the E-C conditions in the superheater section of a circulating fluidized-bed combustor by a burner-rig type working at elevated temperature. The gas temperature was 850 °C and the specimen temperature was adjusted to 550 °C by cooling the specimen internally with pressurized air. In E-C tests in presence of chlorine, nickel-based HVOF coatings performed the best, whereas carbide containing HVOF coatings and diffusion coatings wore away.

Kaur et al. (2011) D-gun sprayed Cr_3C_2–NiCr coating on T22 boiler steel. Coated and not coated boiler steel were subjected to high-temperature oxidation in air and oxidation–erosion in actual boiler environment at 700 °C. The uncoated boiler steel suffered from a catastrophic degradation in the form of intense spalling of the scale in both environments. The Cr_3C_2–NiCr coating showed good adherence to the boiler steel during the exposures with no tendency for spallation of its oxide scale.

Kim and Walker (2007) developed a nanostructured titania coating for ball valves destined for high-pressure acid-leach (HPAL) service. The nanostructured titania coating provided dramatically superior resistances against abrasive and erosive wear compared to titania conventional coatings. The enhanced wear performance seemed to be due to improved toughness. The nanostructured titania coating has been applied onto ball valve components in ten locations around the world and has performed very well. PTA coatings are also successful against corrosion and wear at high temperatures.

19.3.3 Thermal Barrier Coatings

Thermal barrier coatings (TBCs) help to protect the base metal/alloy from high-temperature exposure, allowing for the running of engine parts at higher temperatures and achieving higher energy efficiencies. The successful use of TBCs in a given application depends, however, on the ability to overcome the often-significant mismatch between the expansion coefficient of the coating and that of the substrate. The challenge lies in the fact that good heat flux protection requires the use of low thermal conductivity materials that are generally either refractory metals (W, Mo, Ta, Nb) or oxides (Al_2O_3, or ZrO_2), which generally has low thermal expansion coefficients compared to those of the metals or alloy substrate. On thermal cycling, such a mismatch of thermal expansion coefficient between the coating and the substrate would result in the development of cracks in the coating followed by its spalling and catastrophic failure. One of the options used to mitigate such a problem is the spraying of an intermediate "bond coat" to bridge the expansion coefficient mismatch. Moreover, because of the inherent porosity of oxide-based TBCs, bond coats contribute to the added protection of the substrate metal or alloy from oxidation by the high-temperature oxidizing environment to which it is exposed. In this section, a review is presented of the range of materials commonly used as TBCs and the influence of their stabilization chemistry and the thermal spray technique used for their deposition on their performance. Examples of their industrial applications is given in the next section: 19.4 Thermal Spray Coating by Industry.

Among oxide-based TBCs, alumina and zirconia are among the most widely used materials. Alumina can generally be used up to 900 °C since at higher temperature the γ phase of plasma-sprayed alumina coatings transform into α phase, with an important volume change resulting in coating cracking and peeling off. Zirconia, on the other hand, while being by far the most accepted TBC material, must be stabilized to avoid phase transformations with temperature during its service life. The problem is then the associated cost of the stabilizer material used. The lowest-cost stabilizers, being CaO or MgO, mostly used for TBC coatings in diesel engines, are acceptable for exposure to temperatures below 600 °C above which the stabilization becomes inefficient [Billah BM, et al. (2012)]. For TBCs used in higher-temperature environment, yttria is widely used either at a concentration of 7–8 wt.% in yttria partially stabilized zirconia (YPSZ, tetragonal phase) or 12 wt.% in yttria stabilized zirconia (YSZ, cubic phase). Their maximum service temperature in this case is around 1200 °C and the thermal conductivity of plasma-sprayed coatings is around 1 W/m K. When using powder manufactured from chemical route (sol–gel technique with an intimate mixing of zirconia and yttria at the nanometer level) the maximum service temperature reaches 1350 °C, at the expense of higher cost for the powder.

Other stabilizers, such as CeO_2, GeO_2, Nb_2O_5, To_2O_5, and Sc_2O_3, have also been used in spite of their high cost compared to Y_2O_3, and the need for up to 24 wt.% concentration of the stabilizer oxide in the mix for zirconia stabilization. Even if their thermal conductivities are generally slightly lower than that of ZrO_2-7 wt.% Y_2O_3, their maximum service temperature is about the same. Zirconia stabilized with CeO_2 [Hamacha R, et al. (1996), Ma B, et al. (2009)] offers low thermal conductivity, less phase transformation than YSZ, but increased sintering rate compared to YSZ. Zirconia partially stabilized with dysprosia [Markocsan N, et al. (2007), Curry N, Donoghue J (2012)]. On the other hand, while being more resistant to sintering than standard YSZ coatings up to 200 h at 1150 °C, their thermal properties are significantly influenced by the operating conditions with lowest thermal conductivity reached at high temperatures with the 4DyPSZ coatings (0.70 W/m K at 700 °C and 0.76 W/m K at 1000 °C). Zirconia has also been doped by different rare-earth cations with the formation of dopant clusters as in the ZrO_2–Y_2O_3–Nd_2O_3(Gd_2O_3, Sm_2O_3)–Yb_2O_3(Sc_2O_3) [Gupta M, et al. (2012)]. Pyrochlore structure ($A_2B_2O_7$) materials such as La_2ZrO_7, Nd_2ZrO_7, and $Gd_2Zr_2O_7$ that melt at temperatures over 2000 K without phase change offer properties comparable to YSZ with a lower thermal conductivity, especially $La_2Zr_2O_7$, which has excellent thermal stability [Cao XQ, et al. (2004)].

Hexa-aluminates such as (La,Nd)$MAl_{l1}O_{19}$, where M could be Mg and Mn to Zn, Cr, and Sm, present excellent longtime sintering resistance and structural stability up to 1800 °C. For example, Chen et al. (2011a, b, c) have sprayed YSZ-based composite coatings with the addition of $LaMgAl_{11}O_{19}$ (LaMA) as the secondary phase. Unfortunately, composite coatings showed much shorter thermal cycling lifetime than the monolithic YSZ coating due to the presence of as-sprayed LaMA (La $MgAl_{11}O_{19}$) coating with a large amount of amorphous phase reducing the thermal insulating efficiency and accelerating the oxidation and degradation of bond coat. Chen et al. (2012) also sprayed five-layer functionally graded TBCs based on LaMA/YSZ

system. The amorphous LaMA phase underwent recrystallization processes during high-temperature aging, resulting in the formations of LaMA platelet-like grains and imparting the TBC with improved thermal and mechanical properties and a higher strain tolerance. Such coatings presented a good thermal cycling lifetime at the surface testing temperature above 1350 °C.

Perovskites (ABO_3 crystal structure such as $BaZrO_3$ or $SrZrO_3$ or $CaZrO_3$) have also been extensively studied [Cao XQ, et al. (2004)]. Jarligo et al. (2009) synthesized $Ba(Mg_{1/3}Ta_{2/3})O_3$ and $La(Al_{1/4}\ Mg_{1/2}\ Ta_{1/4})O_3$ compositions and plasma sprayed them as ceramic topcoats of TBC either in single layer or in double-layer combination with conventional YSZ. The low value of fracture toughness for the complex perovskites and the thermally grown oxide at the topcoat–bond coat interface of the TBCs were, however, the major factors that led to the coating failure on thermal cycling at about 1250 °C. Similar results were obtained by Ma et al. (2008). Yu et al. (2011) tested $Sm_2Zr_2O_7$ coatings that exhibited low microhardness and elastic modulus, which increased with rise in aging temperature because of the microstructure reconfiguration.

Other ceramics were also tested. $LaTi_2Al_9O_{19}$ (LTA) was synthesized by solid-state reaction at 1773 K by Xie et al. (2010), and the mechanical properties of the LTA bulk were evaluated. A double-ceramic layer LTA/YSZ TBC structure was proposed, and the TBC sprayed by plasma spraying. The LTA/YSZ TBC remained intact even after 3000 cycles, exhibiting a promising potential as new TBC materials. Guo et al. (2009) produced $BaLa_2Ti_3O_{10}$ (BLT) by solid-state reaction and plasma sprayed it. The coating contained segmentation cracks and had a porosity of around 13%. Thermal cycling result showed that the BLT-TBC had a lifetime of more than 1100 cycles of about 200 h at 1100 °C and the failure occurred by cracking at thermally grown oxide (TGO). Ceramic mixtures were also proposed: Liu et al. (2008) showed that the La_2O_3 addition can effectively alleviate the grain growth of YSZ coatings under high temperatures.

Besides the materials choice, attention was also given to the effect of powder properties such as purity and particle morphology on the TBC coatings obtained using different thermal spray technologies. Paul et al. (2007) reported that improvement in the purity of the YSZ powder used in the process, through a reduction in its free alumina and silica content, from 0.1–0.2 wt.% down to 0.01–0.05 wt.%, gave rise to significant reduction in the sintering rates of produced TBC. Tan et al. (2012) showed that with proper process mapping strategies and spraying hollow powders, it was feasible to produce tailored microstructures with substantially lower thermal conductivity than generally reported for YSZ-TBCs. It also allowed enhancing thermo-structural compliance and reducing propensity to sintering during elevated temperature exposure. Guo et al. (2004) studied the segmentation cracks density of thick TBCs (1.5 mm) for thermal protection of combustor. A segmentation crack density of 3.65/mm exhibited a thermal cycling lifetime of more than 1500 cycles at 1250 °C for the surface/950 °C for the bond coat, indicating an excellent thermal shock resistance.

Zhu et al. (2004) tested conventional TBCs (APS sprayed ZrO_2–8 wt.% Y_2O_3 with a NiCrAlY VPS bond coat) sprayed onto 25.4-mm diameter and 3.2-mm thick nickel base superalloy specimens. A high-power CO_2 laser was used to test the TBC specimens under high-temperature (1287 °C) and high-thermal-gradient cyclic conditions. If the initial average crack propagation rates were in the range of 3–8 μm/cycle, the crack propagation rates increased to 30–40 μm/cycle at later stages of testing and the critical spalling crack size ranged from 3 to 5 mm. According to Shin et al. (2011), the failure of TBC is directly connected to the failure of the blades because the spallation of the ceramic layer accelerates the local corrosion and oxidation. They performed thermal fatigue tests at 1100 °C and 1151 °C for coin-type specimens. Delamination cracks occurred at the edge of a specimen first and then the area of the edge delamination gradually increased toward the center. A thermally grown oxide (TGO) was formed and grew at the interface between the topcoat and the bond coat. The crack propagated with increase in cycle number, growth resulting from the TGO formation, and the high normal stress at the edge. Kim et al. (2010) also investigated the failure mechanisms of coin-shaped plasma-sprayed TBCs for gas turbine blades due to cyclic thermal fatigue. Hernandez et al. (2009) quantified, through finite element analyses, the thermomechanical response of the bond coat (NiCoCrAlY) and the thermally grown oxide (TGO) for a YPSZ. The models they developed include nonlinear and time-dependent behavior such as creep, TGO growth stress, and thermomechanical cyclic loading. Eriksson et al. (2011) for the same type of TBCs studied the effect of three different heat treatments—isothermal oxidation, thermal cycling fatigue (TCF), and Burner Rig Test (BRT)—using a thermal shock rig (TSR). The specimens subjected to BRT gave much thinner interface TGO due to their shorter exposure time to high temperature, and the TGO consisted almost exclusively of Al_2O_3. TCF-subjected specimens had areas of cracked interface TGO, while the thin interface TGO in the BRT-subjected specimens did not contain any cracks. Jang et al. (2006) studied TBC bond coats (0.08, 0.14, and 0.28 mm) HVOF sprayed. The TGO layer with the thickness of 2.8–3 μm was formed after thermal fatigue tests, showing the same effects in both the temperature and the dwell time. The bond coat thickness did not affect the formation of the TGO layer. As the thickness of the bond coat increased, the damage zone in the substrate decreased, the bond coat acting as a buffer layer under applied loads. Re-sintering of the top coating during the thermal fatigue tests was evident from

the fatigue damage and the observed increase in the hardness values. Li et al. (2010a, b) examined through thermal cyclic test TBCs' behavior with the NiCoCrAlTaY bond coats deposited by cold spraying and low-pressure plasma spraying. The surface of the cold-sprayed bond coat presented a smoother configuration than that of the LPPS-sprayed bond coat. Ni/Cr oxides easily formed on the LPPS bond coat during oxidation. In contrast, TGO on the cold-sprayed bond coat was uniform in both thickness and composition. The uniform protective TGO enhanced the thermal cyclic behavior of the TBCs. These results suggested that cold spraying is a promising process to deposit MCrAlY bond coat for high performance of TBCs.

The evolution of TBCs for aero engines is well summarized when comparing review papers published at the end of 1990s [Musil J, et al. (1997), Soechting FO (1999), Beele W, et al. (1999)] with more recent ones [Cao XQ, et al. (2004), Vaßen R, et al. (2010), Gupta M, et al. (2012)] and also those related to coating materials [Haynes JA, et al. (2000), Hamacha R, et al. (1996), Ma B, et al. (2009), Markocsan N, et al. (2007), Curry N, Donoghue J (2012), Chen X, et al. (2011a, b, c), Chen X, et al. (2012), Jarligo MO, et al. (2009)]. In 1999, Miller (1997) said that TBCs have evolved from the laboratory to low-risk turbine section applications and then on to an integral part of engine design. Beele et al. (1999) underlined that if partially stabilized zirconia became the standard material very early on, thermal spraying and electron beam physical vapor deposition (EBPVD) in the early 1990s were even considered as competing technologies. In 2008, Feuerstein et al. (2008) emphasized that "the most advanced thermal barrier coating (TBC) systems for aircraft engine and power generation hot section components consisted of electron beam physical vapor deposition (EB-PVD)-applied yttria-stabilized zirconia and platinum-modified diffusion aluminide bond coating. Thermally sprayed ceramic and MCrAlY bond coatings, however, are still used extensively for combustors and power generation blades and vanes. However, as for any industrial production, the coating cost is a key parameter. For thermal spray processes, the labor and material costs are the major ones, while for EBPVD, the equipment cost is substantial (up to 50% of the cost is for depreciation interest) [Feuerstein A, et al. (2008)] and its utilization must be effective. During the last decade many works were devoted to bond coats: see Toscano et al. (2006). Yttria partially stabilized zirconia (YPSZ) was identified as the best ceramic topcoat material and has been established as standard for the last 30 years. However, correlatively, especially the last decade, other ceramic materials have been studied.

Plasma spray physical vapor deposition (PS-PVD), recently developed by Sulzer Metco [von Niessen K, et al. (2010)], is a low-pressure plasma spray technology to deposit TBC coatings out of the vapor phase. PS-PVD is a part of the family of new hybrid processes. It is then possible to deposit a coating by vaporizing the injected material. Coatings show a unique columnar microstructure, so far only known from other vapor phase deposition processes like EB-PVD. But economical evaluations for columnar coatings on turbine components under production conditions show a clear saving potential when using the PS-PVD process. Hospach et al. (2012) showed that quasi-vapor deposition from clusters resulted in columnar coatings with high porosity and growth rate. The low working pressure (about 100 Pa) increased the size of the plasma plume and enabled homogeneous coatings, which made this process interesting, in particular for large-scale applications.

New developments in suspension or solution plasma spraying seem also very promising (see Chap. 16, Nanocrystaline and Nanostructured Coatings). Vaßen et al. (2010) pointed out that suspension spraying offers the manufacture of strain-tolerant, segmented TBCs with low thermal conductivity. In addition, highly reflective coatings, which reduce the thermal load of the parts from radiation, can be produced. Gell et al. (2008) showed that solution-sprayed TBCs have a microstructure characterized by: strain relieving through thickness vertical cracks, and fine, dispersed porosity ultra-fine splats with enhanced splat-to-splat bonding. First tests showed that such coatings have equal or greater durability, lower thermal conductivity, higher in-plane toughness and bond strength, and costs comparable to APS. However, to our best knowledge such coatings have not yet been tested in industry

19.3.4 Electrical and Electronic Coatings

One of the main problems of electrically conductive thermally sprayed materials, except those cold sprayed or plasma sprayed in soft vacuum VPS, is oxidation during the process, which increases the electrical resistance of the coating. Some thermally sprayed coatings are used to produce resistance heating panels. The choice of the resistance material must be such that the variation of its electrical resistance with temperature is as low as possible because otherwise electronic devices must be used to adapt the voltage to the resistance variation.

Alumina is probably the most used material. The α and γ phases present different dielectric constants and loss tangent at high frequency. The γ phase resulting from the spray process can be avoided either by keeping the substrate at 1000 °C, which is not easy to do with most substrates and requires a careful temperature control during cooling to avoid cracks, or by stabilizing it with elements such as MgO or Cr_2O_3. If the γ phase is not the phase suitable for high-frequency applications, as the α phase, the voltage breakdown is close for both phases. The dielectric

properties of alumina coatings depend strongly upon their microstructure and spray conditions [Pawlowski L (1995), Beauvais S, et al. (2005)]. One of the drawbacks is that the alumina coating's electrical resistivity is strongly dependent on the air humidity due to the increase in water adsorption in the porous coating, generating ionic conductivity. Toma et al. (2011) made the comparative study of the electrical properties and characteristics of thermally sprayed alumina and magnesium spinel coatings sprayed by HVOF and plasma. At low humidity levels, the electrical resistivity of alumina and spinel coatings was comparable (on order of magnitude of 10^{11} Ω m). At a very high humidity level (95% relative air humidity [RH]), a dramatic decrease in resistivity of about five orders of magnitude for alumina coatings and about four orders of magnitude for spinel coatings was observed, water adsorption generating ionic conductivity. HVOF spinel coatings presented the best dielectric strength values ($E_d > 30$ kV/mm against 20 kV/mm for sprayed alumina) and were less sensitive to moisture. Thus, these coatings can be considered as potential candidates for use in insulating applications. Toma et al. (2012) studied microstructural characteristics and electrical insulating properties of thermally sprayed alumina coatings produced by suspension HVOF (S-HVOF) and conventional HVOF spray processes. The better electrical resistance stability of the suspension-sprayed Al_2O_3 coatings could be explained by their specific microstructure and retention of a higher content of α-Al_2O_3. Kim et al. (2001) studied, for plasma-sprayed Al_2O_3–13% TiO_2 coatings, the effect of two commercial sealants based on polymers on the electrical insulation properties before and after the impregnation treatment. Cipri et al. (2007) studied the interesting electromagnetic properties (complex permittivity) of Al_2O_3–SiO_2 compounds plasma sprayed. For microwave and nuclear fusion applications, BeO is sprayed by inert plasma-spraying process but its toxicity requires very stringent spray conditions.

Prudenziati et al. (2006, 2008a, b) have studied Ni, Ni20Cr, or Ni5Al coatings plasma sprayed onto alumina films deposited onto steel plates. They compared electrical properties of resistors prepared with Ni and Ni–20Cr powders by thermal spray processes (APS and HVOF). The resistivity of Ni resistors decreased after annealing at temperatures in the range 200–400 °C, which may be due to healing of structural defects. On the contrary, the observed increase in resistivity of Ni–20Cr-based resistors were possibly due to ordering of the atoms. The temperature dependence of resistance for Ni-based resistors was invariably the same as for Ni bulk, regardless of sample origin. On the other hand, a large spread in temperature coefficient of resistance (TCR) values of Ni–20Cr-based resistors was observed. Ni-based resistors had an excellent reproducibility of the resistance versus the temperature curves, making them excellent candidates for temperature sensors and self-controlled high-temperature heaters.

To limit oxidation in flight, cold spray can be used. In spite of the low flattening degree of cold-sprayed (CS) coatings, the anisotropy does not disappear even after annealing [Champagne VK (2007)]. However, when compared to thermally sprayed coatings, the electrical resistivity of cold-sprayed ones is lower (three to five times) [Gärtner F, et al. (2006), Marx S, et al. (2006), Wu X-K, et al. (2012a, b)].

For electronics, the following applications and development areas of cold spray process can be indicated [Gärtner F, et al. (2006)]:

- Deposition of electric screening coatings on plastics
- Generation of conducting structures on nonmetals
- Deposition of brazing and soldering alloys

For example, Gui et al. (2004) plasma sprayed, onto a graphite substrate, Al matrix composites with high-SiC volume fraction. Al-55SiC and Al-75SiC powders were milled by stainless steel and ZrO_2 balls in a conventional rotating ball mill for 1–10 h. The SiC particles exhibited a reasonably uniform distribution in the composites sprayed from the milled powders. The Fe contamination occurred to the milled powders when stainless steel balls were used. Waveguide devices for microwave applications were achieved by spraying ferrites and dielectrics.

Yamakawa et al. (2009) have studied ceramic trays (a type of kiln furniture) used for firing multilayer ceramic capacitors (MLCC) that are used in a large number of electronic appliances. They are being required in more compact sizes, larger capacities, and with reduced costs year by year. High thermal-shock resistance and reaction resistance are desired properties for these ceramic trays. They showed that the application of plasma-sprayed ZrO_2 topcoat and an Al_2O_3-sintered basecoat made it possible to enhance longevity and reduce cost.

Thermal spray coatings cannot compete with PVD techniques to manufacture electronic devices, but wire arc sprayed coatings are used as shielding material to eliminate electromagnetic and radio frequency interference and dissipate static discharge sparks. Zn and Al are currently used to protect computers, electronic office equipment, medical monitoring devices, housing constructed of temperature-sensitive plastic, and rooms containing military computers. Donner et al. (2011) have cold sprayed copper coatings onto previously thermally sprayed Al_2O_3 coatings. They either applied a bond coat on the ceramic layer or used heated substrates during the cold spray process. By both alternatives, dense copper layers were produced. The electrical conductivity reached 98% of International Annealed Copper Standard (IACS) in the as-sprayed condition on heated substrates, or

90% of the IACS value after spraying on cold substrates with aluminum bond coat and additional heat treatment, thus meeting the requirements for electronic applications. Lin et al. (2011) plasma sprayed surfaces of copper plates with a thick alumina layer to fabricate a composite with a dielectric performance suitable as substrate in electronic devices with high thermal dissipation. They concluded that an alumina layer thickness of 20 μm provided low surface roughness, low thermal resistance, and highly reliable breakdown voltage (38 V/μm). Most telecommunication systems and wireless networks operate at radio and microwave frequencies. However, due to the ever-increasing exploitation of these frequencies, both electromagnetic interference (EMI) pollution and interference occur [Osbond P (1992)]. Various plastic- and foam-layered instruments and computer equipment cases require shielding. That can be achieved by wire arc spraying zinc coating on the case—zinc because of its low melting temperature and wire arc because of the low heat flux of the process. Of course, it is better using nitrogen atomization to keep the electrical conductivity of the coating as low as possible with as less as possible oxide within coating. For military applications, the whole room can be shielded with a zinc or aluminum film wire arc sprayed outside of it.

Broadband electromagnetic wave absorbers usually correspond to spinel ferrites and hexa-ferrites operating at 45–75 GHz. Unfortunately, these materials are usually decomposed when sprayed. Lisjak et al. (2011) found a solution by plasma spraying atomized particles of hexa-ferrite and polymer. The hexa-ferrite crystalline structure was preserved during the spraying, while the polyester partly melted and resolidified during cooling. The coupling of the hexa-ferrite magnetic and dielectric losses with the polyester dielectric losses resulted in the superior properties of the composite coating with respect to the pure single-phase coating of the constituent phases.

Nd–Fe–B permanent magnets have been sprayed by vacuum plasma spraying [Rieger G, et al. (2000)]. The review by Sampath (2010) presents a few ferrites and soft magnetic materials plasma and HVOF sprayed that could be interesting for industrial applications.

According to the review paper by Sampath (2010), interesting prospective seems to be the innovative direct write thermal spray (DWTS), which is a new and exciting manufacturing technology capable of depositing a large number of electronic materials on a wide range of substrates, enabling direct write fabrication of multilayer thick film electronic devices. One of the exciting prospects of this technology is the fabrication of integrated, embedded sensors directly onto thermal spray-coated components. Sampath (2010) also presents the past, present, and future of thermal spray applications in electronics and sensors. The different dielectrics that are used or that have been used are presented: alumina, beryllia, $MgO–3Al_2O_3$ spinel, alumina–titania, cordierite ($2MgO–2Al_2O_3–5SiO_2$), and forsterite ($MgO–SiO_2$); perovskite-based dielectric systems including lead zirconate titanate (PZT), $BaTiO_3$, and strontium-doped $BaTiO_3$, and the like, deposited by plasma or HVOF.

Cold-sprayed nickel or further ferromagnetic metals and alloys are used as induction heating coats on cooking appliances or cooking pots [Marx S, et al. (2006)]. Superficial metallization on polymer improves the corrosion-resistant and antiaging property but also achieves some special features such as electrical conductivity, thermal conductivity, electromagnetic shielding, and radial protection [Wu X-K, et al. (2012a, b)].

Electrically conductive and flexible aluminum coatings (flame sprayed with powder or wire) were deposited onto diverse polyester textiles for wearable electronics, lighting, or communication in medical techniques [Voyer J, et al. (2008)]. Coatings produced using wire as raw material had much better morphologies than those produced using powder as starting material. Successful preliminary test results for Al–polyester composites used as current collectors showed that application-specific electrically conductive composites with adjustable specific surface conductivity values and microstructures can be produced without inducing any thermal or chemical damages to the fabric material [Voyer J, et al. (2008)].

19.3.5 Medical Applications

Orthopedic and dental market is developing very fast with either bioinert coatings (Ti-6Al-4V, Ti-6Al-7Nb, Ti-13Nb-13Zr) or bioactive ones (hydroxyapatite [HA], tricalcium phosphate) [Yang Y, et al. (2006a, b), Ong JL, et al (2006)]. Two types of coatings are used [Davis JR (ed) (2004)]:

First, bioinert ones, with no activity between them and the bone or soft tissues, the most used materials being Ti and Ti-6Al-4V. These coatings must be porous (at least 30%).

Second, bioactive coatings, interacting with bone to promote bonding interfaces, are ceramic coatings with material compositions similar to that of bone tissue (calcium phosphate). The most used ceramic is hydroxyapatite ($Ca_{10}[PO_4]_6[OH]_2$) exhibiting a strong activity to join the bone. Examination of four retrieved HA-coated orthopedic prostheses by Gross et al. (2004) has indicated bone attachment, along with coating removal, from a range of areas on the prosthesis surface. Coating removal occurred by dissolution provided by the higher bone-remodeling rate accompanied by the release of calcium and phosphate. Coatings dissolved faster on elevated areas or those subjected to a higher level of loading. Coatings located in less loaded areas provided a higher longevity. In fact,

very different methods have been tested to spray HA [Khor KA, et al. (1997a, b)].

RF induction plasma-sprayed coatings [Roy M, et al. (2011)], where the HA coatings, prepared with supersonic plasma nozzle, were highly crystalline in nature with insignificant phase decomposition. Both the crystallinity and purity of HA decreased when sprayed with normal plasma nozzle.

Air plasma-sprayed coatings and HA- and HVOF-sprayed nano-titania coatings on Ti-6Al-4V and fiber-reinforced polymer composite substrates [Legoux J-G, et al. (2006)] were compared. The surface cell coverage after 7 days of incubation was more complete on nano-TiO_2 than HA. Preliminary results indicated that osteoblast activity after 15 days of incubation on nano-TiO_2 was equivalent to or greater than that observed on HA. Chang et al. (1998) studied hydroxyapatite coatings sprayed with a vacuum plasma spray system at different power levels. They showed that the spray power greatly affected the crystallinity, chemical composition, and microstructure of as-sprayed hydroxyapatite coatings, which were linked to the melting state of hydroxyapatite powder. Prevéy (2000)], to overcome the complexities of characterizing plasma-sprayed HA coatings, has developed an external standard method of XRD quantitative analysis that can be applied nondestructively. Khor et al. (1997a, b) have studied the formation of a composite made of HA and Ti-6Al-4V, APS or HVOF sprayed, to enhance the poor mechanical properties of hydroxyapatite (HA). The composite presented excellent bond strength due to the superior interfacial bond between the Ti-6Al-4V rich splats and the substrate. Wang et al. (1998) have studied the preparation of a functionally graded bio-ceramic coating composed of essentially calcium phosphate compounds.

HVOF-sprayed HA compared to plasma-sprayed one: The HVOF system has proven to be a novel method for HA deposition with maximum crystallinity and purity values of 93.81 and 99.84%, respectively. With U.S. Food and Drug Administration (FDA)-approved plasma spray technique, values of only 87.6 and 99.4% crystallinity and purity, respectively, were found [Hasan S, Stokes J (2011)].

HVOF-sprayed nanostructured titania (n-TiO_2) and 10 wt.% hydroxyapatite (n-TiO_2-10 wt.% HA) powders have been engineered by Lima et al. (2010) as possible future alternatives to HA coatings deposited via air plasma spray (APS).

The n-TiO_2-10 wt.% HA coatings exhibited bond strength levels higher than 77 MPa, that is, at least twice those of APS HA coatings deposited on Ti-6Al-4V substrates. In addition, due to the high stability of TiO_2 in the human body, longevity-related concerns of HA coatings, such as dissolution and osteolysis, were unlikely to occur. HA coatings with a high content of both crystalline HA and nanostructures were preferred for cell proliferation [Lima RS, Marple BR (2007)].

Coatings resulting from agglomerated nanostructure coatings: It was demonstrated by using an osteoblast cell culture (in vitro) that the type of HA coating phase is more important than the nanostructure character of the coating; however, HA coatings with a high content of both crystalline HA and nanostructures were preferred for cell proliferation [Lima RS, Marple BR (2007), Lima RS, et al. (2006, 2010)]. Based on cell culture (in vitro) results observed for bulk nanostructured ceramics, the nanostructure zones being found on the TiO_2 coating surface may have played an important role in producing good biocompatibility results. However, up to this point there is no experimental evidence to prove this [Lima RS, Marple BR (2007)].

ZrO_2/SiO_2 composite coatings have high-abrasive wear resistance compared with pure HA and HA/ZrO_2 coatings because they exhibit high hardness and dense structure. The in vitro test of the composite coatings in simulated body fluid showed a growth of nanometer-sized particles apatite after the immersion of the coatings for 20 days [Morks MF, Kobayashi A (2008)].

Well-adherent, flawless, glass–ceramic (SiO_2-CaO-K_2O) coatings on alumina and Ti6-Al-4V substrates were realized [Vitale-Brovarone C, Verné E (2005), Xie Y, et al. (2009)]. The obtained results were reproducible and the applied techniques were low cost and not complex. When tested in vitro, the coatings showed an extensive precipitation of a thick HA layer, well adherent to the coatings.

SiO_2-CaO-P_2O_5-based bioactive glasses (BAGs) and glass–ceramics are attractive materials for biomedical applications, because of the excellent levels of bioactivity, which can be achieved by formulating and selecting appropriate compositions [Bolelli G, et al. (2009a, b)]. Preliminary results with high-velocity suspension flame spraying bioactive glasses seemed to be promising.

HA coatings deposited by HVOF spraying showed similar advantages as coatings obtained by APS, but with higher crystallinity. Heat treatment of the coating allowed crystallization of the amorphous calcium phosphate (ACP) present in the coatings [Fernandez J, et al. (2007)]. XRD analysis confirmed that the ACP transforms directly to HA and not to other calcium phosphate phases. Similarly, functionally graded calcium phosphate coatings were produced on Ti-6Al-4V substrates by plasma spraying [Fernandez J, et al. (2007)]. The microstructure of the coating was dense with the typical lamellar structure. The top layer of the coating was mainly composed of tricalcium phosphate (TCP), which suggested high bio-resorbability. After post-spray heat treatment, the TCP phase, from either the decomposition of HA or the TCP feedstock, and the tetracalcium

phosphate (TTCP) phase were no longer detected by XRD, but the CaO phase remained.

Yu et al. (2003) plasma sprayed HA coatings and post spray treated them by the Spart Plasma Sintering (SPS) technique at 500 °C, 600 °C, and 700 °C for duration of 5 and 30 min. The HA coatings treated in SPS for 5 min revealed rapid surface morphological changes during in vitro incubation (up to 12 days), indicating that the surface activity is enhanced by the SPS treatment.

Bellucci et al. (2012) coated titanium plates by high-velocity suspension flame spraying (HVSFS) technique using a novel bioactive glass composition based on the K_2O–CaO–P_2O_5–SiO_2 composition ("Bio-K"). On half of the samples, an atmospheric plasma-sprayed (APS) TiO_2 bond coat was preliminarily deposited; suspensions of attrition-milled micron-sized glass powders, dispersed in a water and isopropanol mixture, were then sprayed onto both bare and bond-coated plates using five different process parameter sets. All coatings exhibited analogous behavior when soaked in a simulated body fluid (SBF) solution. Their interaction with the SBF involved ion release from the glass, conversion of its surface into an amorphous and hydrated silica layer followed by nucleation, and growth of a carbonated hydroxyapatite film on top of the latter. This interaction seemed particularly fast, as the hydroxyapatite film started to appear after 3 days of soaking.

Other materials were tested for their potential application in biomedicine: Liang et al. (2010) plasma sprayed three kinds of powders composed of Ca_2SiO_4, ZrO_2, and $CaZrO_3$ with different Ca_2SiO_4. Results showed that the chemical stability of the coatings was significantly improved compared with pure calcium silicate coatings and increased with the increase in Zr contents. Results indicated that plasma-sprayed coating with 40 wt.% of Ca_2SiO_4 had medium dissolution rate and good biological properties, suggesting its potential use as bone implants.

Preliminary results showed that thermally sprayed nanostructure TiO_2 coatings exhibited photocatalytic bactericidal activity with *Pseudomonas aeruginosa* [Jeffery B, et al. (2010)].

The antibacterial behavior of HA–Ag (silver-doped hydroxyapatite) nanometer-sized powder and their composite coatings were investigated against *Escherichia coli* (DH5a). HA–Ag nanometer-sized powder and PEEK (poly-ether-ether-ketone)-based HA–Ag composite powders were synthesized using in-house powder processing techniques. These nanometer-sized composite powders were cold sprayed. The results indicated that the antibacterial activity increased with increasing HA–Ag nanometer-sized powder concentration in the composite powder feedstock and cold-sprayed coating [Sanpo N, et al. (2009a)].

The antibacterial behavior of chitosan–copper complex (CS–Cu) powder and their composite coatings were investigated against *E. coli* (DH5a). The cold-sprayed coatings retained the antibacterial properties of the original feedstock powders [Sanpo N, et al. (2009b)].

19.3.6 Clearance Control Coatings

In compressors, gas turbines, and turbochargers, dimensional changes take place between the rotor and stator components because of thermal and mechanical effects during operation. These dimensional changes affect sealing and clearance control systems, consisting of a sacrificial element and a cutting component, that are used. Thermal spray coatings, called abradables, and honeycomb seals form effective sacrificial systems. Abradable coatings are machined in situ and consist of a soft metal with polymer particles in cold sections and Ni–graphite or MCrAlY with polyester or BN particles in hot areas [Davis JR (ed) (2004), Ma X, Matthews A (2009), Johnston RE (2011)]. Additives provide the necessary friability, as well as aid in dry lubrication. Other thermally sprayed coatings can also be used on the "cutting" side of the clearance control system, and when the dynamic member of the system is too soft to cut without a coating.

Abradable materials have a strong impact on the turbine efficiency and fuel consumption [Rajendran R (2012)]. At rotating speeds of the order of 10,000 rpm, rotating blade tip may rub against the stationary casing, due to either thermal expansion or misalignment or rotation, inducing strains [Ma X, Matthews A (2007)]. Abradable seals act as sacrificial layers between the blades and the casing and are soft enough to avoid significant wear to blade tips, thus allowing much smaller clearances. They also offer a wear protection to the shroud material and rubbing blades. High-temperature abradable seals are used in high-pressure gas turbine of jet engines [Rajendran R (2012)].

Abradable materials are rather complex because they must be abradable with a good resistance and strength as well as with a good resistance to oxidation and corrosion. Their porosity also plays a key role and is often achieved by spraying also polymers, whose size and volume percentage are critical for optimizing both the "abradability" and erosion-resistance performance. The polymer is then removed by heating the sprayed coating. At last, the coating composition must be such that particle debris, released from the coating into the engine, are kept to a minimum. Their composition must also be adapted to the blade materials: titanium or nickel or steel. They are classified in low- and mid- (<540 °C) and high-temperature (540–980 °C) abradables. Low-temperature abradables are aluminum based with graphite or polyester or polyimide or boron nitride, or nickel based with graphite or calcinated bentonite clay [Sun F, et al. (2012), Puranen J, et al. (2011)]. In the cold compressor section, aluminum base is preferred due to the

high risk of moisture. At high temperatures one uses super alloys (MCrAlY with M=Ni or Co or both) with polyester and/or boron nitride or bentonite or graphite. Recently, ceramic mixed with softer material (BN and polyester) abradable coatings have been developed to reduce slightly the alloy surface temperature. Other seals, which do not interact with the blades, are coatings composed of Babbit (tin–copper–lead), bronze, and AlSi-polyimide. They are used against labyrinth seals along the engine shafts in the compressor and turbine, sealing either gas or oil paths [Davis JR (ed) (2004)].

A few examples are presented below. For high temperatures, Bardi et al. (2008) have tested, for the first stage of industrial gas turbines, the behavior of composite coatings: plasma-sprayed CoNiCrAlY/Al_2O_3 and laser-cladded CoNiCrAlY/graphite coatings. After 1000 h at 1100 °C both coatings did not show relevant microstructural modifications. Steinke et al. (2010) showed that the hardness could be used as an indication for the abradability. It should be in the range of 500 $HV_{0.5N}$. A hardness of approximately 600 $HV_{0.5N}$ seemed to be the upper end at which a good cut-ins was no longer reliably reproducible. Sporer et al. (2007) performed abradability tests of YSZ abradables with the Sulzer Innotec test rig that can operate up to 1200 °C with blade tip speeds up to 410 m/s.

At intermediate temperatures (<450–480 °C), AlSi-hexagonal BN or NiCrAl–bentonite is popular [Johnston RE (2009, 2011), Stringer J, Marshall MB (2012), Faraoun HI, et al. (2006), Bounazef M, et al. (2004)]. For example, the AlSi–hBN coating was characterized by a proportion of about 40% of hBN "lubricant" particles trapped in the metallic matrix [Faraoun HI, et al. (2006)]. The amount of porosity was about 5%. The NiCrAl–bentonite coating contained about 25% of relatively spherical bentonite particles together with about 30% porosity constituted mainly of large pores [Faraoun HI, et al. (2006)]. Comparatively to the hBN particles, the majority of the large bentonite particles and pores in this coating are distributed without significant preferred orientation [Faraoun HI, et al. (2006)].

Johnston (2011) studied the net thermal spraying residual stress (NTSRS) and showed that it was most sensitive to changes in substrate thickness, abradable deposit thickness, and deposit modulus. Such results could be used for the creation of new abradable materials with optimum stress profiles and greater mechanical integrity. Stringer and Marshall (2012) studied the wear at high speed: impact velocities between 100 and 200 m/s and incursion rates between 3.4 and 2000 μm/s. They suggested that the adhesion of abradable material was due to plucking out of complete phases from the abradable coating, rather than a conventional cutting mechanism. Ma and Matthews (2007) suggested using "progressive abradability hardness" (also called "specific grooving energy"), abbreviated as "PAH," to measure abradability in the scratch test. At low temperatures, Ma and Matthews (2007) studied, for abradable seals to centrifugal compressors and steam turbines, the development of a new abradable silicon rubber adhesively bonded to a metal substrate.

Lima and Marple (2007) showed that a material that was generally considered as being hard and stiff, as YSZ, could be engineered to produce a nanostructured 100% ceramic coating with a friable structure possessing attributes required for an abradable coating. In order to engineer a friable ceramic coating, the molten part of a semi-molten agglomerate particle must not fully infiltrate into the capillaries of its nonmolten core during thermal spraying. The porous nano-zones spread throughout the coating microstructure acted as weak links, thereby making the coating friable. Abrasive wear-resistant coatings are applied to blade tips and labyrinth seal teeth. They are often made of alumina, alumina–titania, nickel–aluminum cermet, and Ni–Cr–Cr_3C_2 cermet.

19.3.7 Bond Coatings

Bond coats are very important to:

- Improve the coating adhesion by forming an anchoring sub-coat or adhering to clean and smooth surfaces that cannot be grit blasted properly
- Form a buffer layer with an expansion coefficient between that of substrate and topcoat
- Provide an oxidation- or corrosion-resistant barrier to the substrate

According to the oxidation or corrosion barrier, and the working temperature of the coated part, the bond coat must be properly chosen.

For example, Mo can be used up to 315 °C [American Welding Society (1985)]. NiAl bond coats are oxidation resistant up to 650 °C with Ni–Al (20 wt.%) and 800 °C with Ni–Al (5 wt.%), but they can also be used against corrosion. For example, Lekatou et al. (2008) have investigated the corrosion behavior of an HVOF Ni–5Al/WC–17Co coating on Al-7075 in 0.5 M H_2SO_4. In the temperature range of 25–45 °C, the coating exhibited pseudo-passivity that effectively protected from localized corrosion. In case of surface film disruption, the bond coat successfully hindered corrosion propagation into the Al alloy. Yılmaz (2009) has shown that the application of NiAl (5 wt.%) bond coat layer in the plasma spraying of Al_2O_3 and Al_2O_3–13 wt.% TiO_2 on pure titanium substrate has increased the hardness and bonding strength of coatings. Ni–Cr (20 wt.%) bond coats can be used up to 980 °C and are

designed to resist oxidation and corrosive gases. Cho et al. (2009) coated micron-sized WC–Co powder onto a 420J2 steel substrate and bond coats of Ni, NiCr, and Ni/NiCr using HVOF spraying. The fracture locations were at interfaces with top coatings of WC–Co and NiCr indicating that adhesion between metal and similar metal is much stronger than between metal and cermet (WC–Co) because of the easy diffusion between similar metal atoms. Bond coats for TBCs have been extensively studied. They are of the MCrAlY type with M = Ni, Co, and the like that can be doped with Pt, Hf, and the like and can support temperatures of 1100–1200 °C. A few examples are presented below. Schulz et al. (2008a, b) have studied NiPtAl bond coats as well as NiCoCrAlY(X) deposited by LPPS and EBPVD underneath conventional EBPVD yttria-stabilized zirconia topcoats on three different substrate alloys. The longest lifetimes were achieved on a novel Hf-doped EBPVD NiCoCrAlY bond coat owing to a differing TGO formation and failure mechanism. Zhao and Xiao (2008) investigated the effect of the Pt content on the durability of thermal barrier coatings (TBCs) with a Pt-enriched $\gamma + \gamma'$ bond coat. During oxidation, impurities such as S, C, and refractory elements segregating to the interface would degrade the TGO adherence to the bond coat. However, a higher content of Pt can inhibit this segregation and thus improve the TBCs life. Tang and Schoenung (2005) observed multilayered accumulation of thermally grown oxide (TGO) locally on the tops of the roughness protrusions of the bond coat in thermal barrier coatings. Chen et al. (2011a, b, c) have compared TGO growth and cracking behaviors in TBC systems with APS-, HVOF-, and CGDS-CoNiCrAlY bond coats during thermal exposure. Results pointed the potential advantage of using CGDS technique to produce TBC bond coats, for its significantly improved durability over the commercial air plasma spray bond coat, as well as its fast deposition rate and low deposition temperature. The TBCs with HVOF bond coats had an extended durability, compared to that obtained by APS but lower than that by CGDS. Other materials than superalloy were tested for TBC bond coat, such as glass–ceramics [Das S, et al. (2009)]. The TBC with YSZ topcoat, glass–ceramic bond coat, and nickel base superalloy substrate was subjected to static oxidation test at 1200 °C for 500 h in air. No TGO layer was found between the bond coat and the topcoat in the case of glass–ceramic bonded TBC system, while the conventional TBC system exhibited a TGO layer of about 16 μm thickness at the bond coat–topcoat interface region.

Bond coats are also used for other applications, discussed below.

Lu et al. (2004) plasma sprayed two-layer hydroxyapatite (HA)/HA + TiO_2 bond coat composite coating (HTH coating) on titanium. The HA + TiO_2 bond coat (HTBC) consisted of 50 vol.% HA and 50 vol.% TiO_2 (HT). The positive effect of the HTBC on the decrease of residual stress in HA top coating (HAT coating) was evidenced through the observation on the surface cracking. The toughening and strengthening of HTBC was thought to be mainly due to TiO_2. Goller (2004) plasma sprayed bioglass, known as 45S5 (45% SiO_2, 6% P_2O_5, 24.5% CaO, and 24.5% Na_2O, all in weight percent), onto a titanium substrate with and without Amdry 6250 (60% Al_2O_3–40% TiO_2) as bond coating layer. The adhesive bonding observed at the bioglass metal interface turned into cohesive bonding by application of the bond coating layer.

Guanhong et al. (2011) have deposited on polymer matrix composites (PMCs; carbon-fiber-reinforced unsaturated polyester) the Al bond coat and Al_2O_3 top coating by APS. The highest shear adhesion strength of the bond coating was 5.21 MPa and the hardness of the surface was much improved by the alumina coating. Liu et al. (2006) arc sprayed Al and Zn and plasma sprayed Al, Zn, Ni_3Al, and Cu on carbon-fiber-reinforced polyimide substrate as bond coats for erosion and thermal-resistant coating. Ni_3Al or Cu damaged the substrate. Arc-sprayed and plasma-sprayed Al and Zn could be used as bond coat materials. For Zn as bond coat material, depositing method had little influence on shear adhesion strength. For Al as bond coat material, plasma spray was superior to arc spray, preheating improving shear adhesion strength.

19.3.8 Freestanding Spray-Formed Parts

The freestanding bodies are produced by plasma spraying for refractory or ceramic materials [Geibel A, et al. (1996), Devasenapathi A, et al. (2002), Chráska P, et al. (1997), Neufuss K, et al. (1997), Shi S, Hwang J-Y (2003), Patel RR, et al. (2010), Brožek V, et al. (2009)], by HVOF spraying for thin alloys or cermets [Helali M, Hashmi MSJ (1996)], and also by cold spray [Pattison J, et al. (2007)]. Of course, rotationally symmetrical shapes are preferred: the core is easy to produce, the stress in the sprayed material is low and evenly distributed, and at last separating the core from the coating is easier. In most cases the core is made of smooth graphite or other material coated by atomization of a product preventing the substrate–coating adhesion. It is also possible to achieve very complex shapes, such as manifolds of racecar engines, by spraying on special materials that can be afterward dissolved. It becomes then possible to coat externally the sprayed ceramic thermal barrier by an alloy to achieve the hot gases tightness. This technique, having a high cost, is hardly suitable for large-scale production, but it offers advantages as far as cost and fast delivery are concerned. For example, sprayed ceramic bodies offer good mechanical strength at high temperatures, and excellent electrical insulation at temperatures where glass insulators give-

up chemical resistance against corrosive gases or liquids. For example, in rocketry nozzle inserts are achieved that way. Ceramic tubing is used in furnace construction as well as in chemistry. The production of crucibles for the melting of materials is also an important application. Such crucibles are made of partially (YPSZ) or totally (YSZ) stabilized zirconia, strontium zirconate, alumina, tungsten, and molybdenum. A relatively new application of PTA deposition is the fabrication of freestanding shapes, or solid free form fabrication.

A few examples of freestanding coatings are presented below.

Chen et al. (1993) vacuum plasma sprayed dense, oxide-free, and pore-free freestanding forms of NiAl and NiAl-B. The deposits retained the same phase structure as the starting powders. The as-sprayed freestanding deposits exhibited a large grain size due to self-annealing during vacuum plasma spray processing. The hardness of NiA1-B was about 10% higher than that of NiAI.

Saeidi et al. (2009) produced freestanding VPS- and HVOF-sprayed CoNiCrAlY coatings. The as-sprayed HVOF coating retained the γ/β microstructure of the feedstock powder, and the VPS coating consisted of a single γ phase. A 3 h, 1100 °C heat treatment in vacuum converted the single-phase VPS coating to a two-phase γ/β microstructure and coarsened the γ/β microstructure of the HVOF coating. Oxidation of the freestanding as-sprayed coatings produced a dual-layer oxide consisting of an inner layer of α-Al_2O_3 and an outer spinel layer.

Fan and Ishigaki (2001) used induction plasma spraying (IPS) to produce freestanding parts of Mo_5Si_3-B composite and $MoSi_2$ materials. The oxidation resistance, up to 1210 °C, of the former composite was compared with that of the latter, known to be resistant to high-temperature oxidation. At boron contents greater than 1 wt.%, composites demonstrated encouraging oxidation resistance and with 2 wt.% boron it was comparable to $MoSi_2$.

Waki et al. (2009) sprayed freestanding circular tube specimen of CoNiCrAlY by VPS, HVOF, and APS. They studied the effect of post-spray thermal treatments, in vacuum and in air, on the mechanical properties in the 400–1100 °C temperature range. High-temperature thermal treatment in air was effective in increasing the bending strength and Young's modulus. It was especially effective on the APS coatings, which were produced using powders with average size of 60 μm, and on HVOF coatings, those bending strengths increased by approximately three times.

Plasma-sprayed freestanding zircon pipes (inside diameter 83 mm, wall thickness 1.5–2 mm, lengths up to 2000 mm) are used in furnaces as shields for heating elements [Chráska P, et al. (1997)]. The plasma deposits contained glassy silica and various modifications of zirconia in addition to a small amount of the amorphous phase. This combination of zirconia and silica exhibited properties such as a high thermal-shock resistance, good corrosion resistance, and low wettability.

Chen et al. (2011a, b, c) obtained by plasma spraying freestanding $La_2Zr_2O_7$ coatings, using an amorphous La–O–Zr precursor as the feedstock. During thermal spraying, the amorphous powder crystallized, and fine grains were formed, while with crystallized feedstock powder the average grain size was 750 nm. The thermal conductivity of the as-sprayed coating with the amorphous feedstock powder was approximately 0.42 W/m K and its average coefficient of thermal expansion (CTE) was 11.1×10^{-6}/K, value similar to that of metallic bond coatings.

Henne et al. (1999) processed by induction plasma spraying the material of metallic bipolar plates for solid oxide fuel cells, a chromium alloy with the composition 94% Cr, 5% Fe, and 1% Y_2O_3. Freestanding parts had a density above 95% of the theoretical density of the material. From the deposits obtained, it was positively concluded that, as long as the deposit thickness did not exceed about half the characteristic substrate dimension, the contour of the free side of the deposit sufficiently followed the contour of the substrate.

Agarwal et al. (2003) plasma sprayed a mixture of commercially available aluminum oxide powder (99.8% pure), in the 15–45 μm particle size range, with nanosized aluminum oxide powder (99.9% pure) thoroughly mixed in a rotating ball (alumina ones) mill for 24 h. Coatings were sprayed on conical mandrels. Spray parameters were controlled with an innovative proprietary cooling technique to retain a large fraction of nanosize Al_2O_3 powder particles in the spray deposit. Nanosize particles were partially melted and trapped between the fully melted coarser (micrometer size) Al_2O_3 grains.

Laha et al. (2004) plasma sprayed freestanding structures, hollow conoid (100 m taper-length, 62 mm diameter, 2 mm thickness), of Al-based nanostructured composite with carbon nanotubes (CNT) as second phase. Carbon nanotubes (CNT) were successfully retained in the spray-formed composite structure. The CNTs were observed largely between the consecutive Al–Si splats with dangling structure.

Hussain et al. (2011) cold sprayed titanium freestanding coatings, some of them being vacuum heat-treated to further decrease porosity levels. Cold spraying using N_2 as a process gas heated to 800 °C deposited titanium with less interconnected porosity than N_2 gas at 600 °C due to a higher degree of particle deformation on impact. Pores above 1 μm were reduced to 0.2 vol.% and the total interconnected porosity to 1.8 vol.% after heat treatment of deposits produced at a process gas temperature of 800 °C.

Herman et al. (1994) sprayed by the VPS process dense deposits of unreinforced and composite matrices of Ni_3A1 alloy and $MoSi_2$. Geibel et al. (1996) showed that plasma spray deposition was a suitable technique to produce

freestanding, near-net-shaped components of the difficult-to-shape NiAl intermetallic compound.

Weiss et al. (1992) described a new spray-forming process based on thermal spray shape deposition. Shape-deposition processes built three-dimensional (3-D) shapes by incremental material build-up of thin, planar, cross-sectional layers. These processes did not require preformed mandrels and can be used to directly build three-dimensional structures of arbitrary geometrical complexity. The basis for the thermal spray approach was to spray each layer using a disposable mask that had the shape of the current cross section. Masks could be produced from paper rolls, for example, with a CO_2 laser.

19.3.9 Emerging Thermal Spray Applications

19.3.9.1 Solid Oxide Fuel Cells

A solid oxide fuel cell (SOFC) is an electrochemical conversion device that produces electricity directly from oxidizing fuel. They are made of four layers comprising three ceramic layers, which are not electrically and ionically active below about 600 °C. Such high operating temperatures result in mechanical and chemical compatibility issues. To achieve an affordable manufacturing cost, the whole SOFCs have been manufactured by plasma spraying: cathode, electrolyte, and anode. One of the disadvantages of the process is the thickness of the electrolyte that must be below a few tens of micrometers and impervious. However, it seems that thin and impervious electrolyte (around 10 μm) can be achieved by suspension plasma spraying. Henne (2007) presented in 2007 an excellent overview of thermally sprayed coatings to make SOFC components and also entire cells. Among the numerous studies, essentially with plasma spraying, published before that year, "only few have already proven their potential for a reliable and efficient production of relevant layers and components and promised the status for a technical breakthrough for mass production where a continuous operation with high throughput and yield producing the desired quality is required" [Henne R (2007)]. Henne recommends for further developments to improve plasma sources, increase deposition efficiency, work on less costly materials, and combine synthesis and deposition of cell materials based on low-cost precursors. He also evokes the possibility of the recycling of "plasma gas" and overspray [Henne R (2007)]. A few examples are given below.

Takenoiri et al. (2000) developed a seal-less planar SOFC consisting of a cell supported with a porous metallic substrate and a metallic separator. The anode and electrolyte were fabricated using flame spraying and APS, respectively, and APS was also used to form a protective coating of the separator. It was shown that the electrical resistance of the separator could be kept lower than $25 \times 10^{-3}\ \Omega\ cm^2$ for at least 3000 h by the application of (LaSr)MnO_3 protective coatings.

Barthel et al. (2000) deposited by thermal spray processes (VPS and flame spraying) porous composite cathodes of $(La_{0.8}\ Sr_{0.2})_{0.98}MnO_3$ (LSM) and ZrO_2–12% Y_2O_3 (YSZ). The electrochemical performance of the cathodes, evaluated by impedance spectroscopy, indicated significant improvements, especially for the bilayer technique, whereas the concentration profiles of the multilayer gradients still must be optimized. Flame spraying seemed promising.

$La_{10}\ Mg_{0.2}\ Si_{5.8}\ O_{26.8}$ was prepared by solid-phase sintering and also plasma sprayed by Sun et al. (2012). The amorphous transformation of lanthanum silicates happened during APS process. The heat treatment effectively ameliorated phase composition of as-sprayed coatings, complete recrystallization being achieved after 1000 °C for 4 h. However, it decreased the permeability of coatings.

Puranen et al. (2011) plasma sprayed Mn–Co–Fe spinel coating on the thin metallic interconnectors in SOFCs. They optimized spray conditions to produce coatings with low thickness and low amount of porosity. The original spinel structure decomposed because of the fast transformation of solid–liquid–solid states but was partially restored by using post-annealing treatment.

Harris et al. (2012) manufactured by axial-injection APS (Mettech Axial torch) single-phase and composite cathodes based on $La_{0.6}\ Sr_{0.4}\ Co_{0.2}\ Fe_{0.8}\ O_{32\text{-}\delta}$ (LSCF) and $Sm_{0.5}\ Sr_{0.5}\ Co\ O_3$ (SSC). An average surface temperature of approximately 2200 °C was needed for adequate melting of LSCF particles and approximately 2100 °C to melt SSC. But too much particle heating resulted in coarser and denser microstructures.

Suspension plasma spraying [Fauchais P, et al. (2011)] seems to be promising for the SOFC cathode deposition, as coatings with high porosity levels in combination with fine pore size can be produced. Shen et al. (2011), using induction plasma technology and solution plasma spraying, achieved a homogeneously mixed nanosized composite $Ce_{0.8}\ Gd_{0.2}\ O_{1.9}$ (GDC)/LSCF powder without using a prolonged period of mechanical mixing. The nano-powders exhibited a perovskite structure and a fluorite structure as well as separated GDC ($Ce_{0.8}\ Gd_{0.2}\ O_{1.9}$) and LSCF phases. The coatings were homogeneous and porous (51% porosity) with cauliflower structures. Wang et al. (2012) successfully deposited with Axial III Mettech torch Ni–YSZ anode and YSZ electrolyte half-cells on porous Hastelloy X substrates by SPS. The thickness of the anode and electrolyte layers was ~40 μm and 10–20 μm, respectively. The density of YSZ electrolyte coatings increased as plasma torch input power increased. The anodes of the deposited half-cells were porous and electrolytes dense, with no interconnected pores. Michaux et al. (2010) prepared and characterized porous anode layers with homogeneous nickel distribution and nanometer-sized microstructure for SOFC application. They investigated the

effects of some spray parameters on the layer architecture and composition.

19.3.9.2 Sensors

For oxygen permeation membranes, Zotov et al. (2012) prepared $La_{1-x}Sr_xFe_{1-y}$ $Co_yO_{3-\delta}$ (LSFC) coatings by low-pressure plasma spraying–thin film processes using different plasma spray parameters. The microstructures of the investigated LSFC coatings depended sensitively on the oxygen partial pressure, the substrate temperature, the plasma jet velocities, and the deposition rate. Coatings deposited with Ar-rich plasma and higher plasma jet velocities were most promising.

Oxygen sensors based on ionic conduction of plasma-sprayed ZrO_2 (measurement of the small electrical current caused by oxygen ions diffusing through the layer) are now extensively used in catalytic car exhaust pipes [Fedtke P, et al. (2004)].

19.3.9.3 Decorative Coatings

Thermal spraying is not widely adapted to decorative coatings, and the main efforts were achieved on relatively large structures such as bridges, water tower, chimneys, and so on that were sprayed with zinc or aluminum for corrosion protection. They can be left as-sprayed or sealed with plain or colored sealers. The liquid flame spraying process has been developed to uniformly color hot glass objects [Gross KA, et al. (1999)]. Thermal spraying of concrete or bricks have been performed with glazing materials. Arcondéguy et al. (2007, 2008) manufactured glaze layers by flame spraying onto substrates that decomposed when heated and for which the traditional glazing process was not appropriate. Adjusting the chemical composition permitted to adjust the transition temperature of the materials. Adjusting their morphology by posttreatment permitted to increase the deposition efficiency and reduce the pore content of the coatings. Of course, the decorative value of such coatings is important for the aesthetic but it has a cost.

19.3.9.4 Spent Nuclear Fuel

Many works are now devoted to the containment of spent nuclear fuel that poses a challenge from the perspective of materials science. These applications require to safely provide neutron absorption and corrosion resistance at reasonable costs for very long periods. Identifying a single material that can meet all these requirements has been quasi-impossible and the introduction of coatings seems promising. Alternate coating materials such as amorphous metals and ceramics have been developed and studied to better resist corrosion. Amorphous coatings with boron or other neutron-absorbing element have demonstrated promising results against corrosion [Blink J, et al. (2009), Farmer JC, Choi J-S (2007), Blink J, et al. (2007), Farmer J, et al. (2009), Branagan D (2004)]. The absence of long-range structure (grain boundaries, dislocations, and segregations), in corrosion-resistant materials further enhances the corrosion resistance of amorphous alloys. One of the most promising formulations was found to be $Fe_{49.7}Cr_{17.7}Mn_{1.9}Mo_{7.4}W_{1.6}B_{15.2}C_{3.8}Si_{2.4}$ (SAM2X5), which included chromium (Cr), molybdenum (Mo), and tungsten (W) for enhanced corrosion resistance, and boron (B) to enable glass formation and neutron absorption [Branagan D (2004)]. The parent alloy for this series of amorphous alloys, which is known as SAM40 and represented by the formula $Fe_{52.3}Cr_{19}Mn_2Mo_{2.5}W_{1.7}B_{16}C_4Si_{2.5}$, has less molybdenum than SAM2X5 and was originally developed by Branagan (2004). Coatings, HVOF sprayed, have demonstrated phase stability well above 500–600 °C and at high neutron dose (equivalent to 4000 years inside the container) [Blink J, et al. (2007)].

Alumina plasma-sprayed coatings, manufactured with graded alumina–titania coatings, and phosphate-sealed alumina coatings were investigated to improve the properties of metallic substrates operating in extreme environments of spent nuclear fuel. The effects of particle size distribution, phosphate sealant, and graded titania additions on the dielectric strength of the as-sprayed, thermally cycled, and thermally aged coatings were investigated [Berard G, et al. (2008)]. Spinel ($MgAl_2O_4$) coatings were also investigated [Haslam JJ, et al. (2005)]. All studies demonstrated the necessity to have impervious coatings.

19.3.9.5 Combined Cycle Power Plant Combinations

Hardwicke and Lau (2013) emphasized that recent power generation company announcements centered on integrating renewable resources onto the power grid for cleaner, more efficient energy generation. They think that these technical breakthroughs can certainly utilize the new developments in the thermal spray industry.

19.3.9.6 Future Nuclear Fusion Reactor

While thermonuclear fusion is a potential source of cleaner and safer energy for the future, its technological realization depends on the development of materials able to survive and function under extreme conditions. According to the review by Matejicek et al. (2007), materials to be applied in a fusion reactor will be subjected to extreme and complex loading conditions and have to fulfill very complex and sometimes contradicting requirements. A number of the demands on fusion materials can be fulfilled by the application of coatings. Thermal spraying is just one of the available coating technologies. Thermal spray (especially plasma spray) coatings were developed and tested for a variety of applications in fusion environments, including plasma facing components, tritium permeation barriers, and electrical insulation.

19.4 Thermally Sprayed Coatings by Industry

In his paper [Longo FN (1992)], based on the 1990 multiclient study prepared by Gorham Advanced Materials Institute, entitled "The Expanding Business Opportunities and Challenges in Thermal Sprayed Coatings," Frank Longo, who is a thermal spray industry consultant and is a principal author of this study, identified 34 industrial sectors where thermal spray and other coatings were used. The broad base of end-user activity with thermal spray coatings for 12 industrial sectors is profiled in Tables 19.1, 19.2, and 19.3. These show that the main activities have been in the gas turbine and aircraft industry, turbine and steam, engines and automotive, engines and diesel, transportation, oil and gas exploration, chemical processing, paper and pulp, defense and aerospace, medical and dental, and electric/electronic industry. Longo (1992) estimated that the total market was projected to reach 1.8 to 2.0 billion US dollars by the end of the decade (2000) with strong growth in the powder/consumable business, and standard equipment such as APS and VPS systems and a growing demand for contract coating services which represented close to 50% of the (1990) TS market.

Two decades later, Dorfman and Sharma (2013a, b) estimated that the annual thermal spray industry is worth approximately US$6.5 billion [Hanneforth P (2006)] with the majority of revenue generation in coating services, thus underlying the growth of thermal processes. In terms of market segmentation, approximately 60% of the total TS market at that time belongs to the turbine industry, 15% to automotive, and the remaining 25% is distributed over a large number of other industries.

Dorfman and Sharma (2013a, b) also point out that while future growth of the TS market will continue to depend on the growth of turbine industry, a greater growth potential exists in the "other" industries where currently the penetration of TS is low such as in the area of energy generation using conventional or renewable resources, oil and gas, pulp and paper, metal processing, and biomedical and electronics industries.

The last *ASM Handbook, Volume 5A: Thermal Spray Technology* [Tucker RC (ed) (2013)], which is a replacement for the *Handbook of Thermal Spray Technology* [Davis JR (ed) (2004)], provides a good insight of developments in terms of thermal spray industrial-scale applications including electronics and semiconductors, automotive, energy, and biomedical. Traditional thermal spray market sectors such as aerospace and industrial gas turbines as well as important areas of growth such as advanced thermal barrier materials, wear coatings, clearance control coatings, and oxidation/hot corrosion-resistant alloys are reviewed.

19.4.1 Aerospace

Aero engines are probably those where thermally sprayed coatings, especially APS, VPS, or HVOF sprayed, were extensively developed since the 1970s–1980s. The fan, compressor, combustion chamber, and turbine must be protected with coatings against oxidation, hot gas corrosion, erosion, and wear. As illustrated in Figs. 19.3, and Fig. 19.4, hundreds of components are presently sprayed in aero engines used both for military and traditional industrial gas turbine (IGT) engine units worldwide. Their main role is to reduce friction and wear, corrosion, clearance control, and for high-temperature protection (TBCs) to improve engine efficiency, and extend service life. In aero engines, almost all types of sprayed materials are used (carbides, iron and steel, nickel alloys, cobalt alloys and superalloys, nonferrous metals) except the self-fluxing alloys. HVOF coatings have also been used to replace hard chromium in landing gear. For more details see [Davis JR (ed) (2004), Thintri Inc. (2013)].

TBCs were first successfully tested in the turbine section of a research gas turbine engine in the mid-1970s. By the early 1980s they had entered revenue service on the vane platforms of aircraft gas turbine engines [Billah BM, et al. (2012), Miller RA (1997)], and today they are flying in revenue service on vane and blade surfaces [Miller RA (1997)]. Thermal insulation benefits provided by TBCs and the resulting impact on component creep and thermomechanical fatigue life have made them enablers of high-thrust gas turbine engines. As underlined by Pratt and Whitney, of particular importance is the EB-PVD-based TBC—presenting an excellent compliance upon thermal cycles were then anticipated to improve blade life by a factor of 3 [Schulz U, et al. (2008a, b)].

The aging of TBC's topcoat strongly depends upon the spray conditions and powder morphologies used to spray or deposit it, conditions acting on its sintering properties [Bose S, de Masi-Marcin J (1997), Cipitria A, et al. (2009)]. The second problem is the oxidation of bond coat with the formation of thermally grown oxide (TGO) [Markocsan N, et al. (2009), Golosnoy IO, et al. (2009), Hernandez MT, et al. (2009), Vaßen R, et al. (2009a, b), Toscano J, et al. (2006), Pint BA, et al. (2010)] as well as the bond coat corrosion with oxides such as CMAS (acronym for CaO, MgO, Al_2O_3, and SiO_2) [Mohan P, et al. (2010), Jones RL (1997), Li L, et al. (2010a, b), Hernandez MT, et al. (2009)] or vanadium oxide [Chen Z, et al. (2009)]. Feuerstein et al. (2008) have shown that the most advanced thermal barrier coating (TBC) systems for aircraft engine and power generation hot section components (combustors, blades, and

Table 19.1 Thermal spray processes used by industry [Longo FN (1992)]

	O_2/fuel powder low velocity	Spray and fuse torch	HVOF	Air plasma	Vacuum plasma	Inert gas shroud plasma	Plasma transfered arc	Laser-assisted plasma	D-gun	Gator gard	O_2/fuel wire spray	Electric arc	Electric arc with inert cover or vacuum	Rokide
Gas turbine, aircraft	X	…	X	X	X	X	X	X	X	X	X	X	…	…
Gas turbine, industrial	…	…	…	X	…	X	X	…	…	…	X	…	…	…
Turbine, steam	…	X	…	X	…	X	X	…	…	…	…	…	…	…
Engines, automotive	X	…	…	X	…	…	X	…	…	…	X	X	…	X
Engines, diesel	X	…	…	X	…	…	X	…	…	…	X	X	…	X
Transportation	X	…	…	X	…	…	X	…	X	…	…	X	…	…
Oil and gas exploration	X	X	X	X	…	…	X	…	X	…	X	X	…	X
Chemical processing	X	…	…	X	X	…	…	…	X	…	…	X	X	…
Paper and pulp	X	…	X	X	…	…	X	…	…	…	X	X	…	X
Defense and aerospace	X	…	X	X	X	…	X	…	X	…	X	X	…	…
Medical and dental	…	…	…	X	X	…	…	…	X	…	…	…	…	…
Electric and electronic	…	…	…	X	X	…	…	…	X	…	…	…	…	…

Table 19.2 Thermal spray coating function by industry [Longo FN (1992)]

Industries	Adhesive wear resistance	Adhesive wear resistance tribology	Antifretting	Erosion resistance	Cavitation resistance	Thermal barriers	Clearance control abradability	Restoration of dimension and repair	Corrosion resistance	Corrosion resistance, iron and steel	Near-net shape forming	Electric resistance	Electric conductivity	Impact	Oxidation
Gas turbine, aircraft	X	X	X	X	…	X	X	X	X	X	X	…	…	…	X
Gas turbine, industrial	X	X	X	X	…	X	X	X	X	…	…	…	…	…	X
Turbine, steam	X	X	…	X	X	…	…	X	…	X	…	…	…	…	…
Engines, automotive	X	X	X	X	…	X	X	X	X	X	X	X	…	X	X
Engines, diesel	X	X	…	X	…	X	…	X	…	X	X	…	…	X	X
Transportation	X	X	…	…	…	…	X	X	X	X	…	X	X	…	…
Oil and gas exploration	X	X	…	X	…	…	…	X	X	X	…	…	…	X	…
Chemical processing	X	…	…	X	…	…	…	X	X	X	…	…	…	…	X
Paper and pulp	X	…	…	…	X	…	…	X	X	X	…	…	…	X	…
Defense and aerospace	X	…	…	…	…	X	X	X	…	…	X	…	…	…	…
Medical and dental	…	…	X	…	…	…	…	…	X	…	…	…	…	…	…
Electric and electronic	…	X	X	…	…	…	…	…	…	…	…	X	X	…	…

Table 19.3 Thermal spray powder materials used by industry [Longo FN (1992)]

Industries	Cemented Co-WC	Chromium carbides	Mixed WC, TiC or Cr_3C_2	Oxide ceramics	Non-oxide ceramics	Fluxed alloys	Iron and steel alloys and composites	Nickel and nickel alloys	Super-alloys, MCRALY's	Cobalt and cobalt alloys	Refractory metals	Plastics	Special composites	Glasses	Cermets	Non-ferrous metals
Gas turbine, aircraft	X	X	…	X	X	…	X	X	X	X	X	X	X	…	X	X
Gas turbine, industrial	X	X	X	X	…	X	X	X	X	X	X	…	X	…	X	…
Turbine, steam	X	X	…	…	…	X	X	X	…	X	…	…	…	…	…	X
Engines, automotive	…	…	…	X	…	…	X	X	…	X	X	…	…	…	…	…
Engines, diesel	X	…	…	X	…	…	X	X	…	X	X	…	…	…	X	…
Transportation	…	…	…	…	…	…	X	X	…	…	X	…	…	…	…	X
Oil and gas exploration	X	…	…	X	…	X	X	X	…	X	…	X	…	…	…	X
Chemical processing	X	…	…	X	…	…	X	X	…	X	X	X	…	X	…	…
Paper and pulp	X	…	…	X	…	X	X	X	…	…	X	…	…	…	…	…
Defense and aerospace	X	X	…	X	…	…	X	…	X	X	X	…	…	X	X	…
Medical and denial	…	…	…	X	…	…	…	…	…	X	…	…	…	…	…	X
Electric and electronic	…	…	…	X	X	…	…	…	…	…	…	…	…	…	…	X

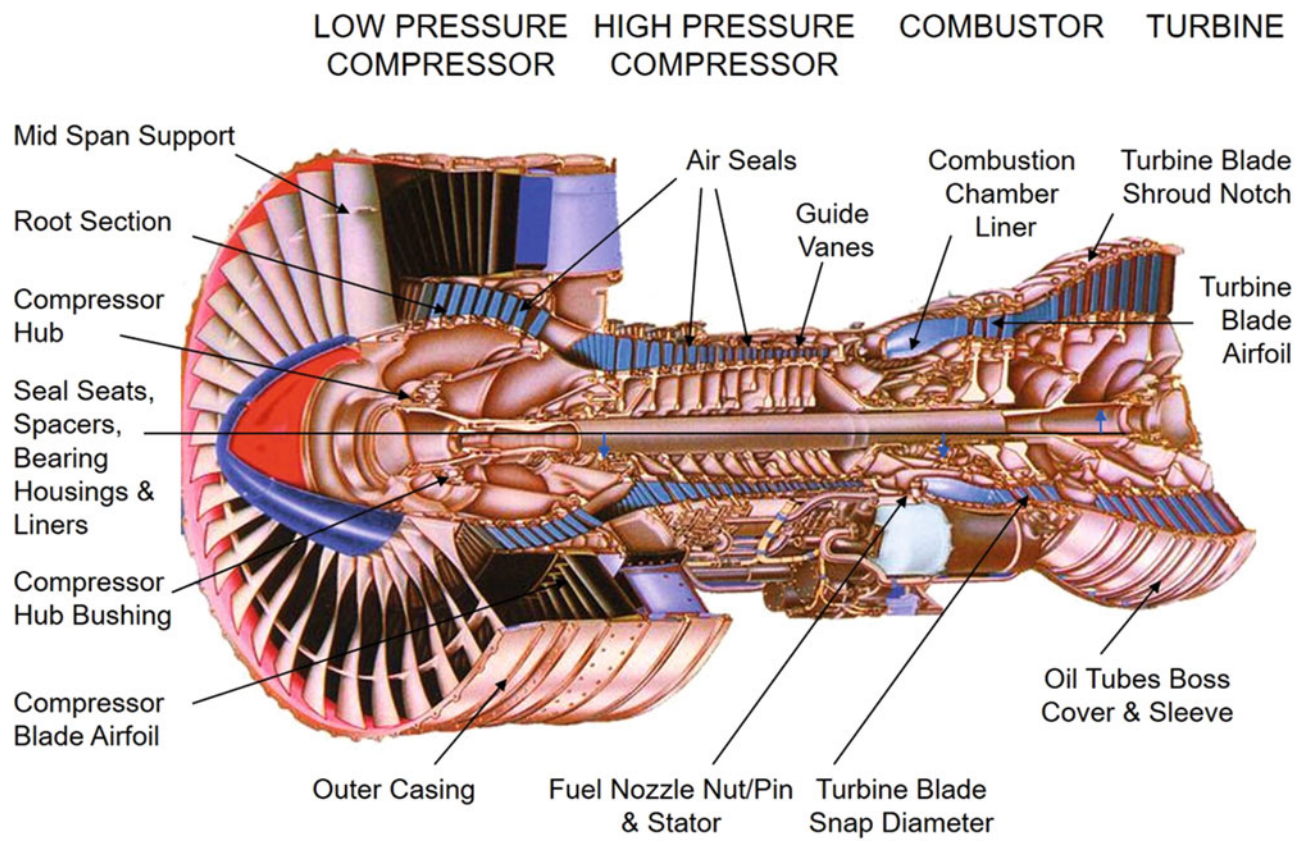

Fig. 19.3 Thermally sprayed coatings on aircraft turbine engine parts. (Reproduced with kind permission from Oerlikon-Metco Corp.)

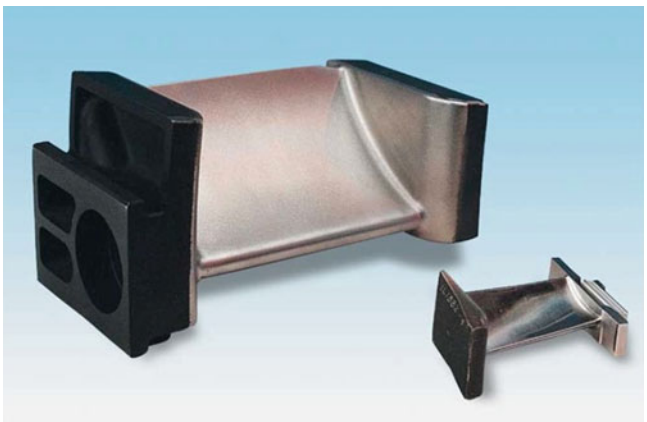

Fig. 19.4 TBC-coated gas turbine vanes. (Courtesy of Sulzer-Metco)

vanes) consist of electron beam physical vapor deposition (EB-PVD)-applied YSZ and platinum-modified diffusion aluminide bond coating. Thermally sprayed ceramic and MCrAlY bond coatings, however, are still used extensively for combustors and power generation blades and vanes. Feuerstein et al. (2008) have reviewed and compared the state-of-the-art processes for the deposition of TBC systems: shrouded plasma and HVOF for MCrAlY bond coat, plasma for low-density YSZ, and dense vertically cracked Zircoat, platinum aluminide diffusion coatings, and EB-PVD-TBC. They outlined and compared key features of coatings and their cost elements actually used in industry. Vaßen et al. (2009a, b, 2010) have presented last developments using advanced processing: methods allowing obtaining highly segmented TBCs [Richer P, et al. (2010)] and the important recent directions of development for TBC systems, including improved processing routes and advanced TBC materials are discussed. Numerous studies were devoted to the resistance of the bond coat [Toscano J, et al. (2006)] and the way to improve it [Billah BM, et al. (2012), Hernandez MT, et al. (2009)] by bond coat treatment, or the choice of the spray process [Richer P, et al. (2010), Karger M, et al. (2011)]. For the TBC topcoat, promising new technologies such as low-pressure plasma spraying–thin film (LPPS-TF) [Hospach A, et al. (2012), Muehlberger E, Meyer P (2009)] or solution or suspension or nanometer-sized agglomerated particles plasma sprayed will probably play an increasing role in future applications [Fauchais P, et al. (2011)].

Against fretting wear, occurring in both lower- and higher-temperature sections of engines, carbides and refractory metals are used, while for clearance control CuNiIn, Nickel–Aluminum-base coatings, where rotating parts need some sealing to reduce bypass of hot combustion or cold compressor gases (through spaces between blade tips and

stationary housing), abradable seals are used. For example, in cold sections they are made of polymers and soft metals, while in the hot nickel–graphite, superalloy–polyester or boron carbide, YPSZ with polyester or boron carbide, NiCrAl, and bentonite are used. Seal coatings are also used in the labyrinth seal knife-edges.

For the high-temperature sections, thermal barrier coatings are used for protection against high-temperature metal fatigue, as well as for reduction in the temperature of the metallic substrate to improve component's durability and increase fuel efficiency by higher turbine inlet temperatures. Besides the fuel consumption reduction, emissions of nitrogen oxide, hydrocarbon gases, and smoke are reduced, which is important to have environmental-friendly engines.

Against corrosion, materials of the family MCrAlYs are used with M being nickel, cobalt, molybdenum, iron, or alloys of these elements (NiCo, CoNi, etc.). These alloys are VPS, HVOF, and for some of them cold sprayed. It is important for these materials to reduce or suppress oxidation during spraying and achieve excellent adhesion. The latter is obtained by keeping the substrates clean from any oxide layer, and at high temperature to achieve diffusion bonding between coating and substrate, which can be achieved using VPS.

Thermal barrier coating (TBC) systems are also widely used in modern gas turbine engines to lower the metal surface temperature in combustor and turbine section hardware. The engine components exposed to the most extreme temperatures are the combustor and the initial rotor blades and nozzle guide vanes of the high-pressure turbine. Metal temperature reductions of up to 165 °C are possible when TBCs are used in conjunction with external film cooling and internal component air cooling [Feuerstein A, et al. (2008)]; TBCs are applied on vane bases, burner cans, after burners, and also on other small engine components. An example of coated gas turbine vane is presented in Fig. 19.4 and that of a TBC-sprayed combustion chamber in Fig. 19.5.

Rotating vane assemblies in aircraft engines require limiting the bypass flow of either hot combustion gases or cold compressor gases through the spaces between the blade tips and the stationary housing. These seals can improve significantly the engine efficiency. Two types of seals are used: abradable ones that are machined in situ by the rotating components (blades, for example), and labyrinth ones to match stator and rotor components with an intermeshing saw tooth geometry.

Against wear, chrome plating has been intensively used because of its durability, ease of application, and low cost. It suffers, however, from pitting, spalling, and other failures under stress. Moreover, for commercial airlines the downtime in which the aircraft is out of service, for the replacement of traditional industrial chromium plating, used in landing gear, is simply too long and prohibitively expensive.

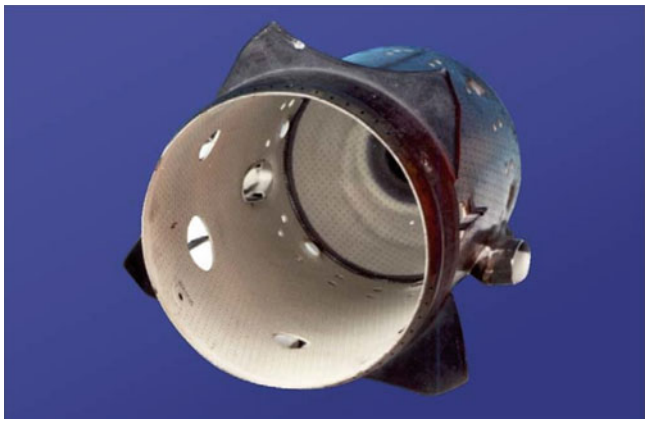

Fig. 19.5 TBC-coated combustion chamber. (Courtesy of Sulzer-Metco)

Alternative coating solutions had also to be developed for the replacement of chrome plating because of serious environmental and health problems associated with hexavalent chromium emissions. Hard trivalent chrome coating, and HVOF- or plasma-sprayed tungsten carbide coatings, present viable alternatives, each with their respective advantages and limitations such as limited coating thickness for trivalent chrome, and only line-of-sight geometries for thermally sprayed coatings [Thintri Inc. (2013)]. Coatings of tungsten carbides especially developed for landing gears and HVOF sprayed have considerably increased the service life of exposed cylinders and seals used in landing gears. Figure 19.6 presents a robot coating a landing gear.

19.4.2 Land-Based Turbines

Compared to aero engines, land-based turbines (LBT) such as the one shown in Fig. 19.7 work in different conditions: the external environment might range from cold (−40 °C) to high temperature (55–60 °C) and corrosive and erosive contaminants due to the environment and fuel are present. Coatings are applied onto bearing journals, bearing seals, sub-shaft journal, labyrinth seals, blades, tip seals, inlet and exhausts, and housing [Davis JR (ed) (2004)]. A detailed description of the different land-based turbines can be found in the paper by Lebedev and Kostennikov (2008). Pomeroy (2005) gives a good description of coatings for gas turbine materials and long-term stability issues. Due to the demand to increase turbine inlet temperatures and thus cycle efficiencies, ceramic insulating coatings can be applied to decrease the temperature of the hottest parts of the turbine components by up to 170 °C. A review of the next generation of TBCs for gas turbines is presented by Curry et al. (2011).

Coatings are applied on bearing journals, bearing seals, stub shaft journals, labyrinth seals, blade nozzles, tip seals,

inlets and exhausts, and housings [Davis JR (ed) (2004), Tucker RC (ed) (2013)]. The overview by Rajendran (2012) presents the different coatings used, methods of application and characterization, and degradation mechanisms, and indicates future directions, which are of use to a practicing industrial engineer. Coatings are applied to the compressor blades and vanes for enhanced erosion resistance. Anti-fretting coating protects the contact area of the dovetail part of the compressor blade root from fretting fatigue failure. Abradable coatings offer close clearance control thereby increasing the engine efficiency. Wear-resistant coatings give extended life to the parts that undergo rotary and reciprocating rubbing motion. Oxidation and corrosion-resistant coatings are applied through either diffusion or overlay process. YPSZ (7 wt.%) thermal barrier coatings offer increased component life with a decrease in operating temperature of the metal. Hardwicke and Lau (2013), in their review paper about advances in thermal spray coatings for gas turbines and energy generation, describe functional coatings widely used in energy generation equipment in industries such as renewables, oil and gas, propulsion engines, and gas turbines. They present the current status of materials, equipment, processing, and properties' aspects for key coatings in the energy industry, especially the developments in large-scale gas turbines. In addition to the most recent industrial advances in thermal spray technologies, future technical needs are also highlighted.

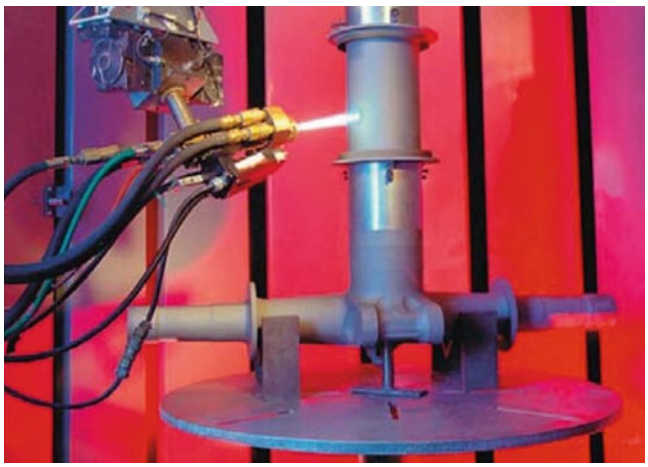

Fig. 19.6 Robot coating a landing gear. (Courtesy of Oerlikon-Metco)

Coating life for land-based turbines (time to refurbish aircraft turbines) should be approximately 24,000 h, with a majority of all service time at maximum conditions, against 8000 h for aircraft turbines with only 5–15% at maximum conditions. Thus, problems of bond coat oxidation, interdiffusion of bond coat and substrate, coating densification, and

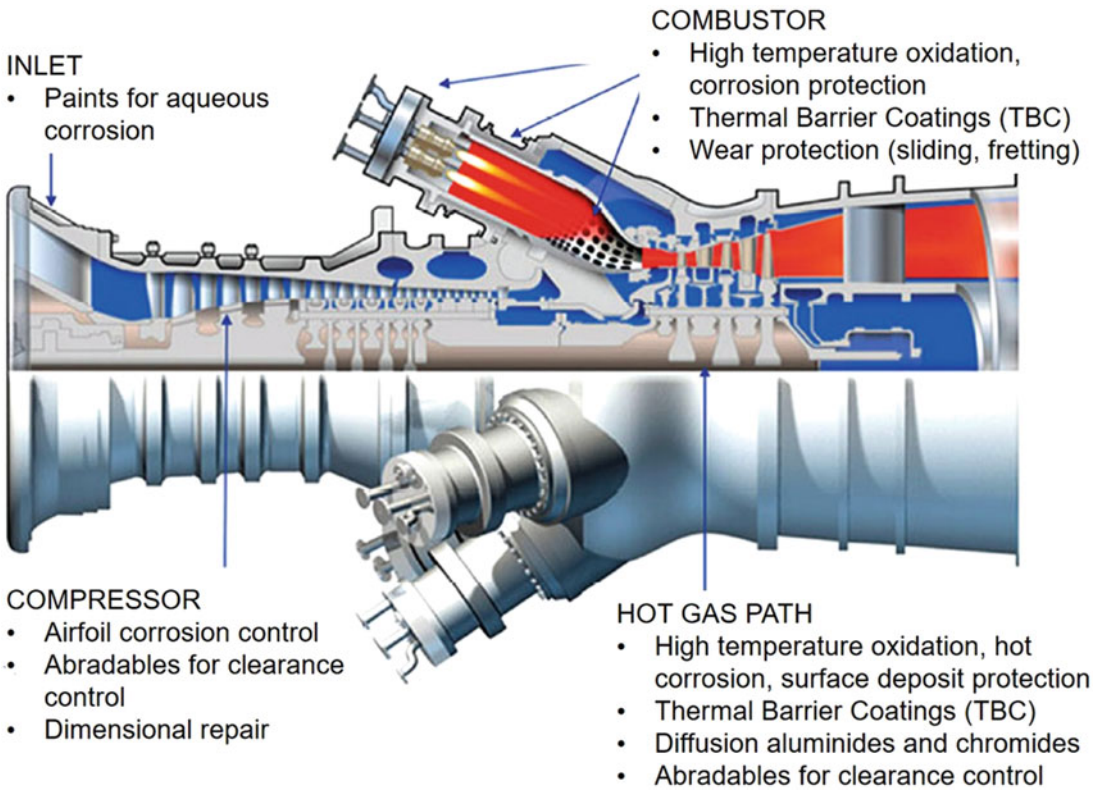

Fig. 19.7 Challenges in traditional industrial gas turbine (IGT) applications for thermal spray coatings with respect to turbine locations. (Schilke 2004; Singh et al. 2019)

changes in thermal or mechanical properties of the coating are more important. Accessibility for inspection, repair, and refurbishment is also more difficult for power generation machines than for aircraft engines. Component size is also more important (a factor of 10 for turbine blades), thus requiring adapted spray processes. At last, the quality of the combustible is far from that used in aircraft engines [Mutasim Z, Brentnall W (1997), Nelson WA, Orenstein RM (1997), Parks WP, et al. (1997), Tamura M, et al. (1999), Wright IG, Gibbons TB (2007)].

Turbines are also exposed to excessive amounts of moisture and chlorides, giving rise to development of two types of hot corrosion and oxidation:

- Type II hot corrosion, occurring at temperatures in the range 500–800 °C and involving the formation of base metal (nickel or cobalt) sulfates that require a certain partial pressure of sulfur trioxide for their stabilization.
- Type I hot corrosion, observed in the range 750–950 °C, involving the transport of sulfur from a sulfate deposit (generally Na_2SO_4) across a preformed oxide into the metallic material with the formation of the most stable sulfides. Once stable sulfide formers (e.g., Cr) are fully reacted with the sulfur moving across the scale, then base metal sulfides can form with catastrophic consequences as they are molten at the temperatures at which Type I hot corrosion occurs.

Sprayed materials with a good corrosion and oxidation resistance are nickel- and/or cobalt-based alloyed coatings [Davis JR (ed) (2004)], such as NiCrMo (Hastelloy or Nistelle), CoCrSiMo (Triballoy), and MCrAlYs plasma or HVOF sprayed. Oxidation- and corrosion-resistant coatings are applied on air inlets, combustor liners, injectors, turbine tip shoes, nozzles, and exhausts [Davis JR (ed) (2004)]. On blades and vanes, MCrAlY coatings are used as bond coats and for corrosion–oxidation protection.

For thermal barrier coatings, mainly ZrO_2–Y_2O_3 (6–8 wt. %), ceria, or dysprosia-stabilized zirconia are used [Wright IG, Gibbons TB (2007)] and also ceria and yttria-stabilized zirconia or for certain applications calcium titanate [Davis JR (ed) (2004)]. It is worth underlying that for abradable and seals in the low-temperature areas, where moisture is important, porous aluminum-base coatings containing polyester, polyimide, or BN, as well as nickel–graphite coatings are used. For higher temperatures (over 450 °C), abradables are made of MCrAlY with BN or polyester [Wright IG, Gibbons TB (2007)]. Ceramic abradables have also been introduced but the expansion mismatch with the metal substrate must be accounted for with the cooling of the superalloy.

19.4.3 Automotive

Thermal spraying has been rather slow in penetrating the automotive industry due to its extreme sensitivity to manufacturing cost and to strict demand on coating reliability. Nevertheless, early signs of acceptability for high-end luxury and racing cars started around the turn of the century. As illustrated in Fig. 19.8, after Oerlikon-Metco Corp., an increasing number of car parts is being treated by different surface modification technologies (from sprayed coatings to PVD or plasma-enhanced chemical vapor deposition [PECVD]). The different coating applications are related to [Davis JR (ed) (2004), Vetter J, et al. (2005), Barbezat G (2003, 2005, 2006)] the power train components, thermal barriers protecting certain components from overheating, brake disks, cylinder bore in diesel engines, aluminum alloy cylinder bore, exhaust valves, crankshaft, transmission and rear end gear clusters, body and chassis, synchronizer rings, shifter forks, valve seats, and connecting rods. Examples of some of these components are given in Fig. 19.9.

Against hot corrosion: Exhaust system components (exhaust headers, exhaust pipes) are protected from hot corrosion by aluminum coatings wire arc sprayed.

Against wear: Piston rings are commonly coated with molybdenum and molybdenum-bearing compounds using the plasma spray process in general. The HVOF spray process is used in the case of high-performance piston rings for diesel engines. Molybdenum coatings are also used on aluminum piston skirts to prevent galling. Some aluminum piston tops are coated with molybdenum to limit erosion due to the impingement of fuel from injectors. Cylinder bore in diesel engines are coated with molybdenum plasma sprayed or WC–Co and WC–Co–Cr HVOF sprayed. Such coatings, slightly porous, retain oil and improve friction. Coated transmission parts such as synchronizing rings and shift forks are widely coated using wire flame spraying with molybdenum to provide a constant coefficient of friction and prevent scuffing.

In order to reduce the weight and size of the engine, iron cylinder blocks are replaced by aluminum ones, usually equipped with cast-iron cylinder linings. Instead of them, Sulzer-Metco has been the first to propose aluminum cylinder bores coated with a special iron alloy, to replace the cast-iron cylinder lining. This plasma coating acts as a direct running surface for the similarly coated piston rings, which reduces diesel or gasoline consumption and the amount of oil needed. The process called "Rota-plasma" developed by Sulzer-Metco was introduced in 2000 for automobile production. It allows coating aluminum alloy (cast aluminum–silicon) cylinder bores to provide a good wear resistance. Coating materials can be carbon steel with its own oxides wustite and magnetite as solid lubricant, composite of carbon tool

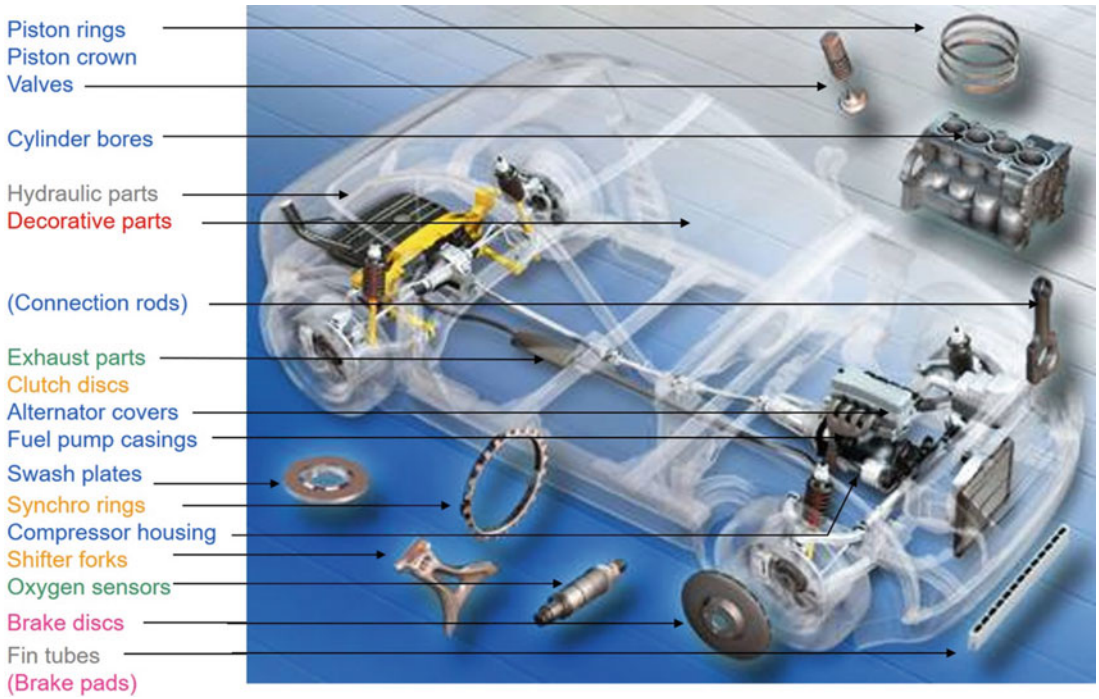

Fig. 19.8 Selected parts to be treated by surface technologies in cars. (Reproduced with kind permission of Oerlikon Metco Corp)

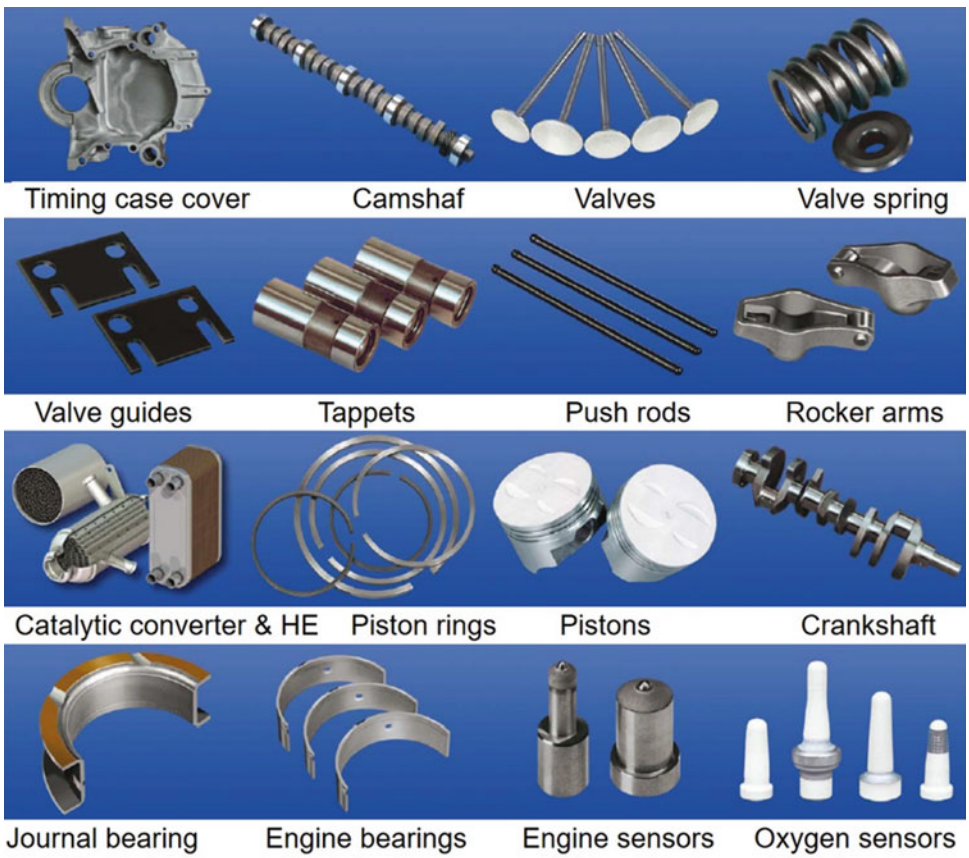

Fig. 19.9 Examples of some of the plasma-coated automobile parts for enhanced longevity and improved performance. ([After Oerlikon-Metco, automotive solutions kit, 2008] Reprinted with kind permission)

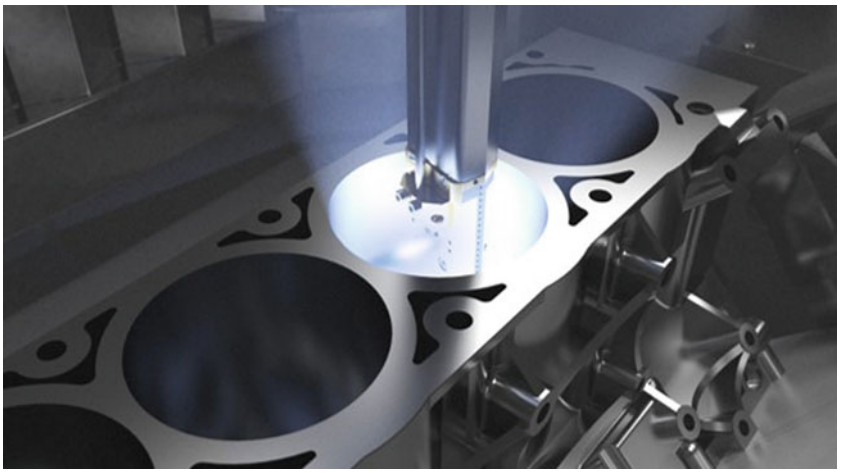

Fig. 19.10 Photo of the Rota plasma process. (Courtesy of Oerlikon-Metco Corp.)

steel and molybdenum, corrosion-resistant steel (Cr and Mo alloyed), and metal matrix composite with ceramic particles. The process is entirely automated and lasts about 1 minute for a bore of conventional car engine (see Fig. 19.10).

The process advantages are the following:

- The pitch distance between the cylinders can be reduced allowing a further reduction in the engine block weight.
- The friction between the piston rings and the liner surface can be significantly reduced (more than 30% in gasoline engines).
- Considering that the majority of the energy losses in the engine is due to thermodynamic cycle efficiency, the potential fuel savings is limited to 4–5%.
- Very low surface wear rate (about 5 nm/h of service).
- Transmission and rear end gear clusters receive often Mo thin coatings plasma sprayed to lessen the friction and produce smoother movement.

TBCs have also been used on piston heads and valves and exhaust ports of high-performance engines. TBC for diesel engines either thick (0.5–1 mm) [Beardsley MB (1997)], or eventually phosphate sealed [Ahmaniemi S, et al. (2002a, b)], or thin [Hejwowski T, Weronski A (2002)] are used to:

- Increase the piston head temperature and improve the fuel combustion [Buyukkaya E, Cerit M (2007)]
- Reduce NO_x emissions [Buyukkaya E, Cerit M (2007)]
- Reduce the heat rejection [Parlak A, et al. (2005)]
- Improve the usability of vegetable oils as a fuel [İşcan B, Aydın H (2012)]

They can also be applied externally on manifolds and other exhaust systems when the air cooling becomes insufficient. They increase the efficiency of turbochargers.

Metal matrix composites are used in brake disks to tailor the mechanical resistance and the thermal conductivity. The wire arc spray provides low-cost filler for weld seam and is also used for dimensional restoration. Ceramic overlays are sprayed for oxygen sensor protection, the sensor itself using zirconia-sprayed coating.

19.4.4 Land-Based and Marine Applications

When metal coatings are needed to enhance the properties of a given surface, wire combustion spray systems or wire arc spray systems are very good solutions to spray protective coatings, especially sacrificial ones. The investment is rather low and coating adherence is generally good (over 20 MPa), with almost no heating of the substrate. However, coatings obtained by these methods are relatively porous (up to 20%), which is not a problem for sacrificial ones. These coatings are extensively used throughout the maritime, paper/pulp/printing, manufacturing, steel, aerospace, automotive, and railroad industries.

19.4.4.1 Sacrificial Coatings

The corrosion protection of large steel structures such as bridges, pipelines, oil tanks, towers, radio and television masts, overhead walkways, and large manufacturing facilities in the metallurgical, chemical, energy, and other industries is a key issue. The protection of structures exposed to moist atmospheres and seawater such as ships, offshore platforms, and seaports is even more difficult [Evdokimenko Yu I, et al. (2001), Sørensen PA, et al. (2009)]. In most cases the surface to be protected is thousands and even tens of thousands of square meters, requiring that coating costs be competitive with those of traditional painting methods. The coating rate must be equal or higher than 10 m^2/h and if possible

Fig. 19.11 Photograph of typical suspension bridge normally WAS with zinc coat followed by painting for environmental protection against corrosion

deposited in one unique pass. The equipment must be mobile and autonomous for operation in field conditions and must work under manual control, automation being generally difficult for large-scale operations, and, at last, the spray gun can be up to 30 m from its power supply and control center [Evdokimenko Yu I, et al. (2001), Sørensen PA, et al. (2009)]. Flame wire arc spraying meets such requirements.

Sacrificial coatings (cathodic behavior relatively to ions, for example, Zn or Al on steel) are mainly used: the thicker they will be the longer will be the protection. Typical thicknesses vary from 50 to 500 μm; the most frequent ones being around 230 μm. Such coatings must have a cathodic behavior relatively to the ions of the metal to be protected, in almost all cases steels. Metals used are then zinc, aluminum, and zinc–aluminum. Zinc performs better than aluminum in alkaline conditions, while aluminum in acidic conditions. Zinc and aluminum replace more and more painting and galvanizing because their lifetime is predictable, they have good erosion resistance, and require one application with no drying problems. Sluice gates and canal lock gates of the St. Denis Canal in France, that have been zinc coated in the early 1930s, have remained in perfect condition with virtually no maintenance for decades. According to literature [Davis JR (ed) (2004), Tucker RC (ed) (2013) *ASM Handbook, Volume 5A*], the lifetime of a 255 μm thick zinc or zinc aluminum coating is about 25 years and it can be extended 15 years by sealing it with vinyl paint. Painting is not the only sealer used; impregnation with special compositions (epoxy resin, silicon resin, etc.) is also being intensively used. As soon as sealing is considered, the porosity of these coatings becomes an advantage for the adhesion of the sealer. Figure 19.11 represents a typical suspension iron bridge which is normally protected against environmental corrosion by WAS with a zinc coat followed by a paint finish.

Zinc–aluminum (Zn–15 wt.% Al) seems to combine advantages of both materials. If resistance to wear must be improved, aluminum coatings can be sprayed with alumina particles, for example, using cored wires.

In case of the protection of steel reinforcement in concrete, zinc is generally used, but titanium has also been used in spite of the fact it is an anodic protection. In that case the coating is applied directly on the concrete substrate [Davis JR (ed) (2004), Tucker RC (ed) (2013) *ASM Handbook, Volume 5A*]. Aluminum must be avoided where thermite sparkling may occur. That is due to the reaction of rusted steel and aluminum smears when this combustible mix is ignited by an impact [Davis JR (ed) (2004), Tucker RC (ed) (2013) *ASM Handbook, Volume 5A*]. Another interest of such coatings is their antifouling properties. Marine biofouling is the undesirable accumulation of marine organisms on artificial surfaces that are immersed in the sea. For example, when marine biofouling occurs on ship hulls, it leads to an increase in weight of the ship and friction to sail.

In the protection from corrosion and/or erosion of industrial gas turbine compressor airfoils, a sacrificial aluminum-filled metallic coating has been recently developed by Sulzer-Metco. The aluminum-filled metallic coating is made conductive via mechanical abrasive finishing. The thickness of these coatings is typically between 25 and 75 μm and the maximum operating temperature 870 °C. Figure 19.12 presents the coated blades of the compressor airfoil.

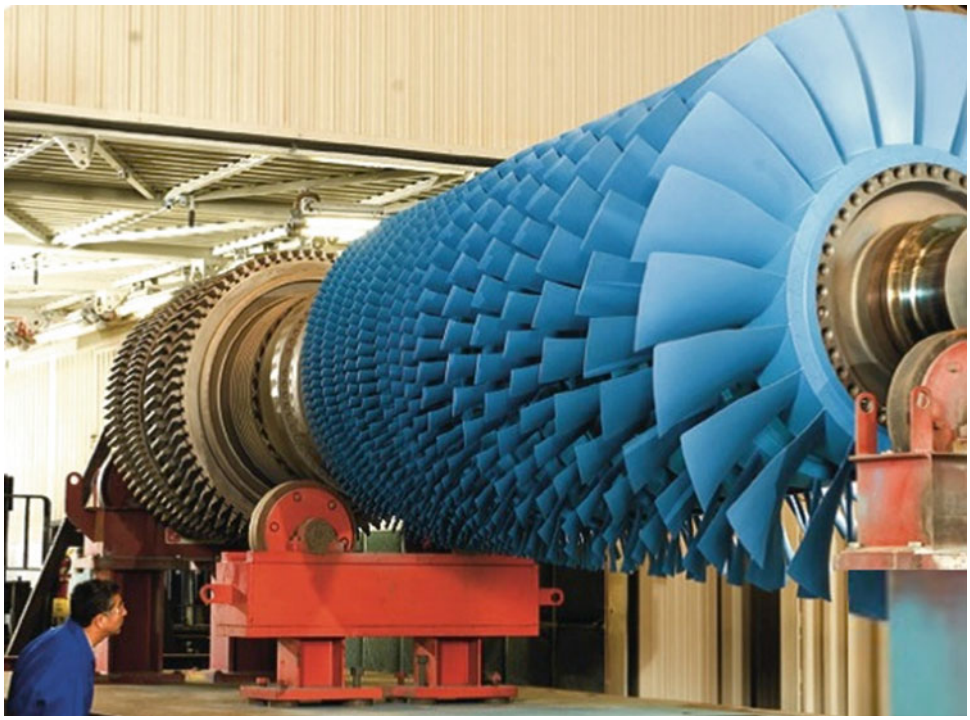

Fig. 19.12 Coated blades of the compressor airfoil of an industrial gas turbine compressor. (Courtesy of Oerlikon-Metco Turbo)

19.4.4.2 Non-sacrificial Coatings

Austenitic stainless steels, aluminum bronze, nickel-base alloys, MCrAlY, cermets with WC, Cr_2C_3, and matrices containing chromium or nickel, or both, are used against corrosion, often associated with wear. However, such coatings, presenting no galvanic protection, will never protect the substrate if connected porosities and oxide networks exist, which is the case of most thermally sprayed coatings. The substrate protection requires using a protective bond coat or producing dense coatings or sealing them, which is not always possible if the service temperature is over a few hundreds of Celsius degrees.

Coatings of corrosion-resistant alloys for severe petroleum industry corrosion applications, such as type 316L stainless steel and Hastelloy C-276, were shown to act as true corrosion barriers. The oxide content also plays a role (see Sect. 19.3.2.1.2: Chemical or Parachemical Corrosion).

For applications with a severe wear in oil and gas industry, cermets are used, with however some problems for offshore installations. According to Meng (2010), the corrosion resistance is improved by the proper choice of binder between the wide varieties of tungsten carbides.

19.4.5 Electrical and Electronics Industry

First of all, thermal spray coatings that allow achieving thick coatings cannot compete with the thin film technology (chemical vapor deposition [CVD], PECVD, sputtering, ion plating, etc.) used in electronic devices. However, they can be very useful in capacitors, insulators, resistors, and inductors. Coatings of oxide ceramics (alumina, titanate, beryllia) are used as dielectrics, while metals and alloys are used for current carrying and bonding to ceramic substrates, metals for electromagnetic shielding, and so on [Davis JR (ed) (2004), Tucker RC (ed) (2013) *ASM Handbook, Volume 5A*]. A few examples are presented below.

Alumina plasma-sprayed coatings are currently used in ozonizers. Standard ozonizer tubes consist of a borosilicate glass tube serving as dielectric with a metal coating applied to the inner surface of the tube serving as the high-voltage electrode. In order to increase the ozone production efficiency, a material with a higher permittivity is needed. Alumina coatings with a thickness up to 1000 μm and serving as dielectric are deposited together with the metal electrode on top of the glass tube in ozonizers. Alumina is also used for high-temperature strain gages and insulation of induction heating coils.

Multilayer ceramic chip capacitors (MLCC) are used in a large number of electronic appliances. According to Yamakawa et al. (2009), they are being required in more compact sizes, larger capacities, and reduced costs year by year, and ceramic trays (a type of kiln furniture) are used for firing them. Normally, this ceramic tray consists of an Al_2O_3–SiO_2 body, an Y_2O_3-stabilized ZrO_2 topcoat, and Al_2O_3 basecoat. The application of plasma-sprayed ZrO_2

topcoat and an Al_2O_3-sintered basecoat makes it possible to enhance longevity and reduce cost.

Pure beryllia (BeO) presents excellent thermal and dielectric properties and is used in many high-performance semiconductor parts for applications such as radio equipment. Some power semiconductor devices use beryllia between the silicon chip and the metal mounting base of the package in order to achieve a lower value of thermal resistance than the alumina currently used. It is also used as a structural ceramic for high-performance microwave devices, vacuum tubes, magnetrons, and gas lasers. Vacuum plasma-sprayed beryllia coatings present excellent properties. Unfortunately, their handling, especially that of fine powders, is highly toxic resulting in very stringent safety conditions such as keeping the rooms where spraying is achieved at pressure lower than atmospheric one. These conditions are often economically prohibitive and such coatings are essentially used for army and nuclear applications [Davis JR (ed) (2004)), Tucker RC (ed) (2013) *ASM Handbook, Volume 5A*].

According to Smyth and Anderson (1975), for electrical heaters, arc-sprayed coatings are used, masking permitting to define the geometry. The choice of the material (NiCr, NiAl, etc.) depends on its resistance variation with temperature that must be as low as possible because the electricity source is a constant voltage one. The resistance depends on the coating oxide content that can also modify the alloy composition, chromium being preferentially oxidized compared to nickel, for example. Most sprayed resistors are used at relatively low temperatures (<250 °C). The resistance value can also be increased when adding alumina particles. Coatings can be sprayed on ceramic material, even polished ones, with a very good adhesion, when eutectics are formed or diffusion occurs. It requires heating the substrate to temperatures close to the sprayed alloy or metal temperature.

Cold-sprayed copper coatings are used to improve the heat conductivity between electronic devices, an underlying copper plate, and a soldered copper-coated heat sink, which is fabricated out of aluminum [Gärtner F, et al. (2006)]. Cold spray also permits the generation of solderable surfaces on materials with poor wettability (for example, heat sinks, such as copper on aluminum) [Marx S, et al. (2006)]. Similarly, PTA allows spraying very thick (up to 10 mm or more) copper coatings that are used in powerful computer systems to improve their cooling. These copper layers, Fig. 19.13, achieve a good heat distribution and remove the heat more easily.

Alumina films plasma sprayed are more and more used as insulators in electronic devices. Plasma-sprayed alumina is used for electronic package mount in automotive industry.

Wire arc sprayed coatings are used as shielding material to eliminate electromagnetic and radio frequency interference and dissipate static discharge sparks. Zn and Al are currently used to protect computers, electronic office equipment, medical monitoring devices, housing constructed of temperature-sensitive plastic, and rooms containing military computers.

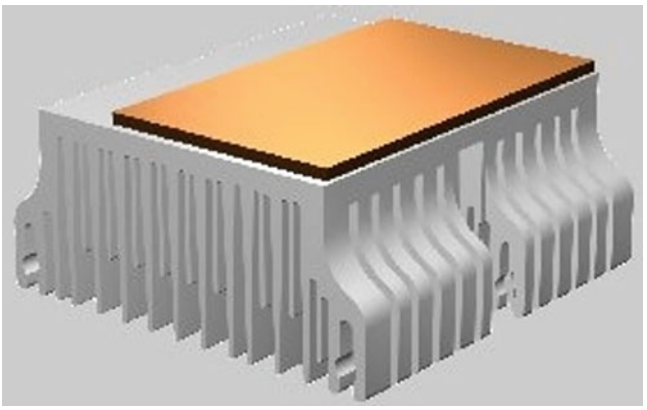

Fig. 19.13 Example of flame wire spraying: copper layer on a computer cooling system. (Ducos 2006a, b)

The review paper by Sampath (2010) points out the industrial success of the lambda sensor for exhaust gas oxygen measurement for engine fuel control. This sensor uses a porous plasma-sprayed zirconia membrane coating between electrodes. When subjected to a differential partial pressure of oxygen, a rapid variation in electric resistance related to the oxygen partial pressure can be monitored through an electrical circuit [Sampath S (2010)].

Aluminum coatings, wire arc sprayed, are used in the production of electrolytic condensers. A thin film of copper is sprayed on carbon and ceramic resistors and carbon brushes to provide the electrical connection of high electrical conductivity. Thermally sprayed coatings are also used to produce thick films' electrical circuits that can carry higher current than printed ones. The most used materials for these applications are Cu, Al, Zn, and Ag.

19.4.6 Medical Applications

Orthopedic and dental market is developing very fast with either bioinert coatings (Ti–6Al–4V, Ti–6Al–7Nb, Ti–13Nb–13Zr, etc.) or bioactive ones (hydroxyapatite, tricalcium phosphate). Both orthopedic and dental implants receive coatings designed to aid fixation in bone tissues. For example, according to Yang et al. (2006a, b) and Ong et al. (2006), the report published in *Implant Dentistry* estimated that 910,000 dental implant procedures were performed in 2000, and the numbers grew at an annual rate of 18.6% through 2005. By 2005, annual sales exceeded half a billion dollars. The implant success is dependent on quality bone formation, optimization of the local surface structure, chemistry, morphology, and use of bioactive factors that are equally important [Ong JL, et al. (2006)]. Coated implants

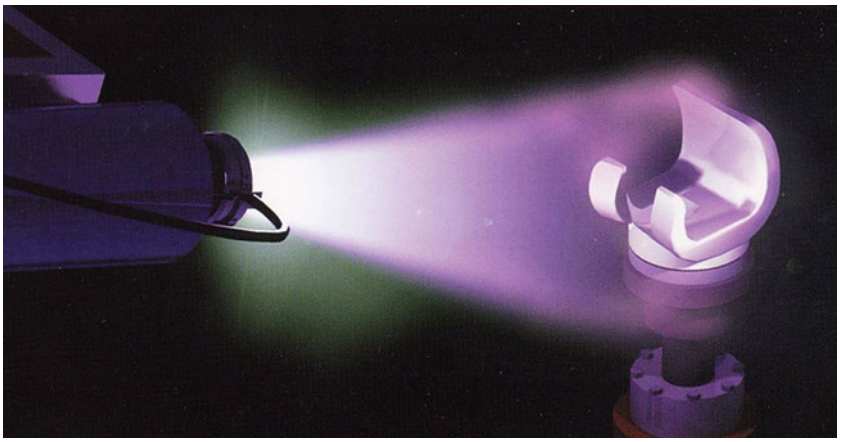

Fig. 19.14 Vacuum plasma spraying of HA coating on a knee prosthesis

are now currently used for tooth, hip, knee, elbow, and shoulder. Two types of coatings are used [Davis JR (ed) (2004), Tucker RC (ed) (2013) *ASM Handbook, Volume 5A*]:

First, bioinert ones, with no activity between them and the bone or soft tissues, the most used materials being Ti and Ti–6Al–4V. These coatings must be porous (at least 30%). Plasma spraying allows preparing porous-graded coatings with dense coating close to substrate to achieve a strong adhesion with substrate and very porous outermost layer (with pore sizes over 100 up to 400 μm). To achieve that, the plasma power was gradually reduced, and the particle sizes increased while regulating the degree of powder melting layers to achieve porous graded coatings [Yang Y, et al. (2006a, b), Ong JL, et al. (2006), Tucker RC (ed) (2013)].

Second, bioactive coatings, interacting with bone to promote bonding interfaces, are ceramic coatings with material compositions similar to that of bone tissue (calcium phosphate). The most used ceramic is hydroxyapatite (HA), $Ca_{10}(PO_4)_6(OH)_2$, exhibiting a strong activity to join the bone. The provision of a high calcium- and phosphorus-rich environment promotes rapid bone formation within the vicinity of the implant. Unfortunately, when HA is plasma sprayed in air, calcium oxide (CaO) is usually formed, thereby affecting the integrity of plasma-sprayed HA coatings. Plasma-sprayed HA coatings also contain other bioresorbable phases, such as tricalcium phosphate (TCP) α or β forms, tetracalcium phosphate (TTCP), and amorphous calcium phosphate (ACP) [Prevéy PS (2000)]. Gross et al. (2004) investigated four HA-coated hip components recovered from patients during revision surgery. Analysis of the coating surface indicated dissolution, osteoclastic resorption, and carbonate apatite precipitation identical to observations from previous in vitro studies. The coating microstructure differed between three coatings that remained on the prosthesis surface, ranging from completely crystalline coatings made by vacuum plasma spraying to less crystalline coatings manufactured by air plasma spraying. Increasing the amorphous and TCP concentration predisposes the coatings to higher dissolution rates [Gross KA, et al. (2004)]. Nelson et al. (2011) have deposited by flame spraying powders of titanium alloy (Ti–6Al–4V) and bioactive glass (45S5) to fabricate composite porous coatings for potential use in bone fixation implants. Bioactive glass and titanium alloy powder were blended and deposited in various weight fractions and with two sets of spray conditions, which produced different levels of porosity. The HA formation on the alloy–bioactive glass composite coating suggested that the addition of bioactive glass to the blend may greatly increase the bioactivity of the coating through enhanced surface mineralization. Drnovšek et al. (2012) studied the ability of nanoparticle bioactive glass (BAG) to infiltrate into the porous titanium (Ti) layer on Ti-based implants to promote osseointegration. Juhasz and Best (2012) reviewed bioactive implants, coatings, and scaffolds made of ceramics, glasses, glass–ceramics, and composites that were able to form a chemical interfacial bond with tissue and can be resorbable or non-resorbable.

The ratio of HA to TCP has been reported to be crucial for bone regeneration. The dissolution rate of HA coating is dependent on the biochemical calcium phosphate phase of the coating as well as coating crystallinity. With adapted spray conditions, it is possible to achieve up to 75% crystallinity for APS, 80% for HVOF spraying, and 95% for VPS [Gross KA, et al. (2004), Khor KA, et al. (1997a, b), Chang C, et al. (1998), Lima RS, et al. (2010), Lima RS, et al. (2006)]. The result also depends on powder preparation, best results being obtained with dense HA particles. In Fig. 19.14 is presented the vacuum plasma spraying (VPS) of HA coating on a knee prosthesis and in Fig. 19.15 biocompatible coating on the lower part of hip joints.

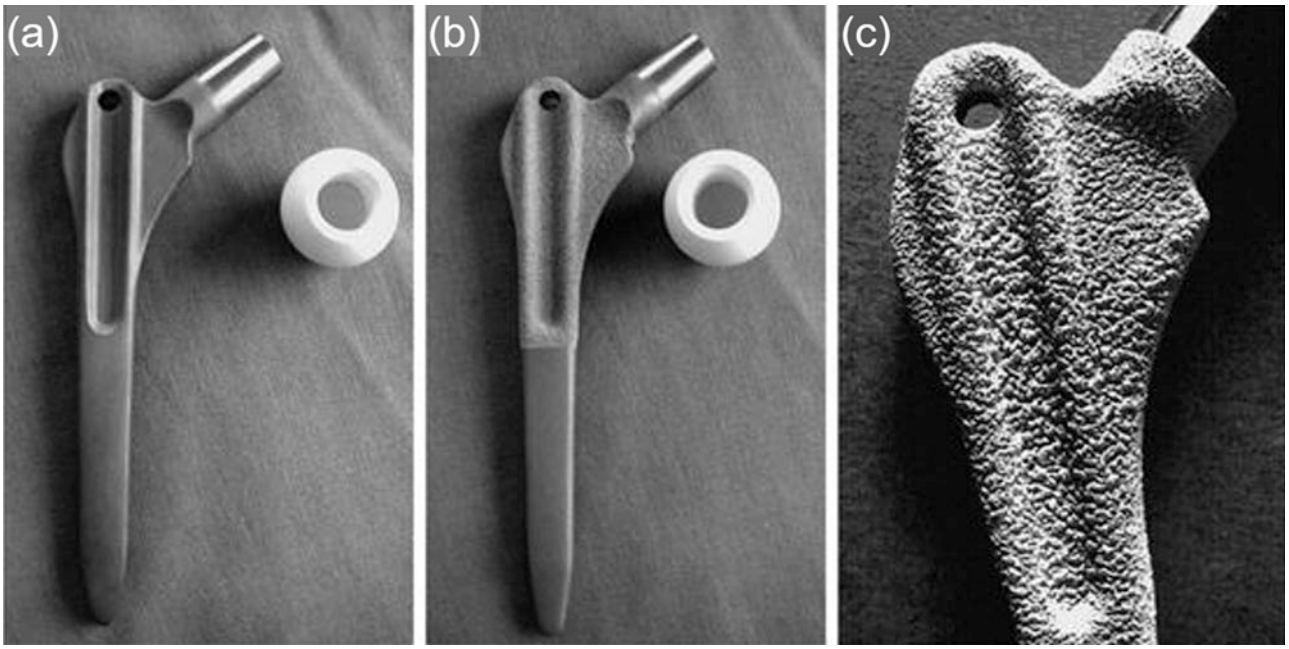

Fig. 19.15 (**a**) Femoral stem Walter, without coating. (**b**) Femoral stem with titanium alloy/hydroxyapatite coating. (**c**) Magnified view of the coating at the proximal end of the porous coated femoral stem. (Landor et al. 2007)

19.4.7 Ceramic and Glass Manufacturing

For the production of a variety of glasses, platinum is currently used thanks to its high melting point, strength, and resistance to corrosion that allows withstanding the abrasive action of molten glass. Rhodium is often alloyed with platinum to increase the strength of the alloy and extend the life of the equipment. According to the prices of these metals, instead of using them as plates or sheets, they are often plasma sprayed in inert atmosphere chambers where oversprayed powder can be collected. A ceramic coating, that is reapplied regularly according to its wear [Davis JR (ed) (2004), Tucker RC (ed) (2013) *ASM Handbook, Volume 5A*], can protect these precious metal coatings. The electric glass melting for homogenizing, feeding, and shaping was developed with molybdenum electrode materials, since stirrers, mixing paddles, and some mold surfaces are plasma coated with molybdenum and its alloys [Davis JR (ed) (2004), Tucker RC (ed) (2013)].

Mold glass material must have sufficient strength, hardness, and accuracy (no deforming process) at high temperature and pressure. Of course, its oxidation resistance must be good, its thermal expansion low, and its thermal conductivity high. Therefore, the mold material choice depends critically on the transition temperature of the glass material. For low-temperature transition glasses, steel molds with a nickel alloy coating can be used. For example, self-fluxing alloy NiCrBSi flame sprayed and refused. For higher transition temperatures, NiCr–Cr_2C_3 or TiC cermets are used.

Hamashima (2007) has developed a new boride cermet coating consisting of Mo-system ternary boride and iron-group metal alloys. MoCoB–Co/Cr cermets have a very low friction coefficient with glass at high temperature. The cermet coating has been applied to the lower mold on an industrial scale and the results were very satisfactory. In particular, the production efficiency of the forming process was improved substantially.

19.4.8 Printing Industry

According to Döering et al. (2008), all printing presses need an ink transferring unit, a print form, and an impression cylinder. They differ in the process of transferring the print image to the substrate, leading to additional cylinders for generating the inverted image—in case of offset printing the so-called offset cylinder—or even a shortcut from the ink transferring roller to the print form and directly to the substrate if gravure printing is regarded. Additionally, dampening units require other surface energy than ink leading rollers. Moreover, the precision of shape and surface roughness of these core components is rather high. Therefore, not only the requirements for an appropriate coating in terms of the function but also the requirements for the grinding and finishing step after the coating process are rather high. This will be illustrated with few examples.

The ink transporting system in offset printing machines consists of several different rollers, providing a homogenous

Fig. 19.16 SUME™CAL coating after super-finishing on calendar roll. (Courtesy of Oerlikon-Metco)

film of ink for the print form. For example, the duct-roller elevates the ink from the ink box to the ink conditioning system. Its surface roughness R_z must be better than 2 μm and tolerances must be better than 2/1000 mm in concentricity. Such conditions are achieved with chromia-rich coating consisting of a bond coat (Ni, NiCr, NiAl) and the ceramic topcoat [Pawlowski L (1996)].

Rollers in the paper industry are subject to various operating environments resulting in wear, chemical attack from dyes, thermal stress on heated rollers, and mechanical stress from doctor blades. They also must exhibit a high surface finish lasting as long as possible. Figure 19.16 presents a calendar roll coated with the so-called Oerlikon-Metco SUME^{TM}CAL developed to meet these requirements.

In contrast to common offset inking units, the anilox unit consists of a laser-engraved roller, taking the ink from a chamber doctor blade system [Döring J-E, et al. (2008)]. The gravure procedure is performed after finishing the roller surface. Producing pure chromia coatings implies using carefully adapted plasma spray conditions and adapted powders. For more details, see the works of Pawlowski [Pawlowski L (1995, 1996)].

Many other rolls are used in printing machines [Pawlowski L (1996)], where different oxides (chromia, alumina–titania [3 or 13 wt.%]) are plasma sprayed. Lima and Marple (2005) have proposed to replace the alumina–titania conventionally plasma sprayed by HVOF-sprayed nanostructured titania coating exhibiting a very dense (nearly pore free) and uniform isotropic microstructure with an excellent wear and corrosion resistance. Plasma-sprayed chrome oxide coatings for inking rollers exhibit very fine microstructures, which can then be laser engraved with a very small and tight pattern (Fig. 19.17).

Other rolls such as blanket cylinders are coated with Hastelloy-C by either APS or HVOF and at last draw rolls are coated with nickel–chromium [Davis JR (ed) (2004), Vetter J, et al. (2005)].

19.4.9 Pulp and Paper

Machines producing paper and cardboard comprise many parts that can be rather important (for example, rolls over one meter in diameter and ten meters in length) with high wear and corrosion problems. Coatings are used in several types of rolls and cylinders, including, for instance, center press rolls, dryer cylinders, calendar rolls, traction rolls, and Yankee cylinders [Vuoristo P, Nylén P (2009)]. Coating materials used are iron- and nickel-base alloys, nickel–chromium self-fluxing alloy, carbides, oxide ceramics, and various multilayers, again depending on the application. For example, rolls are coated by NiCrBSi coatings flame sprayed and others by WC–Co coatings HVOF sprayed. Figure 19.18 presents calendar roll of a paper machine protected by thermal spraying.

Functionally graded (FG) coatings are considered as an option to increase compatibility between ceramic coatings and metallic substrates. In this concept material properties such as coefficient of thermal expansion (CTE) and elastic modulus are designed to gradually change in order to reduce the thermal stresses within the coating. Posttreatments such as coating with fluoropolymers or sealing coatings against corrosive process environments are also used. A few examples are presented below.

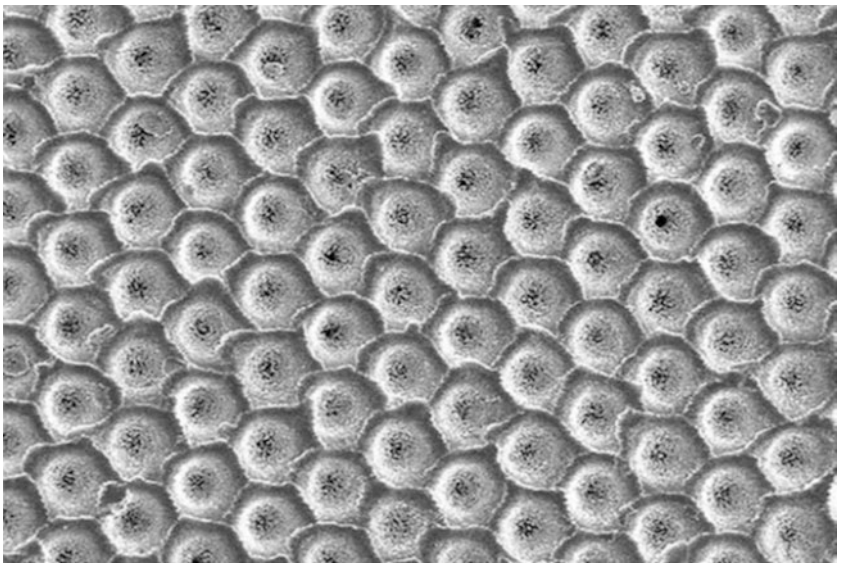

Fig. 19.17 Anilox printing roll with a laser-engraved chromium oxide coating. (Courtesy of Orelikon-Metco)

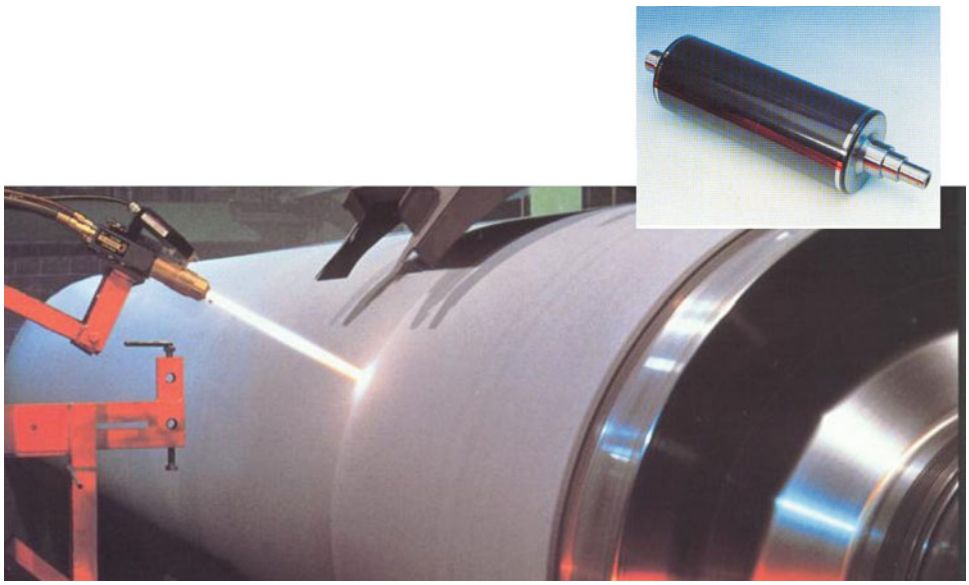

Fig. 19.18 Plasma spray applications in the paper and printing industry. (Reproduced with kind permission from Oerlikon-Metco Corp.)

Press rolls are used to remove as much water as possible from the sheet using mechanical forces. Initially they were made of granite rock and were very expensive with limited rotation velocity. Now one uses cast iron or steel roll bodies with coatings that are application specific and tailored to perform optimally in various different types of paper production conditions. Factors such as wear and corrosion resistances, and the functionality of the roll surface in the paper manufacturing process, are key properties in these applications [Vuoristo P, Nylén P (2009)]. In most cases alumina–titania and chromia coatings are used with HVOF-deposited bond coat [Davis JR (ed) (2004), Tucker RC (ed) (2013)]. According to the size of the coated cylinders, high-power plasma torches, such as Plazjet, are used for deposition.

Dryer cylinders of paper machines and large Yankee drying cylinders of tissue paper machines are HVOF thermal spray coated with cermets containing various carbides. According to their weight and size, these components are commonly coated on-site (surface preparation, coating, surface finish) in the paper factory. Ceramic-coated center press rolls are, nowadays, used to replace conventional granite rolls [Vuoristo P, Nylén P (2009)]. Ceramic coatings are based on

Fig. 19.19 Paper machine center press roll with a thermally sprayed ceramic coating (Metso Paper Inc.). (Reproduced with kind permission from ASM [Vuoristo P, Nylén P (2009)])

aluminum and chromium oxides with an underlying bond coat and corrosion barrier. They are application specific and tailored to perform optimally in various different types of paper production conditions. According to the size of the components, Metso Paper is the world's leading manufacturer, both in Finland and elsewhere. Figure 19.19 represents a ceramic center press roll of a paper machine after finishing.

Sprayed coatings can also be top-coated with a fluoropolymer layer to improve the release properties of the roll surfaces [Vuoristo P, Nylén P (2009)]. Steels with high molybdenum contents (better corrosion resistance and thermal conductivity) HVOF sprayed are also used [Davis JR (ed) (2004), Tucker RC (ed) (2013) *ASM Handbook, Volume 5A*]. Machine knives (slitters, guillotine, blades) are coated with HVOF-sprayed WC–Co coatings and then sharpened [Davis JR (ed) (2004), Tucker RC (ed) (2013) *ASM Handbook, Volume 5A*].

Carbon-fiber-reinforced plastic (CFRP) rolls, exhibiting excellent characteristics including lightweight, high stiffness, and low flexure, have been increasingly employed in industrial manufacturing fields. Compared to conventional metal rolls, CFRP roll is lighter and stiffer and exhibits lower inertia moment [Yoshiya A, et al. (2009)]. Unfortunately, carbide-cermet coatings failed because of their poor thermal shock resistance on CFPR rolls. Ni-base composite porous coating including ceramic particles developed by Nagai et al. (2009) showed high thermal-shock resistance. Five coated rolls were installed in the actual papermaking line. They achieved successful results with 10% improvement in the line speed, whereby outstanding performance and maintenance-free functioning have been confirmed even after 4 years of use. Yoshiya et al. (2009) have developed a 5.4-m long thermally sprayed carbon roller, installed in a paper slitter/winder, that is moving stably at ultrahigh speed, 2300 m/min, with no abrasive wear. The roller has a three-layer structure, especially a tungsten carbide cermet layer on grooved metal sleeve, which covers the CFRP substrate roller shell. The thermal spray process is the finishing process because no after-grinding is performed.

Blow tanks, that are storage bins, are also on-site HVOF sprayed with WC–Co coatings to improve their wear resistance.

19.4.10 Metal Processing Industries

Many parts in metal working industries are submitted to severe wear and corrosion; however, its consequences can be reduced by thermally sprayed coatings. The main parts that can be sprayed are [Davis JR (ed) (2004), Vetter J, et al. (2005), Iyengar RK (2009)] components of electric arc furnace (EAF) and basic oxygen furnace (BOF), molds, casting dies, casting salvage, molten metal containment and delivery, and steel mill rolls working in both wet and dry mill environment, for example, entrance and exit rolls of steel processing line, or rolls for galvanized and aluminized steel sheets. PTA coatings are also used in processing industries.

19.4.10.1 Components of Furnaces or Boilers

Boilers are large and expensive installations that suffer enormously from wear caused by corrosion and erosion, aggravated by very high temperatures. The exact type of wear experienced varies from one part of a boiler to another and is influenced by the overall design of the boiler and the

Table 19.4 Different parts of the boiler that can be affected with the corresponding wear phenomena [http://www.castolin.com]

Part of boiler affected	Principal wear phenomena
Combustion chamber waterwalls	Corrosion/abrasion/erosion
Secondary superheater	Corrosion/oxidation/erosion (ash)
Economizer	Erosion (ash)/corrosion
Primary superheater	Erosion (ash)/corrosion
Reheater	Corrosion/oxidation/erosion (ash)
Superheater soot blowers	Erosion (steam)
Combustion chamber soot blowers	Erosion (steam)

Reproduced with kind permission from Castolin, copyright © Castolin Eutectic

type of combustible fuel. For example, Table 19.4 from www.Castolin.com presents the different parts of the boiler that can be affected with the corresponding wear phenomena.

A wide variety of components associated with electric arc furnace (EAF) and basic oxygen furnace (BOF) are under severe attack from heat, particulate, and acidic gases. Water-cooled components, in the off-gas duct systems such as pans, roofs, boxes, and panels, are subjected to high-velocity combustion gases that contain a number of corrosive chemicals that condense and attack the heat transfer surfaces [Kaushal G, et al. (2011)]. Coatings used are those developed for high-temperature wear and corrosion resistance; see for example [Iyengar RK (2009), Kaushal G, et al. (2011), Espallargas N, et al. (2008), Wang B-Q, Verstak A (1999), Higuera HV, et al. (2001a, b), Sidhu TS, et al. (2005), Sidhu HS, et al. (2006a, b), Sanz A (2001), Gross KA, Kovalevskis A (1996)].

19.4.10.2 Molds

In continuous casting the cast shell in the lower half of the mold abrades and wears the bottom of the mold. Diffusion of the copper substrate from the mold into the surface of the cast product leads to a quality defect called "star cracking" [Iyengar RK (2009)]. Chrome- and nickel-based coatings protect copper molds from wear and also enhances caster product quality by greatly reducing cast product contamination and star cracking problems [Iyengar RK (2009)]. Thermal barrier coatings are also used to control the heat flow and retard rapid chilling [Davis JR (ed) (2004), Tucker RC (ed) (2013) *ASM Handbook, Volume 5A*, Sanz A (2001)]. For very corrosive melts, pure yttria is used instead of zirconia partially stabilized with yttria. Of course, bond coats are necessary, and sometimes multilayer coatings, to achieve a good compliance between the expansion coefficients of mold and topcoat. Sanz (2001) has studied different coatings to protect the mold wall. Casting salvage is also achieved by filling the voids, after grinding of porosity or wear zones, with plasma or wire arc coatings that are then re-machined [Davis JR (ed) (2004), Tucker RC (ed) (2013) *ASM Handbook, Volume 5A*]. Gross and Kovalevskis (1996) have shown that metallic molds from iron, nickel, Ni–Al, and Ni–Cr–B–Si can be produced by air plasma spraying onto steel and chrome-plated steel models. The main processing criterion was the mold temperature that must be heated above 400 °C to avoid coating warpage and fragmentation. Heating to 600–700 °C is required to remove coating porosity and reduce coating pullout. Weiss et al. (1994) have demonstrated the feasibility of making sprayed steel-faced tooling. Kim and Kweon (1996) investigated various flame- and plasma-sprayed coatings to extend the life of these molds. Coating materials studied include plasma-sprayed ceramic coatings with bond coats as well as flame for casting pig iron ingots. Cyclic furnace tests from room temperature to 1100 °C in air, simulating the thermal cycle in casting, indicated that failure occurred along the interface between the bond coat and the gray iron substrate because of iron oxidation, and not at the interface between the ceramic top coating and the bond coating. The field test results indicated that plasma-sprayed alumina coatings with 200 μm top coating thickness are the most promising materials for pig iron casting.

19.4.10.3 Die Casting

Gibbons and Hansell (2006) have shown that two thermal spray materials, one Cr_2C_3–25(Ni–20Cr) and one WC–10Co–4Cr, deposited using JP-5000 HVOF hardware, offered properties that could enable low-cost, low-volume production aluminum injection mold tooling to be upgraded to higher-volume production tooling. Hot dipping rolls—MoB/CoCr, a novel cermet material for thermal spraying, with high durability in molten alloys—have been developed to utilize for aluminum die-casting parts, and for hot continuous dipping rolls in Zn and Al–Zn plating lines [Gibbons GJ, Hansell RG (2008)]. The tests revealed that the MoB/CoCr coating had much higher durability without dissolution in the molten Al–45 wt.% Zn alloy. Using undercoat was effective to reduce the influence of large difference in thermal expansion between the MoB/CoCr topcoat and substrate of stainless steel of AISI-316L, widely used for the hot continuous dipping [Mizuno H, Kitamura J (2007)]. MoB-based cermet feedstock powders (MoB/NiCr and MoB/CoCr) were deposited on SKD61 (AISI H-13) substrates used as a preferred die (mold) material [Khan FF, et al. (2011)]. The durability of these coatings on cylindrical specimens against soldering also has been investigated by immersing in molten aluminum alloy (ADC-12) for 25 h at 670 °C and, subsequently, compared with that of NiCr and CoMoCr coatings. Both types of MoB-based cermet coatings have shown high soldering resistance as negligible intermetallic formation occurred during the immersion test [Khan FF, et al. (2011)]. Weiss et al.

(1994) have used arc-sprayed steel-faced tooling to create matched die sets for injection molding applications.

19.4.10.4 Entrance and Exit Rolls of Steel Processing Line

When coating bridle and accumulator rolls in entrance and exit ends of a steel processing line with tungsten carbide coating surface damage on the roll is eliminated and proper grip provided, and slippage prevented. The surface coating is properly textured to provide the required characteristics or profile on the strip surface [Iyengar RK (2009)]. Multicomponent white cast iron is a new alloy that belongs to system Fe–C–Cr–W–Mo–V, HVOF sprayed, and seems to be promising for rolls [Khan FF, et al. (2011)].

19.4.10.5 Galvanized and Aluminized Steel Sheets

They require very high surface quality, particularly in exposed panels. In continuous galvanizing and aluminizing, the steel strip is dipped in the molten bath through a series of rolls that control the speed and tension of the strip and guide the steel strip through the molten metal bath. The rolls operating in the molten Zn–Al alloy are subjected to severe corrosive environment and require frequent change and repair [Davis JR (ed) (2004), Tucker RC (ed) (2013) *ASM Handbook, Volume 5A*]. Seonga et al. (2001) have shown that WC–Co coatings were not very good with molten Zn–Al. By coating the sink and stabilizer rolls with molybdenum boride, tungsten carbide, and other materials, the rolls remained smoother and produced an improved strip surface.

19.4.11 Petroleum and Chemical Industries

The main problem is to prevent corrosion and wear, all forms of wear, especially those linked to corrosion arising at low, intermediate, and high temperatures. As previously pointed out, against corrosion dense (non-sacrificial) coatings (no pores or cracks and very low oxide level) of the appropriate material are mandatory. For porous coatings, especially ceramic ones, a dense bond coat with a good resistance to the corrosive media is mandatory. Porous coatings can be sealed but the seal must be adapted to the service temperature. Moreover, many components have sizes that require on-site spraying. Usually, dense coatings are obtained with vacuum plasma spraying or D-gun or HVOF, but soft vacuum plasma and D-gun spraying are not adapted to big parts. Thus, HVOF spraying, that can be used on-site, is extensively used against corrosion and abrasive and erosive wear mainly with carbide-based cermets [Davis JR (ed) (2004), Zeng Z, et al. (2008), Souza VAD, Neville A (2007), Ishikawa Y, et al. (2005), Uusitalo MA, et al. (2002), Henne R, et al. (1999), Iyengar RK (2009), Kaushal G, et al. (2011), Espallargas N, et al. (2008), Wang B-Q, Verstak A (1999), Higuera HV, et al. (2001a, b), Bolelli G, et al. (2008), Godoya C, et al. (2004), Choa JE, et al. (2006)]. Of course, for the protection of external steel structures, pipes, tanks, etc., Al, Zn, or Zn–Al wire arc sprayed or flame sprayed are used [Evdokimenko Yu I, et al. (2001), Sørensen PA, et al. (2009), Murakami K, Shimada M (2009), Pacheo da Silva C et al (1991), Chunlong Y, et al. (2009), Schmidt DP, et al. (2006), Han M-S, et al. (2009)], as well as polymers sprayed by flame, HVOF, or plasma according to the polymer melting temperature [Petrovicova E, Schadler LS (2002)]. For example, Fig. 19.20 presents an aluminum protection flame sprayed on a refinery pipe.

Fig. 19.20 Typical coating against corrosion sprayed on-site onto refinery pipe. (Courtesy of Oerlikon-Metco)

Coatings in chemical industry are used for pressure and storage vessels with Hastelloy B or C, Inconel 600, for heat-affected zones where solutions found in gas turbines are often used. In some chemical reactors, submitted to strong acids in combination with organic solvents, glass lining are used that are repaired by APS-spraying tantalum, bonding well to the glass, and followed by an overlay of chromium oxide [Davis JR (ed) (2004), Tucker RC (ed) (2013)]. For example, Moskowitz (1993) has tested HVOF process using unique inert gas shrouding to produce highly dense, low-oxide coatings of metallic alloys, which were tested in laboratory and plant, with exposures as long as 5 years. Coatings of corrosion-resistant alloys, such as type 316L stainless steel and Hastelloy C-276, were shown to act as true corrosion barriers.

For the oil, gas, and petrochemical industries, the following components are coated using thermal spray technologies: mud drill rotors, pump impellers, plunger, turbine, rotor shaft of centrifugal compressor/pump, pump shafts, boiler tube, thermo-well, mixing screw, mandrels, actuator shafts and housings, housings and valves, valve gates and seats, ball valve with large diameter, progressive cavity mud motor rotors, rock drill bits, riser tensioner rods, impeller/blade drilling and production risers, sub-sea piping, wellhead

Fig. 19.21 General view of practical spraying of ball valve by the MET-JET III system. (Reprinted with kind permission from ASM [Huang XO, et al. (2007)])

Fig. 19.22 Wear band on drilling pipe PTA coated. (Courtesy of Castolin)

connectors, fasteners, compressor rods, mechanical seals, pump impellers, tank linings, external pipe coatings, structural steel coating, etc. [Davis JR (ed) (2004), Tucker RC (ed) (2013) *ASM Handbook, Volume 5A*]. It also seems that wear-coating applications have started to replace hard chrome [Thintri Inc. (2013)].

Two examples of coatings used in oil, gas, and petrochemical industries are presented below. Stainless steel ball valves must be wear resistant, and have a low friction coefficient, a good erosion and heat resistance, good fatigue strength and seal performances, etc.; these are significantly improved by applying HVOF coatings [Huang XO, et al. (2007)] and loping trend of these ball valves for highly harsh working conditions. Figure 19.21 shows the practical spraying of a ball valve having a diameter of over 500 mm. Wear bands on drilling pipes, as shown in Fig. 19.22, are PTA coated.

19.4.12 Electrical Utilities

Coatings against corrosion and wear (C–W) are used in fluidized-bed combustor (FBC) and conventional coal-fired boilers.

19.4.12.1 For Fluidized-Bed Combustor Boilers

The problem is linked to the finely divided mixtures of coal and limestone particles eroding and corroding steam pipes and boiler walls, as well as the high sulfur content of coals or low-grade combustibles resulting in corrosion at high temperatures. Different coatings are used:

- Cr_2O_3 (20 wt.%)–Al_2O_3 on NiCrAlY bond coat (against corrosion through the porous ceramic coating) [Davis JR (ed) (2004), Tucker RC (ed) (2013) *ASM Handbook, Volume 5A*], the addition of approximately 20 wt.% chromia resulting in the formation of one solid solution of $(Al–Cr)_2O_3$ in the α-modification (working temperatures can reach 1000 °C and the transformation of γ phase starts around 900 °C).
- HVOF-sprayed Cr_3C_2–NiCr coatings with high compactness and fine grain size [Wang B (1996)], the wear resistance being due to hard carbide particles homogeneously distributed within coating, the ductile matrix being corrosive resistant.

19.4.12.2 For Coal-Fired Boilers

Plasma-sprayed Stellite-6 coating has been found to be effective in increasing the erosion–corrosion resistance of boiler steels in the coal-fired boiler environment. A less porous structure obtained after laser remelting was found to be effective in increasing erosion–corrosion resistance [Sidhu BS, Prakash S (2006)]. Inconel systems or high-chromium alloy or chromium–nickel alloy coatings, presenting a good resistance to sulfur, have also been used, sprayed with plasma, wire arc, or HVOF [Davis JR (ed) (2004), Tucker RC (ed) (2013)]. Petrovicova and Schadler (2002) have proposed low-cost and high-hardness plasma-sprayed coatings, developed by addition of carbon and hardening elements to high-chromium cast iron (C–Si–Mn–Cr–Mo–V–other–Fe) used for wear-resistant material. Nitrogen gas atomization was applied to manufacture the powder in order to prevent oxidation of particles. These coatings showed the same or more erosion resistance than Cr_3C_2–NiCr cermet coating and had higher reliability for long-period operation and higher practicality.

19.4.13 Textile and Plastic Industries

The abrasive qualities of man-made fibers, particularly nylon and polyester, and the corrosive characteristics of additives, such as fiber finishes and lubricants, combine to deteriorate yarn contact surfaces. High rotation speed of grooved rollers results in considerable abrasion wear. Due to the very high rotational speed, the roller has to be made from aluminum, and therefore, the reduction in wear can only be achieved by the deposition of a coating that also must be as light as possible. For years, thermal spray coatings have been used against wear and corrosion on textile machinery: steel thread guiders, thread breaks, stretch roll, grooved roll, separator roll, oiling roll, draw roll, feed roll, conditioning rollers, snick pins, collets, disk grip, cutter base, feed drum, rotor for open-end, extruder dies, knives, heating bars, heater/hot plate, etc. [Davis JR (ed) (2004), Tucker RC (ed) (2013)]. The high-velocity rotating parts are often coated with alumina or alumina–titania coatings. TiO_2 addition lowers significantly the microhardness of the alumina coating but increases its toughness [Yilmaz R, et al. (2007)]. Parts such as knives and extruder dies are coated by HVOF-sprayed tungsten carbides, while textile rolls are plasma sprayed with alumina–titania (13 wt.%) as illustrated in Fig. 19.23.

Lima and Marple (2005) showed that nanostructured titania feedstock HVOF sprayed exhibited a superior abrasion wear resistance (27% lower volume loss) when compared with an air plasma-sprayed conventional alumina–titania coating, in spite of the fact that the latter is 33% harder than the HVOF-sprayed titania. The higher wear resistance of the HVOF-sprayed nanostructured titania was provided by the nanostructured zones embedded in the dense and uniform coating microstructure acting as crack arrester. They are probably worth to be tested in textile industry.

19.4.14 Polymers

Thermal spraying of the polymers [Davis JR (ed) (2004), Tucker RC (ed) (2013), Petrovicova E, Schadler LS (2002), Lathabai S, et al. (1998), Lins VFC, et al. (2007), Berndt CC, et al. (1998), Leivo E, et al. (2004), Zhang T, et al. (1997), Chen H, et al. (1999), Zhang G, et al. (2007), Zhang G, et al. (2006), Zhang C, et al. (2009), Sweet GK (1993), Brogan JA, et al. (1995), Henne RH, Schitter C (1995), Ivosevic M, et al. (2009)] is one-coat process that acts as both the primer and the sealer, with no additional cure time processes. Polymer thermal spraying is ideally suited for large structures that otherwise could not be dipped in a polymer suspension. Moreover, it seems that functionalized polyethylene polymers such as ethylene methacrylic acid copolymer (EMAA) and ethylene acrylic acid (EAA) can be applied in high humidity. Of course, the use of polymer coatings depends strongly on its service conditions. Especially, it must be kept in mind that melting temperatures vary from 40 to 60 °C for ethylene methacrylic acid copolymer (EMAA) to 300 °C for polyimide. They are deposited onto metals, ceramics, cermets, and composites. As they present a high chemical resistance, a high impact, and abrasion resistance at low temperatures, they are used in many industries, especially in food industry.

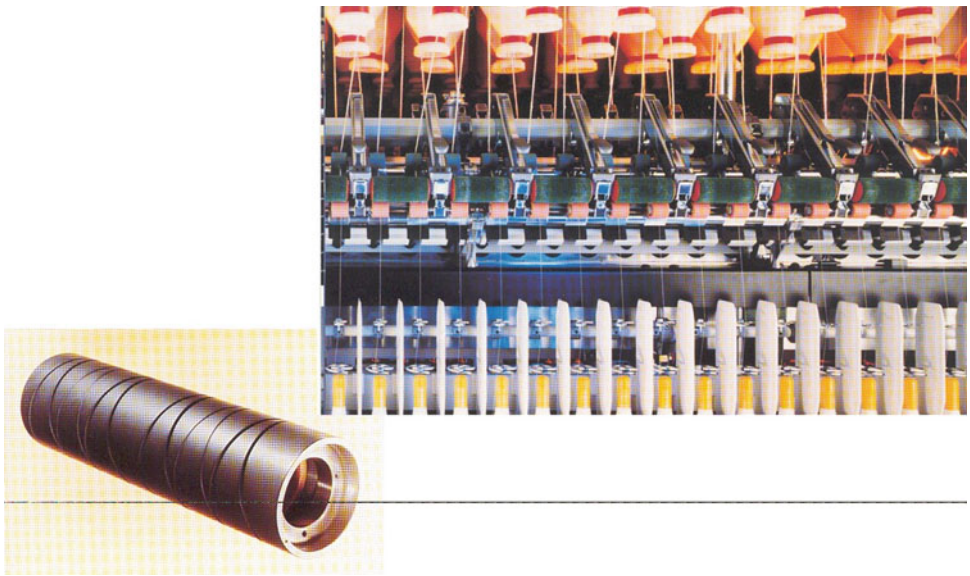

Fig. 19.23 Applications of plasma spray technology for the coating of spools and high-wear parts in the textile industry. (Reproduced with kind permission from Oerlikon-Metco Corp.)

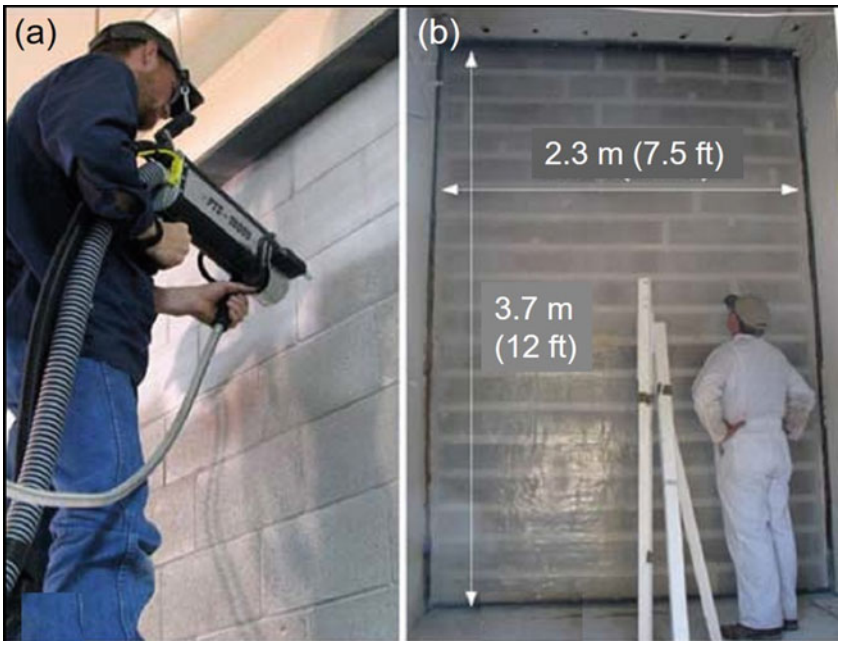

Fig. 19.24 (**a**) Thermal spraying of blast mitigation polymer membrane to the internal side of test walls; (**b**) wall dimensions and appearance of a completed membrane. (Reprinted with kind permission from ASM [Ivosevic M, et al. (2009)])

In food industry, polymer coatings replace paints on the wall because they have a much better resistance to the chemical products used for cleaning (about 1 week for paint against about a quarter for the polymer coating). They are even used on the floors where polymer coatings doped with alumina particles provide an excellent anti-slip lining, the alumina particles rippling out when people walk on it.

A novel coating process (polymer thermal spray, PTS) has been developed by Ivosevic et al. (2009). It utilizes an electro-resistive heating element for rigorous temperature control and for heating the main process gas that could be air, nitrogen, inert, or other gases. They have deposited advanced polymer coatings and structures such as:

- Blast mitigation coatings for protecting civil structures against external explosions.
- Thermal spray forming of syntactic foams based on polyimide micro-balloons.

For blast mitigation, Fig. 19.24 shows thermally sprayed polymer (thermoplastic elastomer) membranes applied to the internal side of the test walls measuring 3.7 × 2.3 m. Figure 19.25 presents the test setup for evaluation of thermally sprayed blast mitigation treatments. The explosion impulse reached 215 kPa and lasted about 50 ms. Both walls successfully passed the test and remained standing. The total wall deflection toward the inside of the test room was 8 in. with no visible damage to the membrane and no flying debris or wall segments penetrating the room.

Spraying syntactic foams based on polyimide micro-balloons was developed [Ivosevic M, et al. (2009)] in the frame of a research project funded by NASA Langley Research Center. The coating was supposed to be used as high-temperature insulation (up to 325 °C) and also satisfy strict flammability regulations relating to the aerospace industry. As shown in Fig. 19.26a, the polyimide syntactic foam consisted of two NASA Langley-licensed materials, polyimide microspheres (PerFoma-H® from GFT Corporation), and a binder. Polyimide microspheres had a bulk density of 0.043 g/cm^3, a size range of 400–800 μm, and service temperature between −253 °C and 315 °C. The binding powder and microspheres were thermally Co-sprayed using the PTS coating system. The thermally sprayed foam did not support a flame and formed a stable isolative char without smoke at higher temperatures. The foam deposited over various complex shapes is shown in Fig. 19.26 and seemed to be interesting for thermal insulation in airspace applications [Ivosevic M, et al. (2009)].

19.4.15 Reclamation

The effects of wear and corrosion can only be retarded, but not be stopped forever and wear parts must be replaced or resurfaced. It is the same for undersize parts due to manufacturing error. The ability to apply coatings by thermal

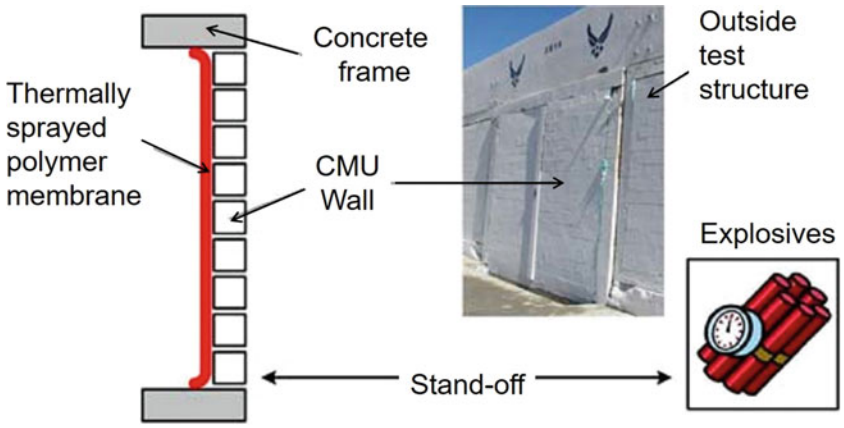

Fig. 19.25 Test setup for evaluation of thermally sprayed blast mitigation treatments. (Reprinted with kind permission from ASM. [Ivosevic M, et al. (2009)])

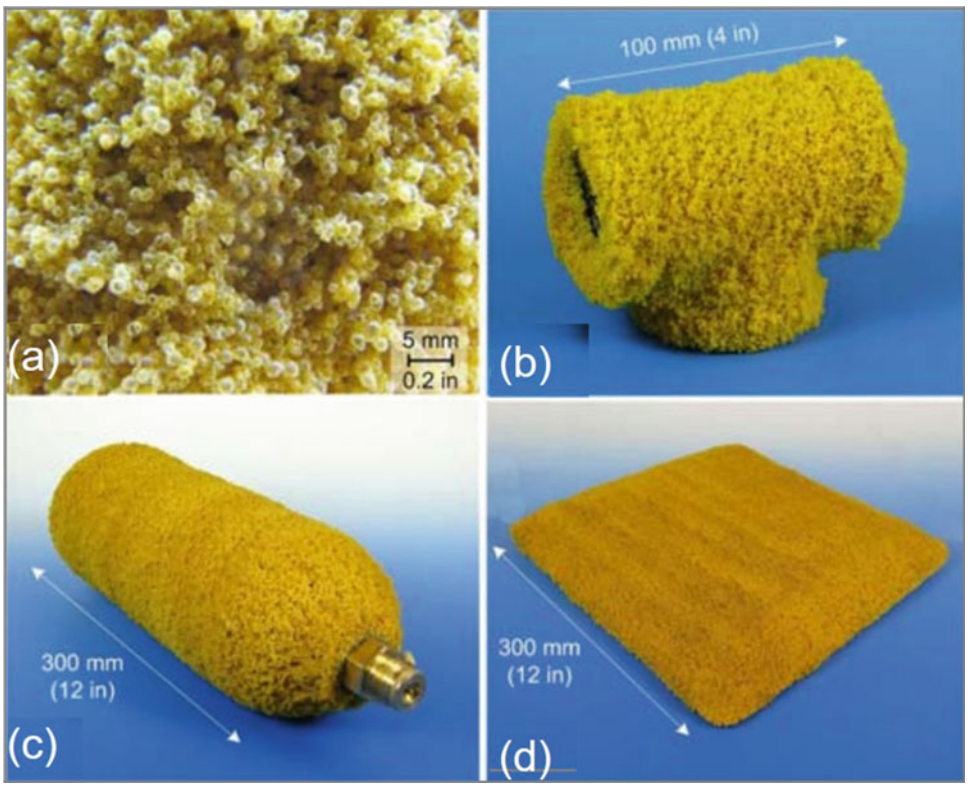

Fig. 19.26 Thermally sprayed syntactic foam based on polyimide micro-balloons: (**a**) foam microstructure; (**b**) thermally sprayed on pipe T joint; (**c**) on a gas cylinder; and (**d**) on a flat aluminum plate. (Reprinted with kind permission from ASM [Ivosevic M, et al. (2009)])

spraying with a broad spectrum of thickness, finish, and composition requirements makes the different thermal spray processes ideal solutions to resurface components, avoiding their costly replacement. Restoration is performed either with the same material as the base metal or with a more corrosion- and/or wear-resistant material. However, it is better to choose coatings that can be machined. In a wide range of industrial applications, thermal coatings are used to renew components by restoring their specified dimensions and matching and sometimes improving their original performance. Very often it is possible to design a coating that meets the functional requirements of the component, and moreover offers better resistance to corrosion, oxidation, and mechanical wear than the original product. Of course, the cost of the resurfacing must be lower than that of a new part (a fraction of it). For example, this technique is particularly used for roller faces and journals, dryer drums for papermaking, pump seals (shafts and sleeves), pump housings, compressor rods,

rotary airlocks and feeders, and conveyer screws [Davis JR (ed) (2004), Tucker RC (ed) (2013)]. PTA also is used for refurbishing components, even with a complex shape as turbine blades.

A few examples are given below to illustrate the use of sprayed coatings in resurfacing components.

The use of aluminum alloy for injection mold tools, especially for the automotive industry, is not new and has been utilized as bridge tooling to support the manufacture of typically up to 10,000 components. Two thermal spray materials, one Cr_2C_3–25(Ni–20Cr) and one WC–10Co–4Cr, deposited using JP-5000 HVOF hardware, have been shown to offer properties that could enable low-cost, low-volume production aluminum injection mold tooling to be upgraded to higher-volume production tooling [Weiss LE, et al. (1994)].

The thermally sprayed Tribaloy T-800 coatings deposited by the HVOF process exhibited lower cavitation wear rates than the stainless-steel bulk material [Hahn M, Fischer A (2010)].

Massive turbines and the valves used to regulate water flow at hydroelectric dams are often exposed to the wearing effects of high-velocity water containing abrasive particulate. As mentioned by Sulzer-Metco, coatings can replace lost material and, at the same time, provide a more wear-resistant surface, increasing useful life by up to 20 times over the original.

Hard chromium plating is usually used to restore to original dimensions the worn surfaces of gas turbine shafts. In the case of shafts repair, hard chromium plating process proved to be time consuming and to involve high costs. High hardness and good wear resistance performances of WC–12%Co HVOF-sprayed coatings support their candidature for the replacement of hard chromium plating in this field [Bolelli G, et al. (2006a, b, c)].

Song et al. (2005) have studied the effect of repair of NiCrAlYSi coating after longtime use on the coherence of coating to substrate and mechanical properties of Ni_3Al-base alloy IC6. For secondary coating repair, the room temperature tensile properties of base alloy had no obvious change, while stress rupture lives decreased, but still were rather long, compared to the alloy with first repair coating. Therefore, they deduced that NiCrAlYSi coating repair is feasible to prolong the service lives of IC6 turbine vanes.

Ducos (1988) has presented a few industries where PTA is used for resurfacing: extruder screw, vanes, turbine blades, engine valves (especially, big diesel engines), and rail train car wheels.

Isakaev et al. (1999) have shown that plasma-sprayed coating of railway frogs, working under contact fatigue and wear-out, provides a good solution for repairing them.

The surfaces of printing press cylinders wear quickly. Coatings of nickel/chrome alloy, Cr_2O_3, and others have supplanted chrome plating as the preferred method of reclaiming worn cylinders because thermal spray processing is far faster.

It has been shown that cold spray is a promising, cost-effective, and environmentally acceptable technology to impart surface protection and restore dimensional tolerances to aluminum alloy [Tapphorn R, et al. (2009)] or magnesium alloy components on helicopters and fixed-wing aircraft [de Botton O (1988)]. Kashirin et al. (2007) have shown that using a portable cold spray system working with air at pressures below 0.8 MPa made possible to restore on-site aluminum alloy molds for plastics, corrosion defects on car aluminum engines, casting defects for various aluminum alloys, antique art objects such as copper sculptures of Isaac Cathedral in Saint-Petersburg, etc.

19.4.16 Other Applications

As previously described, thermal spray coatings provide superior wear (abrasive, erosive, fretting, etc.) resistance and corrosion protection with coatings having low porosity, high hardness, good toughness for cermets, and great flexibility of composition [Davis JR (ed) (2004), Tucker RC (ed) (2013)]. Thus, they are also used in the following:

Mining industry, where good abrasive and/or adhesive resistance is very important. For example, HVOF-, PTA-(alloys doped with ceramic particles), and wire arc-sprayed cored wire coatings are used on conveyor belt idlers, steel oscillating tub, fan components such as removable leading edges, bolt-covers, blades, deflectors and large inlet entrance cone ducts, scraper or excavator teeth, etc., as illustrated in Fig. 19.27.

Nuclear industry, where the use of cobalt-based alloys (stellite or cermet matrix) is limited, thus coatings against wear and corrosion rely on nickel alloy-based coatings (NiCr–WC or Cr_3C_2). Cermets with hafnium carbide have been developed that present a large neutron cross section. However, sprayed coatings are essentially used in pumps, turbines, heat exchangers, vanes, etc.

In numerous applications developed at CEA-DEN, French Atomic Agency, Atomic Energy Department, particularly those encountered in the processing of nuclear wastes, metallic components are subjected to extreme environments in service, in terms, for example, of aging at moderated temperature (several months at about 300 °C) coupled to thermal shocks (numerous cycles up to 850 °C for a few seconds and a few ones up to 1500 °C) under a reactive environment made of a complex mixture of acid vapors in the presence of an electric field of a few hundred volts and a radioactive activity. Berard et al. (2008) have tested alumina plasma-sprayed coatings manufactured with feedstock of different particle size distributions, graded alumina–titania coatings, and

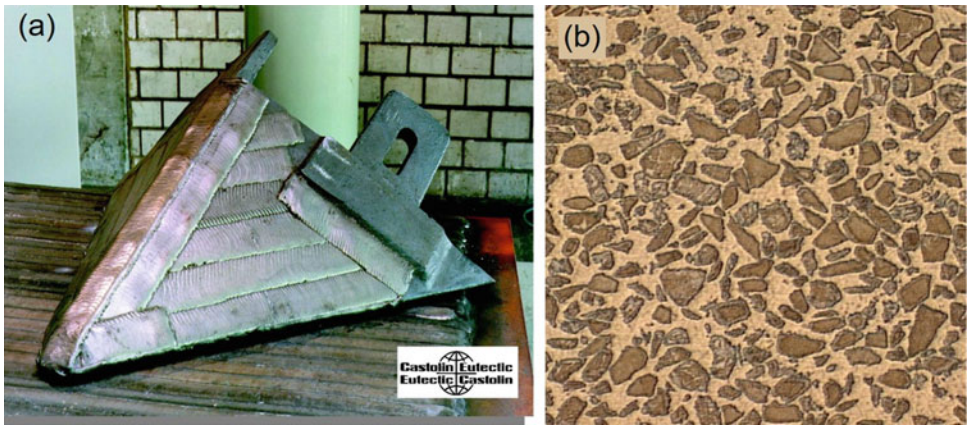

Fig. 19.27 (**a**) Tooth of excavator PTA-coated with a nickel-based composite (**b**) coating microstructure. (Curtesy of Castolin)

phosphate-sealed alumina coatings to improve the properties of metallic substrates operating in such extreme environments. The effects of particle size distribution, phosphate sealant, and graded titania additions on the dielectric strength of the as-sprayed, thermally cycled, and thermally aged coatings were investigated. Thermal aging test was realized in furnace at 350 °C for 400 h and thermal shocks tests resulted from cycling the coating between 850 and 150 °C using oxyacetylene flame and compressed air cooling. Aluminum phosphate impregnation appeared to be an efficient posttreatment to fill connected porosity of these coatings. Alumina as-sprayed coatings manufactured with +22–45 μm and +5–20 μm particle size distributions exhibited good dielectric strengths after thermal solicitations compared to those manufactured with larger size distributions or to graded titania coatings.

Cement industry: Again, the main role of sprayed coatings is against wear and corrosion in mechanical seal, sleeve, burner tip, boiler tube, thermo-well, kiln support roll, pinion shaft, coating for cement preheat tower, impeller blade, calendar roll, cone crusher, and hydraulic rams with acid-resistant coatings.

Drawing machine: Guide roller and ceramic disk, rod breakdown drawing machine, fine drawing machine, and other accessories.

Waste treatment: Steel tube oxidation causes an important problem in municipal solid waste incinerator (MSWI) plants due to burned wastes containing high concentrations of chemically active compounds of alkali, sulfur, phosphorus, and chlorine. Ni-based HVOF coatings are a promising alternative to the MSWI conventional protection against chlorine environments [Guilemany JM, et al. (2007)].

Sheet metal forming dies: Conventionally, mold and dies are manufactured by machining from bulk metallic materials. Tooling by using arc spray process to spray metal directly onto a 3-D master pattern is an alternative method to manufacture mold and dies for plastic injection molding and other applications [Davis JR (ed) (2004), Tucker RC (ed) (2013)].

19.5 Thermally Sprayed Coatings by Country

Dorfman and Sharma (2013a, b) in their "Commentary; Challenges and Strategies for Growth of Thermal Spray Markets," based on the report by Hanneforth (2006), presented interesting statistics, given in Fig. 19.28, about the regional distribution of the thermal spray (TS) markets around the world in 2006, which they estimated at a total value of US$6.5 billion. According to their report, two-thirds of these markets is split evenly between North America and Europe/Middle East. Of the balance, US$1.0 billion was estimated for the Japanese market, US$0.5 billion for each of China and Asia Pacific, and US$0.3 billion for the rest of the world. The growth rate of the industry has been, however, the highest in Asia and South America [Fukumoto M, (2008a, b), Lee C, (2009a, b), Sundararajan, G, et al. (2009a, b), Nakahira A (2009a, b), Valarezo A (2012)]. In particular, there has been a significant increase in research and development activities in China as indicated earlier in Fig. 19.1, giving the number of technical manuscripts submitted to the *Journal of Thermal Spray Technology* (JTST) during the period (2004–2010).

In the following, a brief description is given on the development of the thermal spray (TS) industry in different regions around the world. These are given based on the scarce information available in the open literature on techno-economic developments in this field. Limited information about thermal spraying in Nordic region of Europe [Vuoristo P, Nylén P (2009)], Korea [Lee C (2009a, b)], India [Sundararajan G, et al. (2009a, b)], Japan [Tani K, Nakahira H (1992), Nakahira A (2009a, b)], and China [Fukumoto M (2008a, b)] was available in connection with the Thermal Spray Conference in 2009 (ITSC-2009). The analysis, and observations made, provides general technological trends, and indications of emerging technologies in this rapidly developing field.

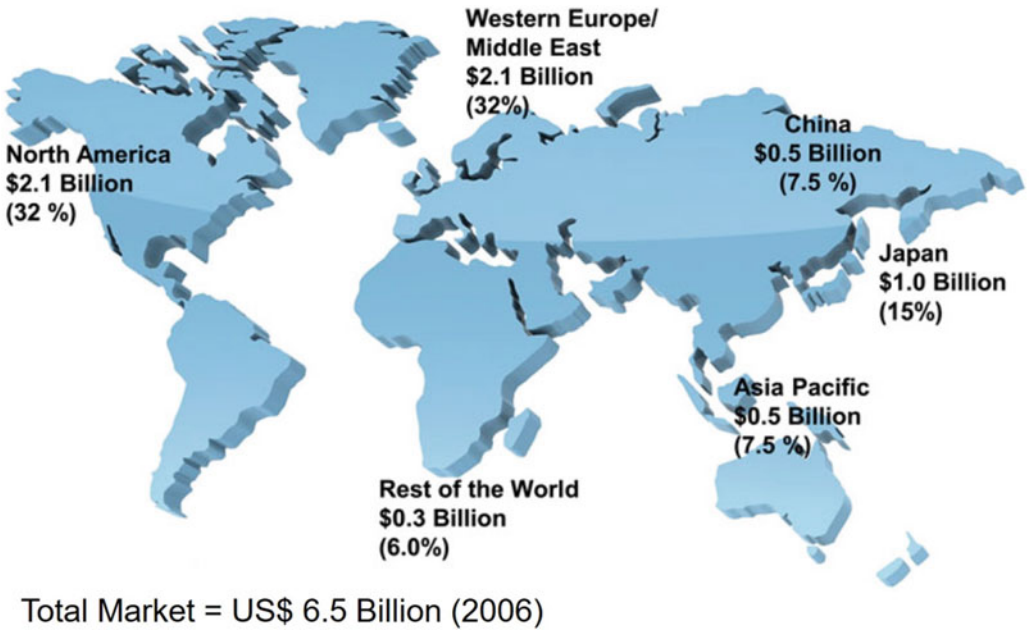

Fig. 19.28 International breakdown of annual thermal spray markets. [Dorfman M, Sharma A (2013a, b)]

19.5.1 North America

Thermal spraying has been in rapid development since the 1970s and 1980s, evolving from an art to a science over the period 1980–2000 [Wigren J, Kristina Täng (2007)]. Extensive research and development efforts were devoted in leading laboratories in this field, which resulted in the emergence of new spray technologies such as HVOF, HVAF, wire arc spraying, and, more recently, solution and suspension plasma spraying. This is illustrated in Fig. 19.29, after TAFA, representing percentages of the different spray techniques in 2000. Flame spraying is now reduced to 50% and the rest of the market comprises all other techniques except of course cold spray that had not yet fully integrated on an industrial scale at that period.

Besides new products and marketing issues, the development and integration of TS technologies at the design stage of new products has been linked to a better reproducibility and reliability of substrate surface preparation, spraying, and posttreatment of coatings. Particularly consistent effort has been made in the following areas:

- Better control of surface preparation with a grit-residue level as low as possible and a roughness adapted to sprayed particles and a desired grit blasting residual stress level.
- Better control of the spray process parameters thanks to computer-control process equipment coupled with adequate online sensors.

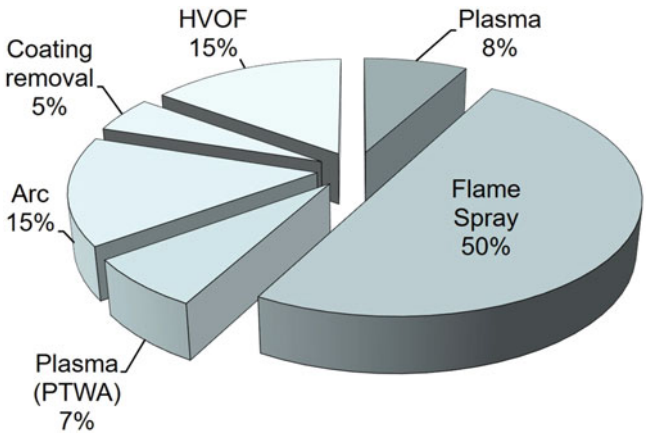

Fig. 19.29 Percentages of the different spray processes in industry in 2000. (After M. L. Thorpe, Oral presentation ITSC)

- Development of robust sensors to follow the key parameters of coating manufacturing.
- Advances in fundamental understanding of correlations between coating properties, particle impact parameters, as well as coating and substrate temperature during spraying.
- Better control of ambient dust fume, especially that resulting from the condensation of vaporized material, in the spray booth and close to the sprayed part.
- Standardization of coating characterization methods.

- Education at the operators and designers' levels coupled with the development of expert systems and proper engineering and material science tools for quality control (QC).

19.5.2 Europe

According to Ducos and Durand (2001), the rapid development of TS technologies in Europe is well illustrated by the breadth of technologies used on an industrial scale with a total annual market value of 615 M€ for 1998 as illustrated in Fig. 19.30 based on the [MAGETEX] study. Particularly significant is the developments of HVOF, D-gun, and wire arc spraying in this period. The spread of the use of TS coating in different industrial sectors in Europe in 1998 is illustrated in Fig. 19.31. As can be seen, these are almost split with one-third mostly devoted to high-end, high-value coating applications, used in aircraft, industrial gas turbines, printing rolls, or medical and dental fields. The balance is equally split between a wide range of applications in the chemical process industries such as primary metals, polymer processing and food, glass, pulp and paper, chemical, oil and gas, textile, and "low end" applications such as mechanical repair and metallic coatings for heavy wear or corrosion protection (including pipes and gas bottles).

Thermal spraying is also used widely in many industrial sectors in the Nordic countries [Vuoristo P, Nylén P (2009)]. Important areas where thermal spraying is used are in the manufacture of products for the petroleum, paper, metals, transport, defense, and high-tech machinery industries. In Finland, thermal spray technology has wide areas of application in the pulp and paper industries. In Sweden, thermal spray technology is of great importance in the manufacture of aero engines and in industrial gas turbine applications. In Norway, thermal spraying is widely used in various offshore applications, including sub-sea oil drilling enterprises. Unfortunately, if the paper indicates that all of the major spray processes are currently used (from flame and arc spraying, to plasma, HVOF, and HVAF), depending on the application and type of coating applied, no details are given about their distribution between different industrial sectors.

19.5.3 Japan

According to Tani and Nakahira (1992) and Nakahira (2009a, b), the growth rate of the thermal spray (TS) market over the period 2004–2006 is estimated to be more than 5%. Thermal spraying output for fiscal year 2004 for the three sectors of the Japanese market were contract job shop productions just under 40 billion Yen (≈ US$0.4 billion), in-house production by large enterprises about 45 billion Yen (≈ US$0.45 billion), and consumables and spray equipment manufacturing 10–15 billion Yen (≈ US$0.1–0.15 billion). Figure 19.32 represents the repartition of coating services by

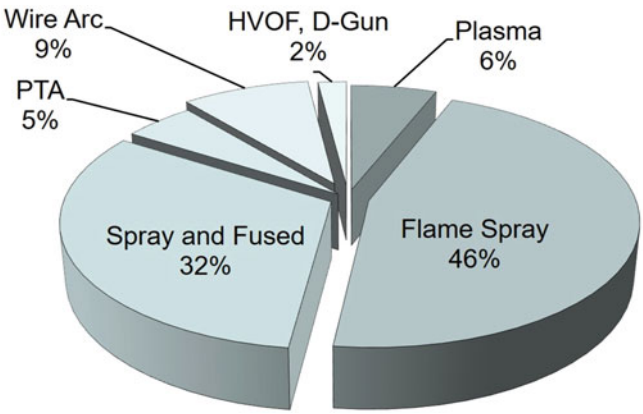

Fig. 19.30 Percentages of the different spray processes in European industry in 1998 (After Ducos and Durand). (Reprinted with kind permission from ASM [Ducos M, Durand JP (2001)])

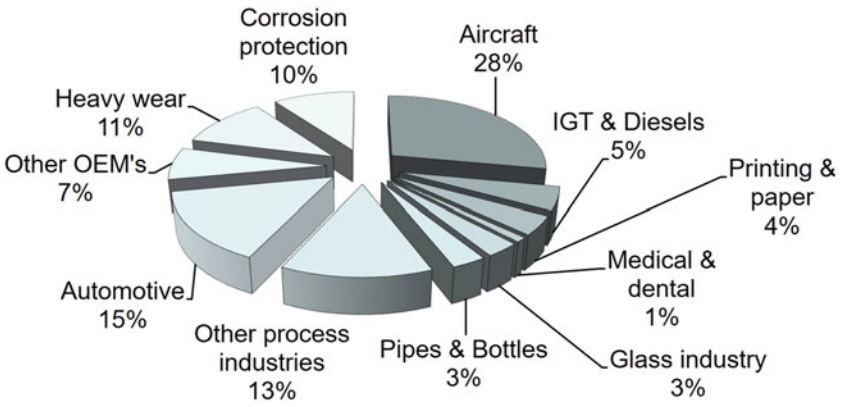

Fig. 19.31 Repartition of the 615 M€ coating activities across end-use sectors in Europe in 1998. (Reprinted with kind permission from ASM [Ducos M, Durand JP (2001)])

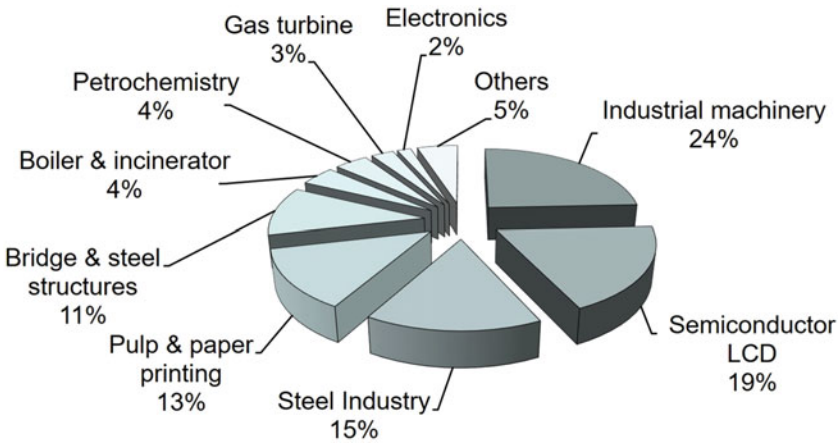

Fig. 19.32 Coating services by job shops in Japan in 2004: total market size, 45 billion Yen (≈ US$0.45 billion). (Reprinted with kind permission from Springer Science Business Media [Nakahira A (2009a, b)], copyright © ASM International)

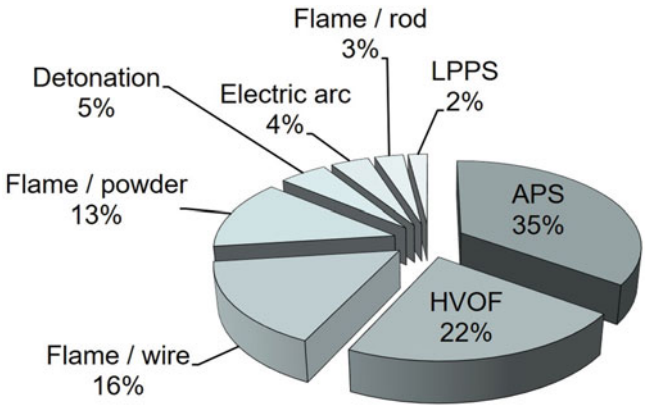

Fig. 19.33 Segmentation of spray process/turnover of contract job shops in fiscal year 2004 in Japan. (Reprinted with kind permission from Springer Science Business Media [Nakahira A (2009a, b)]. copyright © ASM International)

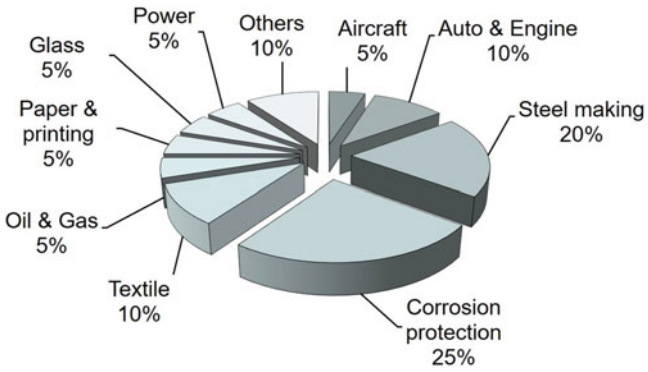

Fig. 19.34 Estimated share of different thermal spray application fields in China. (Reprinted with kind permission from Springer Science Business Media [Fukumoto M (2008a, b)], copyright © ASM International)

job shops in 2004, with total amount of 45 billion Yen (≈ US $0.45 billion) [Nakahira A (2009a, b)]. It is worth noting that the growth rate in the semiconductor/liquid crystal display (LCD) field is very high. Figure 19.33 shows the corresponding distribution among spray processes with the important contribution of APS and HVOF, at the expense of a reduction in flame-sprayed coatings.

19.5.4 China

Statistical data [Fukumoto M (2008a, b)] show that according to Professor Chang-Jiu Li, of the School of Materials Science and Engineering, Xi'an Jiaoton University in China, the total output of the thermal spray industry in China increased from about 1.2 billion RMB (US$0.14 billion) in 2002 to 2.1 billion RMB (US$0.24 billion) in 2005. While this amount corresponds to an annual growth rate of about 20%, which is significantly higher than the growth rate of 6.1% in North America, the total thermal spray industry output in China in 2005 was only 4% of the North American market, and 20% of the corresponding market in Japan. According to Professor Chang-Jiu Li, the fast and sustained growth of the Chinese economy in the last three decades at an average rate of 10% has provided unique opportunities for China's thermal spray industry to grow the fastest worldwide, a trend that is expected to continue over the next few years.

In terms of thermal spray applications in China, the technology has been widely used in different industrial fields, including steelmaking, textiles, paper and pulp, energy, petroleum and chemicals, aeronautics, and others (Fig. 19.34). The application of thermal spray coatings in the steel industry has been the fastest growing field in the last several years. The energy industry mainly includes coatings for coal-fired power plants and hydroelectric power plants. Applications of thermal spray technology to the aeronautics industry in China are mainly performed in five large job shops that share 5% of the total thermal spray output in

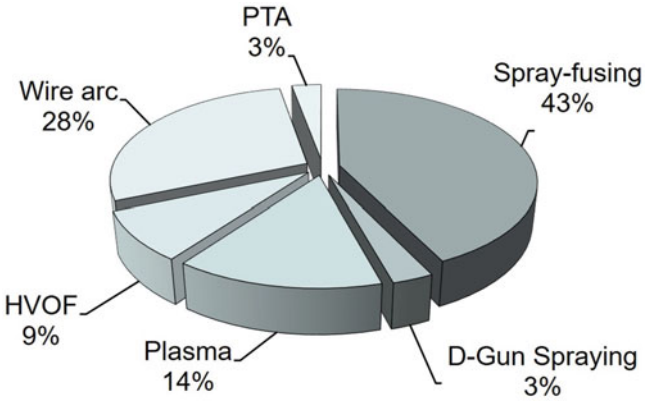

Fig. 19.35 Estimated share of different spray processes in China. (Reprinted with kind permission from ASM International [Lee C (2009a, b)])

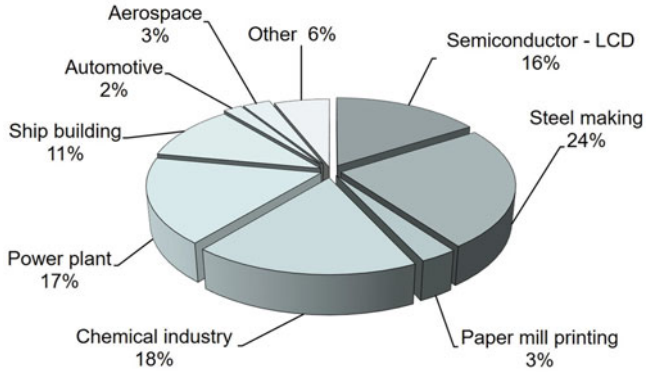

Fig. 19.36 Estimated annual sales of different spray application fields in Korea. (Reprinted with kind permission from ASM International [Lee C (2009a, b)])

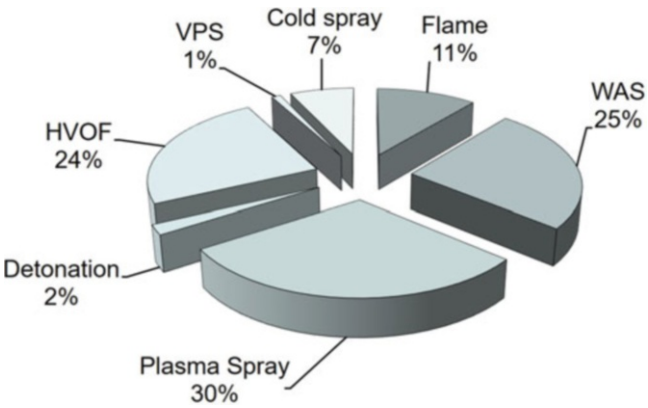

Fig. 19.37 Estimated share of different spray application fields in Korea. (Reprinted with kind permission from ASM International [Lee C (2009a, b)])

China. The national program to develop different types of aircraft is expected to promote further fast expansion of R&D and thermal spraying applications in this field at an annual rate greater than 30%, including domestic and foreign job-shop contracts.

Statistical data also show that Chinese applications in 2003 was mainly driven by flame spraying/spray fusing, which constituted around 43% of the TS market as shown in Fig. 19.35. Wire arc spraying accounted for 28% of the market, plasma 14%, HVOF 9%, and each of PTA and D-gun spraying equally representing 3% of the markets. It is believed that the market share of HVOF and plasma spraying has increased markedly in the last 3 years, surpassing the corresponding figures shown in Fig. 19.35 based on 2003 data.

19.5.5 South Korea

According to Fukumoto (2008a, b), thermal spraying in Korea began about 40 years ago during an industrialization period in the 1970s. A few small companies started spraying zinc and aluminum during this initial period. Major developments in thermal spraying technology were initiated by companies related to aerospace and steel production in 1980s. Korean Air started flame spraying for commercial airplane repair. Samsung Aerospace Company (now Sermatech Korea) started original equipment manufacturer (OEM) coating for military aircraft-related repair and maintenance. Union Carbide Coating Service (now Praxair Surface Technologies) and Daeshin Metallizing Company initiated industrial applications of thermal spraying such as hearth roll coatings. During a growth period in the 1990s, numerous new thermal spraying companies were established related to steel industries, textile industries, paper industries, and power generation plants. The general thermal spray market increase has been steady with the exception of aerospace applications because of limited activities in this field.

Figures 19.36 and 19.37, after Lee (2009a, b). show the distribution in 2008 of the thermal spray markets in S. Korea in terms of industrial sectors, for an estimated market of US $0.1 billion, and TS technologies used respectively. As noted, chemical and power plants clearly dominate the market share. Semiconductor and shipbuilding industries also have significant share of the pie. In terms of revenue, semiconductor/LCD, steel making, and power plant industries are the dominant sectors, based on the current fiscal reports.

19.5.6 India

In India the perceptible change in the thermal spray industry occurred in the 1990s and a good indicator of its success is the growth in sale of spray-grade powders [Sundararajan G, et al. (2009a, b)] that has multiplied by a factor of 3 between 2000 and 2008. The number of systems, as shown in

Fig. 19.38, is still low for a country of India's size but it is an important change compared to that prevailing not so long ago. The distribution of the country's thermal spray system installations among the various segments is presented in Fig. 19.39. The data clearly reveal that the highest number of thermal spray units operate as "job-shops." They play a crucial role both in addressing the needs of a vast majority of industrial users and running a crusade to demonstrate "new" applications to the industry and facilitating further growth [Sundararajan G, et al. (2009a, b)].

19.6 Techno-Economic Analysis

19.6.1 Different Cost Contribution Factors

In spite of its fundamental importance toward the acceptance of a new technology, few papers have been devoted to the economic analysis of thermal spray processes [American Welding Society (1985), Feuerstein A, et al. (2008), Ducos M (2006a, b), de Botton O (1988), Ducos M, Durand JP (2001), MAGETEX, Lee C (2009a, b), Sundararajan G, et al. (2009a, b), Tani K, Nakahira H (1992), Nakahira A (2009a, b), Fukumoto M (2008a, b), de Munter AJ, et al. (2002), Celotto S, et al. (2007), Molz R, Hawley D (2007)]. This is due to the generally confidential nature of the relevant information in an industrially competitive environment. Moreover, in our rapidly evolving global economy, process economics changes rapidly with time and location. In the context of this book, it is more important to focus on the methodology of carrying out a detailed economic analysis, rather than on the absolute values. These can and will change with time. Emphasis is placed on understanding of the relative importance of the different cost factors in the overall process economics and means of controlling them. Typical examples are provided at the end of this section for the illustration of the methodology and a comparative analysis of the different thermal spray technologies. For a more precise economic analysis, it is best to work with your local provider of thermal spray equipment and materials supplier.

The first step in an overall cost analysis is to identify the different steps of the operation, which can involve a single or multiple process technologies. A typical coating process often involves all or most of the following process steps:

(a) Substrate preparation
- Machining
- Masking
- Degreasing
- Grit blasting
- Ultrasonic cleaning

(b) Coating
- Part setting-up
- Preheating
- Coating
- Online posttreatment (whenever necessary)
- Part removal

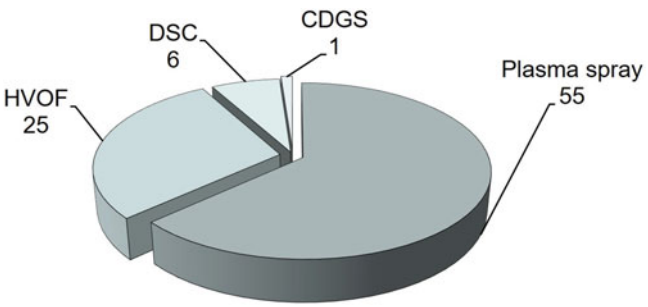

Fig. 19.38 Thermal spray installations in India—distribution in terms of spraying technology used, for a total number of 87 installations (excludes flame, arc, and wire spray systems). ([Sundararajan G, et al. (2009a, b)]. Reprinted with kind permission from ASM International)

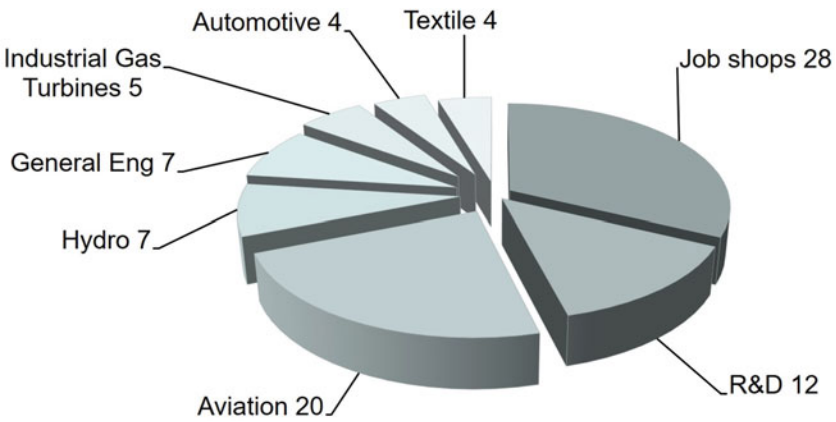

Fig. 19.39 Number of thermal spray installations in India used by different industrial sectors, for a total number of 87 installations (excludes flame, arc, and wire spray systems). ([Sundararajan G, et al. (2009a, b)]. Reprinted with kind permission from ASM International)

(c) Post-coating operations
- Off-line posttreatment, annealing, austempering, laser glazing, hot isostatic pressing (whenever necessary)
- Surface machining, grinding, and polishing
- De-masking
- Cleaning
- Quality control
- Packing and labeling

The overall cost for the coating of a given part constitutes essentially of two broad categories of cost contributing factors:

Direct costs (S_{di}), which includes all cost items directly related to each of the different process steps. These depend directly on the complexity of the technology used, the number, size, shape, and complexity of the parts to be coated, and the nature of the coating material. Direct costs are usually calculated on a per hour basis of the operation. Their conversion to cost per part depends on the number of parts that could be produced in 1 h. The principal factors that contribute to the direct cost of a coating operation are:
- The cost of material to be sprayed (powder, wires, rods, etc.)
- The cost of gases, electricity, and consumables supplied for the operation
- Direct labor cost for each of the different stages of the operation
- Quality control, packing, and labeling

Indirect costs (S_{in}), often referred to as *fixed cost* or *overhead costs*, include all other expenses, which are related to the investment needed and general running cost of the coating site. The indirect cost factors are usually calculated on a yearly basis of the operation. Their conversion to a per hour basis depends on the number of hours of operation of the coating center per year (N_{hy}). They include, though not limited to, the following:
- Equipment acquisition and amortization of the capital investment
- Building, ancillary equipment, and necessary infrastructure
- Maintenance workshop
- Quality control laboratory
- General administration and services
- Marketing and financial expenses

The total cost of the coating of a single part, S_T, is the sum of all direct, S_{di}, and indirect, S_{in}, cost factors, on a per hour basis, multiplied by the number of hours needed per part (N_{hp}).

$$S_T = \left[S_{di} + \frac{S_{in}}{N_{hy}}\right] \times N_{hp} \tag{19.2}$$

Where;

S_T Total cost per part ($/part)
S_{di} Direct cost per hour ($/h)
S_{in} Indirect cost per year ($/y)
N_{hy} Operating hours per year (h/y)
N_{hp} Number of hours per part (h/part)

19.6.2 Direct Cost Factors

19.6.2.1 Cost of Materials

This is often the most important single cost item of the coating operation. It varies widely depending on the nature of the coating material, its purity, and its form. As presented in Chap. 13, Powders, Wires, and Cords, coating material are available as powders, wires, cords, or rods depending on the coating technology used. Powders are by far the most common form of materials used in coating operations with particle size ranging from 10 μm up to a few hundred microns in diameter or more. Generally, the cost of a powder increases rapidly with the following parameters:

- *The purity level of the material*: For example, a 5N Si powder would cost almost one order of magnitude higher than a 3N Si.
- *Oxygen level*: For example, a "grade 1" titanium powder with an oxygen level lower than 1200 ppm will cost considerably more than a "grade 2" powder of the same particle size but with an oxygen level in the 2500 ppm or "grade 4" with an oxygen level of 4000 ppm.
- *Particle size distribution*: The narrower the particle size distribution of the powder, the higher will be the cost of the powder on a $/kg basis.
- *Powder morphology*: Generally, spherical, free-flowing, dense powders will have a higher cost than a standard spray dried or fused and crushed powder.
- *Specialty alloys*: When custom made, with tightly controlled specification of its elemental analysis, the powder will cost considerably more than standard materials.

It is important to underline that these parameters are also interactive between them. For example, a titanium powder with a particle size $\leq$45 μm and an oxygen content of less than 1300 ppm (grade 1) will be more difficult to obtain and would be significantly more expensive than a titanium powder with the same oxygen level (grade 1), but a coarser particle size range (45–106 μm). Delivery time and volume

of annual consumption can also have a significant influence on the cost of powders. The same reasoning equally applies for other materials in the form of cords, wires, or rods.

The key parameters that influence the quantity of material needed to spray a part are:

- *The surface to be coated*, A_c, taking into account its shape complexity, its holes distribution that must be protected, and the sprayed material lost at edges.
- *The average thickness of the coating*, δ_c (including the mean thickness that has to be removed from the as-sprayed part to achieve the final specified dimensions, sprayed coatings' dimensional precision being in the range of tenths of millimeters).

These two quantities, together with the feedstock specific mass, ρ_p (kg/m^3), and the deposition efficiency, η_c (%), which depends strongly on the spray process and the geometry of the part to be coated, allow calculating the powder quantity necessary for each part, m_{part} (kg):

$$m_{part} = \frac{\delta_c A_c \rho_p}{\eta_c} \tag{19.3}$$

It is important to stress the very important impact of the deposition efficiency, η_c (%), on the overall cost of materials in the coating process. This is because overspray powders, which do not end up in the coating, are collected from the exhaust gases or ambient air strictly for environmental reasons and are never recycled in the coating operation because of the risk of introducing major contaminants or defects in the coating. Moreover, scrap/over-sprayed powders, while they represent a loss of value based on their procurement cost, would also often require additional costs, as a waste material, for their discharge in an environmentally safe way.

Automation is one way of reducing powder waste, and accordingly reduce powder consumption in the spray process, through close control of the spray process. For example, if a multi-axis robot handles the arc spray gun, the operation of powder feeder can be synchronized with the robot, thus stopping the powder feeding during substrate transfer or repositioning, to reduce feedstock losses and coating costs. It is be noted, however, that stopping the powder feeding does not imply stopping the powder carrier gas flow since, in the absence of powder carrier gas, any powder in transient in the powder feeding line would sediment in the transport line and could end blocking it when the powder feeding is resumed.

19.6.2.2 Cost of Gases, Electricity, and Consumables

The cost of gases can represent an important component of the operating cost of the coating operation and often the next cost item in a spray operation after the cost of the spray material. This depends significantly on the nature of the gases used, their purity level, and overall volume flow rates required for the coating operation. The unit cost of gases ($/m^3) also depends on the overall size of the operation and the associated gas consumption. A compilation of typical cost of gases used in thermal spray and cold spray coating operations in North America and Europe is given in Table 19.5. These values are based on 2020 prices and should be adjusted for inflation and price changes in subsequent years.

It is important to note that the decision on which size of gas packaging to use is essentially based on the volume of the operation. For example, the cost for industrial purity argon gas in North America can be more than three times higher when in the form of compressed gas cylinders compared to cryogenic form in industrial-scale Dewar's. The use of cryogenic gases, on the other hand, while generally less expensive per m^3 of gas used, can be completely offset by the constant loss factor that has to be bled to the atmosphere from cryogenic containers for any prolonged period of time in which the gas is not in use. Compressed gas cylinders, or bulk packs, required manual handling and rental fee for the cylinders, which in large-volume operation can be important especially if the operation requires a wide range of different specialty gases. Generally, the cost of the gas varies with its consumption and on-site storage linked to the corresponding delivery mode [Celotto S, et al. (2007)] (from cylinder, vehicles delivering liquid gases with different storage volumes and pressures, trailer for He, bulk vehicle).

The total cost of the gas component in the spray operation depends obviously on the nature of the spray operation, and the operating conditions. For example, with cold spray process, which is one of the highest gas consumer spray operations, the gas consumption rate, as illustrated in Fig. 19.40, depends on the process variables, the type of gas, operating pressure and temperature, and internal diameter of the spray nozzle; see Table 19.6 for system configurations associated with Fig. 19.40 [Celotto S, et al. (2007)]. The use of helium in cold spray requires flow rates that are 4.2 times higher than those for N_2, due to the large

Table 19.5 Range of cost of spray gases and electric energy in North America and Europe

Gas	Cost range
Argon (Ar)	0.8–2.4 US$/m^3
Nitrogen (N_2)	0.2–1.5 US$/m^3
Oxygen (O_2)	0.2–1.3 US$/m^3
Hydrogen (H_2)	6.0–14 US$/m^3
Helium (He)	15–80 US$/m^3
Natural gas (CH_4)	0.2–1.5 US$/m^3
Propane (C_3H_6)	0.2–2.0 US$/m^3
Electric energy	0.09–0.20 US$/kWh

Table 19.6 System configurations associated with Fig. 19.40

System configuration	1	2	3	4	5	7	7	8
Nozzle i.d. (mm)	2.0	2.0	2.0	2.7	2.0	2.7	2.0	2.0
Gas used	N_2	N_2	N_2	N_2	He	He	He	He
Gas pressure (MPa)	2.0	3.0	3.0	3.0	3.0	2.0	2.0	2.0
Gas temperature (°C)	25	25	350	350	25	25	25	350

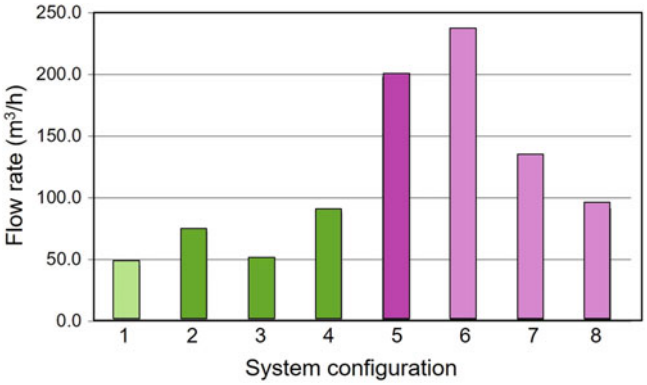

Fig. 19.40 Gas consumption rates for different cold spray system configurations. [Celotto S, et al. (2007)]

difference in sonic velocity. Increasing the gas temperature, on the other hand, allows for the decrease in the gas consumption.

Gas recycling and on-site gas generation are two of the common means of reducing the cost of gases in the coating operation. Gas recycling is generally limited to operation in a closed environment such as in vacuum plasma spraying (VPS), whether DC or RF induction plasma. More recently, gas recycling has been increasingly introduced in cold spray operations, which requires often the use of helium at relatively large volume flow rates with a significant financial burden on the operation. Gas recycling in this case has to be associated with a gas cleaning and recompression operation. On-site gas generation on the other hand is only used in large volume operation, which justifies the capital investment whether for the generation of oxygen or nitrogen on site through cryogenic distillation or hydrogen through water electrolysis.

The cost of energy, whether in the form of fuels in combustion spraying, or electrical power, in plasma spray operations, varies considerably with type of technology used and the scale of operation. A comparison of the power requirement by different spray technologies is given in Fig. 19.41. This shows that HVOF and high-velocity liquid fuel (HVLF) technologies are among the largest energy consumers in which the supplied fuel is in the form of liquid or gas. Comparative data on the energy efficiency and the associated specific energy requirement (SER) of different

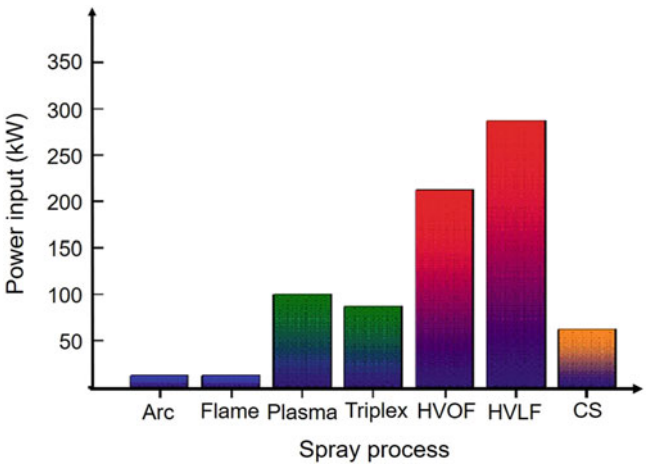

Fig. 19.41 Total power consumption by different spray processes. ([Molz R, Hawley D (2007)]. Reprinted with kind permission from ASM International)

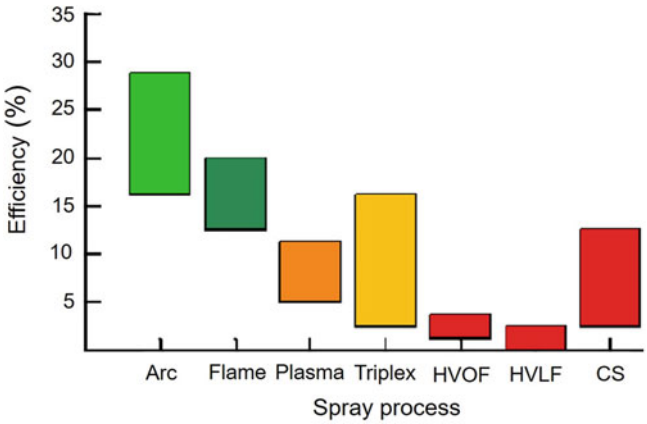

Fig. 19.42 Spray process efficiencies for different spray processes. ([Molz R, Hawley D (2007)]. Reprinted with kind permission from ASM International)

spray processes are provided in Figs. 19.42 and 19.43, respectively.

Molz and Hawley (2007) pointed out that the comparison of the effective performance of alternate thermal spray processes for a given application is not straightforward and often hampered by detailed particularities of each process. They consequently proposed a more generic and global method, based on deriving a unified process efficiency formula that takes into account all energy inputs and energy outputs of a process in the same energy units. They made a direct comparison of process efficiency for each process and specific coating conditions. For example, the energy input to the "system" could either be already included in the supply to the thermal spray gun or created (as in combustion guns) within the gun itself. Two sources exist, one for the gas itself

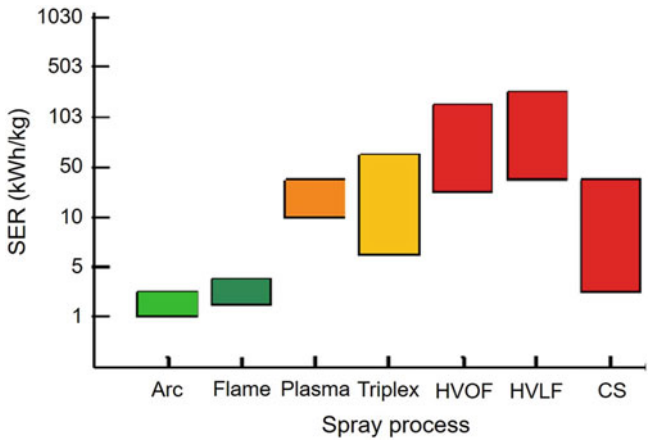

Fig. 19.43 Specific energy requirement (SER) in kWh/kg of coating deposited for different spray processes. ([Molz R, Hawley D (2007)]. Reprinted with kind permission from ASM International)

being used (in raw form prior to any reaction) and one for the material input into the system. This is illustrated in Fig. 19.41, after Molz and Hawley D (2007), representing the total energy required (input) for a few thermal spray processes. As expected, flame and wire arc spraying exhibit the lowest energy consumptions.

Figure 19.42, after Molz and Hawley (2007), represents the process efficiency for each thermal spray process based on the measured power output in terms of particle temperatures and velocities. The drawback of these calculations is that they are based on the particle temperature measured assuming that it is representative of the total thermal energy state of the sprayed powder. As noted in Fig. 19.42, wire arc spraying, while having the highest energy efficiency of all TS processes, barely manages to achieve 30% efficiency. The lowest efficiency (≈2% range) is found to be with the HVOF and HVLF processes.

Figure 19.43, after Molz and Hawley (2007), represents the specific energy requirement (SER) defined as the energy consumed per kg of coating deposited. It is to be noted that the scale in this case is logarithmic in order to fit the entire range of values. The typical high-velocity coatings of carbides, with lower deposit efficiency and higher energy input, require considerably more energy to deposit per unit mass, almost one order of magnitude higher than that to spray pure ceramics or metals.

Electric energy-based technologies, such as plasma spraying and wire arc spraying, use typically industrial electricity rates, which are composed of two components:

- *Power* (*kW*), which is set by an annual agreement with the electric energy utilities reflecting the overall size of the operation and its peak energy demand.
- *Energy* (*kWh*), which is the electrical energy consumption by the operation for running the plasma system as well as all of the ancillary equipment.

Electricity cost for building illumination, heating, and other operations is not included under direct cost of the operation. These constitute part of the indirect costs. Electricity rates vary widely between locations and period of operation over the range 0.09–0.20 US$/kWh or more.

The cost of consumables and spare parts also varies widely with the nature of the spray process and the complexity of the part. For example, in DC plasma-spraying operation, whether atmospheric or under vacuum, a close monitoring of the state of the electrodes is essential for ensuring a consistent quality of the coating. Generally, the allowed life of the electrodes is based on the recommendations of the equipment manufacturer and/or the operator experience. It is generally accepted practice to replace consumable parts in a setup after a well-defined lifetime, rather than wait for a disruption of the operation and a failure of the quality of the coating. It has to be recognized that the cost of a failed coating is not only limited to the loss of the coating martial and associated labor and expenses, but also to the damage caused to the part being coated, which can be order of magnitude higher than that of the coating operation itself. The cost of consumables is not limited to torch components; it can also include certain important components of the plasma generating equipment. In induction plasma spraying, for example, the RF power supply has a triode tube that needs to be replaced depending on its projected lifetime, which can be in the 10,000–20,000 h. The triode life also depends on the mode of operation and the number of starts and stops per hour of unit. In a 100-kW installation, the cost of such a component can be in the US $10,000–15,000 range.

The cost of consumables also includes the cost of masking tapes used to protect the surface, which should not be exposed to sand blasting or coating, the cost of the grit used in the sand blasting operation prior to coating, and cost of grinding and polishing materials and supplies used for surface finishing of the part.

19.6.2.3 Direct Labor Cost

In thermal spray operations, direct labor cost is inversely proportional to the degree of automation of the operation. The higher is the level of automation and the larger is the scale of the operation, the lower will be the direct cost of labor per part. In a typical coating operation, direct labor is needed for:

- Preparation of the part to be coated, including its masking, sandblasting, and cleaning

- Setting-up of the part in the coating booth: starting of the operation, preheating, and coating, followed by removal of the part from the rig
- Cleaning of the part, surface machining, grinding, and polishing
- De-masking and cleaning
- Quality control
- Packing and labeling

The total cost of labor for the coating operation is also relatively sensitive to the overall management of the facility and the efficient definition of the operation steps and the definition of responsibilities.

19.6.2.4 Direct Cost for Quality Control, Packing, and Labeling

This depends on the maturity of the technology used for the coating operation and on the nature of the parts to be coated. The most stringent quality control rules are generally applied for medical and aerospace applications, where very rigorous quality control (QC) procedures are needed and have to be strictly enforced. In other applications, with generally lower-value items, such as in automobile industry, QC on individual parts would be too expensive. The industry has to rely in this case on well-developed, mature, and reliable technologies.

The overall cost of quality control includes direct and indirect cost factors. Basic investment in QC in instrumentation and laboratory equipment will go under *indirect cost*, while the labor cost associated with the QC procedures will go under *direct cost* and will depend on whether it is applied on all of the coated parts or on randomly selected parts. For obvious reasons, QC procedures tend to use nondestructive testing as much as possible in order to avoid sacrificing the part being tested. In the development stage of a new part, both nondestructive and destructive testing procedures are generally needed.

19.6.3 Indirect or Fixed Cost Factors

19.6.3.1 Capital Investments

This covers the total investment needed for the setting-up of the operation. It includes:

- *Cost of land and building*, including building permits and environmental studies necessary for the setting-up of the operation
- *Ancillary equipment and infrastructure*, including spray booth, dust collection and disposal, air cleaners, sound control, and operator safety equipment
- *Production equipment*, including spray system and associated operations, instrumentation, and data acquisition
- *Equipment for posttreatment and finishing*, including heat treatment furnaces, laser glazing, hot isostatic pressing, machining, and grinding and polishing equipment
- *Maintenance workshop*
- *Quality Control laboratory*
- *Storage space* for materials, supplies, spare parts, and finished part
- *Office space*

Direct investment for the acquisition of the coating production equipment rarely exceeds 15–20% of the total investment needed for the setting-up of a new production facility. The investment structure needed for the expansion of an existing facility can be different with a considerably higher percentage needed for the acquisition of the production equipment.

Capital investment contributes to indirect production cost through the amortization of the investment made. It is important to note that the amortization rules vary from country to country as well as between the different types of investments. For example, investments for the building and infrastructure are generally depreciated over a 25-year period, production equipment, over a 5–7-year period, while computers, automation, and information technology (IT) equipment may need to be amortized over a 3–5-year period due to the rapid evolution of the technology. The simplest method of calculating amortization cost per hour of operation, S_{ih}, is based on a linear amortization over the projected number of years considered as useful life of the equipment, N_y, divided by the number of operating hours per year, N_{hy}, as follows:

$$S_{ih} = \frac{P_e}{N_y \times N_{hy}} \tag{19.4}$$

where P_e is the procurement cost of the equipment. For more information on investment cost calculation, the interested reader can go through the paper by de Munter et al. (2002). Typical investment cost estimate for coating equipment and ancillary equipment are given in Tables 19.7 and 19.8, respectively, based on a 2006 study by MAGETEX and presented by Ducos (2006a, b).

19.6.3.2 Other Indirect or Fixed Costs

These include essentially the cost of general administration and services, insurances, marketing, and financial services. These are strongly dependent on the scale of the operation and its location.

Table 19.7 Investment costs of equipment for spray processes in 2006 [Ducos M (2006a, b)]

	Value in Euro (€)	Value in US$
Manual powder or wire flame	About 5000	About 6500
Automated powder or wire flame	5000–10,000	6500–13,000
HVOF–HVAF	50,000–100,000	65,000–130,000
Wire arc spray	9000–22,500	11,700–29,250
APS	75,000–185,000	97,500–240,500
VPS/CAPS	600,000 to >2 M	780,000 to >2.6 M
PTA	50,000–75,000	65,000–97,500

Reprinted with kind permission from Dr. M. Ducos

APS air plasma spraying, *CAPS* controlled atmosphere plasma spraying, *HVAF* high-velocity air fuel, *HVOF* high-velocity oxy fuel, *PTA* plasma-transferred arc, *VPS* vacuum plasma spraying

Table 19.8 Investment costs of ancillary equipment in 2006 [Ducos M (2006a, b)]

	Value in Euro (€)	Value in US$
Grit blasting	10,000–40,000	13,000–52,000
Linear movements	35,000–75,000	45,500–97,5000
Robot	75,000–150,000	97,500–195,000
Spray booth	12,000–25,000	15,600–32,500
Ventilation and filtering	30,000–45,000	39,000–58,500
Machining and grinding	200,000–1 M	260,000–1.3 M
Quality control	75,000–200,000	97,500–260,000

Reprinted with kind permission from Dr. M. Ducos

19.6.4 Few Examples

19.6.4.1 Cost of DC Atmospheric Plasma Spraying of YPSZ

To illustrate the relative importance of each of these cost factors, de Botton (1988), in his Master of Science Study, calculated the costs for DC atmospheric plasma spraying (APS) of yttria partially stabilized zirconia (YPSZ) coatings on a flat 1 m^2 surface. The coating thickness was 300 µm. The spray rate was 3 kg/h, with a deposition efficiency of 60% and a coating relative density of 0.9. Losses at holes and edges were assumed to be of 10%.

For the cost calculations, he assumed:

- 5 years to recover capital investment (cost of 10% per year)
- Maintenance cost of 4% of capital investment
- 250 production days, 2 shifts per day, for a total of 4000 h/year production time

Results are summarized in Figs. 19.44 and 19.45, which represent the different factors of prices per sprayed part. It is obvious from this figure that the most important one is the powder, followed by labor (automation can reduce it notably) and capital cost. Figure 19.45 reveals that after the coating cost (81.9%), the grinding process is the most important

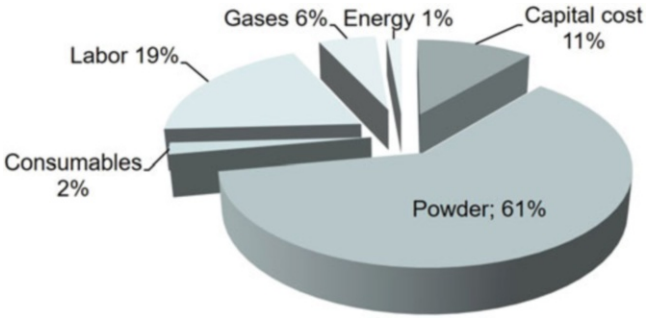

Fig. 19.44 Spray costs distribution of YPSZ coatings. ([de Botton O (1988)]. Reprinted with kind permission from MIT)

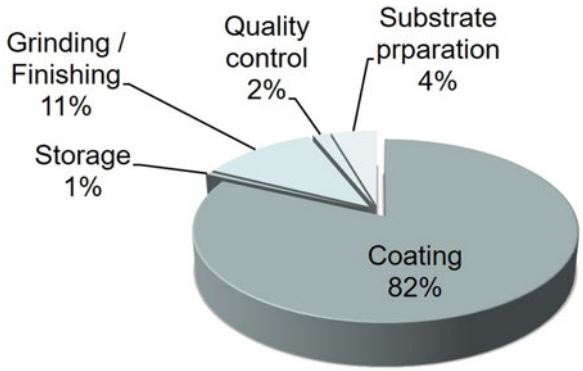

Fig. 19.45 Total costs distribution of YPSZ coatings. ([de Botton O (1988)]. Reprinted with kind permission from MIT)

(11.5%) followed by the surface preparation (4.4%). The quality control and storage represent only 2.1%.

19.6.4.2 MCrAlY Coatings Sprayed Using HPPS and Wire Arc Spray

In a study by Sacriste et al. (2001), the bond coat of TBCs was deposited on a nickel-based super alloy, with a surface area of 100 × 50 mm^2 and a thickness of 2 mm. As the thickness of the topcoat was limited to 200 µm for this application, a relatively low roughness of the bond coat was

Table 19.9 Cost analysis[a] for the production of NiCrAlY coating using Plazjet-7070 and twin-wire arc spray (Arc Jet-9000) processes operating using nitrogen or air as atomizing gas [Sacriste D, et al. (2001)]

Parameter	Plazjet-7070	Arc Jet-9000	
		Nitrogen	Air
System cost (US$)	198,000	23,800	23,800
Amortization time (years)	5	5	5
Material feed rate (kg/h)	12	12	12
Spraying time per year (h)	278	278	278
Amortization (US$/kg of coating)	19.83	2.38	2.38
NiCrAlY powder and wire (US$/kg)	90	63	63
Powder cost (US$/kg of coating)	1.26	0.11	0.11
Electric power (kW)	115	10	10
Electric energy cost (US$/100 kWh)	7.90	7.90	7.90
Energy cost (US$/kg of coating)	1.26	0.11	0.11
Plasma and atomization gas flow rates (m^3/h)	9.6	105	65
Gas cost (US$/100 m^3)	3.40	3.40	0.50
Gas consumption (m^3/year)	2670	29,200	18,000
Electrodes and tips costs (US$)	635	6	6
Electrodes and tips lifetime (h)	12	6	6
Consumable cost (US$/kg of coating)	7.39	0.63	0.18
Production cost (US$/kg of coating)	162.10	154.80	107.30
Labor cost (US$/kg of coating)	8.45	8.45	8.45
Production cost without amortization (US$/kg)	158.65	105.74	105.29
Total production cost (US$/kg of coating)	178.48	108.12	107.67

[a]The production cost was calculated per kilogram of coating at a deposition rate of 12 kg/h and a deposition efficiency of 60%. The total production was set to two tons per year. Coatings were sprayed without substrate cooling

needed (*Ra* <10 μm). Two different TS technologies were used for the deposition of the bond coat:

- The high-power plasma spray (HPPS) TAFA, PlazJet-7070 equipped with a 120-mm long anode and working with a mixture of nitrogen and hydrogen, the powder being injected at feed rates up to 12 kg/h.
- The TAFA twin-wire arc spray system used in this study was Arc Jet-9000 model. Wires were fed with the push–pull system capable to work with wires and cored wires 7.50 m long. The NiCrAlY material was available as cored wire with a NiCr envelope containing particles of Al, Cr, and Y. Air and nitrogen were used as atomization gases with different air caps.

Coatings obtained by arc spraying exhibited a higher surface roughness due to a relatively low particle velocity compared to that obtained with the Plazjet-7070 process. The deposition efficiency was the same as that obtained with the Plazjet-7070 gun, for both air and nitrogen atomizing gas. The use of nitrogen atomization resulted in a 10 wt.% reduction in the oxygen content, but no changes were observed in the bond strength (higher than 40 MPa). The composition of the arc-sprayed NiCrAlY coatings was very heterogeneous, which was attributed to the wire manufacturing method.

A summary of the cost analysis of the optimized results using the three coating conditions (Plazjet-7070, and Arc Jet-9000 operating with N_2 and Air) is presented in Table 19.9, after Sacriste et al. (2001).

Table 19.9 shows that the Arc Jet-9000 process, using air or nitrogen atomization, is about 40% less expensive than the Plazjet-7070 process. As with the majority of spraying systems, the material feedstock is the most expensive parameter for both systems. In this study, it represents about 84% of the total coating price for Plazjet-7070 and 97% for Arc Jet-9000. Because of the high deposition rates, labor cost was relatively low with both systems, representing less than 5% for Plazjet-7070 and of the order of 7% for Arc Jet-9000. One of the major differences between the two systems is in the capital investment, which, for the Plazjet-7070 system, was more than eight times higher than the Arc Jet-9000, representing 11% of total production cost for the Plazjet-7070 compared to about 2% for the Arc Jet-9000 system. The difference in the electric power shows that Arc Jet-9000 is more thermally efficient than plasma spraying, as it requires a power of only 10 kW to spray 12 kg of NiCrAlY

Table 19.10 Different costs for manually wire arc-spraying zinc on 1 m^2 of steel [Ducos M (2006a, b)]

Parameter	Cost in €/m^2
Surface preparation	7.3
Spraying (air atomization)	6.9
Amortizing	1.0
Total	15.2 €/m^2

Reprinted with kind permission from Dr. M. Ducos

material per hour, in sharp contrast to 110 kW needed for the Plazjet-7070 system.

19.6.4.3 Manual Wire Flame Zn Coating

According to Ducos (2006a, b) and calculations of MAGETEX, the different costs for manually wire arc-spraying zinc on steel substrate are summarized in Table 19.10. These were based on a coating thickness of 120 µm, labor cost at 40 €/h., and system amortization over 3 years of an operation of 1200 h/y. The cost of zinc wire consumption was estimated at 2 €/h. With this spray process, which is one of the cheapest of surface modification technologies, the surface preparation becomes slightly more important than the spray cost. Because of the low investment cost, amortizing is also rather low as can be noted in Table 19.10.

19.6.4.4 Cost Analysis for NiAl Coatings Using APS Versus WAS

Ducos (2006a, b) has evaluated the cost of a NiAl coating, 1.8 mm thick, for aeronautic application, using atmospheric plasma spraying (APS) in comparison with wire arc spraying (WAS). Coatings are performed with robotized setups according to conditions and costs summarized in Table 19.11.

Figure 19.46 presents the cost distribution of the different items of the spray process for APS. It can be seen that the most important cost factor is the powder (51%), followed by the investment amortization (22%) and labor (18%). Gases, electricity, and consumable parts represent only 9%. The distribution of other costs (surface preparation, grit blasting and cleaning, finishing, and quality control) is presented in Fig. 19.47. It can represent 50–80% of the spray costs. Figure 19.48 represents the cost distribution per sprayed hour for the APS and WA coatings. The WA coating cost per hour is about 60% that of the APS coating, which is mainly due to the investment and labor costs.

19.6.4.5 Cost Comparison for Hard Chromium Replacement

Based on same principles, Ducos and Durand (2001) calculated the costs per m^2 of Al_2O_3–TiO_2 (13 wt.%) APS sprayed, WC–Co HVOF sprayed, and NiCrBSi HVOF sprayed to replace electrolytic hard chromium. Results are presented in Fig. 19.49, which shows that the cheapest coating is that of NiCrBSi HVOF sprayed at a cost 21.6 € higher than that of hard chromium (18 €). APS ceramic coating comes next to which the cost of the bond coat must be added (46.6 + 20.0 = 66.6 €), followed by the HVOF-sprayed WC–Co coating (122.5 €), which is at a considerably higher cost due to the cost of the powder.

Table 19.11 Spray conditions and costs of APS and WAS deposition of NiAl (5 wt.% Al) 1.8 mm thick coatings for aeronautic application [Ducos M (2006a, b)]

Parameter	APS	WAS
Deposition rate (kg/h)	2.5	11.2
Deposition efficiency (%)	60	70
Material costs (€/kg)	35 (powder)	45 (wire)
Spray time (h)	2.93	0.56
Material used (kg)	7.33	6.29
Consumable parts (€)	13.49	0.45
Gases and electricity (€)	30.26	1.4

Reprinted with kind permission from Dr. M. Ducos

APS air plasma spraying, *WAS* wire arc spraying

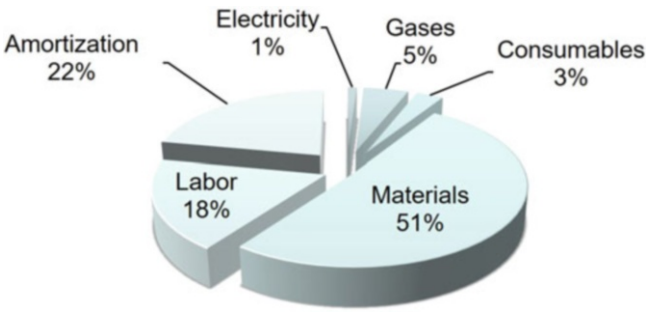

Fig. 19.46 Distribution of direct spray costs for a 1.8 mm thick NiAl (5 wt.% Al) coating plasma sprayed in air. ([Ducos M (2006a, b)]. Reprinted with kind permission from Dr. M. Ducos)

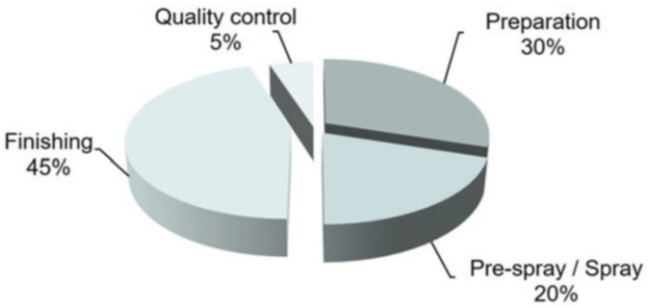

Fig. 19.47 Distribution of pre- and post-spray costs for a 1.8 mm thick NiAl (5 wt.%) coating plasma sprayed in air. ([Ducos M (2006a, b)]. Reprinted with kind permission from Dr. M. Ducos)

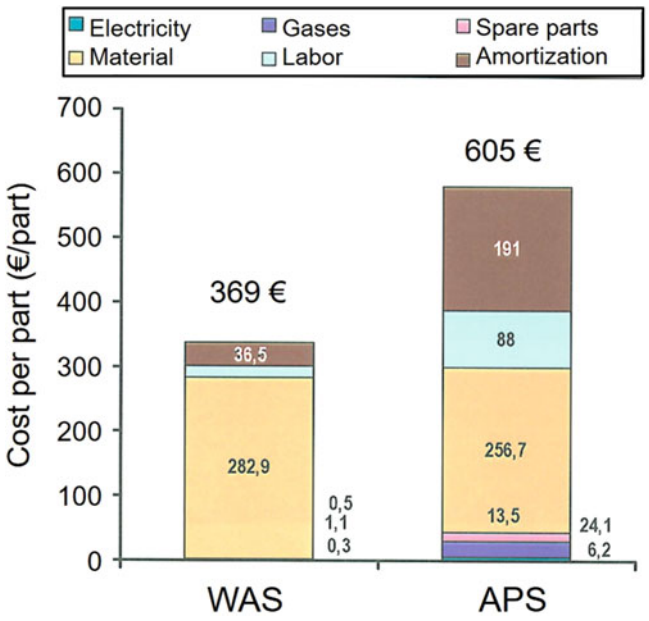

Fig. 19.48 Comparison of the cost per part of 1.8 mm thick NiAl (5 wt. %) coatings plasma sprayed in air or wire arc sprayed. ([Ducos M (2006a, b)]. Reprinted with kind permission from Dr. M. Ducos)

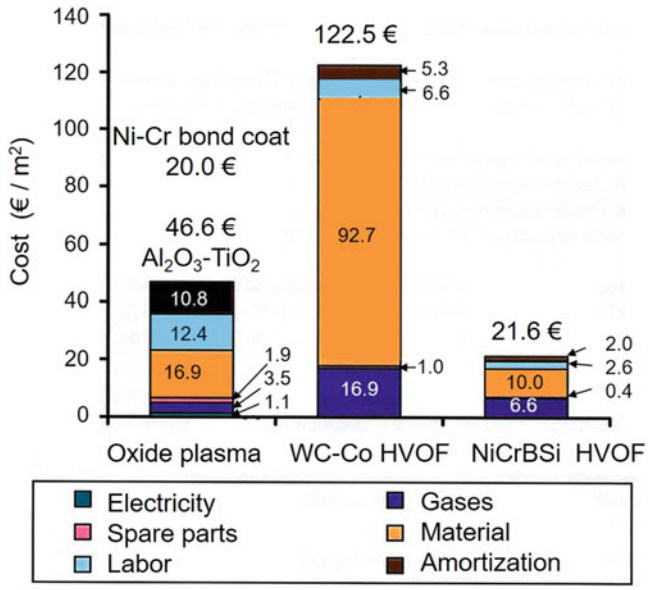

Fig. 19.49 Comparison of the costs per m^2 of Al_2O_3–TiO_2 (13 wt.%) APS sprayed, WC–Co HVOF sprayed, and NiCrBSi HVOF sprayed to replace hard chromium. ([Ducos M, Durand JP (2001)]. Reprinted with kind permission from ASM International)

19.7 Summary and Conclusions

In this chapter, a brief comparative analysis of different thermal spray processes is presented, grouping them in into five subgroups: cold spray, combustion-based thermal spray, plasma spray, wire arc spray, and plasma-transferred arc deposition. In this section, emphasis is placed on the unique features of each of these technologies, its advantages, and limitation. As demonstrated in the different parts of this book, these technologies are essentially complimentary rather than competing for the same application. The choice of a specific coating and/or thermal spray process, for a given service condition, depends on the service needs, expectation of the end user, and the cost that could be tolerated for the application.

This is followed by a review of different TS coating applications described in terms of surface modification for the enhancement of its resistant to wear, corrosion, and oxidation; providing thermal protection; clearance control; good bonding; electrical and electronic properties; and the deposition of freestanding spray-formed parts. The coating design process is often complicated by the fact that in practice components are not always devoted to a single requirement such as wear or corrosion or electrical insulation or thermal insulation. In most cases, coatings must resist to different combined needs: for example, wear is often linked to corrosion.

The subsequent section provides a review of present and potential industrial applications of the technology in a wide range of industrial sectors including aerospace, land-based turbines and power generation, automotive, land-based and marine applications, application in the electrical and electronic industries, medical applications, ceramics and glass industries, and chemical process industries. This is followed by a brief overview of evolution of this industry on an international scale by country.

In the last section of this chapter, techno-economic analysis is presented discussing different cost contributing factors with typical examples of cost estimation for a few applications. Due to the dependence of the economic parameters on the regional infrastructure and local cost factors, emphasis is placed more on the methodology and the identification of the principal cost factors affecting the process economics rather than their absolute value that can change rapidly with time depending on the local economic context. On this point, it is important to stress that the evaluation of the cost of a coating has to be placed in contrast to cost savings that it could generate either by extending the lifetime of a part, refurbishing a worn part avoiding the extra cost of its replacement, or sometimes simply by reducing the "downtime" of a rather expensive installation simply for repair or the replacement of a worn part.

The following tables prepared by the International Thermal Spray Association [http://www.thermalspray.org] summarize the different TS technologies used in various industrial segments (Table A.1), coating application according to industry served (Table A.2), and materials sprayed in various industrial sectors (Table A.3).

Table A.1 Thermal spray technologies used by various industrial segments

Industry	Oxy fuel	Spray/fuse	HVOF	D-gun	Air plasma	Vacuum plasma	Shroud plasma
Aero gas turbine	✓		✓	✓	✓	✓	✓
Stationary gas turbine	✓		✓	✓	✓	✓	
Hydro-steam turbine	✓		✓	✓	✓	✓	✓
Automotive engines	✓		✓		✓		
Diesel engines	✓		✓		✓		
Transportation non-engine	✓			✓	✓		
Agriculture implementations	✓	✓			✓		
Railroad	✓		✓		✓		
Iron and steel manufacture	✓	✓			✓		
Steel rolling mills	✓	✓	✓		✓		
Iron and steel casting			✓		✓		
Forging	✓		✓				
Copper and brass mills	✓						
Ship and boat manufacture and repair	✓						
Oil and gas exploration	✓	✓	✓	✓	✓		
Mining, construction, and dredging	✓	✓	✓		✓		
Rock products	✓	✓	✓		✓		
Screening							
Cement and structural clay	✓	✓	✓				
Chemical processing	✓	✓	✓	✓	✓		
Rubber and plastic manufacture	✓	✓	✓		✓		
Textile	✓		✓	✓	✓		
Food processing	✓	✓	✓	✓	✓		
Electrical utilities			✓		✓		
Pulp and paper	✓		✓		✓		
Printing equipment			✓	✓	✓		
Defense and aerospace	✓		✓	✓	✓	✓	
Nuclear			✓	✓	✓		
Medical			✓	✓	✓	✓	✓
Business equipment			✓	✓	✓		
Electrical and electronics			✓	✓	✓	✓	
Architectural	✓	✓			✓		
Glass manufacture		✓		✓	✓		

Reprinted with kind permission from *SPRAYTIME*—a publication of the International Thermal Spray Association, a standing committee of the American Welding Society

Table A.2 Thermal spray applications in various industrial segments

	Wear							Clearance control				Electrical	
Industry	Abrasive	Adhesive	Fretting	Erosion	Cavitation	Impact	TBC	Abradable	Abrasive	Restoration	Corrosion/ Oxidation	Resistance	Conductivity
Aero gas turbine	✓	✓	✓	✓			✓	✓	✓	✓	✓		
Stationary gas turbine	✓	✓	✓	✓			✓	✓	✓	✓	✓		
Hydro-steam turbine	✓	✓	✓	✓	✓					✓	✓		
Automotive engines	✓	✓		✓		✓	✓	✓	✓	✓	✓	✓	
Diesel engines	✓	✓		✓		✓	✓			✓	✓		
Transportation non-engine	✓	✓					✓			✓	✓	✓	
Agriculture implementations	✓			✓		✓				✓			
Railroad	✓	✓				✓				✓	✓		✓
Iron and steel manufacture	✓			✓		✓				✓	✓		
Steel rolling mills	✓	✓				✓				✓	✓		
Iron and steel casting	✓			✓		✓				✓	✓		
Forging	✓	✓				✓				✓	✓		
Copper and brass mills	✓									✓	✓		
Ship and boat manufacture/ repair	✓			✓						✓	✓		
Oil and gas exploration	✓	✓		✓		✓				✓	✓		
Mining, construction, and dredging	✓			✓	✓	✓				✓	✓		
Rock products	✓					✓				✓	✓		
Screening	✓					✓				✓	✓		
Cement and structural clay	✓					✓				✓	✓		
Chemical processing	✓			✓						✓	✓		
Rubber and plastic manufacture	✓			✓		✓				✓	✓		
Textile	✓									✓			
Food processing	✓									✓			
Electrical utilities	✓	✓		✓	✓	✓				✓	✓		
Pulp and paper	✓				✓	✓				✓	✓		
Printing equipment	✓	✓								✓			
Defense and aerospace	✓	✓	✓	✓	✓	✓	✓			✓			
Nuclear											✓		
Medical	✓		✓								✓		
Business equipment	✓	✓	✓										
Electrical and electronics										✓	✓		
Architectural	✓					✓							
Glass manufacture	✓	✓								✓	✓		

Reprinted with kind permission from *SPRAYTIME*—a publication of the International Thermal Spray Association, a standing committee of the American Welding Society

Table A.3 Thermal spray-coating materials used in various industrial sectors

Industry	Chrome carbide	Self-fluxing	Iron and steel	Nickel alloys	Superalloys	MCrAlY	Cobalt alloys	Nonferrous
Aero gas turbine	✓		✓	✓	✓	✓	✓	✓
Stationary gas turbine	✓		✓	✓	✓	✓	✓	✓
Hydro-steam turbine	✓	✓	✓	✓	✓		✓	✓
Automotive engines	✓			✓	✓	✓	✓	
Diesel engines	✓		✓	✓	✓	✓	✓	
Transportation non-engine			✓	✓				✓
Agriculture implementations		✓	✓	✓				✓
Railroad		✓	✓	✓				✓
Iron and steel manufacture		✓	✓	✓	✓		✓	✓
Steel rolling mills		✓	✓	✓	✓		✓	✓
Iron and steel casting		✓	✓					✓
Forging		✓	✓	✓	✓		✓	
Copper and brass mills							✓	
Ship and boat manufacture/ repair			✓	✓				✓
Oil and gas exploration		✓	✓	✓			✓	✓
Mining, construction, and dredging		✓	✓					✓
Rock products		✓	✓					✓
Screaming			✓					
Cement and structural clay		✓	✓					✓
Chemical processing			✓	✓	✓		✓	
Rubber and plastic manufacture		✓	✓	✓			✓	
Textile			✓					
Food processing		✓	✓					
Electrical utilities		✓	✓	✓			✓	✓
Pulp and paper		✓	✓	✓				✓
Printing equipment								✓
Defense and aerospace	✓	✓	✓	✓	✓	✓	✓	✓
Nuclear								
Medical								✓
Business equipment								✓
Electrical and electronics								✓
Architectural	✓							✓
Glass manufacture	✓	✓	✓					

Reprinted with kind permission from *SPRAYTIME*—a publication of the International Thermal Spray Association, a standing committee of the American Welding Society

Appendices

Appendix A: Processes and Coating Applications by Industry

Appendix B: Use of the Different Spray Materials

In this appendix only basic information about the most frequently sprayed materials are presented. For more detailed information, the reader must consult the different powder and wire suppliers. It must also be kept in mind that the coating resulting from the spray process has properties (thermal and electrical conductivities, for example) different from those of powder or wire properties. Such differences result from the increase in the oxide content, the pores generated during spraying, the real contacts between layered splats, etc. Properties also depend on the way the sprayed material has been manufactured. In the following, X-20Y-10Z means 20 wt.% of Y, 10 wt.% of Z, the balance being X.

B.1 Metals

Aluminum: Al (99 wt.%) $T_m = 660$ °C:

- Good corrosion resistance in industrial atmospheric conditions
- Good electrical and thermal conductivity
- Soft and ductile → repair Al alloys
- Nonmagnetic (electromagnetic shielding)
- Sprayed by flame (powder or wire), wire arc, plasma, and cold spray

Aluminum base: Al–Si (95/5 or 12 wt.%):

- Salvage of parts made of Al, Mg, and their alloys—excellent finish
- Sprayed by flame (powder or wire), wire arc, plasma, and cold spray
- Cobalt-based powders (pure cobalt $T_m = 1495$ °C)

Stellite® (Co–xCr–yW–zC):

- Against galling and cavitation
- For metal friction, high-angle erosion, high-temperature hardness, good resistance to abrasion, and rather good wettability
- Very good oxidation resistance
- Replace WC in high-temperature applications
- Repair of cobalt-based parts
- Sprayed by HVOF, flame, PTA, and plasma

Triballoy® (Co–xCr–yMo–zSi) or (Co–xCr–yMo–zSi–tNi):

- Against galling for metal-to-metal friction
- High-temperature hardness
- Good resistance to corrosion and oxidation
- Very good wear properties from room temperature to 860 °C
- Sprayed by HVOF, flame, PTA, and plasma

Co–25.5Cr–10.5Ni–7.5W–0.5C:

- High abrasive, sliding fretting, and cavitation wear resistance up to 800–850 °C
- Good oxidation resistance
- Behave well between 540 and 840 °C
- Sprayed by HVOF, flame, PTA, and plasma

Co–28Mo–8Cr–2Si:

- Up to 760 °C low coefficient of friction
- Good corrosion resistance
- Sprayed by HVOF, flame, PTA, and plasma

Co–28Mo–17Cr–3Si:

- Excellent sliding wear resistance
- Good hot corrosion resistance and moderate oxidation resistance up to 800 °C
- Sprayed by HVOF, flame, PTA, and plasma

Copper Cu (99 wt.%) ($T_m = 1084$ °C):

- Very good electrical and thermal conductivities
- Good resistance to inks (paper and printing)
- Used to repair Cu-base alloys
- Nonmagnetic (electromagnetic shielding)
- Sprayed by flame (powder or wire), wire arc, plasma, HVOF, and cold spray

Copper-based powder: Cu–36Ni–5In ($T_m = 1150$ °C):

- Very dense coatings with good resistance to galling and fretting
- Sprayed by flame (powder or wire), wire arc, plasma, HVOF, and cold spray

Aluminum bronze: Cu–9.5Al–1Fe:

- For pumps (against cavitation)

- Piston guides (soft-bearing surfaces)
- Shifter forks and compressor air seals (friction)
- Strength and hardness twice that of other bronzes
- Sprayed by flame (powder or wire), wire arc, plasma, HVOF, and cold spray

Supra bronze: Cu–40Zn–0.8Sn–0.75Fe–0.24Mn:

- For metallizing work
- Sprayed by flame (powder or wire), wire arc, plasma, HVOF, and cold spray
- Iron-based powders (pure iron $T_m = 1538$ °C)
- Low-carbon steels (C < 0.25 wt.%)
- An inexpensive low-carbon steel powder
- Corrosion resistant → repair + good wear resistance in lubricated service
- May contain martensitic phases
- Produces machinable coatings
- Sprayed by flame, wire arc, plasma, HVOF, and cold spray

High-carbon steels (C > 0.8 wt.%):

- Reclamation
- Wear and erosion resistance
- Sprayed by flame, wire arc, plasma, and HVOF

Stainless steels (SS): Fe-13 or 14Cr–1Ni:

- Good resistance to wear and corrosion
- Best for all purposes (SS)
- Sprayed by flame, wire arc, plasma, and HVOF

Stainless steels (SS): Fe–18Cr–8Mg–5Ni:

- Reclamation
- Corrosion protection
- Low shrinkage and good machinability
- Sprayed by flame, wire arc, plasma, and HVOF

Stainless steels (SS): Fe–17Cr–12NI–2.5Mo–1Si–0.1C (ASI 316):

- Corrosion protection
- Dimensional restoration
- Cavitation and low-temperature erosion resistance
- Sprayed by wire or powder flame, wire arc, and HVOF

Cored wires (wire arc sprayed):

- Some of them (Fe–Cr–P–C–, etc.) form amorphous phases upon spraying
- Rather good resistance to corrosion (for example, with H_2SO_4)
- Good resistance to abrasion

Molybdenum: Mo (pure molybdenum $T_m = 2623$ °C):

- Self-bonding to most metallic surfaces, especially steels
- Natural lubricity and high hardness: good wear properties
- Maximum service temperature 316 °C

Salvage and build-up of Ni-base alloy components:

- High-density coatings
- Fretting resistant
- Used for pump parts, diesel engine fuel, injectors, piston rings, synchronized ring, press fits, valves, gears, cam followers, etc.
- Sprayed by HVOF, flame (powder or wire), wire arc, and plasma

Self-fluxing alloys: Mo+25 (Ni–Cr–B–Si–Fe):

- High wear resistance, low friction coefficient
- Against steel, good scuff resistance
- Can be used for hard-facing, hard-bearing surfaces
- Against abrasion

Nickel: Ni (99.5 wt.%) (pure nickel $T_m = 1455$ °C):

- Good bonding to steel
- Good corrosion and oxidation resistance up to 980 °C
- Resist heat and prevent scaling of carbon and low-alloy steels in hot atmospheres

Salvage and build-up of Ni-base alloys:

- Easily machined
- Sprayed by HVOF, flame (powder or wire), wire arc, and plasma

Ni–20Cr:

- Good surface appearance
- Good machinability
- Protective coatings against oxidizing gases at high temperature (up to 980 °C)
- Electrical conductors
- Surfacing

Other different types of NiCr (Cr 10–17 wt.%) but also addition of Fe, Mo with specific applications:

- See supplier guides for example

Ni–16Cr–8Fe:

- Machinable "stainless" coatings for salvage and build-up applications on corrosion-resistant steels
- Sprayed by HVOF, flame (powder or wire), wire arc, and plasma

Ni–18Cr–6Al (composite or clad):

- Good oxidation resistance
- Good machinability
- Bonding and surfacing layers
- Self-bonds to most metallic surfaces
- Sprayed by HVOF, flame (powder or wire), wire arc, and plasma

Ni–20Cr–10W–9Mo–4Cu–1C–1B–1Fe:

- Wear and corrosion protection
- Coatings contain some amounts of glassy phases (due to addition of refractory metals and metalloids)
- Sprayed by HVOF, flame (powder or wire), wire arc, and plasma

Ni–5Al (clad):

- Good hardness and refractoriness (formation of nickel aluminide)
- Oxidation and abrasion resistant
- Adhere very well to smooth substrates
- Bond coat
- Resizing of over-machined parts or of worn-out parts
- Possible: Al 20 wt.% (clad) → self-bonds to most metal surfaces
- Sprayed by HVOF, flame (powder or wire), wire arc, and plasma

Nickel-based self-fluxing alloys:
Ni–10Cr–2.5B–2.5Fe–2.5Si–0.15C:

- The only one producing machinable-fused coating
- Resistance to abrasive wear, fretting, cavitation, and erosion up to 840 °C

Ni–17Cr–4Fe–4Si–3.5B–1C:

- Dense coating good corrosion resistance
- Ni–17Cr–4Fe–4Si–3.5B–1C
- Dense, hard, and oxide-free coating
- Piston rings, cylinder liners, and utility exhaust fan

Superalloys: M.Cr.Al.Y with M = Ni, Co, Fe, Ni–Co:

- Composition optimized: for substrate compatibility and environmental resistance
- Protection against corrosion and oxidation in high-temperature applications
- Aero gas turbines
- Marine turbines
- Stationary gas turbines
- Design criteria—avoid phase transformation during engine start up and shut down; avoid brittle phases (e.g., μ, σ, αCr)
- Limit brittleness increasing with oxide content
- Form a stable and adherent oxide scale of Al_2O_3 with the addition of active elements (0.5% wt. Y)
- Increase corrosion resistance (by increasing Cr content)
- Control thermal expansion coefficient: increasing with Cr and decreasing with Al
- Keep ductile coatings (ductile to brittle temperature influenced by Cr and Al contents)
- Many compositions exist
- Sprayed by HVOF and plasma (if possible, under soft-vacuum to limit oxidation)

B.2 Ceramics

For most oxides the thermal expansion coefficient is low compared to that of most metals and it has to be taken into account because they are often used at high temperature.

luAmina: Al_2O_3 (T_m = 2050 °C):

- Main problem: Starting from α phase, melting and fast cooling (spraying) result in γ phase. Unfortunately, around 1000 °C γ phase transforms into α phase with a volume increase of about 4% resulting in coating peeling off. Thus, coatings should be used below 900 °C.
- They are not too sensitive to oxygen losses.
- They have a good resistance to abrasive, sliding, and friction wear up to approximately 800 °C.
- Poor resistance to shock or impact loading.
- High dielectric strength and good electrical insulating coatings.
- Reactive with molten salts.
- Porous coatings.
- Sprayed mainly by plasma, sometimes by HVOF (particles below 22 μm in diameter), and also by flame (rods or cords).

itTanium dioxide: TiO_2 (T_m = 1843 °C):

- Very sensitive to oxygen losses resulting in strong modifications of coating properties: color from white to black and especially electrical properties
- Loss and gain of oxygen reversible
- Very good wettability
- Excellent surface finish
- Excellent adhesion
- Rather low porosity
- Sprayed by plasma, HVOF, and also by flame (rods or cords)

Alumina–Titanium dioxide: Al_2O_3–$xTiO_2$:

- TiO_2 in the range 2–50 wt.% (most common: 3–13–40 wt.%): lowers Al_2O_3 coating porosity
- Al_2O_3–$3TiO_2$ can be used with most acids and alkalis
- Good for abrasion, erosion, and sliding wear
- Maximum service temperature, 840 °C
- Less brittle but lower dielectric strength than pure Al_2O_3 coatings sprayed by plasma

Al_2O_3–$13TiO_2$:

- Applications similar to those of Al_2O_3–$3TiO_2$ but with lower hardness and dielectric strength and less resistance to chemical attack
- Maximum service temperature, 540 °C
- Sprayed by plasma

Al_2O_3–$40TiO_2$:

- Formation of Al_2TiO_5
- Softer and less resistant to chemicals
- Excellent finishing properties
- Sprayed by plasma
- Other compositions are used, for example, with SiO_2 below 2 wt.%

Chromium oxide: Cr_2O_3 ($T_m = 2435$ °C):

- Its stoichiometry depends strongly upon spray conditions (high oxygen pressure needed), and sub-stoichiometric coatings have a metallic behavior with a poor corrosion resistance
- Coatings have high hardness (1900–2000 HV_{5N})
- Excellent wear resistance
- Low porosity
- Excellent finish
- Used on sliding surfaces
- Good wear resistance
- Insoluble in acids, alkalis, and alcohol
- Maximum service temperature, 540 °C
- Excellent engraving properties
- Sprayed by plasma, HVOF, and also by flame (rods or cords)

Cr_2O_3–$3TiO_2$–$5SiO_2$:

- TiO_2 limits oxygen losses
- Resists better than Cr_2O_3 to impacts
- High wear and corrosion resistance
- Hydroxyapatite: $Ca_5(PO_4)_3OH$
- For coating medical and dental implants
- Biocompatible and bioactive (main constituent of bones)
- Sprayed by plasma

Zirconia: ZrO_2:

- Interesting mechanical properties.
- Good wear resistance.
- Low thermal conductivity (1–5 W/m K).
- Three phases: monoclinic (m), tetragonal (t), and cubic (c). Upon cooling around 1000 °C, cubic or tetragonal phases transform into monoclinic with volume increase of about 10% and coating peeling off. Thus, only totally (c phase) or partially (t' non-transformable t phase) stabilized zirconia can be sprayed.
- Most used stabilizers are CaO, MgO, Y_2O_3, and CeO_2. CaO and MgO are rather cheap but the maximum service temperature is about 500 °C. Very good results are obtained with Y_2O_3; with about 8 wt.% t' phase is obtained, while with 13 wt.% c phase is obtained, as with 24–25 wt.% CeO_2. The maximum service temperature (about 1350 °C at the best) depends not only on the phase (best results with c phase) but also on the way the powder is manufactured (see Sect. 11.1.2.9), best results being obtained when zirconia and stabilizer particles are very small and uniformly distributed.
- Coatings have excellent thermal shock resistance and good oxidation and corrosion resistance.
- They are mainly used as thermal barriers.
- Sprayed by plasma and also by flame (rods or cords).

Zircon: $ZrSiO_4$ (infusible):

- Dissociated during spraying (65% ZrO_2, 35% SiO_2)
- Not wetted by liquid metals: used for casting
- Good resistance to liquid glass
- Good resistance to combustion gases

B.3 Cermets

They are made of a metal matrix, to achieve a good toughness, in which are embedded ceramic particles either of oxides or carbides for the hardness and wear resistance.

Here again the manufacturing process plays a key role, for example, sintered particles behaving very differently than blended ones.

With oxides: In most cases they are blends. For example: Al_2O_3–30(Ni–20Al):

- Denser coatings than pure ceramic, more abrasion, and shock resistant, hard, and smooth
- Addition of alumina particles modifies the electrical resistance of the metal matrix

MCrAlY + Al_2O_3 (<3 μm):

- Hardness increases with Al_2O_3 content
- Electrical resistance decreases with Al_2O_3 %

With carbides (the most used):

- Most used ones are: WC, Cr_3C_2, and also sometimes TiC
- If all of them have melting temperatures over 1900 °C (for example, $T_m = 2870$ °C for WC), they are relatively sensitive to oxidation.
- WC oxidation starts at 500–600 °C and oxidation produces W_2C decomposing into W over 1300 °C.

Cr_3C_2:

- Is not the only chromium carbide: Cr_7C_3 ($T_m = 1782$ °C), $Cr_{23}C_6$ ($T_m = 1518$ °C). Cr_3C_2 is mostly used in spraying and its oxidation starts at 800–900 °C; however, $Cr_{23}C_6$ has an excellent wear resistance.

TiC:

- Has a unique cubic phase ($T_m = 3170$ °C), in which oxidation starts at 800–900 °C.
- At last, carbides dissolve more or less in the liquid metal or alloy matrix, the dissolution increasing with temperature over the matrix melting temperature. The metal matrix lowers the wear resistance of carbides but increases resistance to mechanical or thermal shock. Phase changes of metal matrix must be avoided during the service (for example, that of Co occurs at about 480 °C). To conclude, chemical changes occur during spraying especially in air atmosphere: oxidation, decomposition, and dilution. Thus, microstructural properties of sprayed cermets depend strongly on spray conditions (VPS, IPS, APS, HVOF, HVAF, etc.), particle morphology and manufacturing process, and ceramic mean grain size. Only a few examples are given below:

WC–8Co:

- Dense, hard, and wear-resistant coating
- Sprayed by plasma, HVOF, and HVAF

WC–12Co:

- Excellent low-temperature wear resistance
- Sprayed by plasma, HVOF, and HVAF

WC–17Co:

- Higher Co level improves toughness and fretting resistance
- Cannot be used in corrosive media

Cr_3C_2–25(Ni–20Cr):

- Oxidation resistant up to 900 °C
- Good corrosion resistance
- Excellent for high-temperature cavitation, abrasion, and sliding wear

Cr_3C_2–7(Ni–20Cr):

- Very good resistance to high-temperature fretting and wear (higher carbide content increases hardness)

B.4 Abradables

They are designed to wear preferentially upon contact with mating part in order to automatically establish clearance. They comprise a metal matrix and nonmetallic filler such as graphite, polyester, polyimide, boron nitride, and friable material, the role of filler being to weaken the matrix integrity. The metal matrix is made of Ni, Al, Cu, Co bases, and superalloys.

The main difference in the base material is related to service temperature:

- Al–Si with C: up to 315–425 °C
- Al–Si with polyester: up to 350 °C

The filler content can be varied:

- Both are used for the compressor section of jet engines

Co–polyester–BN:

- They are used up to 700 °C

Cu: Aluminum bronze alloy–polyester or Cu–14polyester–8Al–1Fe–5Binder

- Maximum service temperature: 650 °C

Ni–graphite:

- They are used up to 480 °C
- Self-lubricating

MCrAlY–polyester and/or BN:

- Temperatures up to 1200–1300 °C

Nomenclature

Units are indicated in parentheses; when no units are indicated, the parameter is dimensionless.

Latin Alphabet

A_c	Surface to be coated (m^2)
f	Friction coefficient
m_{part}	Mass of coating required for each part (kg/part)
N_{hy}	Operating hours per year (h/y)
N_{hp}	Number of hours per part (h/part)
p	Pressure (Pa)
Pc	Cost per kg powder deposited (US$/kg or €/kg)
Pcc	Cost of spare parts (US$ or €)
Pcp	Powder cost per hour (US$/h or €/h)
Pe	Cost of equipment's (US$ or €)
Pee	Energy cost per 100 kW (US$ or €)
Pen	Energy cost per deposited kg powder (US$/kg or €/kg)
Pep	Component cost per deposited kg powder (US$/kg or €/kg)
Pg	Gas cost per 100 m^3 (US$ or €)
Pgp	Gas cost per deposited kg powder (US$/kg or €/kg)
Pt	Plasma torch power (kW)
qp	Powder quantity necessary for each part (kg)
Qp	Powder spraying rate (kg/h)
Ra	Surface roughness (μm)
S_T	Total cost per part ($/part)
S_{di}	Direct cost per hour ($/h)
S_{in}	Indirect cost per year ($/y)
S_{ih}	Amortization rate per hour (US$/h or €/h)
T	Tangential force (N)
tc	Mean component lifetime (h)
tp	Time necessary to spray the part (h)
v	Velocity (m/s)

Greek Alphabet

η_e	Percentage corresponding to effective spray due to loss at holes and edges (%)
η_c	Powder or wire deposition efficiency (%)
ρ_p	Feedstock specific mass (kg/m^3)
δ_c	Coating thickness (mm)

References

Abdi, S., and S. Lebaili. 2008. Alternative to chromium, a hard alloy powder NiCrBCSi (Fe) coatings thermally sprayed on 60CrMn4 steel. Phase and comportements. *Physics Procedia* 2: 1005–1014.

Agarwal, A., T. McKechnie, and S. Seal. 2003. Net shape nanostructured aluminum oxide structures fabricated by plasma spray forming. *Journal of Thermal Spray Technology* 12 (3): 350–359.

Ahmaniemi, S., M. Vippola, P. Vuoristo, T. Mäntylä, M. Buchmann, and R. Gadow. 2002a. Residual stresses in aluminum phosphate sealed plasma sprayed oxide coatings and their effect on abrasive wear. *Wear* 252: 614–623.

Ahmaniemi, S., J. Tuominen, P. Vuoristo, and T. Mäntylä. 2002b. Sealing procedures for thick thermal barrier coatings. *Journal of Thermal Spray Technology* 11 (3): 320–332.

Ahmed, R., and M. Hadfield. 2002. Mechanisms of fatigue failure in thermal spray coatings. *Journal of Thermal Spray Technology* 11 (3): 333–349.

Ahn, H.-S., and O.-K. Kwon. 1999. Tribological behaviour of plasma-sprayed chromium oxide coating. *Wear* 225–229: 814–824.

Ahn, J., B. Hwang, and S. Lee. 2005. Improvement of wear resistance of plasma-sprayed molybdenum blend coatings. *Journal of Thermal Spray Technology* 14 (2): 251–257.

Akebono, H., J. Komotori, and M. Shimizu. 2008. Effect of coating microstructure on the fatigue properties of steel thermally sprayed with Ni-based self-fluxing alloy. *International Journal of Fatigue* 30: 814–821.

Alam, S., S. Sasaki, and H. Shimura. 2001. Friction and wear characteristics of aluminum bronze coatings on steel substrates sprayed by a low pressure plasma technique. *Wear* 248: 75–81.

Al-Fadhli, H.Y., J. Stokes, M.S.J. Hashmi, and B.S. Yilbas. 2006. The erosion–corrosion behaviour of high velocity oxy-fuel (HVOF) thermally sprayed inconel-625 coatings on different metallic surfaces. *Surface and Coating Technology* 200: 5782–5788.

American Welding Society. 1985. *Thermal spraying, practice, theory and application*. Miami: American Welding Society.

Aoh, J.-N., and J.-C. Chen. 2001. On the wear characteristics of cobalt-based hardfacing layer after thermal fatigue and oxidation. *Wear* 250: 611–620.

Arcondéguy, A., A. Grimaud, A. Denoirjean, G. Gasgnier, C. Huguet, B. Pateyron, and G. Montavon. 2007. Flame-sprayed glaze coatings: effects of operating parameters and feedstock characteristics onto coating structures. *Journal of Thermal Spray Technology* 16 (5–6): 978–990.

Arcondéguy, A., G. Gasgnier, G. Montavon, B. Pateyron, A. Denoirjean, A. Grimaud, and C. Huguet. 2008. Effects of spraying parameters onto flame-sprayed glaze coating structures. *Surface and Coating Technology* 202: 4444–4448.

Arrabal, R., A. Pardo, M.C. Merino, M. Mohedano, P. Casajús, and S. Merino. 2010. Al/SiC thermal spray coatings for corrosion protection of Mg–Al alloys in humid and saline environments. *Surface and Coating Technology* 204: 2767–2774.

Bala, N., H. Singh, and S. Prakash. 2010. Accelerated hot corrosion studies of cold spray Ni–50Cr coating on boiler steels. *Materials and Design* 31: 244–253.

———. 2011. Characterization and high-temperature oxidation behavior of cold-sprayed Ni-20Cr and Ni-50Cr coatings on boiler steels. *Metallurgical and Materials Transactions A* 42A: 3399–3416.

Barbezat, G. 2003. Low-cost high-performance coatings produced by internal plasma spraying for the production of high efficiency engines. In *International thermal spray conference 2003*, ed. C. Moreau and B. Marple, 139–142. Materials Park: ASM International.

———. 2005. Advanced thermal spray technology and coating for lightweight engine blocks for the automotive industry. *Surface and Coating Technology* 200: 1990–1993.

———. 2006. Application of thermal spraying in the automobile industry. *Surface and Coating Technology* 201: 2028–2031.

Bardi, U., C. Giolli, A. Scrivani, G. Rizzi, F. Borgioli, A. Fossati, K. Partes, T. Seefeld, D. Sporer, and A. Refke. 2008. Development and investigation on new composite and ceramic coatings as possible

abradable seals. *Journal of Thermal Spray Technology* 17 (5–6): 805–811.

Barthel, K., S. Rambert, S. Barthel, S. Rambert, and S. Siegmann. 2000. Microstructure and polarization resistance of thermally sprayed composite cathodes for solid oxide fuel cell use. *Journal of Thermal Spray Technology* 9 (3): 343–347.

Beardsley, M.B. 1997. Thick thermal barrier coatings for diesel engines. *Journal of Thermal Spray Technology* 6 (2): 181–186.

Beauvais, S., V. Guipont, M. Jeandin, D. Juve, D. Treheux, A. Robisson, and R. Saenger. 2005. Influence of defect orientation on electrical insulating properties of plasma-sprayed alumina coatings. *Journal of Electroceramics* 15: 65–74.

Beele, W., G. Marijnissen, and A. van Lieshout. 1999. The evolution of thermal barrier coatings—Status and upcoming solutions for today's key issues. *Surface and Coating Technology* 120–121: 61–67.

Bellucci, D., G. Bolelli, V. Cannillo, R. Gadow, A. Killinger, L. Lusvarghi, A. Sola, and N. Stiegler. 2012. High velocity suspension flame sprayed (HVSFS) potassium-based bioactive glass coatings with and without TiO_2 bond coat. *Surface and Coating Technology* 206: 3857–3868.

Berard, G., P. Brun, J. Lacombe, G. Montavon, A. Denoirjean, and G. Antou. 2008. Influence of a sealing treatment on the behavior of plasma-sprayed alumina coatings operating in extreme environments. *Journal of Thermal Spray Technology* 17 (3): 410–419.

Berger, L.-M., K. Lipp, J. Spatzier, and J. Bretschneider. 2011. Dependence of the rolling contact fatigue of HVOF-sprayed WC–17%Co hard metal coatings on substrate hardness. *Wear* 271: 2080–2088.

Berndt, C.C., J.A. Brogan, G. Montavon, A. Claudon, and C. Coddet. 1998. Mechanical properties of metal- and ceramic-polymer composites formed via thermal spray consolidation. *Journal of Thermal Spray Technology* 7 (3): 337–339.

Billah, B.M., F. Ahmad Khalid, and A. Nusair Khan. 2012. Behavior of calcia-stabilized zirconia coating at high temperature, deposited by air plasma spraying system. *Journal of Thermal Spray Technology* 21 (1): 121–131.

Blink, J., J. Choi, and J. Farmer. 2007. Applications in the nuclear industry for thermal spray amorphous metal and ceramic coatings, UCRL-CONF-232603. *Lawrence Livermore National Laboratory* 9: 1–14.

Blink, J., J. Farmer, J. Choi, and C. Saw. 2009. Applications in the nuclear industry for thermal spray amorphous metal and ceramic coatings. *Metallurgical and Materials Transactions A* 40A: 1344–1354.

Bolelli, G., and L. Lusvarghi. 2006. Heat treatment effects on the tribological performance of HVOF sprayed Co-Mo-Cr-Si coatings. *Journal of Thermal Spray Technology* 15 (4): 802–810.

Bolelli, G., V. Cannillo, L. Lusvarghi, and T. Manfredini. 2006a. Wear behaviour of thermally sprayed ceramic oxide coatings. *Wear* 261: 1298–1315.

Bolelli, G., V. Cannillo, L. Lusvarghi, and S. Ricco. 2006b. Mechanical and tribological properties of electrolytic hard chrome and HVOF-sprayed coatings. *Surface and Coating Technology* 200: 2995–3009.

Bolelli, G., R. Giovnardi, L. Lusvarghi, and T. Manfredini. 2006c. Corrosion resistance of HVOF-sprayed coatings for hard chrome replacement. *Corrosion Science* 48: 3375–3397.

Bolelli, G., L. Lusvarghi, and R. Giovanardi. 2008. A comparison between the corrosion resistances of some HVOF-sprayed metal alloy coatings. *Surface and Coating Technology* 202: 4793–4809.

Bolelli, G., J. Rauch, V. Cannillo, A. Killinger, L. Lusvarghi, and R. Gadow. 2009a. Microstructural and tribological investigation of high-velocity suspension flame sprayed (HVSFS) Al_2O_3 coatings. *Journal of Thermal Spray Technology* 18 (1): 35–48.

Bolelli, G., V. Cannillo, R. Gadow, A. Killinger, L. Lusvarghi, and J. Rauch. 2009b. Microstructural and in vitro characterisation of high-velocity suspension flame sprayed (HVSFS) bioactive glass coatings. *Journal of the European Ceramic Society* 29: 2249–2257.

Bolelli, G., B. Bonferroni, J. Laurila, L. Lusvarghi, A. Milantia, K. Niemi, and P. Vuoristo. 2012a. Micromechanical properties and sliding wear behaviour of HVOF-sprayed Fe-based alloy coatings. *Wear* 276–277: 29–47.

Bolelli, Cannillo V., L. Lusvarghi, R. Rosa, A. Valarezo, W.B. Choi, R. Dey, C. Weyant, and S. Sampath. 2012b. Functionally graded WC–Co/NiAl HVOF coatings for damage tolerance, wear and corrosion protection. *Surface and Coating Technology* 206: 2585–2601.

Bose, S., and J. de Masi-Marcin. 1997. Thermal barrier coating experience in gas turbine engines at Pratt & Whitney. *Journal of Thermal Spray Technology* 6 (1): 99–104.

Bounazef, M., S. Guessasmaa, and B. Ait Saadi. 2004. The wear, deterioration and transformation phenomena of abradable coating BN–SiAl–bounding organic element, caused by the friction between the blades and the turbine casing. *Materials Letters* 58: 3375–3380.

Branagan, D. 2004. *Properties of amorphous/partially crystalline coatings*. US Patent 20040253381.

Branagan, D.J., M. Breitsameter, B.E. Meacham, and V. Belashchenko. 2005. High-performance nanoscale composite coatings for boiler applications. *Journal of Thermal Spray Technology* 14 (2): 196–204.

Brogan, J.A., S. Margolies, H. Sampath, C.C. Herman, and S.D. Berndt. 1995. Adhesion of combustion-sprayed polymer coatings. In *Thermal spray science and technology*, ed. C.C. Berndt and S. Sampath, 521–526. Materials Park: ASM International.

Brožek, V., P. Ctibor, D.I. Cheong, and S.-H. Yang. 2009. Plasma spraying of zirconium carbide-hafnium carbide-tungsten cermets. *Powder Metallurgy Progress* 9: 1–49.

Buyukkaya, E., and M. Cerit. 2007. Thermal analysis of a ceramic coating diesel engine piston using 3-D finite element method. *Surface and Coating Technology* 202: 398–402.

Cao, X.Q., R. Vaßen, and D. Stöver. 2004. Ceramic materials for thermal barrier coatings. *Journal of the European Ceramic Society* 24: 1–10.

Carrasquero, E.J., J. Lesage, E.S. Puchi-Cabrera, and M.H. Staia. 2008. Fretting wear of HVOF Ni–Cr based alloy deposited on SAE 1045 steel. *Surface and Coating Technology* 202: 4544–4551.

Cartier, M. 2003. *Handbook of surface treatments and coatings*, 412 p. New York: ASME Press.

Celotto, S., J. Pattison, J.S. Ho, A.N. Johnson, and W. O'Neill. 2007. The economics of the cold spray process. In *Cold spray materials deposition process - fundamentals and applications*, ed. V. Champagne. Sawston: Woodhead.

Champagne, V.K. 2007. *The cold spray materials deposition process; fundamental and applications*, 362 p. Cambridge: Woodhead.

Chang, C., J. Shi, J. Huang, Z. Hu, and C. Ding. 1998. Effects of power level on characteristics of vacuum plasma sprayed hydroxyapatite coating. *Journal of Thermal Spray Technology* 7 (4): 484–488.

Chatha, S.S., H.S. Sidhu, and B.S. Sidhu. 2012a. High temperature hot corrosion behaviour of NiCr and Cr_3C_2–NiCr coatings on T91 boiler steel in an aggressive environment at 750 °C. *Surface and Coating Technology* 206: 3839–3850.

———. 2012b. The effects of post-treatment on the hot corrosion behavior of the HVOF-sprayed Cr_3C_2–NiCr coating. *Surface and Coating Technology* 206: 4212–4224.

Chattopadhyay, R. 2001. *Surface wear: Analysis, treatment, and prevention*, 307 p. Materials Park: ASM International.

Chen, H., and I.M. Hutchings. 1998. Abrasive wear resistance of plasma-sprayed tungsten carbide–cobalt coatings. *Surface and Coating Technology* 107: 106–114.

Chen, J.Z., H. Herman, and S. Safai. 1993. Evaluation of NiAI and NiAI-B deposited by vacuum plasma spray. *Journal of Thermal Spray Technology* 2 (4): 357–361.

Chen, H., H. Zhao, J. Qu, and H. Shao. 1999. Erosion-corrosion of thermal-sprayed nylon coatings. *Wear* 233–235: 431–435.

Chen, Z., J. Mabon, J.-G. Wen, and R. Trice. 2009. Degradation of plasma-sprayed yttria-stabilized zirconia coatings via ingress of vanadium oxide. *Journal of the European Ceramic Society* 29: 1647–1656.

Chen, X., B. Zou, Y. Wang, H. Ma, and X. Cao. 2011a. Microstructure and thermal cycling behavior of air plasma-sprayed YSZ/LaMgAl11O19 composite coatings. *Journal of Thermal Spray Technology* 20 (6): 1328–1338.

Chen, W.R., E. Irissou, X. Wu, J.-G. Legoux, and B.R. Marple. 2011b. The oxidation behavior of TBC with cold spray CoNiCrAlY bond coat. *Journal of Thermal Spray Technology* 20 (1–2): 132–138.

Chen, H., Y. Gao, H. Luo, and S. Tao. 2011c. Preparation and thermophysical properties of $La_2Zr_2O_7$ coatings by thermal spraying of an amorphous precursor. *Journal of Thermal Spray Technology* 20 (6): 1201–1208.

Chen, X., L. Gu, B. Zou, Y. Wang, and X. Cao. 2012. New functionally graded thermal barrier coating system based on LaMgAl11O19/YSZ prepared by air plasma spraying. *Surface and Coating Technology* 206: 2265–2274.

Cho, T.Y., J. Hong Yoon, J. Young Cho, Y. Kon Joo, J. Ho Kang, S. Zhang, H. Gon Chun, S. Young Hwang, and S. Chol Kwon. 2009. Surface properties and tensile bond strength of HVOF thermal spray coatings of WC-Co powder onto the surface of 420J2 steel and the bond coats of Ni, NiCr, and Ni/NiCr. *Surface and Coating Technology* 203: 3250–3253.

Choa, J.E., S.Y. Hwang, and K.Y. Kim. 2006. Corrosion behavior of thermal sprayed WC cermet coatings having various metallic binders in strong acidic environment. *Surface and Coating Technology* 200: 2653–2662.

Chráska, P., K. Neufuss, and H. Herman. 1997. Plasma spraying of zircon. *Journal of Thermal Spray Technology* 6 (4): 445–448.

Chun-long, Y., A. Yun-qi, and S. Ya-tan. 2009. Three years corrosion tests of nanocomposite epoxy sealer for metalized coatings on the East China Sea. In *Thermal spray 2009: Proceedings of the international thermal spray conference*, ed. B.R. Marple, M.M. Hyland, Y.-C. Lau, C.-J. Li, R.S. Lima, and G. Montavon, 1090–1093. Materials Park: ASM International.

Cipitria, A., I.O. Golosnoy, and T.W. Clyne. 2009. A sintering model for plasma-sprayed zirconia TBCs. Part I: Free-standing coatings. *Acta Materialia* 57: 980–992.

Cipri, F., C. Bartuli, T. Valente, and F. Casadei. 2007. Electromagnetic and mechanical properties of silica-aluminosilicates plasma sprayed composite coatings. *Journal of Thermal Spray Technology* 16 (5–6): 831–838.

Cramer, S.D., B.S. Covino Jr., G.R. Holcomb, S.J. Bullard, W.K. Collins, R.D. Govier, R.D. Wilson, and H.M. Laylor. 1999. Thermal sprayed titanium anode for cathodic protection of reinforced concrete bridges. *Journal of Thermal Spray Technology* 8 (1): 133–145.

Curry, N., and J. Donoghue. 2012. Evolution of thermal conductivity of dysprosia stabilised thermal barrier coating systems during heat treatment. *Surface and Coating Technology* 209: 38–43.

Curry, N., N. Markocsan, X.-H. Li, A. Tricoire, and M. Dorfman. 2011. Next generation thermal barrier coatings for the gas turbine industry. *Journal of Thermal Spray Technology* 20 (1–2): 108–115.

D'Ans, P., J. Dille, and M. Degrez. 2011. Thermal fatigue resistance of plasma sprayed yttria-stabilised zirconia onto borided hot work tool steel, bonded with a NiCrAlY coating: experiments and modeling. *Surface and Coating Technology* 205: 3378–3386.

Dallaire, S. 2001. Hard arc-sprayed coating with enhanced erosion and abrasion wear resistance. *Journal of Thermal Spray Technology* 10 (3): 511–519.

Darut, G., H. Ageorges, A. Denoirjean, G. Montavon, and P. Fauchias. 2008. Effect of the structural scale of plasma-sprayed alumina coatings on their friction coefficients. *Journal of Thermal Spray Technology* 17 (5–6): 788–797.

Das, S., S. Datta, D. Basu, and G.C. Das. 2009. Glass–ceramics as oxidation resistant bond coat in thermal barrier coating system. *Ceramics International* 35: 1403–1406.

Davis, J.R., ed. 2004. *Handbook of thermal spray technology. Sections introduction to applications for thermal spray processing and selected applications*. Materials Park: ASM International.

de Botton, O. 1988. *Master of Science in Technology and Policy*. Cambridge, MA: MIT.

de Munter, A.J., A. Bult, and J.A. de Jong. 2002. On the economical and environmental aspects of TSA coatings. In *International thermal spray conference 2002*, ed. E. Lugscheider. Düsseldorf: DVS. e-Proc.

Deng, C., M. Liu, C. Wu, K. Zhou, and J. Song. 2007. Impingement resistance of HVAF WC-based coatings. *Journal of Thermal Spray Technology* 16 (5–6): 604–609.

Dent, A.H., A.J. Horlock, D.G. McCartney, and S.J. Harris. 1999. The corrosion behavior and microstructure of high-velocity oxy-fuel sprayed nickel-base amorphous/nanocrystalline coatings. *Journal of Thermal Spray Technology* 8 (3): 399–404.

Devasenapathi, A., H.W. Ng, S.C.M. Yu, and A.B. Indra. 2002. Forming near net shape free-standing components by plasma spraying. *Materials Letters* 57: 882–886.

Ding, Z.-X., W. Chen, and Q. Wang. 2011. Resistance of cavitation erosion of multimodal WC-12Co coatings sprayed by HVOF. *Transactions of the Nonferrous Metals Society of China* 21: 2231–2236.

Donner, K.-R., F. Gärtner, and T. Klassen. 2011. Metallization of thin Al_2O_3 layers in power electronics using cold gas spraying. *Journal of Thermal Spray Technology* 20 (1–2): 299–306.

Dorfman, M.R., and A. Sharma. 2013a. Challenges and strategies for growth of thermal spray, keynote lecture presented at ITSC-2012, Houston, TX, USA. *Journal of Thermal Spray Technology* 22 (5): 559–563.

Dorfman, M., and A. Sharma. 2013b. Commentary challenges and strategies for growth of thermal spray markets: the six-pillar plan. *Journal of Thermal Spray Technology Comment* 22 (5): 559–563.

Döring, J.-E., F. Hoebener, and G. Langer. 2008. Review of applications of thermal spraying in the printing industry in respect to OEMs. In *Thermal spray conference: Crossing the border*, ed. E. Lugscheider. Düsseldorf: DVS. e-Proc.

Drnovšek, N., S. Novak, U. Dragin, M. Čeh, M. Gorenšek, and M. Gradišar. 2012. Bioactive glass enhances bone ingrowth into the porous titanium coating on orthopaedic implants. *International Orthopaedics* 36: 1739–1745.

Ducos, M. 1988. Plasma transferred arc reclamation. In *Plasmas in industry. Dopee Diffusion, France*, ed. G. Laroche and M. Orfeuil, 251–262. (in French).

———. 2006a. *Evaluation des coûts de projection thermique* (Costs evaluation in thermal spraying). Cours, ALIDERTE, Limoges.

———. 2006b. *Evaluating the costs of thermal spraying*, ALIDERTE course. ALIDERTE, Limoges (in French)

Ducos, M., and J.P. Durand. 2001. Thermal coatings in Europe, a business perspective. In *Thermal spray 2001*, ed. C.C. Berndt, K.H. Khor, and E. Lugscheider, 1267–1276. Materials Park: ASM International.

Eriksson, R., H. Brodin, S. Johansson, L. Östergren, and X.-H. Li. 2011. Influence of isothermal and cyclic heat treatments on the adhesion of plasma sprayed thermal barrier coatings. *Surface and Coating Technology* 205: 5422–5429.

Esfahani, E.A., H. Salimijazi, M.A. Golozar, J. Mostaghimi, and L. Pershin. 2012. Study of corrosion behavior of arc sprayed aluminum coating on mild steel. *Journal of Thermal Spray Technology*. https://doi.org/10.1007/s11666-012-9810-x.

Espallargas, N., J. Berget, J.M. Guilemany, A.V. Benedetti, and P.H. Suegama. 2008. Cr_3C_2–NiCr and WC–Ni thermal spray

coatings as alternatives to hard chromium for erosion–corrosion resistance. *Surface and Coating Technology* 202: 1405–1417.

Evdokimenko Yu, I., V.M. Kisel', V.K. Kadyrov, A.A. Korol', and O.I. Get'man. 2001. High-velocity flame spraying of powder aluminum protective coatings. *Powder Metallurgy and Metal Ceramics* 40 (3–4): 121–126.

Factor, M., and I. Roman. 2002. Use of microhardness as a simple means of estimating relative wear resistance of carbide thermal spray coatings: Part 2. Wear resistance of cemented carbide coatings. *Journal of Thermal Spray Technology* 11 (4): 482–495.

Fan, X., and T. Ishigaki. 2001. Mo_5Si_3-B and $MoSi_2$ deposits fabricated by radio frequency induction plasma spraying. *Journal of Thermal Spray Technology* 10 (4): 611–617.

Faraoun, H.I., T. Grosdidier, J.-L. Seichepine, D. Goran, H. Aourag, C. Coddet, J. Zwick, and N. Hopkins. 2006. Improvement of thermally sprayed abradable coating by microstructure control. *Surface and Coating Technology* 201: 2303–2312.

Farmer, J.C., and J.-S. Choi. 2007. Criticality-control applications in the nuclear industry for thermal spray amorphous metal and ceramic coatings, UCRL-TR-234171. *Lawrence Livermore National Laboratory* 31: 1–7.

Farmer, J., J. Choi, C. Saw, J. Haslam, D. Day, P. Hailey, T. Lian, R. Rebak, J. Perepezko, J. Payer, D. Branagan, B. Beardsley, A. D'Amato, and L. Aprigliano. 2009. Iron-based amorphous metals: high-performance corrosion-resistant material development. *Metallurgical and Materials Transactions A* 40A: 1289–1305.

Fauchais, P., G. Montavon, R.S. Lima, and B.R. Marple. 2011. Engineering a new class of thermal spray nano-based microstructures from agglomerated nanostructured particles, suspensions and solutions: an invited review. *Journal of Physics D: Applied Physics* 44: 093001.

Fedrizzi, L., L. Valentinelli, S. Rossi, and S. Segna. 2007. Tribocorrosion behaviour of HVOF cermet coatings. *Corrosion Science* 49: 2781–2799.

Fedtke, P., M. Wienecke, M.-C. Bunescu, T. Barfels, K. Deistung, and M. Pietrzak. 2004. Yttria-stabilized zirconia films deposited by plasma spraying and sputtering. *Journal of Solid State Electrochemistry* 8: 626–632.

Fernandez, J., M. Gaona, and J.M. Guilemany. 2007. Effect of heat treatments on HVOF hydroxyapatite coatings. *Journal of Thermal Spray Technology* 16 (2): 220–228.

Feuerstein, A., J. Knapp, T. Taylor, A. Ashary, A. Bolcavage, and N. Hitchman. 2008. Technical and economical aspects of current thermal barrier coating systems for gas turbine engines by thermal spray and EBPVD: a review. *Journal of Thermal Spray Technology* 17 (2): 199–213.

Flores, J.F., A. Neville, N. Kapur, and A. Gnanavelu. 2009. An experimental study of the erosion–corrosion behavior of plasma transferred arc MMCs. *Wear* 267: 213–222.

Fossati, A., M. DiFerdinando, U. Bardi, A. Scrivani, and C. Giolli. 2012. Influence of surface finishing on the oxidation behaviour of VPS MCrAlY coatings. *Journal of Thermal Spray Technology* 21 (2): 314–324.

Fukumoto, M. 2008a. The current status of thermal spraying in Asia. *Journal of Thermal Spray Technology* 17 (1): 5–13.

———. 2008b. The current status of thermal spraying in Asia; Hwang SY Status of thermal spraying in Korea; Li C-J The current state of thermal spray activities in China; Tani K, Nakahira A The current status of thermal spray in Japan; Khor MKA Thermal spray activities in Singapore. *Journal of Thermal Spray Technology* 17 (1): 5–13.

Ganesh Sundara Raman, S., B. Rajasekaran, S.V. Joshi, and G. Sundararajan. 2007. Influence of substrate material on plain fatigue and fretting fatigue behavior of detonation gun sprayed Cu-Ni-In coating. *Journal of Thermal Spray Technology* 16 (4): 571–579.

Gärtner, F., T. Stoltenhoff, T. Schmidt, and H. Kreye. 2006. The cold spray process and its potential for industrial applications. *Journal of Thermal Spray Technology* 15 (2): 223–232.

Gawne, D.T., Z. Qiu, Y. Bao, T. Zhang, and K. Zhang. 2001. Abrasive wear resistance of plasma-sprayed glass-composite coatings. *Journal of Thermal Spray Technology* 10 (4): 599–603.

Geibel, A., L. Froyen, L. Delaey, and K.U. Leuven. 1996. Plasma spray forming: an alternate route for manufacturing free-standing components. *Journal of Thermal Spray Technology* 5 (4): 419–430.

Gell, M., E.H. Jordan, M. Teicholz, B.M. Cetegen, N. Padture, L. Xie, D. Chen, X. Ma, and J. Roth. 2008. Thermal barrier coatings made by the solution precursor plasma spray process. *Journal of Thermal Spray Technology* 17 (1): 124–135.

Gibbons, G.J., and R.G. Hansell. 2006. Down-selection and optimization of thermal-sprayed coatings for aluminum mould tool protection and upgrade. *Journal of Thermal Spray Technology* 15 (3): 340–347.

———. 2008. Thermal-sprayed coatings on aluminium for mould tool protection and upgrade. *Journal of Materials Processing Technology* 204: 184–191.

Gilbert, A., K. Kokini, and S. Sankarasubramanian. 2008. Thermal fracture of zirconia–mullite composite thermal barrier coatings under thermal shock: a numerical study. *Surface and Coating Technology* 203: 91–98.

Godoya, C., M.M. Lima, M.M.R. Castro, and J.C. Avelar-Batista. 2004. Structural changes in high-velocity oxy-fuel thermally sprayed WC–Co coatings for improved corrosion resistance. *Surface and Coating Technology* 188–189: 1–6.

Goller, G. 2004. The effect of bond coat on mechanical properties of plasma sprayed bioglass-titanium coatings. *Ceramics International* 30: 351–355.

Golosnoy, I.O., A. Cipitria, and T.W. Clyne. 2009. Heat transfer through plasma-sprayed thermal barrier coatings in gas turbines: a review of recent work. *Journal of Thermal Spray Technology* 18 (5–6): 809–821.

Gorlach, I.A. 2009. A new method for thermal spraying of Zn–Al coatings. *Thin Solid Films* 517: 5270–5273.

Gross, K.A., and A. Kovalevskis. 1996. Mold manufacture with plasma spraying. *Journal of Thermal Spray Technology* 5 (4): 469–475.

Gross, K.A., J. Tikkanen, J. Keskinen, V. Pitkänen, M. Eerola, R. Siikamaki, and M. Rajala. 1999. Liquid flame spraying for glass coloring. *Journal of Thermal Spray Technology* 8 (4): 583–589.

Gross, K.A., W. Walsh, and E. Swarts. 2004. Analysis of retrieved hydroxyapatite-coated hip prostheses. *Journal of Thermal Spray Technology* 13 (2): 190–199.

Gu, L., X. Chen, X. Fan, Y. Liu, B. Zou, Y. Wang, and X. Cao. 2011. Improvement of thermal shock resistance for thermal barrier coating on aluminum alloy with various electroless interlayers. *Surface and Coating Technology* 206: 29–36.

Guanhong, S., H. Xiaodong, J. Jiuxing, and S. Yue. 2011. Parametric study of Al and Al_2O_3 ceramic coatings deposited by air plasma spray onto polymer substrate. *Applied Surface Science* 257: 7864–7870.

Gui, M., S.B. Kang, and K. Euh. 2004. Al-SiC powder preparation for electronic packaging aluminum composites by plasma spray processing. *Journal of Thermal Spray Technology* 13 (2): 214–222.

Guilemany, J.M., N. Espallargas, P.H. Suegama, A.V. Benedetti, and J. Fernández. 2005. High-velocity oxyfuel Cr_3C_2-NiCr replacing hard chromium coatings. *Journal of Thermal Spray Technology* 14 (3): 335–341.

Guilemany, J.M., M. Torrell, and J.R. Miguel. 2007. Properties of HVOF coating of Ni based alloy for MSWI boilers protection. In *Thermal spray 2007: Global coating solutions*, ed. B.R. Marple, M.M. Hyland, Y.-C. Lau, C.-J. Li, R.S. Lima, and G. Montavon, 1115–1119. Materials Park: ASM International. e-Proc.

Guo, H.B., R. Vaßen, and D. Stöver. 2004. Atmospheric plasma sprayed thick thermal barrier coatings with high segmentation crack density. *Surface and Coating Technology* 186: 353–363.

Guo, H., H. Zhang, G. Ma, and S. Gong. 2009. Thermo-physical and thermal cycling properties of plasma-sprayed $BaLa_2Ti_3O_{10}$ coating as potential thermal barrier materials. *Surface and Coating Technology* 204: 691–696.

Gupta, M., N. Curry, P. Nylén, N. Markocsan, and R. Vaßen. 2012. Design of next generation thermal barrier coatings—Experiments and modeling. *Surface and Coating Technology* 220: 20–26.

Habibi, M.H., Li Wang, and S.M. Guo. 2012. Evolution of hot corrosion resistance of YSZ, $Gd_2Zr_2O_7$, and $Gd_2Zr_2O_7$ + YSZ composite thermal barrier coatings in Na_2SO_4 + V_2O_5 at 1050 °C. *Journal of the European Ceramic Society* 32: 1635–1642.

Hager, C.H., Jr., J.H. Sanders, and S. Sharma. 2008. Un-lubricated gross slip fretting wear of metallic plasma-sprayed coatings for Ti6Al4V surfaces. *Wear* 265: 439–451.

Hager, C.H., Jr., J. Sanders, S. Sharma, and A.A. Voevodin. 2009. The use of nickel graphite composite coatings for the mitigation of gross slip fretting wear on Ti6Al4V interfaces. *Wear* 267: 1470–1481.

Hahn, M., and A. Fischer. 2010. Characterization of thermal spray coatings for cylinder running surfaces of diesel engines. *Journal of Thermal Spray Technology* 19 (5): 866–872.

Hamacha, R., P. Fauchais, and E. Nardou. 1996. Influence of dopant on the behaviour under thermal cycling of two plasma sprayed zirconia coatings, Part 1: Relationship between powder characteristics and coating properties. *Journal of Thermal Spray Technology* 5 (4): 431–438.

Hamashima, K. 2007. Application of new boride cermet coating to forming of glass sheets. *Journal of Thermal Spray Technology* 16 (1): 32–33.

Han, M.-S., Y.-B. Woo, S.-C. Ko, Y.-J. Jeong, S.-K. Jang, and S.-J. Kim. 2009. Effects of thickness of Al thermal spray coating for STS 304. *Transactions of the Nonferrous Metals Society of China* 19: 925–929.

Hanneforth, P. 2006. The Global Thermal Spray Industry—100 Years of Success: So What's Next?. iTTSe, Vol 1, No 1, ASM International, Materials Park, May 2006, 14–16

Hardwicke, C.U., and Y.-C. Lau. 2013. Advances in thermal spray coatings for gas turbines and energy generation: a review. *Journal of Thermal Spray Technology* 22 (5): 564–576.

Harris, J., M. Qureshi, and O. Kesler. 2012. Deposition of composite LSCF-SDC and SSC-SDC cathodes by axial-injection plasma spraying. *Journal of Thermal Spray Technology* 21 (3–4): 461–468.

Hasan, S., and J. Stokes. 2011. Design of experiment analysis of the Sulzer Metco DJ high velocity oxy-fuel coating of hydroxyapatite for orthopedic applications. *Journal of Thermal Spray Technology* 20 (1–2): 186–194.

Haslam, J.J., J.C. Farmer, R.W. Hopper, and K.R. Wilfinger. 2005. Ceramic coatings for a corrosion-resistant nuclear waste container evaluated in simulated ground water at 90 °C. *Metallurgical and Materials Transactions A* 36A: 1085–1095.

Hawthorne, H.M., B. Arsenault, J.P. Immarigeon, J.G. Legoux, and V.R. Parameswaran. 1999. Comparison of slurry and dry erosion behavior of some HVOF thermal sprayed coatings. *Wear* 225–229: 825–834.

Haynes, J.A., M.K. Ferber, and W.D. Porter. 2000. Thermal cycling behavior of plasma-sprayed thermal barrier coatings with various MCrAIX bond coats. *Journal of Thermal Spray Technology* 9 (1): 38–48.

Hejwowski, T., and A. Weronski. 2002. The effect of thermal barrier coatings on diesel engine performance. *Vacuum* 65: 427–432.

Helali, M., and M.S.J. Hashmi. 1996. Production of free-standing objects by high velocity oxy-fuel (HVOF) thermal spraying process. *Journal of Materials Processing Technology* 56: 431–438.

Henne, R. 2007. Solid oxide fuel cells: a challenge for plasma deposition processes. *J. Thermal Spray Technology* 16 (3): 381–403.

Henne, R.H., and C. Schitter. 1995. Plasma spraying of high performance thermoplastics. In *Thermal spray science and technology*, ed. C.C. Berndt and S. Sampath, 527–532. Materials Park: ASM International.

Henne, R., M. Müller, E. Proß, G. Schiller, F. Gitzhofer, and M. Boulos. 1999. Near-net-shape forming of metallic bipolar plates for planar solid oxide fuel cells by induction plasma spraying. *Journal of Thermal Spray Technology* 8 (1): 110–116.

Herman, H., S. Sampath, R. Tiwari, and R. Neiser. 1994. Plasma spray forming of intermetallics and their composites. *Journal of Thermal Spray Technology* 3 (3): 295–296.

Hernandez, M.T., A.M. Karlsson, and M. Bartsch. 2009. On TGO creep and the initiation of a class of fatigue cracks in thermal barrier coatings. *Surface and Coating Technology* 203: 3549–3558.

Heydarzadeh, S.M., and F. Ghadami. 2010. Comparative tribological study of air plasma sprayed WC–12% coating versus conventional hard chromium electro deposit. *Tribology International* 43: 882–886.

Higuera, H.V., J. Belzunce Varela, A. Carriles Menéndez, and S. Poveda Martiınez. 2001a. High temperature erosion wear of flame and plasma-sprayed nickel–chromium coatings under simulated coal-fired boiler atmospheres. *Wear* 247: 214–222.

Higuera, H.V., F.J. Belzunce Varela, A. Carriles Menéndez, and S. Poveda Martinez. 2001b. A comparative study of high-temperature erosion wear of plasma-sprayed NiCrBSiFe and WC–NiCrBSiFe coatings under simulated coal-fired boiler conditions. *Tribology International* 34: 161–169.

Hill, H., S. Weber, U. Raab, W. Theisen, and L. Wagner. 2012. Influence of processing and heat treatment on corrosion resistance and properties of high alloyed steel coatings. *Journal of Thermal Spray Technology* 21 (5): 987–994.

Hirata, T., S. Ota, and T. Morimoto. 2003. Influence of impurities in Al_2O_3 ceramics on hot corrosion resistance against molten salt. *Journal of the European Ceramic Society* 23: 91–97.

Hitchman, L.N., and J. Knapp. 2010. Failure of thermal barrier coatings subjected to CMAS attack. *Journal of Thermal Spray Technology* 19 (1–2): 148–155.

Holcomb, G.R., S.D. Cramer, S.J. Bullard, B.S. Covino Jr., W.K. Collins, R.D. Govier, and G.E. McGill. 1997. Characterization of thermal-sprayed titanium anodes for cathodic protection. In *Thermal spray: A united forum for scientific and technological advances*, ed. C.C. Berndt, 141–150. Materials Park: ASM International.

Hospach, A., G. Mauer, R. Vaßen, and D. Stöver. 2012. Characteristics of ceramic coatings made by thin film low pressure plasma spraying (LPPS-TF). *Journal of Thermal Spray Technology* 21 (3–4): 435–440.

Houdkova, S., M. Kasparova, and F. Zahalka. 2010. The influence of spraying angle on properties of HVOF sprayed hardmetal coatings. *Journal of Thermal Spray Technology* 19 (5): 893–901.

Huang, X.O., R.J. Wang, T.J. Zhang, H.J. Luo, and Y.F. Lü. 2007. Several application cases of thermal spraying technology on industrial components and its considerations. In *Thermal spray 2007: Global coating solutions*, ed. B.R. Marple, M.M. Hyland, Y.-C. Lau, C.-J. Li, R.S. Lima, and G. Montavon. Materials Park: ASM International. e-Proc.

Hussain, T., D.G. McCartney, P.H. Shipway, and T. Marrocco. 2011. Corrosion behavior of cold sprayed titanium coatings and free standing deposits. *Journal of Thermal Spray Technology* 20 (1–2): 260–274.

Isakaev, E., A. Yablonsky, A. Kogan, V. Katarzhis, V. Kutnov, and P. Ivanov. 1999. The repair of railway frogs using plasma sprayed coatings, heat and mass transfer under plasma conditions. *Annals of the New York Academy of Sciences* 891: 231–235.

İşcan, B., and H. Aydın. 2012. Improving the usability of vegetable oils as a fuel in a low heat rejection diesel engine. *Fuel Processing Technology* 98: 59–64.

Ishikawa, K., T. Suzuki, S. Tobe, and Y. Kitamura. 2001. Resistance of thermal-sprayed duplex coating composed of aluminum and 80Ni-20Cr alloy against aqueous corrosion. *Journal of Thermal Spray Technology* 10 (3): 520–525.

Ishikawa, Y., J. Kawakita, S. Osawa, T. Itsukaichi, Y. Sakamoto, M. Takaya, and S. Kuroda. 2005. Evaluation of corrosion and wear resistance of hard cermet coatings sprayed by using an improved HVOF process. *Journal of Thermal Spray Technology* 14 (3): 384–390.

Ivosevic, M., S.L. Coguill, and S.L. Galbraith. 2009. Polymer thermal spraying: a novel coating process. In *Thermal spray 2009: Proceedings of the international thermal spray conference*, ed. B.R. Marple, M.M. Hyland, Y.-C. Lau, C.-J. Li, R.S. Lima, and G. Montavon, 1078–1083. Materials Park: ASM International.

Iyengar, R.K. 2009. *Thermal spray coating for steel processing*. Littleton: Technovations International.

Jacobs, L., M.M. Hyland, and M. De Bonte. 1999. Study of the influence of microstructural properties on the sliding-wear behavior of HVOF and HVAF sprayed WC-cermet coatings. *Journal of Thermal Spray Technology* 8 (1): 125–132.

Jang, H.-J., D.-H. Park, Y.-G. Junga, J.-C. Jang, S.-C. Choi, and U. Pai. 2006. Mechanical characterization and thermal behavior of HVOF-sprayed bond coat in thermal barrier coatings (TBCs). *Surface and Coating Technology* 200: 4355–4362.

Jansen, F., W. Xi, M.R. Dorfman, J.A. Peters, and D.R. Nagy. 2002. Performance of di-calcium silicate coatings in hot-corrosive environment. *Surface and Coating Technology* 149: 57–61.

Jarligo, M.O., D.E. Mack, R. Vaßen, and D. Stöver. 2009. Application of plasma-sprayed complex perovskites as thermal barrier coatings. *Journal of Thermal Spray Technology* 18 (2): 187–193.

Jeffery, B., M. Peppler, R.S. Lima, and A. McDonald. 2010. Bactericidal effects of HVOF-sprayed nanostructured TiO_2 on Pseudomonas aeruginosa. *Journal of Thermal Spray Technology* 19 (1–2): 344–349.

Ji, G.-C., C.-J. Li, Y.-Y. Wang, and W.-Y. Li. 2007. Erosion performance of HVOF-sprayed Cr3C2-NiCr coatings. *Journal of Thermal Spray Technology* 16 (4): 557–565.

Jiang, S.M., H.Q. Li, J. Ma, C.Z. Xu, J. Gong, and C. Sun. 2010. High temperature corrosion behavior of a gradient NiCoCrAlYSi coating II: oxidation and hot corrosion. *Corrosion Science* 52: 2316–2322.

Jin, O., S. Mall, J.H. Sanders, and S.K. Sharma. 2006. Durability of Cu–Al coating on Ti–6Al–4V substrate under fretting fatigue. *Surface and Coating Technology* 201: 1704–1710.

Johnston, R.E. 2009. The sensitivity of abradable coating residual stresses to varying material properties. *Journal of Thermal Spray Technology* 101318 (5–6): 1004–1013.

———. 2011. Mechanical characterization of AlSi-hBN, NiCrAl-Bentonite, and NiCrAl-Bentonite-hBN freestanding abradable coatings. *Surface and Coating Technology* 205: 3268–3273.

Jones, R.L. 1997. Some aspects of the hot corrosion of thermal barrier coatings. *Journal of Thermal Spray Technology* 6 (1): 77–84.

Juhasz, J.A., and S.M. Best. 2012. Bioactive ceramics: processing, structures and properties. *Journal of Materials Science* 47: 610–624.

Kang, A.S., J.S. Grewal, D. Jain, and S. Kang. 2012. Wear behavior of thermal spray coatings on rotavator blades. *Journal of Thermal Spray Technology* 21 (2): 355–359.

Karger, M., R. Vaßen, and D. Stöver. 2011. Atmospheric plasma sprayed thermal barrier coatings with high segmentation crack densities: spraying process, microstructure and thermal cycling behaviour. *Surface and Coating Technology* 206: 16–23.

Kashirin, A., O. Klyuev, T. Buzdygar, and A. Shkodkin. 2007. DYMET technology evolution and application. In *Thermal spray 2007: Global coating solutions*, ed. B.R. Marple, M.M. Hyland, Y.-C. Lau, C.-J. Li, R.S. Lima, and G. Montavon, 141–145. Materials Park: ASM International.

Kasparova, M., F. Zahalka, and S. Houdkova. 2011. WC-Co and Cr_3C_2-NiCr coatings in low- and high-stress abrasive conditions. *Journal of Thermal Spray Technology* 20 (3): 412–424.

Kaur, M., H. Singh, and S. Prakash. 2011. Surface engineering analysis of detonation-gun sprayed Cr3C2–NiCr coating under high-temperature oxidation and oxidation–erosion environments. *Surface and Coating Technology* 206: 530–541.

Kaushal, G., H. Singh, and S. Prakash. 2011. High-temperature erosion-corrosion performance of high-velocity oxy-fuel sprayed Ni-20Cr coating in actual boiler environment. *Metallurgical and Materials Transactions A* 42 (7): 1836–1846.

Kawakita, J., S. Kuroda, T. Fukushima, and T. Kodama. 2005. Improvement of corrosion resistance of high-velocity oxyfuel-sprayed stainless steel coatings by addition of molybdenum. *Journal of Thermal Spray Technology* 14 (2): 225–230.

Kembaiyan, K.T., and K. Keshavan. 1995. Combating severe fluid erosion and corrosion of drill bits using thermal spray coatings. *Wear* 186–187: 487–492.

Kenichi, S., S. Nakahama, S. Hattori, and K. Nakano. 2005. Slurry wear and cavitation erosion of thermal-sprayed cermets. *Wear* 258: 768–775.

Khan, F.F., G. Bae, K. Kang, H. Na, J. Kim, T. Jeong, and C. Lee. 2011. Evaluation of die-soldering and erosion resistance of high velocity oxy-fuel sprayed MoB-based cermet coatings. *Journal of Thermal Spray Technology* 20 (5): 1022–1034.

Khor, K.A., P. Cheang, and Y. Wang. 1997a. The thermal spray processing of HA powders and coatings. *JOM* 49: 51–57.

Khor, K.A., C.S. Yip, and P. Cheang. 1997b. Ti-6AI-4 hydroxyapatite composite coatings prepared by thermal spray techniques. *Journal of Thermal Spray Technology* 6 (1): 109–115.

Kim, K., and A.M. Korsunsky. 2011. Effects of imposed displacement and initial coating thickness on fretting behaviour of a thermally sprayed coating. *Wear* 271 (7–8): 1080–1085.

Kim, H.-J., and Y.-G. Kweon. 1996. The application of thermal sprayed coatings for pig iron ingot molds. *Journal of Thermal Spray Technology* 5 (4): 463–468.

Kim, S.-J., and S.-J. Lee. 2011. Effects of F−Si sealer on electrochemical characteristics of 15%Al−85%Zn alloy thermal spray coating. *Transactions of the Nonferrous Metals Society of China* 21: 2798–2804.

Kim, G.E., and J. Walker. 2007. Successful application of nanostructured titanium dioxide coating for high-pressure acid-leach application. *Journal of Thermal Spray Technology* 16 (1): 34–39.

Kim, H.J., Y.G. Kweon, and R.W. Chang. 1994. Wear and erosion behavior of plasma-sprayed WC-Co coatings. *Journal of Thermal Spray Technology* 3 (2): 169–178.

Kim, H.-J., S. Odoul, C.-H. Lee, and Y.-G. Kweon. 2001. The electrical insulation behavior and sealing effects of plasma-sprayed alumina-titania coatings. *Surface and Coating Technology* 140: 293–301.

Kim, D.-J., I.-H. Shin, J.-M. Koo, C.-S. Seok, and T.-W. Lee. 2010. Failure mechanisms of coin-type plasma-sprayed thermal barrier coatings with thermal fatigue. *Surface and Coating Technology* 205: S451–S458.

Koiprasert, H., S. Dumrongrattana, and P. Niranatlumpong. 2004. Thermally sprayed coatings for protection of fretting wear in land-based gas-turbine engine. *Wear* 257: 1–7.

Kokini, K., J. DeJonge, S. Rangaraj, and B. Beardsley. 2002. Thermal shock of functionally graded thermal barrier coatings with similar thermal resistance. *Surface and Coating Technology* 154: 223–231.

Koolloos, M.F.J., and J.M. Houben. 2000. Behavior of plasma-sprayed thermal barrier coatings during thermal cycling and the effect of a preoxidized NiCrAIY bond coat. *Journal of Thermal Spray Technology* 9 (1): 49–58.

Krishnamurthy, N., M.S. Murali, B. Venkataraman, and P.G. Mukunda. 2012. Characterization and solid particle erosion behavior of plasma sprayed alumina and calcia-stabilized zirconia coatings on Al-6061 substrate. *Wear* 274–275: 15–27.

Krishnan N, Vardelle A, Legoux JG (2008) A life cycle comparison of hard chrome and thermal sprayed coatings: a case example of aircraft landing gears. In: Lugscheider E (ed) Thermal spray conference: Crossing the border. DVS, Dûsseldorf, e-Proc

Kulu, P., and J. Hailing. 1998. Recycled hard metal-base wear-resistant composite coatings. *Journal of Thermal Spray Technology* 7 (2): 173–178.

Kulu, P., and T. Pihl. 2002. Selection criteria for wear resistant powder coatings under extreme erosive wear conditions. *Journal of Thermal Spray Technology* 11 (4): 517–522.

Kulu, P., L. Hussainova, and R. Veinthal. 2005. Solid particle erosion of thermal sprayed coatings. *Wear* 258: 488–496.

Kumar, A., J. Boy, R. Zatorski, and L.D. Stephenson. 2005. Thermal spray and weld repair alloys for the repair of cavitation damage in turbines and pumps: a technical note. *Journal of Thermal Spray Technology* 14 (2): 177–182.

Kwon, J.-Y., J.-H. Lee, H.-C. Kim, Y.-G. Jung, U. Paik, and K.-S. Lee. 2006. Effect of thermal fatigue on mechanical characteristics and contact damage of zirconia-based thermal barrier coatings with HVOF-sprayed bond coat. *Materials Science and Engineering A* 429: 173–180.

Laha, T., A. Agarwal, T. McKechnie, and S. Seal. 2004. Synthesis and characterization of plasma spray formed carbon nanotube reinforced aluminum composite. *Materials Science and Engineering A* 381: 249–258.

Landor, I., P. Vavrik, A. Sosna, D. Jahoda, H. Hahn, and M. Daniel. 2007. Hydroxyapatite porous coating and the osteointegration of the total hip replacement. *Archives of Orthopaedic and Traumatic Surgery* 127 (2): 81–89.

Lathabai, S., M. Ottmuller, and I. Fernandez. 1998. Solid particle erosion behaviour of thermal sprayed ceramic, metallic and polymer coatings. *Wear* 221: 93–108.

Lebedev, A.S., and S.V. Kostennikov. 2008. Trends in increasing gas-turbine units efficiency. *Thermal Engineering* 55 (6): 461–468.

Lee, C. 2009a. Market direction and application opportunities for TS growth in Korea. In *Thermal Spray-2009: Proceedings (ITSC-2009)*, ed. B.R. Marple, M.M. Hyland, Y.-C. Lau, C.-J. Li, R.S. Lima, and G. Montavon, 505–510. Materials Park: ASM International.

———. 2009b. Market direction and application opportunities for T/S growth in Korea. In *Thermal spray 2009: Proceedings of the international thermal spray conference*, ed. B.R. Marple, M.M. Hyland, Y.-C. Lau, C.-J. Li, R.S. Lima, and G. Montavon, 505–510. Materials Park: ASM International. e-Proc.

Legoux, J.-G., F. Chellat, R.S. Lima, B.R. Marple, M.N. Bureau, H. Shen, and G.A. Candeliere. 2006. Development of osteoblast colonies on new bioactive coatings. *Journal of Thermal Spray Technology* 15 (4): 628–633.

Leivo, E., T. Wilenius, T. Kinos, P. Vuoristo, and T. Mäntylä. 2004. Properties of thermally sprayed fluoropolymer PVDF, ECTFE, PFA and FEP coatings. *Progress in Organic Coating* 49: 69–73.

Lekatou, A., E. Regoutas, and A.E. Karantzalis. 2008. Corrosion behaviour of cermet-based coatings with a bond coat in 0.5 M H_2SO_4. *Corrosion Science* 50: 3389–3400.

Li, J., H. Liao, and C. Coddet. 2002. Friction and wear behavior of flame-sprayed PEEK coatings. *Wear* 252: 824–831.

Li, Y., Y. Ma, B. Xie, S. Cao, and Z. Wu. 2007. Dry friction and wear behavior of flame-sprayed polyamide1010/n-SiO_2 composite coatings. *Wear* 262: 1232–1238.

Li, W.-Y., G. Zhang, C. Zhang, O. Elkedim, H. Liao, and C. Coddet. 2008. Effect of ball milling of feedstock powder on microstructure and properties of TiN particle-reinforced Al alloy-based composites fabricated by cold spraying. *Journal of Thermal Spray Technology* 17 (3): 316–322.

Li, L., N. Hitchman, and J. Knapp. 2010a. Failure of thermal barrier coatings subjected to CMAS attack. *Journal of Thermal Spray Technology* 19 (1–2): 148–155.

Li, Y., C.-J. Li, G.-J. Yang, and L.-K. Xing. 2010b. Thermal fatigue behavior of thermal barrier coatings with the MCrAlY bond coats by cold spraying and low-pressure plasma spraying. *Surface and Coating Technology* 205: 2225–2233.

Liang, B., and C. Ding. 2005. Thermal shock resistances of nanostructured and conventional zirconia coatings deposited by atmospheric plasma spraying. *Surface and Coating Technology* 197: 185–192.

Liang, Y., Y. Xie, H. Ji, L. Huang, and X. Zheng. 2010. Chemical stability and biological properties of plasma-sprayed CaO-SiO_2-ZrO_2 coatings. *Journal of Thermal Spray Technology* 19 (6): 1171–1178.

Lima, R.S., and B.R. Marple. 2005. Superior performance of high-velocity oxyfuel-sprayed nanostructured TiO_2 in comparison to air plasma-sprayed conventional Al_2O_3-13TiO_2. *Journal of Thermal Spray Technology* 14 (3): 397–404.

———. 2007. Thermal spray coatings engineered from nanostructured ceramic agglomerated powders for structural, thermal barrier and biomedical applications: a review. *Journal of Thermal Spray Technology* 16 (1): 40–63.

Lima, M.M., C. Godoy, P.J. Modenesi, J.C. Avelar-Batista, A. Davison, and A. Matthews. 2004. Coating fracture toughness determined by Vickers indentation: an important parameter in cavitation erosion resistance of WC–Co thermally sprayed coatings. *Surface and Coating Technology* 177–178: 489–496.

Lima, R.S., H. Li, K.A. Khor, and B.R. Marple. 2006. Biocompatible nanostructured high-velocity oxyfuel sprayed titania coating: deposition, characterization, and mechanical properties. *Journal of Thermal Spray Technology* 15 (4): 623–627.

Lima, R.S., S. Dimitrievska, M.N. Bureau, B.R. Marple, A. Petit, F. Mwale, and J. Antoniou. 2010. HVOF-sprayed Nano TiO_2-HA coatings exhibiting enhanced biocompatibility. *Journal of Thermal Spray Technology* 19 (1–2): 336–343.

Lima, C.R.C., N.F.C. de Souza, and F. Camargo. 2012. Study of wear and corrosion performance of thermal sprayed engineering polymers. *Surface and Coating Technology* 220: 140–143.

Limarga, A.M., S. Widjaja, and T.H. Yip. 2005. Mechanical properties and oxidation resistance of plasma-sprayed multilayered Al_2O_3/ZrO_2 thermal barrier coatings. *Surface and Coating Technology* 197: 93–102.

Lin, K.H., Z.H. Xu, and S.T. Lin. 2011. A study on microstructure and dielectric performances of alumina/copper composites by plasma spray coating. *Journal of Materials Engineering and Performance* 20 (2): 231–237.

Lins, V.F.C., J.R.T. Branco, F.R.C. Diniz, J.C. Brogan, and C.C. Berndt. 2007. Erosion behavior of thermal sprayed, recycled polymer and ethylene–methacrylic acid composite coatings. *Wear* 262: 274–281.

Lisjak, D., M. Bégard, M. Bruehl, K. Bobzin, A. Hujanen, P. Lintunen, G. Bolelli, L. Lusvarghi, S. Ovtar, and M. Drofenik. 2011. Hexaferrite/polyester composite coatings for electromagnetic-wave absorbers. *Journal of Thermal Spray Technology* 20 (3): 638–644.

Liu, A., M. Guo, J. Gao, and M. Zhao. 2006. Influence of bond coat on shear adhesion strength of erosion and thermal resistant coating for carbon fiber reinforced thermosetting polyimide. *Surface and Coating Technology* 201: 2696–2700.

Liu, Y., Y.F. Gao, S.Y. Tao, X.M. Zhou, W.D. Li, H.J. Luo, and C.X. Ding. 2008. Microstructure of plasma sprayed La_2O_3-modified YSZ coatings. *Journal of Thermal Spray Technology* 17 (5–6): 603–607.

Longo, F.N. 1992. Industrial guide–markets, materials, and applications for thermal-sprayed coatings. *Journal of Thermal Spray Technology* 1 (2): 143–145.

Lu, Y.-P., M.-S. Li, S.-T. Li, Z.-G. Wang, and R.-F. Zhu. 2004. Plasma-sprayed hydroxyapatite-titania composite bond coat for hydroxyapatite coating on titanium substrate. *Biomaterials* 25: 4393–4403.

Lu, W., Y. Wu, J. Zhang, S. Hong, J. Zhang, and G. Li. 2011. Microstructure and corrosion resistance of plasma sprayed Fe-based alloy coating as an alternative to hard chromium. *Journal of Thermal Spray Technology* 20 (5): 1063–1070.

Luo, L., S. Liu, J. Li, and Y. Wu. 2011. Thermal shock resistance of FeMnCrAl/Cr3C2–Ni9Al coatings deposited by high velocity arc spraying. *Surface and Coating Technology* 205: 3467–3471.

Ma, X., and A. Matthews. 2007. Investigation of abradable seal coating performance using scratch testing. *Surface and Coating Technology* 202: 1214–1220.

———. 2009. Evaluation of abradable seal coating mechanical properties. *Wear* 267: 1501–1510.

Ma, W., M.O. Jarligo, D.E. Mack, D. Pitzer, J. Malzbender, R. Vaßen, and D. Stöver. 2008. New generation perovskite thermal barrier coating materials. *Journal of Thermal Spray Technology* 17 (5–6): 831–837.

Ma, B., Y. Li, and K. Su. 2009. Characterization of ceria–yttria stabilized zirconia plasma-sprayed coatings. *Applied Surface Science* 255: 7234–7237.

MAGETEX. n.d. Thermal coatings in Europe: a business prospective. MAGETEX, Les bureaux de Sèvres, 2 rue Troyon, 92316 Sèvres.

Markocsan, N., P. Nylén, J. Wigren, and X.-H. Li. 2007. Low thermal conductivity coatings for gas turbine applications. *Journal of Thermal Spray Technology* 16 (4): 498–505.

Markocsan, N., P. Nylén, J. Wigren, X.-H. Li, and A. Tricoire. 2009. Effect of thermal aging on microstructure and functional properties of zirconia-base thermal barrier coatings. *Journal of Thermal Spray Technology* 18 (2): 201–208.

Marx, S., A. Paul, A. Köhler, and G. Hüttl. 2006. Cold spraying: innovative layers for new applications. *Journal of Thermal Spray Technology* 15 (2): 177–183.

Mary, C., S. Fouvry, J.M. Martin, and B. Bonnet. 2011. Pressure and temperature effects on Fretting Wear damage of a Cu–Ni–In plasma coating versus Ti17 titanium alloy contact. *Wear* 272: 18–37.

Matejıcek, J., P. Chraska, and J. Linke. 2007. Thermal spray coatings for fusion applications—review. *Journal of Thermal Spray Technology* 16 (1): 64–83.

Matsubara, Y., Y. Sochi, M. Tanabe, and A. Takeya. 2007. Advanced coatings on furnace wall tubes. *Journal of Thermal Spray Technology* 16 (2): 195–201.

Matthäus, G., J. Henry, and D. Ackermann. 2009. Further developments in internal diameter HVOF application of WC-CoCr for hard chrome replacement in critical applications such as landing gear. In *Thermal spray 2009: Proceedings of the international thermal spray conference*, ed. B.R. Marple, M.M. Hyland, Y.-C. Lau, C.-J. Li, R.S. Lima, and G. Montavon, 722–724. Materials Park: ASM International.

Mei, H., Y. Liu, L. Cheng, and L. Zhang. 2012. Corrosion mechanism of a NiCoCrAlTaY coated Mar-M247 superalloy in molten salt vapor. *Corrosion Science* 55: 201–204.

Meng, H. 2010. The performance of different WC-based cermet coatings in oil and gas applications–A comparison. In *ITSC 2010 Thermal spray: Global solutions, future applications*. Düsseldorf: DVS. e-Proc.

Michaux, P., G. Montavon, A. Grimaud, A. Denoirjean, and P. Fauchais. 2010. Elaboration of porous NiO/8YSZ layers by several SPS and SPPS routes. *Journal of Thermal Spray Technology* 19 (1–2): 317–327.

Miller, R.A. 1997. Thermal barrier coatings for aircraft engines: history and directions. *Journal of Thermal Spray Technology* 6 (1): 35–42.

Mizuno, H., and J. Kitamura. 2007. MoB/CoCr cermet coatings by HVOF spraying against erosion by molten Al-Zn alloy. *Journal of Thermal Spray Technology* 16 (3): 404–413.

Mohan, P., T. Patterson, B. Yao, and Y. Sohn. 2010. Degradation of thermal barrier coatings by fuel impurities and CMAS: thermochemical interactions and mitigation approaches. *Journal of Thermal Spray Technology* 19 (1–2): 156–167.

Molz, R., and D. Hawley. 2007. A method of evaluating thermal spray process performance. In *Thermal spray 2007: Global coating solutions*, ed. B.R. Marple, M.M. Hyland, Y.-C. Lau, C.-J. Li, R.S. Lima, and G. Montavon. Materials Park: ASM International. e-Proc.

Morks, M.F., and A. Kobayashi. 2008. Development of ZrO_2/SiO_2 bioinert ceramic coatings for biomedical application. *Journal of the Mechanical Behavior of Biomedical Materials* 1: 165–171.

Moskowitz, L.N. 1993. Application of HVOF thermal spraying to solve corrosion problems in the petroleum industry—an industrial note. *Journal of Thermal Spray Technology* 2 (1): 21–29.

Muehlberger, E., and P. Meyer. 2009. LPPS – thin film processes: overview of origin and future possibilities. In *Thermal spray 2009: Proceedings of the international thermal spray conference*, ed. B.R. Marple, M.M. Hyland, Y.-C. Lau, C.-J. Li, R.S. Lima, and G. Montavon, 737–740. Materials Park: ASM International.

Murakami, K., and M. Shimada. 2009. Development of thermal spray coatings with corrosion protection and antifouling properties. In *Thermal spray 2009: Proceedings of the international thermal spray conference*, ed. B.R. Marple, M.M. Hyland, Y.-C. Lau, C.-J. Li, R.S. Lima, and G. Montavon, 1041–1044. Materials Park: ASM International.

Musil, J., M. Alaya, and R. Oberacker. 1997. Plasma-sprayed duplex and graded partially stabilized zirconia thermal barrier coatings: deposition process and properties. *Journal of Thermal Spray Technology* 6 (4): 449–455.

Mutasim, Z., and W. Brentnall. 1997. Thermal barrier coatings for industrial gas turbine applications: an industrial note. *Journal of Thermal Spray Technology* 6 (1): 105–108.

Nagai, M., S. Shigemura, and A. Yoshiya. 2009. Thermal-sprayed CFRP roll with resistant to thermal shock and wear - for papermaking machine. In *Thermal spray 2009: Proceedings of the international thermal spray conference*, ed. B.R. Marple, M.M. Hyland, Y.-C. Lau, C.-J. Li, R.S. Lima, and G. Montavon, 607–611. Materials Park: ASM International.

Nakahira, A. 2009a. Current status and future prospect of thermal spray coating applications and coating service market of job shops in Japan. In *Proceedings (ITSC-2009) Conference*, ed. B.R. Marple, M.M. Hyland, Y.-C. Lau, C.-J. Li, R.S. Lima, and G. Montavon, 499–504. Materials Park: ASM International.

———. 2009b. Current status and future prospect of thermal spray coating applications and coating service market of job shops in Japan. In *Thermal spray 2009: Proceedings of the international thermal spray conference*, ed. B.R. Marple, M.M. Hyland, Y.-C. Lau, C.-J. Li, R.S. Lima, and G. Montavon, 499–504. Materials Park: ASM International. e-Proc.

Nelson, W.A., and R.M. Orenstein. 1997. Land based gas turbines TBC experience in land-based gas turbines. *Journal of Thermal Spray Technology* 6 (2): 176–180.

Nelson, G.M., J.A. Nychka, and A.G. McDonald. 2011. Flame spray deposition of titanium alloy-bioactive glass composite coatings. *Journal of Thermal Spray Technology* 20 (6): 1339–1351.

Neufuss, K., P. Chráska, B. Kolman, S. Sampath, and Z. Trávnícek. 1997. Properties of plasma-sprayed freestanding ceramic parts. *Journal of Thermal Spray Technology* 6 (4): 434–438.

Niebuhr, D., and M. Scholl. 2005. Synthesis and performance of plasma-sprayed polymer/steel coating system. *Journal of Thermal Spray Technology* 14 (4): 487–494.

Ong, J.L., M. Appleford, S. Oh, Y. Yang, W.-H. Chen, et al. 2006. The characterization and development of bioactive hydroxyapatite coatings. *JOM* 58 (7): 67–69.

Osawa, S., T. Itsukaichi, and R. Ahmed. 2005. Influence of substrate properties on the impact resistance of WC cermet coatings. *Journal of Thermal Spray Technology* 14 (4): 495–501.

Ouyang, J.H., S. Sasaki, and K. Umeda. 2001. Microstructure and tribological properties of low-pressure plasma-sprayed ZrO_2–CaF_2–Ag_2O composite coating at elevated temperature. *Wear* 249: 440–451.

Pacheo da Silva, C., et al. 1991. *2nd Plasma Technik Symposium 1*, 363–373. Wohlen: Plasma Technik.

Pan, Z.Y., Y. Wang, C.H. Wang, X.G. Sun, and L. Wang. 2012. The effect of SiC particles on thermal shock behavior of Al2O3/8YSZ coatings fabricated by atmospheric plasma spraying. *Surface and Coating Technology* 206: 2484–2498.

Pantelis, D.I., P. Psyllaki, and N. Alexopoulos. 2000. Tribological behavior of plasma-sprayed Al_2O_3 coatings under severe wear conditions. *Wear* 237: 197–204.

Pardo, A., M.C. Merino, M. Mohedano, P. Casajús, A.E. Coy, and R. Arrabal. 2009. Corrosion behaviour of Mg/Al alloys with composite coatings. *Surface and Coating Technology* 203: 1252–1263.

Parks, W.P., E.E. Hoffman, W.Y. Lee, and I.G. Wright. 1997. Thermal barrier coatings issues in advanced land-based gas turbines. *Journal of Thermal Spray Technology* 6 (2): 187–192.

Parlak, A., H. Yasar, and O. Eldogan. 2005. The effect of thermal barrier coating on a turbo-charged diesel engine performance and exergy potential of the exhaust gas. *Energy Conversion and Management* 46: 489–499.

Patel, R.R., A.K. Keshri, G.S. Dulikravich, and A. Agarwal. 2010. An experimental and computational methodology for near net shape fabrication of thin walled ceramic structures by plasma spray forming. *Journal of Materials Processing Technology* 210: 1260–1269.

Pattison, J., S. Celotto, R. Morgan, M. Bray, and W. O'Neill. 2007. Cold gas dynamic manufacturing: a non-thermal approach to freeform fabrication. *International Journal of Machine Tools and Manufacture* 47: 627–634.

Paul, S., A. Cipitria, I.O. Golosnoy, L. Xie, M.R. Dorfman, and T.W. Clyne. 2007. Effects of impurity content on the sintering characteristics of plasma-sprayed zirconia. *Journal of Thermal Spray Technology* 16 (5–6): 798–803.

Pawlowski, L. 1995. *The science and engineering of thermal spray coatings*. New York: Wiley.

———. 1996. Technology of thermally sprayed anilox rolls: state of art, problems, and perspectives. *Journal of Thermal Spray Technology* 5 (3): 317–334.

Petrovicova, E., and L.S. Schadler. 2002. Thermal spraying of polymers. *International Materials Review* 47 (4): 169–190.

Picas, J.A., A. Forna, and G. Matthäus. 2006. HVOF coatings as an alternative to hard chrome for pistons and valves. *Wear* 261: 477–484.

Pint, B.A., I.G. Wright, and W.J. Brindley. 2000. Evaluation of thermal barrier coating systems on novel substrates. *Journal of Thermal Spray Technology* 9 (2): 198–203.

Pint, B.A., J.A. Haynes, and Y. Zhang. 2010. Effect of superalloy substrate and bond coating on TBC lifetime. *Surface and Coating Technology* 205: 1236–1240.

Pokhmurska, H., B. Wielage, T. Lampke, T. Grund, M. Student, and N. Chervinska. 2008. Post-treatment of thermal spray coatings on magnesium. *Surface and Coating Technology* 202: 4515–4524.

Pomeroy, M.J. 2005. Coatings for gas turbine materials and long-term stability issues. *Materials and Design* 26: 223–231.

Pratap Singh, V., A. Sil, and R. Jayaganthan. 2011. Tribological behavior of plasma sprayed Cr_2O_3–3%TiO_2 coatings. *Wear* 272: 149–158.

Prevéy, P.S. 2000. X-ray diffraction characterization of crystallinity and phase composition in plasma-sprayed hydroxyapatite coatings. *Journal of Thermal Spray Technology* 9 (3): 369–376.

Process Industries: Power, http://www.castolin.com

Prudenziati, M., G. Cirri, and P. Dal Bo. 2006. Novel high-temperature reliable heaters in plasma spray technology. *Journal of Thermal Spray Technology* 15 (3): 329–331.

Puranen, J., J. Lagerbom, L. Hyvärinen, M. Kylmälahti, O. Himanen, M. Pihlatie, J. Kiviaho, and P. Vuoristo. 2011. The structure and properties of plasma sprayed iron oxide doped manganese cobalt oxide spinel coatings for SOFC metallic interconnectors. *Journal of Thermal Spray Technology* 20 (1–2): 154–159.

Qiao, Y., Y.-R. Liu, and T.E. Fischer. 2001. Sliding and abrasive wear resistance of thermal-sprayed WC-CO coatings. *Journal of Thermal Spray Technology* 10 (1): 118–125.

Rajendran, R. 2012. Gas turbine coatings – an overview. *Engineering Failure Analysis* 26: 355–369.

Ramachandran, C.S., V. Balasubramanian, P.V. Ananthapadmanabhan, and V. Viswabaskaran. 2012. Understanding the dry sliding wear behaviour of atmospheric plasma-sprayed rare earth oxide coatings. *Materials and Design* 39: 234–252.

Ramesh, M.R., S. Prakash, S.K. Nath, Pawan Kumar Sapra, and N. Krishnamurthy. 2011. Evaluation of thermocyclic oxidation behavior of HVOF-sprayed NiCrFeSiB coatings on boiler tube steels. *Journal of Thermal Spray Technology* 20 (5): 992–1000.

Ramesha, C.S., D.S. Devaraja, R. Keshavamurthya, and B.R. Sridharb. 2011. Slurry erosive wear behavior of thermally sprayed Inconel-718 coatings by APS process. *Wear* 271: 1365–1371.

Richer, P., M. Yandouzi, L. Beauvais, and B. Jodoin. 2010. Oxidation behaviour of CoNiCrAlY bond coats produced by plasma, HVOF and cold gas dynamic spraying. *Surface and Coating Technology* 204: 3962–3974.

Rieger, G., J. Wecker, W. Rodewald, W. Sattler, F.W. Bach, T. Duda, and W. Unterberg. 2000. Nd-Fe-B permanent magnets (thick films) produced by a vacuum-plasma-spraying process. *Journal of Applied Physics* 87 (9): 5329–533

Rodriguez, J., A. Martin, R. Fernández, and J.E. Fernández. 2003. An experimental study of the wear performance of NiCrBSi thermal spray coatings. *Wear* 255: 950–955.

Roy, M., A. Bandyopadhyay, and S. Bose. 2011. Induction plasma sprayed nano hydroxyapatite coatings on titanium for orthopaedic and dental implants. *Surface and Coating Technology* 205: 2785–2792.

Sacriste, D., N. Goubot, J. Dhers, M. Ducos, and A. Vardelle. 2001. An evaluation of the electric arc spray and (HPPS) processes for the manufacturing of high power plasma spraying MCrAlY coatings. *Journal of Thermal Spray Technology* 10 (2): 352–358.

Saeidi, S., K.T. Voisey, and D.G. McCartney. 2009. The effect of heat treatment on the oxidation behavior of HVOF and VPS CoNiCrAlY coatings. *Journal of Thermal Spray Technology* 18 (2): 209–216.

Sahraoui, T., N.-E. Fenineche, G. Montavon, and C. Coddet. 2004. Alternative to chromium: characteristics and wear behavior of HVOF coatings for gas turbine shafts repair (heavy-duty). *Journal of Materials Processing Technology* 152: 43–55.

Sakata, K., K. Nakano, H. Miyahara, Y. Matsubara, and K. Ogi. 2007. Microstructure control of thermally sprayed Co-based self-fluxing alloy coatings by diffusion treatment. *Journal of Thermal Spray Technology* 16 (5–6): 991–997.

Sampath, S. 2010. Thermal spray applications in electronics and sensors: past, present, and future. *Journal of Thermal Spray Technology* 19 (5): 921–949.

Sanchez, E., E. Bannier, V. Cantavella, M.D. Salvador, E. Klyatskina, J. Morgiel, J. Grzonka, and A.R. Boccaccini. 2008. Deposition of Al_2O_3-TiO_2 nanostructured powders by atmospheric plasma spraying. *Journal of Thermal Spray Technology* 17 (3): 329–337.

Sanpo, N., M. Lu Tan, P. Cheang, and K.A. Khor. 2009a. Antibacterial property of cold-sprayed HA-Ag/PEEK coating. *Journal of Thermal Spray Technology* 18 (1): 10–15.

Sanpo, N., S. Ming Ang, P. Cheang, and K.A. Khor. 2009b. Antibacterial property of cold sprayed chitosan-Cu/Al coating. *Journal Thermal Spray Technology* 18 (4): 600–608.

Santa, J.F., L.A. Espitia, J.A. Blanco, S.A. Romo, and A. Toro. 2009. Slurry and cavitation erosion resistance of thermal spray coatings. *Wear* 267: 160–167.

Sanz, A. 2001. Tribological behavior of coatings for continuous casting of steel. *Surface and Coating Technology* 146–147: 55–64.

Sathish, S., M. Geetha, S.T. Aruna, N. Balaji, K.S. Rajam, and R. Asokamani. 2011. Sliding wear behavior of plasma sprayed nanoceramic coatings for biomedical applications. *Wear* 271: 934–941.

Savarimuthu, A.C., H.F. Taber, I. Megat, J.R. Shadley, E.F. Rybicki, W.C. Cornell, W.A. Emery, D.A. Somerville, and J.D. Nuse. 2001. Sliding wear behavior of tungsten carbide thermal spray coatings for replacement of chromium electroplate in aircraft applications. *Journal of Thermal Spray Technology* 10 (3): 502–510.

Schilke, P.W. 2004. *Advanced Gas Turbine Materials and Coatings*. GER-3569G, General Electric Company, August. 2004.

Schmidt, D.P., B.A. Shaw, E. Sikora, W.W. Shaw, and L.H. Laliberte. 2006. Corrosion protection assessment of sacrificial coating systems as a function of exposure time in a marine environment. *Progress in Organic Coating* 57: 352–364.

Schulz, U., O. Bernardi, A. Ebach-Stahl, R. Vaßen, and D. Sebold. 2008a. Improvement of EB-PVD thermal barrier coatings by treatments of a vacuum plasma-sprayed bond coat. *Surface and Coating Technology* 203: 160–170.

Schulz, U., K. Fritscher, and A. Ebach-Stahl. 2008b. Cyclic behavior of EB-PVD thermal barrier coating systems with modified bond coats. *Surface and Coating Technology* 203: 449–455.

Schwetzke, R., and H. Kreye. 1999. Microstructure and properties of tungsten carbide coatings sprayed with various high-velocity oxygen fuel spray systems. *Journal of Thermal Spray Technology* 8 (3): 433–439.

Seonga, B.G., S.Y. Hwanga, M.C. Kima, and K.Y. Kimb. 2001. Reaction of WC-Co coating with molten zinc in a zinc pot of a continuous galvanizing line. *Surface and Coating Technology* 138: 101–110.

Shen, Y., V. Alexandra, B. Almeida, and François Gitzhofer. 2011. Preparation of nanocomposite GDC/LSCF cathode material for IT-SOFC by induction plasma spraying. *Journal of Thermal Spray Technology* 20 (1–2): 145–153.

Shi, S., and J.-Y. Hwang. 2003. Plasma spray fabrication of near-net-shape ceramic objects. *Journal of Minerals and Materials Characterization and Engineering* 2 (2): 145–150.

Shin, I.-H., J.-M. Koo, C.-S. Seok, S.-H. Yang, T.-W. Lee, and B.-S. Kim. 2011. Estimation of spallation life of thermal barrier coating of gas turbine blade by thermal fatigue test. *Surface and Coating Technology* 205: S157–S160.

Sidhu, B.S., and S. Prakash. 2006. Erosion-corrosion of plasma as sprayed and laser remelted Stellite-6 coatings in a coal fired boiler. *Wear* 260: 1035–1044.

Sidhu, T.S., S. Prakash, and R.D. Agrawal. 2005. Studies on the properties of high-velocity oxy-fuel thermal spray coatings for higher temperature applications. *Materials Science* 41 (6): 805–823.

———. 2006a. Hot corrosion resistance of high-velocity oxyfuel sprayed coatings on a nickel-base superalloy in molten salt environment. *Journal of Thermal Spray Technology* 15 (3): 387–399.

Sidhu, H.S., B.S. Sidhu, and S. Prakash. 2006b. Comparative characteristic and erosion behavior of NiCr coatings deposited by various high-velocity oxyfuel spray processes. *Journal of Materials Engineering and Performance* 5 (6): 699–704.

Sidhu, T.S., A. Malik, S. Prakash, and R.D. Agrawal. 2007. Oxidation and hot corrosion resistance of HVOF WC-NiCrFeSiB coating on Ni- and Fe-based superalloys at 800 °C. *Journal of Thermal Spray Technology* 16 (5–6): 844–849.

Singh, H., D. Puri, S. Prakash, and V.V. Rama Rao. 2006. On the high-temperature oxidation protection behavior of plasma-sprayed stellite-6 coatings. *Metallurgical and Materials Transactions A* 37A: 3048–3056.

Singh, H., A. Ang, S. Matthews, H. DeVilliers-Lovelock, and B. Singh Sidu. 2019. Thermal spray for extreme environments, editorial. *Journal of Thermal Spray Technology* 28: 1339–1345.

Skandan, G., R. Yao, R. Sadangi, B.H. Kear, Y. Qiao, L. Liu, and T.E. Fischer. 2000. Multimodal coatings: a new concept in thermal spraying. *Journal of Thermal Spray Technology* 9 (3): 329–331.

Smyth, R.T., and J.C. Anderson. 1975. Production of resistors by arc plasma spraying. *Electrocomponent Science and Technology* 2: 135–145.

Sobolev, V.V., J.M. Guilemany, and J. Nutting. 2004. *High velocity oxy-fuel spraying*. London: Maney for the Institute of Materials, Minerals and Mining.

Soechting, F.O. 1999. A design perspective on thermal barrier coatings. *Journal of Thermal Spray Technology* 8 (4): 505–511.

Song, J.X., Y.F. Han, S.S. Li, and C.B. Xiao. 2005. Repair of NiCrAlYSi overlay coating on Ni3Al base alloy IC6. *Intermetallics* 13: 351–355.

Sørensen, P.A., S. Kiil, K. Dam-Johansen, and C.E. Weinell. 2009. Anticorrosive coatings: a review. *Journal of Coating Technology and Research* 6 (2): 135–176.

Souza, V.A.D., and A. Neville. 2007. Aspects of microstructure on the synergy and overall material loss of thermal spray coatings in erosion–corrosion environments. *Wear* 263: 339–346.

Sporer, D., M. Dorfman, L. Xie, A. Refke, I. Giovannetti, and M. Giannozzi. 2007. Processing and properties of advanced ceramic abradable coatings. In *Thermal spray 2007: Global coating solutions*, ed. M.R. Marple, M.M. Hyland, Y.-C. Lau, C.-J. Li, R.S. Lima, and G. Montavon, 495–500. Materials Park: ASM International.

Staia, M.H., M. Suárez, D. Chicot, J. Lesage, A. Iost, and E.S. Puchi-Cabrera. 2012. Cr_2C_3–NiCr VPS thermal spray coatings as candidate for chromium replacement. *Surface and Coating Technology* 220: 225–231.

Steinke, T., G. Mauer, R. Vaßen, D. Stöver, D. Roth-Fagaraseanu, and M. Hancock. 2010. Process design and monitoring for plasma sprayed abradable coatings. *Journal of Thermal Spray Technology* 19 (4): 756–764.

Stewart, S., and R. Ahmed. 2002. Rolling contact fatigue of surface coatings—A review. *Wear* 253: 1132–1144.

Stoica, V., R. Ahmed, M. Golshan, and S. Tobe. 2004. Sliding wear evaluation of hot isostatically pressed thermal spray cermet coatings. *Journal of Thermal Spray Technology* 13 (1): 93–107.

Stoica, V., R. Ahmed, and T. Itsukaichi. 2005. Influence of heat-treatment on the sliding wear of thermal spray cermet coatings. *Surface and Coating Technology* 199: 7–21.

Stringer, J., and M.B. Marshall. 2012. High speed wear testing of an abradable coating. *Wear* 294–295: 257–263.

Sun, F., N. Zhang, H. Liao, and J. Li. 2012. Effect of heat treatment temperature on performance of plasma-sprayed apatite-lanthanum silicate coatings as electrolytes for IT-SOFC. *Journal of Thermal Spray Technology* 21 (6): 1257–1267.

Sundararajan, G., Y.R. Mahajan, and S.V. Joshi. 2009a. Thermal Spraying in India: Status and Prospects. In *Proceedings (ITSC-2009)*, ed. B.R. Marple, M.M. Hyland, Y.-C. Lau, C.-J. Li, R.S. Lima, and G. Montavon, 511–516. Materials Park: ASM International.

———. 2009b. Thermal spraying in India: status and prospects. In *Thermal spray 2009: Proceedings of the international thermal spray conference*, ed. B.R. Marple, M.M. Hyland, Y.-C. Lau, C.-J.

Li, R.S. Lima, and G. Montavon, 511–516. Materials Park: ASM International.

Sweet, G.K. 1993. Applying thermoplastic/thermoset powder with a modified plasma system. In *Proceedings of the 1993 national thermal spray conference*, ed. C.C. Berndt and F. Bernicki, 381–384. Materials Park: ASM International.

Takenoiri, S., N. Kadokawa, and K. Koseki. 2000. Development of metallic substrate supported planar solid oxide fuel cells fabricated by atmospheric plasma spraying. *Journal of Thermal Spray Technology* 3639 (3): 360–363.

Tamura, M., M. Takahashi, J. Ishii, K. Suzuki, M. Sato, and K. Shimomur. 1999. Multilayered thermal barrier coating for land-based gas turbines. *Journal of Thermal Spray Technology* 8 (1): 68–72.

Tan, Y., V. Srinivasan, T. Nakamura, S. Sampath, P. Bertrand, and G. Bertrand. 2012. TBC optimizing compliance and thermal conductivity of plasma sprayed thermal barrier coatings via controlled powders and processing strategies. *Journal of Thermal Spray Technology* 21 (5): 950–962.

Tang, F., and J.M. Schoenung. 2005. Local accumulation of thermally grown oxide in plasma-sprayed thermal barrier coatings with rough top-coat/bond-coat interfaces. *Scripta Materialia* 52: 905–909.

Tani, K., and Y. Harada. 2007. Enhancement of service life of steam generating tubes in oil-fired boiler for power generation employing plasma spray technology. *Journal of Thermal Spray Technology* 16 (1): 111–117.

Tani, K., and H. Nakahira. 1992. Status of thermal spray technology in Japan. *Journal of Thermal Spray Technology* 1 (4): 333–339.

Tao, K., X.-L. Zhou, H. Cui, and J.-S. Zhang. 2009. Oxidation and hot corrosion behaviors of HVAF-sprayed conventional and nanostructured NiCrC coatings. *Transactions of the Nonferrous Metals Society of China* 19: 1151–1160.

Tao, S., Z. Yin, X. Zhou, and C. Ding. 2010. Sliding wear characteristics of plasma-sprayed Al_2O_3 and Cr_2O_3 coatings against copper alloy under severe conditions. *Tribology International* 43: 69–75.

Tapphorn, R., J. Henness, and H. Gabel. 2009. Kinetic metallization-a repair process for damaged IVD-Al coatings, Mg, and Al alloy components. In *Thermal spray 2009: Proceedings of the international thermal spray conference*, ed. B.R. Marple, M.M. Hyland, Y.-C. Lau, C.-J. Li, R.S. Lima, and G. Montavon, 261–266. Materials Park: ASM International.

Thintri Inc. 2013. Thermal spray wear coatings find growing markets and greater competition. *Spraytime* 20 (1): 1–36.

Tian, W., Y. Wang, and Y. Yang. 2008. Fretting wear behavior of conventional and nanostructured Al2O3–13 wt%TiO2 coatings fabricated by plasma spray. *Wear* 265: 1700–1707.

Tillmann, W., E. Vogli, I. Baumann, G. Kopp, and C. Weihs. 2010. Desirability-based multi-criteria optimization of HVOF spray experiments to manufacture fine structured wear-resistant $75Cr_3C_2$-25(NiCr20) coatings. *Journal of Thermal Spray Technology* 19 (1–2): 393–408.

Toma, F.-L., S. Scheitz, L.-M. Berger, V. Sauchuk, M. Kusnezoff, and S. Thiele. 2011. Comparative study of the electrical properties and characteristics of thermally sprayed alumina and spinel coatings. *Journal of Thermal Spray Technology* 20 (1–2): 195–204.

Toma, F.-L., L.-M. Berger, S. Scheitz, S. Langner, C. Rödel, A. Potthoff, V. Sauchuk, and M. Kusnezoff. 2012. Comparison of the microstructural characteristics and electrical properties of thermally sprayed Al_2O_3 coatings from aqueous suspensions and feedstock powders. *Journal of Thermal Spray Technology* 21 (3–4): 480–488.

Toscano, J., R. Vaβen, A. Gil, M. Subanovic, D. Naumenko, L. Singheiser, and W.J. Quadakkers. 2006. Parameters affecting TGO growth and adherence on MCrAlY-bond coats for TBC's. *Surface and Coating Technology* 201: 3906–3910.

Tucker, R.C., ed. 2013. *ASM handbook, Vol 5A: Thermal spray technology*. Materials Park: ASM International.

Tuominen, J., P. Vuoristo, T. Mäntylä, M. Kylmälahti, J. Vihinen, et al. 2000. Improving corrosion properties of high-velocity oxy-fuel sprayed inconel 625 by using a high-power continuous wave neodymium-doped yttrium aluminum garnet laser. *Journal of Thermal Spray Technology* 9 (4): 513–519.

Uozato, S., K. Nakata, and M. Ushio. 2003. Corrosion and wear behaviors of ferrous powder thermal spray coatings on aluminum alloy. *Surface and Coating Technology* 169–170: 691–694.

Uusitalo, M.A., P.M.J. Vuoristo, and T.A. Mäntylä. 2002. Elevated temperature erosion–corrosion coatings in chlorine containing environments of thermal sprayed. *Wear* 252: 586–594.

Valarezo, A. 2012. Latin America: An Emerging and Growing Market for Thermal Spray. In *Proceedings (ITSC-2012), Conference Houston, TX, 2012*

Valarezo, A., G. Bolelli, W.B. Choi, S. Sampath, V. Cannillo, L. Lusvarghi, and R. Rosa. 2010. Damage tolerant functionally graded WC–Co/stainless steel HVOF coatings. *Surface and Coating Technology* 205: 2197–2208.

Vaßen, R., S. Giesen, and D. Stöver. 2009a. Lifetime of plasma-sprayed thermal barrier coatings: comparison of numerical and experimental results. *Journal of Thermal Spray Technology* 18 (5–6): 835–845.

Vaßen, R., A. Stuke, and D. Stöver. 2009b. Recent developments in the field of thermal barrier coatings. *Journal of Thermal Spray Technology* 18 (2): 181–186.

Vaßen, R., M.O. Jarligo, T. Steinke, D.E. Mack, and D. Stöver. 2010. Overview on advanced thermal barrier coatings. *Surface and Coating Technology* 205: 938–942.

Venkateswarlu, K., V. Rajinikanth, T. Naveen, and Dhiraj Prasad Sinha. 2009. Abrasive wear behavior of thermally sprayed diamond reinforced composite coating deposited with both oxy-acetylene and HVOF techniques. *Wear* 266: 995–1002.

Vetter, J., G. Barbezat, J. Crummenauer, and J. Avissar. 2005. Surface treatment selections for automotive applications. *Surface and Coating Technology* 200: 1962–1968.

Vitale-Brovarone, C., and E. Verné. 2005. SiO_2-CaO-K_2O coatings on alumina and Ti6Al4V substrates for biomedical applications. *Journal of Materials Science. Materials in Medicine* 16: 863–871.

von Niessen, K., M. Gindrat, and A. Refke. 2010. Vapor phase deposition using plasma spray-PVD™. *Journal of Thermal Spray Technology* 19 (1–2): 502–509.

Voyer, J., P. Schulz, and M. Schreiber. 2008. Electrically conductive flame sprayed aluminum coatings on textile substrates. *Journal of Thermal Spray Technology* 17 (5–6): 818–823.

Vuoristo, P., and P. Nylén. 2009. Industrial and research activities in thermal spray technology in the Nordic region of Europe. In *Thermal spray 2009: Proceedings of the international thermal spray conference*, ed. B.R. Marple, M.M. Hyland, Y.-C. Lau, C.-J. Li, R.S. Lima, and G. Montavon, 517–522. Materials Park: ASM International. e-Proc.

Waki, H., T. Kitamura, and A. Kobayashi. 2009. Effect of thermal treatment on high-temperature mechanical properties enhancement in LPPS, HVOF, and APS CoNiCrAlY coatings. *Journal of Thermal Spray Technology* 18 (4): 500–509.

Wang, B. 1996. Erosion-corrosion of thermal sprayed coatings in FBC boilers. *Wear* 199: 24–32.

Wang, B.Q., and K. Luer. 1994. The erosion-oxidation behavior of HVOF Cr_3C_2-NiCr cermet coating. *Wear* 174: 177–185.

Wang, B.-Q., and A. Verstak. 1999. Elevated temperature erosion of HVOF Cr_3C_2/TiC– NiCrMo cermet coating. *Wear* 233–235: 342–351.

Wang, Y., K.A. Khor, and P. Cheang. 1998. Thermal spraying of functionally graded calcium phosphate coatings for biomedical implants. *Journal of Thermal Spray Technology* 7 (1): 50–57.

Wang, Y., J.-G. Legoux, R. Neagu, S. Hui, and B.R. Marple. 2012. Suspension plasma spray and performance characterization of half cells with NiO/YSZ anode and YSZ electrolyte. *Journal of Thermal Spray Technology* 21 (1): 7–15.

Weiss, L.E., F.B. Prinz, D.A. Adams, and D.P. Siewiorek. 1992. Thermal spray shape deposition. *Journal of Thermal Spray Technology* 1 (3): 231–237.

Weiss, L.E., D.G. Thuel, L. Schultz, and F.B. Prinz. 1994. Arc-sprayed steel-faced tooling. *Journal of Thermal Spray Technology* 3 (3): 275–281.

Wigren, J., and Kristina Täng. 2007. Quality considerations for the evaluation of thermal spray coatings. *Journal of Thermal Spray Technology* 16 (4): 533–540.

Wright, I.G., and T.B. Gibbons. 2007. Recent developments in gas turbine materials and technology and their implications for syngas firing. *International Journal of Hydrogen Energy* 32: 3610–3621.

Wu, Y., S. Hong, J. Zhang, Z. He, W. Guo, Q. Wang, and G. Li. 2012a. Microstructure and cavitation erosion behavior of WC–Co–Cr coating on 1Cr18Ni9Ti stainless steel by HVOF thermal spraying. *International Journal of Refractory Metals and Hard Materials* 32: 21–26.

Wu, X.-K., J.-S. Zhang, X.-L. Zhou, H. Cui, and J.-C. Liu. 2012b. Advanced cold spray technology: Deposition characteristics and potential applications. *Science China Technological Sciences* 55 (2): 357–368.

Xie, Y., X. Zheng, C. Ding, W. Zhai, J. Chang, and H. Ji. 2009. Preparation and characterization of CaO-ZrO_2-SiO_2 coating for potential application in biomedicine. *Journal of Thermal Spray Technology* 18 (4): 678–685.

Xie, X.Y., H.B. Guo, and S.K. Gong. 2010. Mechanical properties of $LaTi_2Al_9O_{19}$ and thermal cycling behaviors of plasma-sprayed $LaTi_2Al_9O_{19}$/YSZ thermal barrier coatings. *Journal of Thermal Spray Technology* 19 (6): 1179–1185.

Xie, X., H. Guo, S. Gong, and H. Xu. 2012. Hot corrosion behavior of double-ceramic-layer $LaTi_2Al_9O_{19}$/YSZ thermal barrier coatings. *Chinese Journal of Aeronautics* 25: 137–142.

Yamakawa, O., H. Nihonmatsu, M. Morisasa, and H. Hotta. 2009. Plasma sprayed ceramic tray members for firing ceramic capacitor. In *Thermal spray 2009: Proceedings of the international thermal spray conference*, ed. B.R. Marple, M.M. Hyland, Y.-C. Lau, C.-J. Li, R.S. Lima, and G. Montavon, 624–627. Materials Park: ASM International.

Yandouzi, M., H. Bu, M. Brochu, and B. Jodoin. 2012. Nanostructured Al-based metal matrix composite coating production by pulsed gas dynamic spraying process. *Journal of Thermal Spray Technology* 21 (3–4): 609–619.

Yang, Q., T. Senda, and A. Hirose. 2006a. Sliding wear behavior of WC–12% Co coatings at elevated temperatures. *Surface and Coating Technology* 200: 4208–4212.

Yang, Y., N. Oh, Y. Liu, W. Chen, S. Oh, M. Appleford, S. Kim, K. Kim, S. Park, J. Bumgardner, W. Haggard, and J. Ong. 2006b. Enhancing osseo-integration using surface-modified titanium implants. *JOM* 58: 71–76.

Yang, G.-J., C.-J. Li, S.-J. Zhang, and C.-X. Li. 2008. High-temperature erosion of HVOF sprayed Cr_3C_2-NiCr coating and mild steel for boiler tubes. *Journal of Thermal Spray Technology* 17 (5–6): 782–787.

Yılmaz, S. 2009. An evaluation of plasma-sprayed coatings based on Al_2O_3 and Al_2O_3–13 wt.% TiO_2 with bond coat on pure titanium substrate. *Ceramics International* 35: 2017–2022.

Yilmaz, R., A.O. Kurt, A. Demir, and Z. Tatli. 2007. Effects of TiO_2 on the mechanical properties of the Al_2O_3–TiO_2 plasma sprayed coating. *Journal of the European Ceramic Society* 27: 1319–1323.

Yoshiya, A., S. Shigemura, M. Nagai, and M. Yamanaka. 2009. Advances of thermal sprayed carbon roller in paper industry. In *Thermal spray 2009: Proceedings of the international thermal spray conference*, ed. B.R. Marple, M.M. Hyland, Y.-C. Lau, C.-J. Li, R.S. Lima, and G. Montavon, 601–606. Materials Park: ASM International.

Yu, L.-G., K.A. Khor, H. Li, and P. Cheang. 2003. Effect of spark plasma sintering on the microstructure and in vitro behavior of plasma sprayed HA coatings. *Biomaterials* 24: 2695–2705.

Yu, J., H. Zhao, X. Zhou, S. Tao, and C. Ding. 2011. Effect of thermal aging on microstructure and mechanical properties of plasma-sprayed samarium zirconate coatings. *Journal of Thermal Spray Technology* 20 (5): 1056–1062.

Yuan, F.H., Z.X. Chen, Z.W. Huang, Z.G. Wang, and S.J. Zhu. 2008. Oxidation behavior of thermal barrier coatings with HVOF and detonation-sprayed NiCrAlY bond coats. *Corrosion Science* 50: 1608–1617.

Zeng, Z., N. Sakoda, T. Tajiri, and S. Kuroda. 2008. Structure and corrosion behavior of 316L stainless steel coatings formed by HVAF spraying with and without sealing. *Surface and Coating Technology* 203: 284–290.

Zhang, T., D.T. Gawne, and Y. Bao. 1997. The influence of process parameters on the degradation of thermally sprayed polymer coatings. *Surface and Coating Technology* 96: 337–344.

Zhang, G., H. Liao, H. Yu, V. Ji, W. Huang, S.G. Mhaisalkar, and C. Coddet. 2006. Correlation of crystallization behavior and mechanical properties of thermal sprayed PEEK coating. *Surface and Coating Technology* 200: 6690–6695.

Zhang, G., H. Liao, M. Cherigui, J. Paulo Davim, and C. Coddet. 2007. Effect of crystalline structure on the hardness and interfacial adherence of flame sprayed (poly-ether–ether–ketone) coatings. *European Polymer Journal* 43: 1077–1082.

Zhang, X.C., B.S. Xu, F.Z. Xuan, S.T. Tu, H.D. Wang, and Y.X. Wu. 2008. Rolling contact fatigue behavior of plasma-sprayed CrC–NiCr cermet coatings. *Wear* 265: 1875–1883.

Zhang, C., G. Zhang, V. Ji, H. Liao, S. Costil, and C. Coddet. 2009. Microstructure and mechanical properties of flame-sprayed PEEK coating remelted by laser process. *Progress in Organic Coating* 66: 248–253.

Zhang, J., Z. Wang, P. Lin, W. Lu, Z. Zhou, and S. Jiang. 2011. Effect of sealing treatment on corrosion resistance of plasma-sprayed NiCrAl/Cr_2O_3-8 wt.%TiO_2 coating. *Journal of Thermal Spray Technology* 20 (3): 508–513.

Zhao, X., and P. Xiao. 2008. Effect of platinum on the durability of thermal barrier systems with a $\gamma+\gamma'$ bond coat. *Thin Solid Films* 517: 828–834.

Zhu, D., S.R. Choi, and R.A. Miller. 2004. Development and thermal fatigue testing of ceramic thermal barrier coatings. *Surface and Coating Technology* 188–189: 146–152.

Zhum Gahr, K.H. 1987. *Microstructure and wear of materials*. Amsterdam: Elsevier.

Zotov, N., A. Hospach, G. Mauer, D. Sebold, and R. Vaßen. 2012. Deposition of La12xSrxFe12yCoyO32d coatings with different phase compositions and microstructures by low-pressure plasma spraying-thin film (LPPS-TF) processes. *Journal of Thermal Spray Technology* 21 (3–4): 441–447.